Frost Resistance of Building Materials : Proceedings of the 2nd Nordic Research Seminar in Lund 1996

Lindmark, Sture

1996

UNIVERSITY OF LUND
LUND INSTITUTE OF TECHNOLOGY
Division of Building Materials

Report TVBM-3072

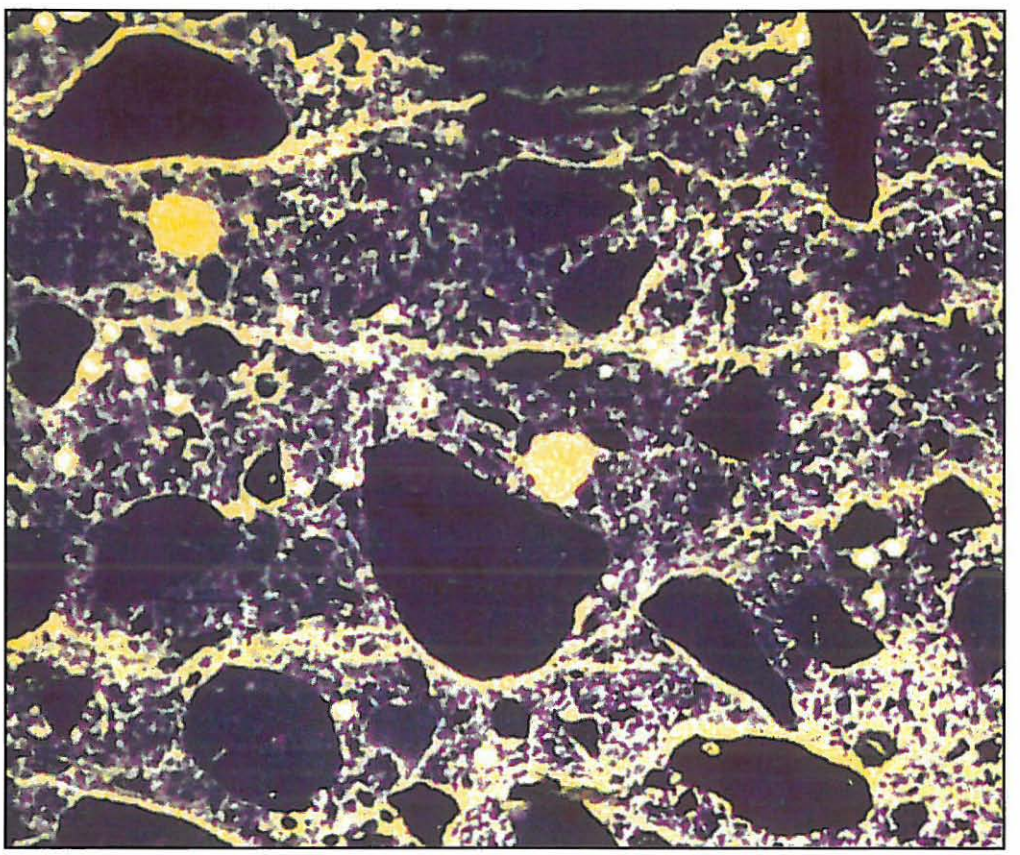

FROST RESISTANCE OF BUILDING MATERIALS

Sture Lindmark, Editor

Proceedings of a Nordic Research Seminar in Lund, April 16-17, 1996

UNIVERSITY OF LUND
LUND INSTITUTE OF TECHNOLOGY
Division of Building Materials

Report TVBM-3072

FROST RESISTANCE OF BUILDING MATERIALS

Sture Lindmark, Editor

Proceedings of a Nordic Research Seminar in Lund, April 16-17, 1996

Coverphoto from the paper by Niemann and Lehtonen

ISRN: LUTVDG/TVBM--96/3072--SE(1-190)
ISSN: 0348-7911 TVBM

Lund Institute of Technology
Division of Building Materials
Box 118
S-221 00 Lund, Sweden

Telephone: 46-46-2227415
Telefax: 46-46-2224427

Foreword

Frost destruction of porous building materials is a big problem in the Scandinavian countries, and in many other countries inside and outside Europe, such as U.K., Germany, countries in eastern Europe, U.S.A., Canada, etc. Much research has been devoted to solving the frost destruction problem, especially concerning the destruction of concrete, but also concerning the destruction of clay brick, roofing tile, cellular concrete, natural stone, etc. Nordic researchers have made important contributions in the past; names such as Poul Nerenst in Denmark, Sven Gabriel Bergström and Birger Warris in Sweden, and Jukka Vuorinen in Finland can be mentioned.

Previously, frost damage was in most cases of type internal damage occurring when the "stone" was frozen in a more than critically saturated condition. During the last decades, surface scaling of concrete is a growing problem in many countries. The reason is an increased use of deicing salts on roads and bridges. Maybe, surface scaling is a rising problem also for other mineral materials, such as natural stone and renderings. In this case, the reason might be that air pollution causes deposition of substances at the stone surface. Eventually, these interact with moisture and frost to cause surface scaling.

The mechanisms behind internal frost damage is fairly well understood due to work done in the fourties, fifties and sixties, primarily in the U.S.A. by T.C Powers, R.A. Helmuth and others. The mechanisms behind surface salt scaling is however still largely unknown, But as can be seen in these proceedings, much work is now being done in order to clarify the salt scaling mechanism. A very important step has also been the development of salt scaling test methods, that can be used for a rational selection of durable concrete.

The purpose of this Nordic research seminar was to get a general view of research going on in the Nordic countries on frost destruction. Naturally, most papers deal with concrete, but there are also some papers on other materials. Researchers from Finland, Denmark Norway and Sweden took part in the seminar.

This seminar was the second in order. The first took part in 1993 with only a few participants. Hopefully, there will be a third seminar within a few years time summarizing all the frost research which is now going on in the Nordic countries, or that will start in the near future.

Lund, June 17, 1996

Göran Fagerlund

CONTENTS

How Does the Frost Action Break Down Concrete in the Laboratory Test and in Field Circumstances

By C. Niemann and V. Lehtonen
Stockholm Konsult
Materialprovningen

Service life is very important for the concrete structures in infrastructure. To assure the right service life the technician has to use fast laboratory test to estimate the natural ageing processes. It would be most desirable that the test made at laboratory acts the very same way as the real circumstances.
We want to reveal our experience on how the frost break down process affects the concrete in the laboratory. Also we expose how the frost is acting on bridge constructions in The Stockholm area.

What the technicians wants

Technicians wants to obtain data which correlate frost actions with the mechanisms. In particular, it is important to compare field observations made on actual concrete structures with the data obtained in the laboratory.

One may also simulate the natural frost cycles in the laboratory like *Saeki et al* did. They measured the cycles in the coastal concrete structures and made the same cycles in the laboratory. The surface layer temperature was controlled in a cycle from 5 °C to -10 °C a day. The temperature inside the specimen was kept at 2 °C in order to simulate the measured temperatures in the coastal structures during the freezing and thawing period of the year. The test specimens were cured in the laboratory at the same atmospheric conditions as on the site. Three different type of curing methods were used, exposed to air, five days water curing, and four weeks water curing. The test age for concretes with 6 % air and different cement types was four weeks.

One can imagine that it is not easy to have tools which show what is happening in the concrete during a freezing and thawing cycle. The laboratory investigation by *Grasenick et al* show how the water penetrates through a capillary pore into the air void and how ice crystals are formed. When an ice crystal melts, it leaves secondary product deposits in the pore. The tool used was a Scanning Electron Microscope with an Energy Dispersive X-ray Micro Analyzer.

The comparison we made was how frost breaks down the concrete in the Swedish laboratory test and in concretes structures. The concrete structures studied are bridges from the Stockholm area with an age varying from 6 to 40 years. The laboratory concrete specimens ranged from 28 days and upwards. The quality of concrete types varies from low to high grade and with or without air entraining.

Studies related not only to frost damage but durability in general must be continued a long period in order to collect enough information. It is extremely important to compare observations made with actually used concrete mixes to the data obtained at the laboratory. Otherwise the results carried out at the laboratory remains inevitably limited. On the other hand it is more difficult to continue over a long time observations made with test specimens exposed to natural weathering. That's why we used the concrete specimens from the structures where detailed data is still available. The concrete, the very same as used today in bridges, was 6-8 years old. The early type of air entrained concrete was about 40 years old.

The Laboratory Test SS 13 72 44 and the Break Down Process

We investigated how the frost act is changing the concrete microstructure in the Swedish Standard laboratory test for frost resistance of concrete specimens.
High scaling is usually related to high amount of calcium hydroxide in the solution on the concrete surfaces. Calcium hydroxide is rapidly carbonated to calcium carbonate and precipitated. It is usual with all types of concrete that the precipitation indicates that the scaling rate is high. Calcium hydroxide is leached out from the surface to the test solution. The scaling residue has also a much lower calcium content than the content in the undamaged areas. Chloride ions are penetrated into the test concrete and pushing ahead also sulphate ions. High levels of chloride ions are measured inside the specimen. The air void system is not affected in the period of 56 cycles. The pores do not have deposits of secondary products. We studied even a specimen which has been tested about eight hundred cycles and found that the layer just 0.5 mm beneath the surface have some deposits in the air pores. Pores are not completely filled and deeper down in the specimen the voids are not affected. Just the surface region is leached out, that means a lower content of calcium hydroxide and higher of silicon dioxide than the usual values for a cement paste.

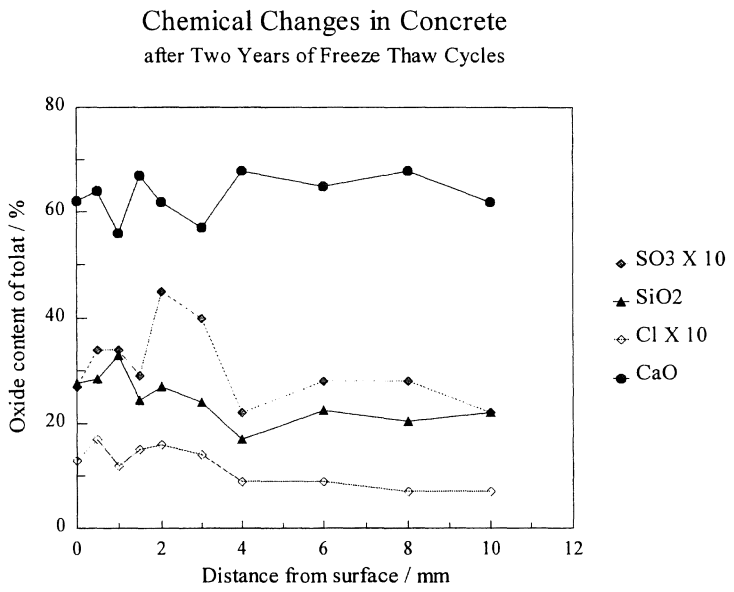

Figure 1. *The changes in the chemical composition of the paste during the freeze/thaw cycles at the laboratory test. Chlorides are penetrating in to the concrete and the close to the surface calcium is leached out.*

Concrete Break Down in Bridges

We have a lot of documentation of the bridges in the Stockholm area. The information is based of hundreds of objects from which concrete specimens are taken. Observations are done partly by ocular inspections in the field and in the laboratory. These ocular observations are completed with thin section, and planar section specimens, which are studied in detail. More than one thousand five hundred thin sections have been prepared from old concrete specimens. SEM-XMA data were used to analyze the chemical changes and the secondary reaction products in the air void system in some specimens.

If we ocularly can see that the concrete is frost damaged, the pores are filled with white deposits. The limit one ocularly can see is the pores down to 200 - 300 microns in diameter.

The thin section specimens studied by optical microscopy show that the small air voids always are first filled up. The same type of results are confirmed by other colleagues working with microscopy; *Pyy*, *Grasenick et al* and *Thaulow*.

In specimens from old concrete roads the pores up to 40 microns in diameter are filled with deposits in twenty-five years, *Grasenick et al.*

We investigated the concretes, which protects the asphalt insulation on the bridge decks, and found that air voids up to 300 microns were filled with secondary products. This concrete is highly moisture loaded and deicing salts are also penetrated through the asphalt pavement into this concrete. The age of this air entrained concrete was about 40 years.

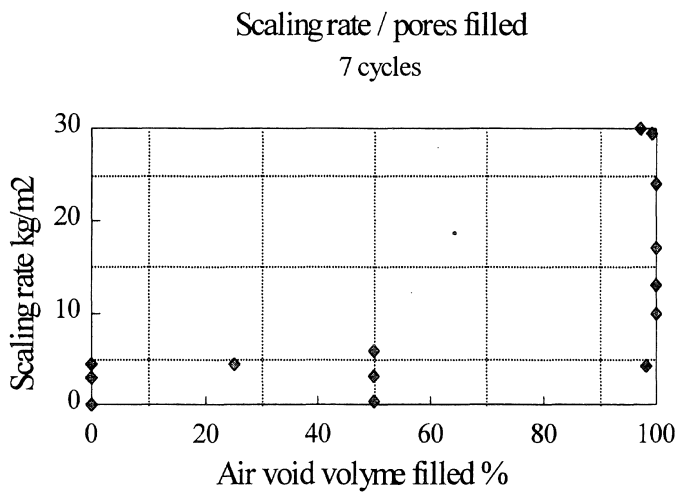

Figure 2. *Pore void filling and the freeze/thaw durability of the same type of concrete. The scaling rate is high if the pores are filled with secondary reaction products. The freeze/thaw scaling rate is rather independent of the original air content.*

We collected information of the same type of concrete with different pore filling and air contents. These concrete specimens were subjected to a freeze/thaw test. This test confirmed our earlier experience that concrete with high level of pore filling is damaged by the frost also in the real service circumstances. The tested concrete specimens failed totally first with a 100 % pore filling. See figure 2.

The air pores in the weathered upper concrete surface are not filled with deposits within a layer thickness 0 to 3 mm. Only this particular layer is also carbonated.

Thin sections show even the stage of the break down process in concrete. It is easy to see the first cracks just a few microns wide. These cracks are always parallel to the surface and the distance from the surface is varying from 10 to 25 mm. If the decomposition has gone further, the concrete is damaged more layer-by-layer. This observation is also documented by *Rösli et al* and the authors suggest that internal stresses are developed in the concrete due to the thermal gradient on the concrete surface.

We found also in the 6 - 8 years old concrete specimens that the pore filling just was starting at the same distance of 10 - 25 mm from the surface. Pores up till 10 microns are almost completely filled in this certain region but at other levels they are empty.

This can explain the observations *by Saeki et al* when they investigated on other parameters correlating to the freezing thawing durability. The surface layer scaling was depending on the surface strength. For example a bad curing gives a lower surface crack resistance capacity, namely the fracture toughness, and the scaling rate is subsequently higher in concrete structures.

A picture of a planar section specimen from a bridge deck shows this layer-by-layer damage clearly. In most of the specimens where we see the frost damage, the pore system is filled up to 100 %. The pore filling appears in the optical microscope is as dense as the aggregates, no fluorescent epoxy is penetrating into the deposit. When pores are filled to 100 % , the concretes can be air entrained or not, we can see different types of damage on the concrete. In the first place all voids are filled, but there is no signs of cracks in the concrete, secondly one can observe the layer-by-layer micro cracking in the optical microscope and finally one can ocularly see the layer-by-layer damage. This means that the complete pore filling is a serious indication that the concrete has been subjected to a high moisture load and to moisture movements. If you do not decrease the moisture load and the moisture movements in the concrete you will get a layer-by-layer damage in the future.

We always find a few pores which are not filled. Pores in neighborhood of those are completely filled with the secondary products. It means that the air void wall do not have capillary openings and the water penetration during the moisture movements and/or freezing is not possible. The very same phenomena has been observed earlier in alkali activated slag concrete by *Byfors et al.* This concrete has a microstructure without capillary porosity and it's permeability is low. This combination makes it impossible to have moisture movements in this concrete and the transport of the freezable water to the air voids is not possible. Frost resistance is just depending on the water to binder ratio for an alkali activated slag concrete.

One may also have an air entraining agent which gives a stable air void system and the spacing factor is correct, but there are no capillary pores leading to the air bubbles. In the freezing test this concrete has the same scaling rate as a concrete without air with the same water to cement ratio.

Conclusions

The laboratory test reveals concrete with poor durability. The test results can not be transformed to estimate the service life, because the pore filling is an important parameter in freeze/thaw durability in real concrete structures.

In structures we need high moisture levels and moisture movements in the concrete before the damage appears. Usually the damage first becomes visible on the surfaces which are more exposed to the sun.
When we first observe complete air void filling in a concrete structure, the cement paste will be damaged by freeze/thawing action. This leads to the layer-by-layer breaking down which is easy to see in the field. This long time frost detoriation process is controlled in the beginning by chemistry and the final stages controlled by physics.

It is important to the technicians that one learns to understand the natural freezing processes. This understanding should create theories so that we can use or develop the laboratory tests. The natural criteria has to be fulfilled in the test and then the fast laboratory tests can be used to estimate the service life of concrete structures.

APPENDIX 1

Parameters which We know to Affect the Freeze/Thaw Durability in Concrete in the Stockholm Area

Structure

Design
Orientation
Loads
Movements

Surface Strength

Water Binder Ratio and Materials Used
Construction Period and Curing
Concrete Quality

Moisture

Moisture Level
Moisture Movements
Drying and Rewetting

Air Void Filling by Moisture Movements and Freeze/Thaw

Capillary Pore System
Secondary Reaction Products in Air Voids

Layer-by-Layer

Air Voids Completely Filled
Internal Stress Due to Thermal Gradient/Suction
Moisture Movements in the Cracks
Concrete Damaged

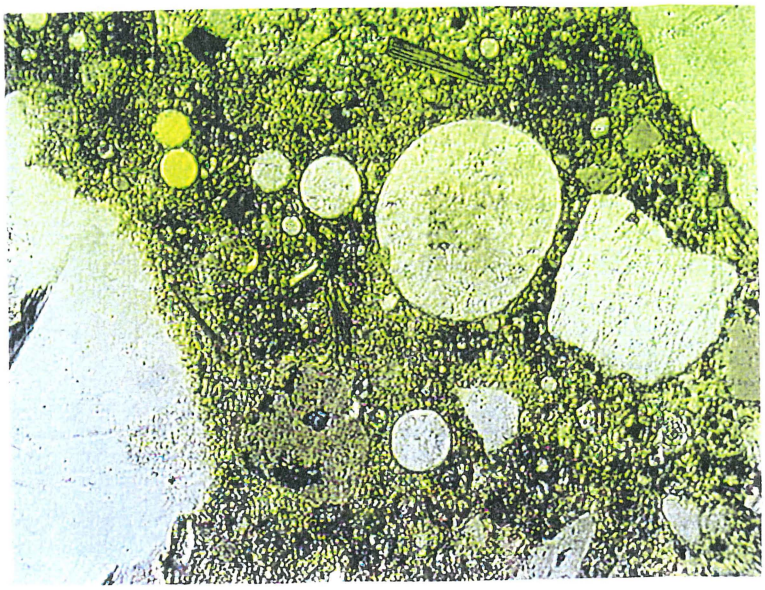

Picture 1. *A picture of concrete specimen in transmitted light in thin section. A few empty air voids and typical "round aggregates" in the completely filled air void system. The size of the photographed area is about 0.8 mm x 1.3 mm.*

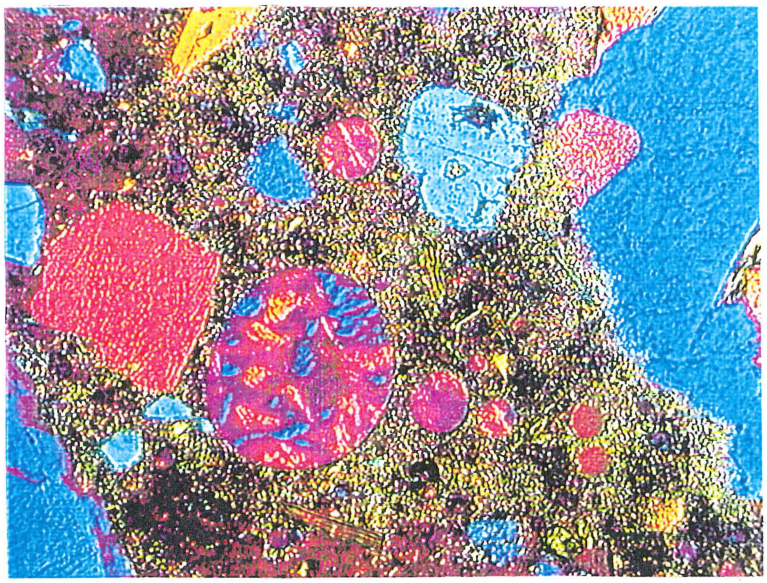

Picture 2. *The same specimen in cross polarized light and lamda plate. "Round aggregates" are calcium hydroxid. The size of the photographed area is about 0.8 mm x 1.3 mm.*

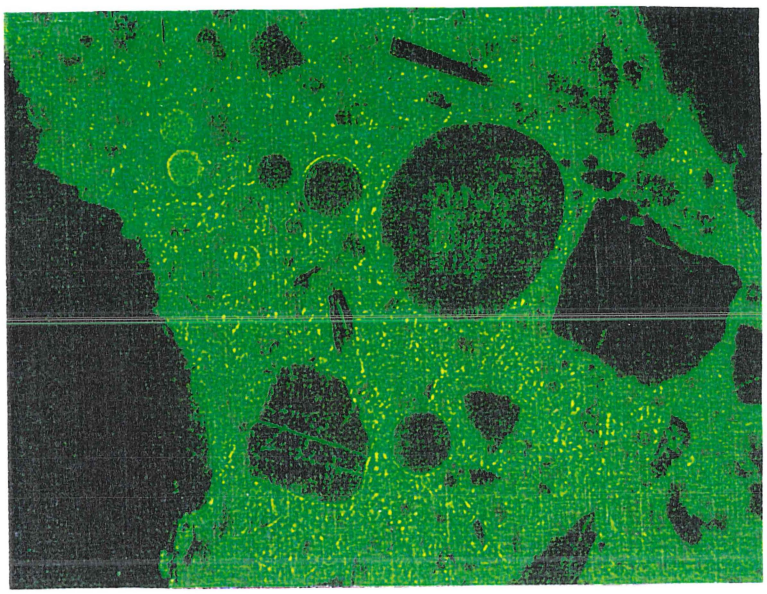

Picture 3. *The same specimen in fluorecent light. The fluorecent expoxi does not penetrate the "round aggregates" or the natural aggregates because both these do have a very dence structure. The size of the photographed area is about 0.8 mm x 1.3 mm.*

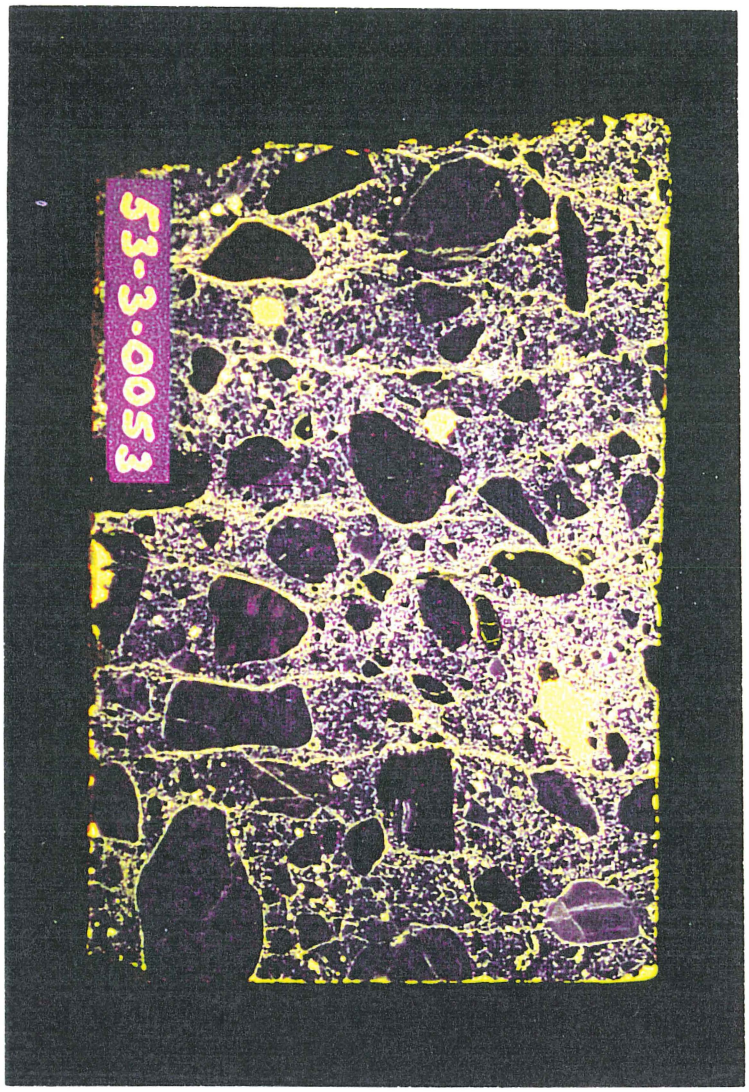

Picture 4. *A planar section concrete sample from a bridge deck. If air voids are completely filled with secondary reaction products we get typical frost cracks. These cracks are always parallel to the surface and the distance from the surface is varying from 10 to 25 mm. If the decomposition has gone further, the concrete is damaged more layer-by-layer, like in this concrete core. The concrete sample size is 98 mm in diameter and the length is 145 mm.*

1 *N. Seaki, N. Takada and Y. Fujita*
Some Experiments for Scaling Resistance of Hardened Concrete
TRANSACTIONS OF THE JAPAN CONCRETE INSTITUTE,
VOL 2, 1980, 101 - 108

2 *Hannu Pyy*
Private communications
TECHNICAL RESEARCH CENTER OF FINLAND VTT , BUILDING TECHNOLOGY

3a *Grasenick, Hans Martin and Johanna Blaha*
Erforschung der Struktur und der Beständigkeit von Luftporen im Luftporenzementsteinsystem mit Hilfe der Elektronmikroskopie
BUNDESMINISTERIUM f. BAUTEN u. TECHNIK,
Straßenforschung Heft 173

3b *Grasenick and Sorentz*
Beitrag der Elektomikroskopie zur Frost-Tausaltz Forschung
Zement und Beton · 27. Jahrgang · Heft 3 (1982) 120 - 121

4 *Niels Thaulow*
VBB Rapport 83-11-04, APPENDIX 6
Editors *Jan Erik Jansson and Hans Klingenberg*

5 *A. Rösli and A. B. Harnik*
Improving the Durability of Concrete to Freezing and Deicing Salts
ASTM Special Publication STP-691, 1980, pp 464 - 473

6 *K. Byfors, G. Klingstedt, V. Lehtonen, H. Pyy and L. Romben*
Durability of Concrete Made With Alkali Activated Slag
ACI SP 114-70, 1989, pp 1429 - 1463

7 **SS 13 72 44, Swedish Standard test for frost resistance**
SIS, Stockholm 1988

8 *F. Karsson, V. Lehtonen och* **C. Niemann**
Uppfyllning av betongs luftporer med kalciumhydroxid/ettringit
Stockholm Konsult, Materialprovningen, Rapport nr 74512.

SCALING RESISTANCE OF CONCRETE FIELD EXPOSURE TESTS

Per-Erik Petersson
SP - Swedish National Testing and Research Institute
Box 857
S-501 15 BORÅS
Sweden

Summary
This paper presents results from field exposure tests to investigate scaling resistance. Concrete specimens were exposed to the marine environment in Träslövsläge on the Swedish west coast and to the environment close to the highway between Borås and Gothenburg. Large amounts of de-icing agents are used on this highway every winter.

Thirty-four different concrete qualities were used in the investigation, ranging from very poor (water/binder ratio=0.90, no entrained air) to very good scaling resistance (water/binder ratio=0.37, air content=6%). Three different Portland cement qualities were used and silica fume, or pulverised fly-ash, was added to some of the concrete mixes.

The scaling resistance at 28 days was determined using Swedish standard SS 13 72 44 for all the concrete qualities. After two to four years of field exposure the specimens were inspected visually and then tested again in the laboratory. The results for the aged specimens were compared with the results for the 28 days old specimens.

The following conclusions can be drawn from the test results:

- SS 13 72 44 is useful for classifying concrete intended for use in environments aggressive to concrete structures.

- The scaling resistance of concrete in a marine environment or in the environment close to a highway normally improves with age.

- The highway environment is much more aggressive than the marine environment, at least as far as scaling resistance is concerned.

Key words: *concrete, scaling resistance, field exposure testing.*

1 Introduction

Knowledge about the scaling resistance of concrete is mainly based on experience. In Sweden, Portland cement has been used as binder in concrete for over a century, and we have had access to air-entraining agents for more than 40 years. This has made it possible to gain experience on how "common" concrete functions under normal conditions in the Swedish climate. It is known that a sufficiently low water/binder ratio, a sufficiently high content of air and a good air pore structure normally produces concrete with good scaling resistance for the majority of areas of use. Testing methods have also been developed, e.g. SS 13 72 44, which make it possible to estimate the quality of concrete. However, it must be kept in mind that our knowledge is based on experience and not on basic knowledge of deterioration mechanisms. If we use other types of cement than Portland cement, other admixtures than pure air-entraining agents, very low water/binder ratios, etc., we often do not have sufficient experience and knowledge either of how a frost-resistant concrete should be composed, or of how it should be tested. Better knowledge and more experience must be gained!

Rapid development takes place in the field of concrete technology. High performance concrete with low water-binder ratios and very high strengths are being produced. It is possible to produce concrete with extremely good casting characteristics. Surface treatment and impregnation affect the characteristics of the concrete. Fibres of steel, polymer and coal give tough concrete, etc. Full use of these products in real structures requires experience from exposure under actual conditions as a complement to the extensive laboratory experiments that have been carried out.

The Swedish tradition is to almost exclusively use Portland cement as the binder in concrete. In other countries, fly-ash, slag, silica fume and other additions are used to a great extent as a complement to Portland cement. Surface treatment products are also used in other countries to a much greater extent than in Sweden. These materials and applications, new to Sweden, can probably contribute to cheaper and perhaps also better constructions and possibly also to more environmentally friendly constructions. It is therefore of great importance that knowledge and experience be gained, for example in field exposure experiments, of how these products function under Swedish environmental conditions and with Swedish construction practices.

The aim of the work presented in this report was to gain experience of the scaling resistance of concrete from realistic exposure conditions and to calibrate results from field exposure tests with laboratory results obtained by the Swedish standardised freeze/thaw testing method SS 13 72 44. The paper gives the results of an extensive field exposure experiment in a marine environment that was carried out in Träslövsläge, south of Varberg on the Swedish west coast, as well as the results of a smaller study performed in a road environment on national highway 40 between Borås and Gothenburg. More detailed information is presented in /1/.

2 Field exposure in a marine environment

2.1 Field exposure site in Träslövsläge

The field exposure site consists of three approximately 20 meter long and three meter wide floating concrete pontoons. They are situated in Träslövsläge harbour about seven kilometres south of Varberg on the Swedish west coast. The pontoons are protected from direct wave forces by a pier, however, they are also exposed to salt spray when the waves hit the protective pier that separates the outer dock from the sea. The pier is located only a few meters beyond the pontoons.

Test panels of concrete, with the dimensions 100x800x1000 mm, were attached to the sides of the pontoons, so that half the height of the panels (500 mm) was over and half under the water line. The surface of the panel that was cast against the mould was turned outward and was usually used as the test surface. Because the pontoons float, the water line was always at half the panel height. The panels were mounted so that it was relatively simple to dismount them when they were to be tested after exposure.

Moreover, on the decks of the pontoons, specimens with the dimensions of 50x150x150 mm were placed with the sawn test surface (150x150 mm) turned upwards. After being aged for different times, the specimens were taken in for testing in the laboratory.

In many ways the climate on the Swedish west coast represents a very aggressive environment for concrete constructions, owing to salt and high humidity. As regards temperature, however, the climate is relatively mild, as the temperature seldom falls below -10° C. This is probably of great significance for the scaling resistance of concrete.

2.2 Concrete qualities

In the investigation, 34 concrete mixtures were tested, see Table 1. The mixtures ranged from concrete with an expected very poor scaling resistance (water/binder ratio=0.75, no air) to very good resistance (water/binder ratio=0.35, 6% air).

Three different types of Swedish Portland cement were used: Slite std, Degerhamn anl and Degerhamn 400. Compared with Slite std, Degerhamn anl is a low alkaline cement with an equivalent alkaline content of below 0.6%. The C_3A content is also low, and the cement can be considered sulphate-resistant. The Degerhamn cement also shows low heat development, making this type of cement generally suitable for use in large, compact constructions in environments aggressive towards concrete. This cement is, for example, used for all bridge constructions in Sweden. Degerhamn 400 is a finer-ground variant of the Degerhamn cement.

The fly-ash was added in the form of dry powder, together with the cement. The silica fume used was in the form of a slurry, which yields a good dispersion of the silica fume particles. The slurry was added with the first mixing water.

TABLE 1 *Concrete qualities used for the field exposure tests in Träslövsläge on the Swedish west coast.*

Quality no.	Cement	Binder content	Silica fume	Fly ash	Water/ binder ratio	Admix-tures[1)]	Air	Slump	Compr strength
		kg/m³	*%*	*%*			*%*	*mm*	*MPa*
1-35	Anl	450			0.35	AE+PL	6.0	105	68
1-40	Anl	420			0.40	AE+PL	6.2	125	57
1-50	Anl	370			0.50	AE	6.4	105	41
1-75	Anl	240			0.75	AE	6.1	100	21
2-35	Slite	450			0.35	AE+PL	5.7	135	60
2-40	Slite	420			0.40	AE+PL	6.2	125	55
2-50	Slite	390			0.50	AE	5.8	95	42
2-60	Slite	310			0.60	AE	6.3	100	35
2-75	Slite	250			0.75	AE	5.8	115	26
3-35	Anl	450	5[2)]		0.35	AE+PL	5.8	60	71
3-40	Anl	420	5		0.40	AE+PL	6.1	75	60
3-50	Anl	370	5		0.50	AE	6.0	80	45
3-75	Anl	245	5		0.75	AE	5.9	140	21
4-40	Anl	420	10		0.40	AE+PL	6.6	60	65
5-40	Anl	420	5		0.40	AE+PL	2.9	90	81
6-35	Anl	450	5		0.35	AE+PL	2.1	45	93
6-40	Anl	420	5		0.40	AE+PL	1.7	70	87
7-35	Anl	450			0.35	PL	2.4	55	91
7-40	Anl	420			0.40	PL	2.1	50	79
7-75	Anl	265			0.75	-	1.1	45	32
8-35	Slite	470			0.35	PL	2.1	85	73
8-40	Slite	440			0.40	PL	2.1	80	67
8-50	Slite	410			0.50	-	1.4	95	56
8-60	Slite	330			0.60	-	1.6	70	45
8-75	Slite	270			0.75	-	1.4	70	37
H1	Anl	500	5		0.30	PL	0.8	>265	112
H2	Anl	500	10		0.30	PL	1.1	145	117
H3	Anl	492			0.30	PL	3.6	>265	90
H4	Anl	420	5		0.40	AE+PL	5.9	180	56
H5	Anl	551	5		0.25	PL	1.3	>265	116
H6	Anl	518		5	0.30	PL	2.8	>265	90
H7	De400	500	5		0.30	PL	1.3	>265	114
H8	Anl	616		20	0.30	PL	3.0	>270	90
H9	De400	500			0.30	PL	2.9	210	99

1) AE=air entraining agent (Cementa 88L or Cementa L14), PL=plasticizer (Cementa 92M))
2) percent by weight of the total binder content

The aggregate used was a frost-resistant natural gravel, primarily gneiss, the largest particle size being 16 mm. The air-entraining agent was Cementa L14 (pine oil) except for the mixtures containing silica fume, in which Cementa 88L (Vinsol resin) was used. Cementa 92M (melamine) was used as plasticizer. The admixtures were added with the mixing water.

As can be seen in Table 1, the concrete qualities can be separated into two groups: "normal" concrete (1-35 to 8-75) and high performance concrete (H1 to H9). The normal concrete strengths are between 21 and 91 MPa, with slump values between 45 and 140 mm. The strength of the high performance concretes is higher (except for H4) and the consistency in all cases is fluid. Air-entrainment admixtures were used in only one of the nine high performance concrete qualities. In spite of this, the air content is often relatively high. One explanation may be that the plasticizer was used in high dosages for the high performance concrete qualities, which may have resulted in the high air content.

2.3 Manufacturing and curing of specimens

2.3.1 Concrete manufacturing

All mixtures were made in a 350-litre paddle mixer. The concrete was mixed for three minutes, after which tests were made of the consistency and air content.

2.3.2 Specimens for normal time testing

For testing the scaling resistance, 150-mm cubes were produced according to process IA in SS 13 72 44, second edition /2/. Directly after casting, the moulds were covered with plastic foil to prevent drying. The cubes were demoulded after 24 hours and then placed in water (20$\pm$ 2° C), where they were stored for six days. They were then placed in a climate chamber with a temperature of 20$\pm$ 2°C, a relative humidity of 50$\pm$5% and an air flow of <0.1 m/s.

After 21 days, 50-mm thick specimens were sawn from the cubes. The specimens were immediately placed in the climate chamber, where they were stored for another seven days.

When the specimens were 26 days old, a rubber sheet was glued to the specimens on all sides except the test surface. The rubber sheet reached 20$\pm$1 mm over the test surface, according to the test set-up shown in Figure 1.

When the concrete was 28 days old, water was poured on to the test surface. This resaturation continued for three days, after which the water was replaced with 3% NaCl solution, and the freeze/thaw testing began.

2.3.3 Specimens for field testing

Specimens with the dimensions 50x150x150 mm were manufactured and cured for 28 days in the exact same way as for the normal time specimens, with the exception of the fact that no rubber sheet was glued to the surfaces. They were then placed at the field exposure site on the decks of the pontoons with the sawn test surface turned upwards.

When the specimens were taken in to the laboratory for testing after certain periods of exposure, they were stored in a climate chamber (20° C, 50% RH) for one week. During this time, rubber sheets were glued onto the sides of the specimens. They were then resaturated for three days, after which the freeze/thaw tests started.

Panels with the dimensions of 100x1000x800 mm were also manufactured for exposure at the test site. Directly after being cast, the specimens were covered with plastic foil. After 24 hours, the panels were removed from the moulds and again covered with plastic foil for another six days. The panels were then stored in the laboratory until they were placed at the field exposure site when they were 28 days old.

After exposure periods, the panels were taken back to the laboratory and specimens with the dimensions of 50x100x100 mm were sawn from the panels. The specimens were then treated in the same way as the specimens for normal time testing.

2.4 Freeze/thaw testing

The freeze/thaw tests were carried out according to SS 13 72 44, version 2, procedure IA.

Before the start of the freeze/thaw testing, all the surfaces of the specimens except for the test surface were insulated with a 20±1 mm thick layer of celluar polystyrene according to Figure 1. A 3 mm thick layer of 3% NaCl solution was poured onto the freeze surface. To prevent evaporation during testing, polyethylene foil was stretched over the salt solution.

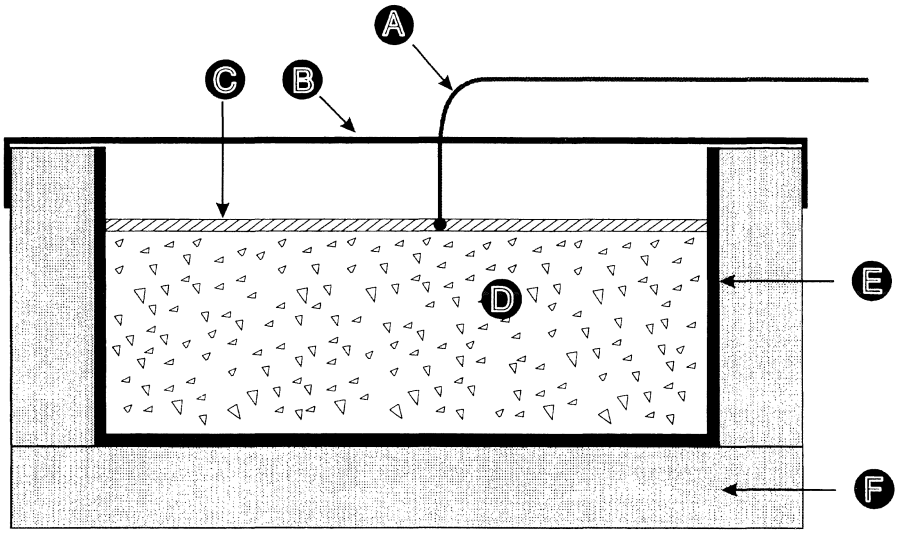

FIGURE 1 *Test set-up according to SS 13 72 44. A=temperature sensor, B=plastic sheet, C=salt solution, D=specimen, E=rubber sheet, F=heat insulation*

The specimens were then exposed to repeated freezing and thawing between -18 and +20°C. The time for each cycle was 24 hours. The temperature was continuously measured in the salt solution for one specimen in each freezer.

The material scaled from the test surface was collected after 7, 14, 28, 42 and 56 cycles and then dried at 105°C and weighed. The results are given as the amount of scaled material per surface unit as a function of the number of freeze/thaw cycles.

Three or four specimens of each quality of concrete were tested.

2.5 Results of the normal time test

The results of the normal time tests are reported in Table 2.

In Table 2, the following observations can be made:

- The requirements for good or very good scaling resistance are fulfilled for all 12 concrete qualities having a water/binder ratio less than or equal to 0.5 and in which air-entraining agents have been used.
- Of the four air-entrained qualities having a water/binder ratio exceeding 0.5, none fulfill the requirement for acceptable scaling resistance.
- Of the 18 qualities in which no air entraining agent was used, 14 do not fulfill the requirement for acceptable scaling resistance. The four concretes without air and with acceptable scaling resistance, all have a water/binder ratio of 0.30 or lower. Moreover, three of these four qualities have a high natural content of air, about 3%.
- Only one quality with a low air content, 1.3%, fulfills the requirement for good scaling resistance. This quality, however, has a low water/binder ratio of 0.25.

The test method thus completely classified the qualities of concrete as could be expected. It can also be seen that the scaling resistance of the concretes were either judged to be very good/good or unacceptable, while no concrete was classified in the region of acceptable, between these levels. Consequently, a functioning test method must primarily differentiate between very good and very poor qualities, and these experiments show that the method used here does that. For the method to be useful, however, it is also necessary that the expected results agree with the results achieved in actual structures. Field experiments must be carried out to obtain answers.

2.6 Results of the field tests

2.6.1 Specimens aged on the decks of the pontoons

For all qualities of concrete, specimens for freeze/thaw tests (50x150x150 mm) were manufactured according to the procedure described in section 2.3.3. The specimens were treated as specimens for normal time testing until the 28th day after casting. Then, between December 1991 and February 1992, they were placed on the pontoons with the sawn test surface turned upwards.

TABLE 2 *Freeze/thaw test results (mean values) for normal time tests. Italicised figures are uncertain owing, for example, to leakage of salt solution during the test.*

Quality No.	Cement	Silica fume	Fly ash	Water/ binder	Air	Scaling (g/m²)					Rating[1]
		%	%		%	*7c*	*14c*	*28c*	*42c*	*56c*	
1-35	Anl			0.35	6.0	56	74	85	95	106	G
1-40	Anl			0.40	6.2	71	91	97	101	105	G
1-50	Anl			0.50	6.4	80	97	111	124	131	G
1-75	Anl			0.75	6.1	400	620	920	1080	1160	NA
2-35	Slite			0.35	5.7	20	27	40	50	56	VG
2-40	Slite			0.40	6.2	57	76	91	104	109	G
2-50	Slite			0.50	5.8	133	203	264	280	290	G
2-60	Slite			0.60	6.3	310	560	940	1160	1290	NA
2-75	Slite			0.75	5.8	700	1280	2090	2650	3090	NA
3-35	Anl	5		0.35	5.8	17	21	28	39	57	VG
3-40	Anl	5		0.40	6.1	9	14	16	19	21	VG
3-50	Anl	5		0.50	6.0	27	32	38	40	43	VG
3-75	Anl	5		0.75	5.9	420	603	880	995	1050	NA
4-40	Anl	10		0.40	6.6	18	22	27	31	38	VG
5-40	Anl	5		0.40	2.9	56	75	92	113	135	G
6-35	Anl	5		0.35	2.1	140	420	1240	2410	4520	NA
6-40	Anl	5		0.40	1.7	350	1020	2540	4510	7550	NA
7-35	Anl			0.35	2.4	210	600	1280	1870	2410	NA
7-40	Anl			0.40	2.1	850	2250	4710	6700	9450	NA
7-75	Anl			0.75	1.1	1910	4810	*12000*	SF[2]	SF	NA
8-35	Slite			0.35	2.1	320	880	1830	2660	3520	NA
8-40	Slite			0.40	2.1	1030	2360	4540	6840	9120	NA
8-50	Slite			0.50	1.4	2180	5070	*11000*	SF	SF	NA
8-60	Slite			0.60	1.6	2460	6790	16610	*33000*	SF	NA
8-75	Slite			0.75	1.4	2510	7130	*23000*	SF	SF	NA
H1	Anl	5		0.30	0.8	29	84	209	352	545	NA[3]
H2	Anl	10		0.30	1.1	43	83	405	923	1958	NA
H3	Anl			0.30	3.6	15	21	33	45	60	VG
H4	Anl	5		0.40	5.9	25	35	48	53	59	VG
H5	Anl	5		0.25	1.3	18	41	78	104	151	G
H6	Anl		5	0.30	2.8	18	29	41	60	77	VG
H7	De400	5		0.30	1.3	12	31	86	306	593	NA[3]
H8	Anl		20	0.30	3.0	25	38	55	88	152	NA[3]
H9	De400			0.30	2.9	14	20	28	42	69	VG

1) Rating of scaling resistance according to SS 13 72 44;
VG=very good, G=good, A=acceptabel, NA= not acceptable

2) SF means that the specimen is totally disintegrated

3) Accelerated scaling (normally not acceptable according to SS 13 72 44

After three years of exposure, the specimens were taken to the laboratory from December 1994 to March 1995 for freeze/thaw testing. The aim was to compare the results with the normal time tests in order to study effects of ageing. All "normal" concrete qualities, i.e. 1-35 to 8-75, were analysed in this way.

No visible freeze/thaw damage could be observed for any specimens on the exposure site, with the exception of those with a water/binder ratio of 0.75. The surfaces of these specimens were weakly etched and the edges showed damage. The specimens were weighed in air and in water, and the volume was determined and compared with corresponding values at an age of 28 days, i.e. before ageing. The reduction in volume did not exceed 1.5% for any specimen. Thus the damage was relatively limited, even in the case of high water/binder ratios.

The results of freeze/thaw testing of the aged specimens are shown in Table 3. It was found that the specimens made of concrete with water/binder ratios of 0.75 often leaked at relatively low scaling. This explains the gaps in the table. The values for the specimens that leaked are not representative and have not, of course, been considered in the analyses.

The results for the aged specimens show even more clearly than the normal time tests that there is a well-defined zone between good and poor qualities of concrete. All qualities but one were classified as having either very good or unacceptable scaling resistance. Only one concrete quality had good scaling resistance, while no quality was classified as having acceptable scaling resistance. It can again be pointed out that a good freeze/thaw test method must primarily be able to distinguish between very good and very poor concrete, as it seems to be rare that concrete qualities are classified in the zone between very good and poor scaling resistance.

In a comparison between the results of Tables 2 and 3, it is seen that aged specimens, almost without exception, showed better scaling resistance than those that were tested at 28 days! In this marine environment on the west cost of Sweden the concrete seems to have experienced positive ageing.

Figures 2 and 3 compare scaling for aged specimens with results from the normal time tests. The two figures represent 14 and 56 freeze cycles, respectively. Almost all of the results lie to the right of the diagonal line, which means that scaling is lower for aged than for non-aged specimens.

As can be seen in the figures, it is possible to divide the qualities of concrete into two clearly identifiable groups: concrete with and without entrained air. The results show that the ageing effect is especially pronounced for the concretes in which no air entraining agent was used. It can also be seen that some of the aged concretes without entrained air showed low scaling even after 56 freeze cycles. This is discussed in greater detail below.

For the air-entrained concrete qualities, the scaling is often 10 times lower for aged than for non-aged specimens. The difference decreases with increasing scaling and, at a value of about 1 kg/m^2 after 56 cycles, there no longer seems to

TABLE 3 *Freeze/thaw test results (mean values) for specimens aged on the decks of the pontoons for about four years at the field exposure site in Träslövsläge. Italicised figures are uncertain due, for example, to leakage of salt solution during the tests.*

Quality no.	Cement	Silica fume	Fly ash	Water/ binder	Air	Scaling (g/m²)					Rating[1]
		%	%		%	*7c*	*14c*	*28c*	*42c*	*56c*	
1-35	Anl			0.35	6.0	6	10	12	14	18	VG
1-40	Anl			0.40	6.2	7	10	12	13	15	VG
1-50	Anl			0.50	6.4	10	14	18	20	23	VG
1-75	Anl			0.75	6.1	617	840	1052			NA
2-35	Slite			0.35	5.7	7	9	11	14	18	VG
2-40	Slite			0.40	6.2	7	10	13	15	17	VG
2-50	Slite			0.50	5.8	13	20	26	34	36	VG
2-60	Slite			0.60	6.3	37	63	140	183	214	G
2-75	Slite			0.75	5.8	268	*378*				?
3-35	Anl	5		0.35	5.8	4	8	12	14	16	VG
3-40	Anl	5		0.40	6.1	4	8	11	14	16	VG
3-50	Anl	5		0.50	6.0	7	12	16	19	23	VG
3-75	Anl	5		0.75	5.9	1030	1260	1580	1740	1880	NA
4-40	Anl	10		0.40	6.6	8	13	17	22	25	VG
5-40	Anl	5		0.40	2.9	6	10	14	18	27	VG
6-35	Anl	5		0.35	2.1	4	7	11	116	2050	NA
6-40	Anl	5		0.40	1.7	4	8	18	2730	SF[2]	NA
7-35	Anl			0.35	2.4	8	11	13	15	18	VG
7-40	Anl			0.40	2.1	8	12	15	18	23	VG
7-75	Anl			0.75	1.1	801	*1010*				NA
8-35	Slite			0.35	2.1	7	9	12	16	19	VG
8-40	Slite			0.40	2.1	6	9	14	17	20	VG
8-50	Slite			0.50	1.4	18	29	51	143	683	NA[3]
8-60	Slite			0.60	1.6	40	57	192	1944	8694	NA
8-75	Slite			0.75	1.4	418	*576*				?

1) Rating of scaling resistance according to SS 13 72 44;
VG=very good, G=good, A=acceptabel, NA= not acceptable
2) SF means that the specimen is totally disintegrated
3) Accelerated scaling (normally not acceptable according to SS 13 72 44

be any difference. This is important, as this value represents the limit between acceptable and unacceptable scaling resistance according to SS 13 72 44. For air-entrained concrete, the present acceptance limit for scaling-resistant concrete thus seems to be applicable to the marine environment of Sweden. For concrete with lower scaling, the method yields results on the safe side, i.e. the scaling in the case of normal time testing is higher than the corresponding results for aged specimens. For concrete without entrained air, scaling for aged concrete is often up to 100 times lower than the normal time values, and the difference does not seem to

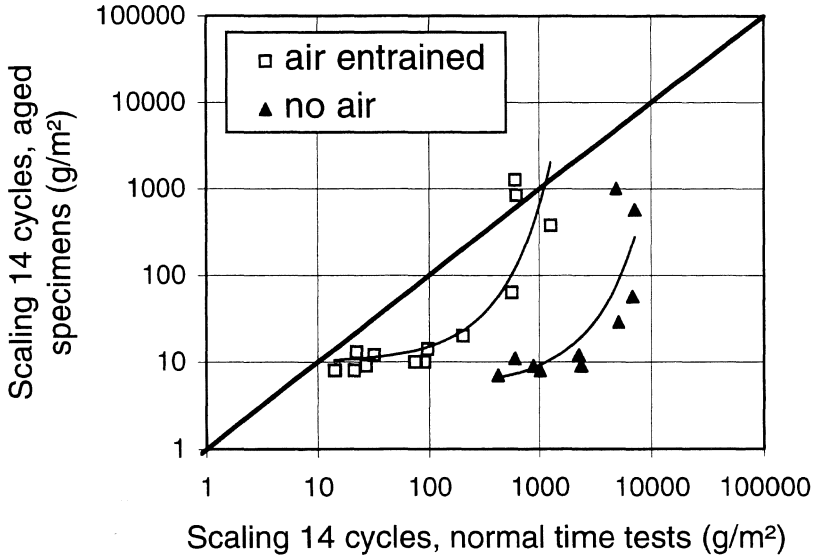

FIGURE 2 *Relation between test results for aged concrete and for concrete tested at 28 days (normal time test) after 14 freeze/thaw cycles.*

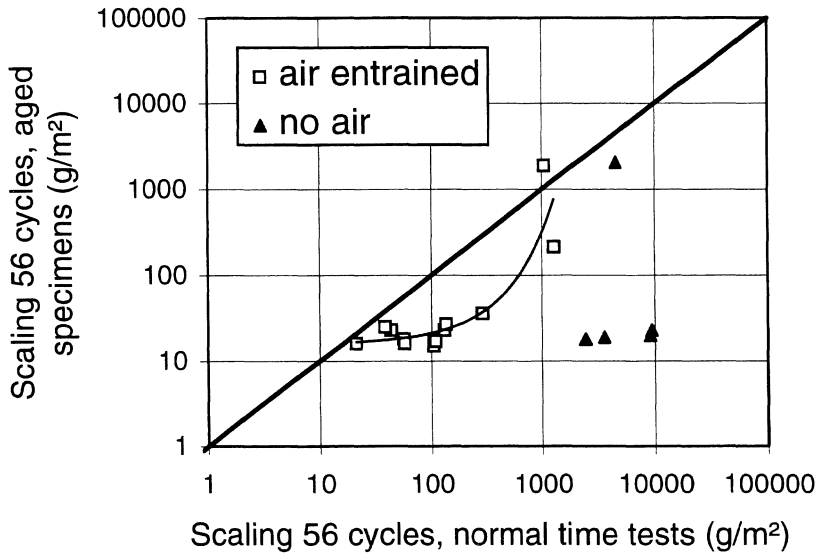

FIGURE 3 *Relation between test results for aged concrete and for concrete tested at 28 days (normal time test) after 56 freeze/thaw cycles.*

disappear until scaling after 56 freeze cycles exceeds about 10 kg/m². According to these results, SS 13 72 44 appears to underestimate the scaling resistance of concrete without entrained air, at least in the marine environment. There is, nevertheless, justification for having a high safety margin for concrete without entrained air until the degradation mechanisms and ageing effects of salt and frost have been completely clarified.

Figure 4 shows scaling as a function of water/binder ratio after different numbers of freeze cycles for the aged qualities of concrete 8-35 - 8-75, i.e. concrete without entrained air and with Slite std as binder. It is clear from the results that the concrete scales in freezing in an accelerated process when the water/binder ratio is 0.50 or higher. On the other hand, scaling is very small, even after 56 freeze/thaw cycles, when the water/binder ratio is equal to or less than 0.40. The low water/binder ratio together with the natural air (about 2%) seems to be sufficient to give good resistance. This indicates that it may be possible to produce concrete without entrained air that has good scaling resistance in the marine environment, providing that the water/binder ratio is sufficiently low.

Concrete with the cement Degerhamn anl without entrained air also has good scaling resistance when the water/binder ratio is 0.4 or lower, see Table 3. However, concrete with 5% silica fume addition (concrete qualities 6-35 and 6-40)

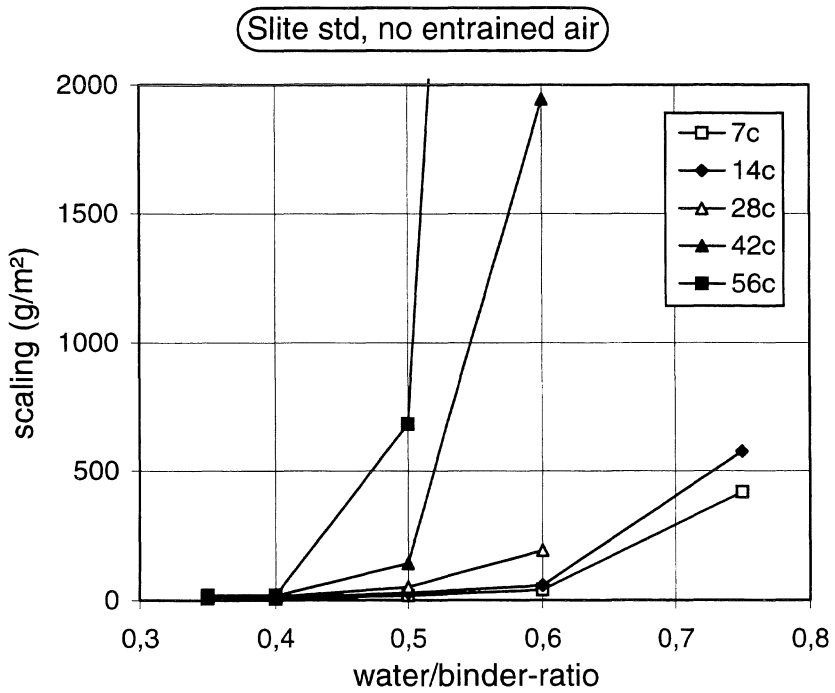

FIGURE 4 *Scaling as function of the water/binder ratio and the number of freeze/thaw cycles for aged concrete without entrained air and Slite std as binder.*

also seems to scale at low water/binder ratios. There is very little scaling for these concrete qualities until 28 or 42 cycles, after which it accelerates rapidly, and the concrete is completely disintegrated within only a few cycles. This is generally the same process as is reported in /3/ for concrete with silica fume. However, it is not possible to explain the reason why the concrete with silica fume disintegrates in freezing on the basis of the results of this investigation. It is indicated in /4/ that the reason might be alkali-silica reactions owing to the silica fume being insufficiently dispersed in the concrete. However, this cannot explain the course of events here, as the silica fume was added as a slurry and was therefore well dispersed in the concrete.

Scaling in concrete without entrained air or silica fume accelerates quickly for higher values of the water/binder ratio, as can be seen in the results for 8-50 and 8-60. To study how stable the scaling resistance is for lower values of water/binder ratio, the freezing experiments were continued for 112 cycles for two of the concrete qualities without entrained air, 7-35 (Degerhamn anl 0.35) and 8-40 (Slite std 0.40). The results are given in Figure 5, together with the results for concrete with silica fume with low water/binder ratios.

It can be seen in Figure 5 that scaling also remains relatively small after 112 freeze/thaw cycles for concrete with Degerhamn anl or Slite std concrete as the binder. There is no rapid acceleration, as for concrete with silica fume, and,

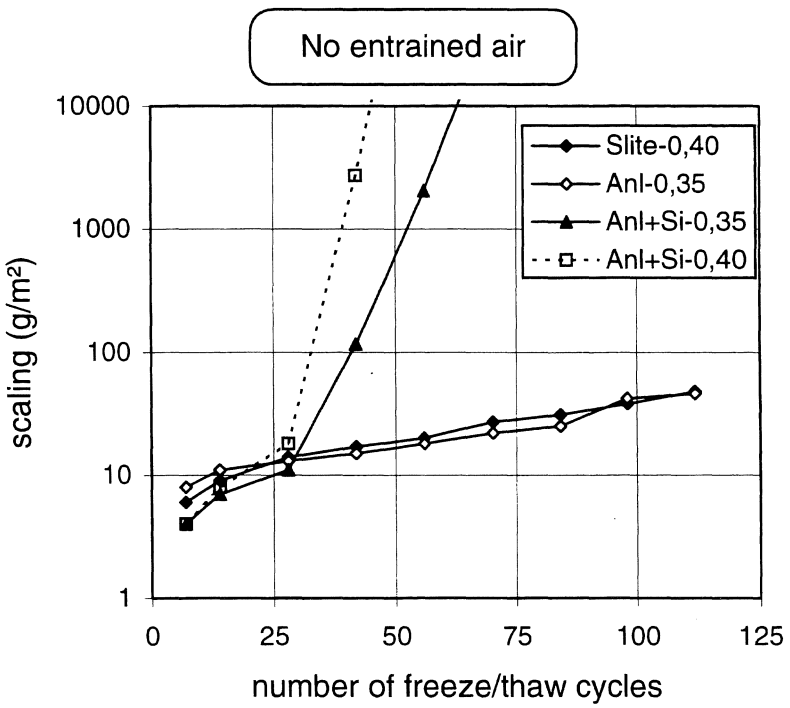

FIGURE 5 *Scaling for concrete qualities with and without addition of silica fume as function of the number (up to 112) of freeze/thaw cycles.*

to judge by these results, the scaling resistance of concrete with OPC as the only binder seems to be stable.

Some experiments were performed with aged specimens to study the influence of the surface layer on ageing effects. For this purpose, a five mm thick layer was sawn from the exposed surface. The specimens were then treated in a normal way, i.e. they were conditioned at +20°C and RH=65% for seven days and then re-saturated for three days before the start of the freeze/thaw testing. The results are given in Table 4. Two specimens were included in each test series. The results for the specimens whose outer layer had been sawn away (Table 4) are compared with the results for the normally aged specimens (Table 3) in Figures 6 and 7.

It can be seen in Figure 6 that there is good agreement between the results for concrete with entrained air, at least in the case of low scaling. In the case of scaling of about 1 kg/m², there is a tendency for the exposed outer layers to have somewhat poorer scaling resistance than the newly-sawn freeze surfaces sawn.

However, Figure 7 shows that the scaling resistance for concrete without entrained air is poorer for the newly-sawn surfaces, at least in the case of low scaling. This implies that after ageing concrete without entrained air is protected by a thin layer that gives significantly improved scaling resistance in the marine environment in question in many cases.

TABLE 4 *Freeze/thaw test results (mean values) for specimens aged for four years on the decks of the pontoons after which a five mm thick layer was sawn from the exposed surfaces of the specimens before the start of the test. Italicised figures are uncertain owing, for example, to leakage of salt solution during the test.*

Quality no.	**Cement**	**Silica fume**	**Fly ash**	**Water/ binder**	**Air**	**Scaling (g/m²)**					**Rating[1)]**
		%	%		%	*7c*	*14c*	*28c*	*42c*	*56c*	
1-40	Anl			0.40	6.2	11	14	20	23	26	VG
1-75	Anl			0.75	6.1	100	261				?
2-40	Slite			0.40	6.2	11	13	19	26	31	VG
2-75	Slite			0.75	5.8	203	600				?
3-40	Anl	5		0.40	6.1	11	15	23	27	28	VG
3-75	Anl	5		0.75	5.9	121	225	435	670	1040	NA
4-40	Anl	10		0.40	6.6	15	21	28	36	40	VG
6-40	Anl	5		0.40	1.7	58	460	2255	6260	SF[2]	NA
7-40	Anl			0.40	2.1	37	525	2595	4660	8090	NA
7-75	Anl			0.75	1.1	705	3860	SF			NA
8-40	Slite			0.40	2.1	29	60	217	520	990	NA[3]
8-75	Slite			0.75	1.4	2125	4880				NA

1) Rating of scaling resistance according to SS 13 72 44;
VG=very good, G=good, A=acceptabel, NA= not acceptable
2) SF means that the specimen is totally disintegrated
3) Accelerated scaling (normally not acceptable according to SS 13 72 44)

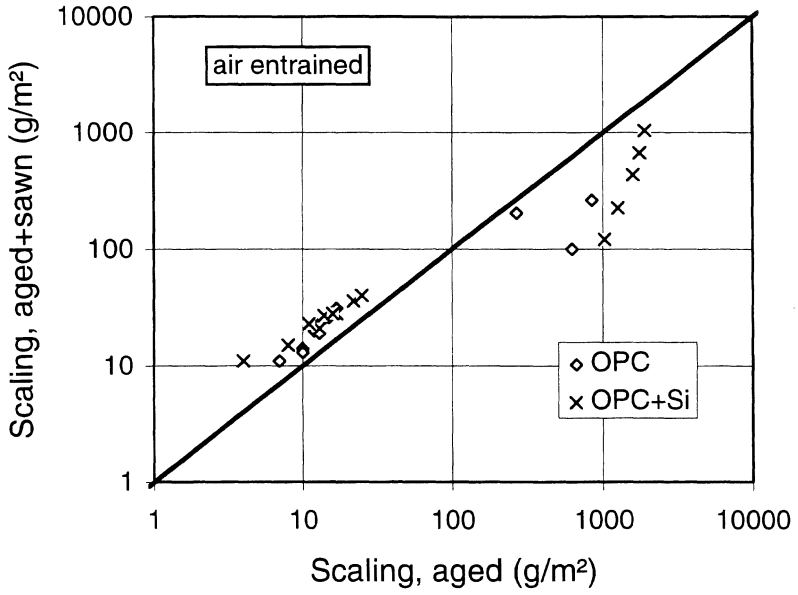

FIGURE 6 *The relation between the scaling resistance for aged specimens and aged specimens where a 5 mm thick layer is sawn from the test surface before testing. The results are relevant for air-entrained concrete.*

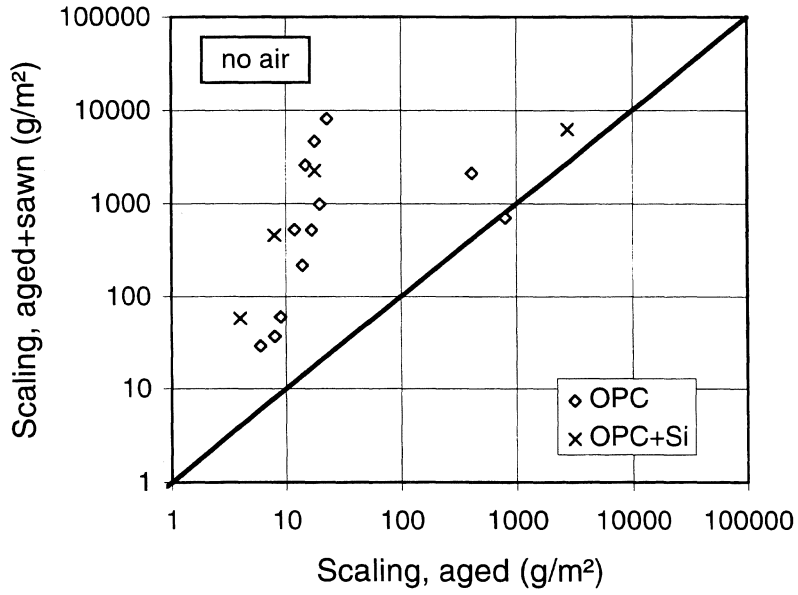

FIGURE 7 *The relation between the scaling resistance for aged specimens and aged specimens where a 5 mm thick layer is sawn from the test surface before testing. No air entraining agent is used.*

Table 5 shows the water absorption during three days of re-saturating directly prior to the freeze/thaw testing for aged specimens and for aged specimens whose surfaces were sawn off. According to the test results, the water absorption is 2 - 3 times lower for the aged surfaces than for the corresponding surfaces whose outer layer were sawn off. Concrete with entrained air seems to tolerate an increased absorption, while concrete without entrained air does not. This explains why the scaling resistance is normally poorer for concrete without entrained air when the outer surface layer has been sawn off. It is not possible, however, on the basis of the results of this investigation, to explain why the surface is so much less water-permeable after ageing.

TABLE 5 *Water suction during the resaturation period directly before the freeze/thaw test. The results are relevant for aged specimens and also for aged specimens where a 5 mm thick layer is sawn off the test surface before the test.*

Quality No.	**Cement**	**Silica fume**	**Fly ash**	**Water/ binder**	**Air**	**Water suction (g/m²)**	
		%	%			*aged*	*aged+sawn*
1-40	Anl			0.40	6.2	132	327
1-75	Anl			0.75	6.1	633	1978
2-40	Slite			0.40	6.2	104	227
2-75	Slite			0.75	5.8	831	1635
3-40	Anl	5		0.40	6.1	97	260
3-75	Anl	5		0.75	5.9	711	1404
4-40	Anl	10		0.40	6.6	127	292
6-40	Anl	5		0.40	1.7	64	140
7-40	Anl			0.40	2.1	142	248
7-75	Anl			0.75	1.1	591	2044
8-40	Slite			0.40	2.1	92	135
8-75	Slite			0.75	1.4	585	1400

2.6.2 Concrete panels aged on the sides of the pontoons

Between December 1991 and March 1992, concrete panels with dimensions of 100x800x1000 mm were placed on the sides of the pontoons so that half the panel was under and half the panel over the water line.

After about two years of exposure, the panels were brought to the laboratory of the Swedish National Testing and Research Institute in Borås for analysis. It should be noted that no frost damage had been observed up to this point in time on the panels in the field, except for concrete with a water/binder ratio of 0.75. On these, a small amount of damage was observed on the horizontal upper surfaces.

A 5 cm wide strip was sawn from one of the sides of the panels to eliminate any possible edge effects. A 100-mm wide strip was then sawn to be used for the tests. The strip was split so that 100-mm cubes were obtained. Some of these cubes were used for freeze/thaw testing.

The cubes used for freeze/thaw testing were divided in the middle, using a diamond saw, so that two specimens with the approximate dimensions of 50x100x100 mm were obtained. For one of the specimens, the cast surface was used as the test surface. This was the surface that was cast against the mould and which had been directly exposed to the sea water. For the other specimen, the sawn surface was used for testing. This was thus concrete from the inner portion of the panel, about 50 mm from the surface that had been exposed to sea water.

Specimens for freeze/thaw testing were taken either from the upper part of the panel, least 150 mm over the water line, or from the part of the panel that had been in the splash zone, i.e. ±150 mm from the water line. Table 6 shows the designations of the specimens with respect to the part of the panel from which they had been taken.

TABLE 6 *Designation of specimens according to their location on the panel.*

	Over the waterline	In the **Sp**lash zone
Cast surface	Ov/Ca	Sp/Ca
Sawn surface	Ov/Sa	Sp/Sa

After sawing, the specimens were treated in the same way as specimens for normal time testing, see section 2.3.2. This means that the specimens were dried for seven days and then resaturated for three days before the start of freeze/thaw testing.

The results are shown in Table 7. Two specimens were normally tested for each combination of concrete quality and location of the specimen, although in some cases only one specimen was tested.

The results for the sawn specimens can not, of course, be expected to be directly comparable with the results for the normal time tests on cast cubes. Production and storage until the 28th day were different. Moreover, sawn surfaces were tested in some cases and cast surfaces in others, etc. It is, however, of interest to examine how well the predictions according to the normal time tests can be used for classifying the aged concrete in the panels.

Scaling for the aged specimens was, without exception, low for the four "normal" qualities of concrete (1-50, 2-40, 3-40, 3-50), which agrees well with the normal time tests. Scaling is higher, however, for the wettest specimen surfaces, i.e. cast surfaces that were exposed to the splash zone (Sp/Ca). The effect is especially pronounced for mixtures with additions of silica fume, and for one of these, 3-50, scaling in the splash zone exceeds the limit for acceptable scaling resistance. The reason for the higher scaling in the splash zone is probably a higher moisture con-

TABLE 7 Test results after 56 freeze/thaw cycles for specimens sawn from panels aged on the sides of the pontoons. The designations of the specimens are given in Table 6.

Quality No.	Cement	Silica fume	Fly ash	Water/ binder	Air	Scaling, 56 cycles (g/m²)				Normal time results[1)]
		%	%		%	Ov/Ca	Ov/Sa	Sp/Ca	Sp/Sa	(g/m²)
1-50	Anl			0.50	6.4	80	60	540	55	131
2-40	Slite			0.40	6.2	65	45	110	50	109
3-40	Anl	5		0.40	6.1	55	60	860	60	21
3-50	Anl	5		0.50	6.0	80	60	1420	75	43
H1	Anl	5		0.30	0.8	9260	19360	170	14650	545
H2	Anl	10		0.30	1.1	12300	5250	210	15900	1958
H3	Anl			0.30	3.6	265	75	130	60	60
H4	Anl	5		0.40	5.9	95	65	155	55	59
H5	Anl	5		0.25	1.3	1660	5500	210	790	151
H8	Anl		20	0.30	3.0	285	220	940	240	152

1) Normal time results, 56 cycles, according to Table 2.

tent owing to long-term capillary suction without the possibility of intermediate drying periods.

For the high performance qualities of concrete, scaling for cast surfaces in the splash zone is low or moderate. However, scaling for sawn surfaces and cast surfaces above the splash zone is high or even very high for some of the concrete qualities. This applies to H1, H2 and H5, all without entrained air and with silica fume. These surfaces seems to have suffered some form of negative ageing. This may have to do with the fact that all surfaces except for the cast surfaces in the splash zone were continuously or periodically exposed to drying, either as exposure to the air or as internal self-drying.

Scaling is low for H3, a concrete without silica fume addition and H4, a concrete with entrained air and silica fume addition. It should be noted, however, that the concrete without silica fume has a high natural air content, 3.6%, which must certainly contribute to the low scaling. H8, which contains fly-ash, also shows relatively low scaling.

The normal time test according to SS 13 72 44 seems to classify the four "normal" concrete qualities satisfactorily, with some doubt in the case where silica fume was added. Moreover, the first four high performance concrete qualities in Table 7 were classified correctly, while the scaling resistance was overestimated for the fifth quality, H5. This is an extreme quality of concrete with a very low water/binder ratio of 0.25. The scaling resistance of H8, containing fly-ash, was somewhat underestimated, although the field specimens from the splash zone are very close to the limit for unacceptable scaling resistance, when tested on the cast surface.

Figure 8 plots all the freeze/thaw results for the high performance qualities of concrete against the air content. As can be seen in the figure, there is a clear correlation between air content and scaling resistance. The results indicate that a relatively low natural content of air of about 2% can yield scaling resistance for low values of the water/binder ratio.

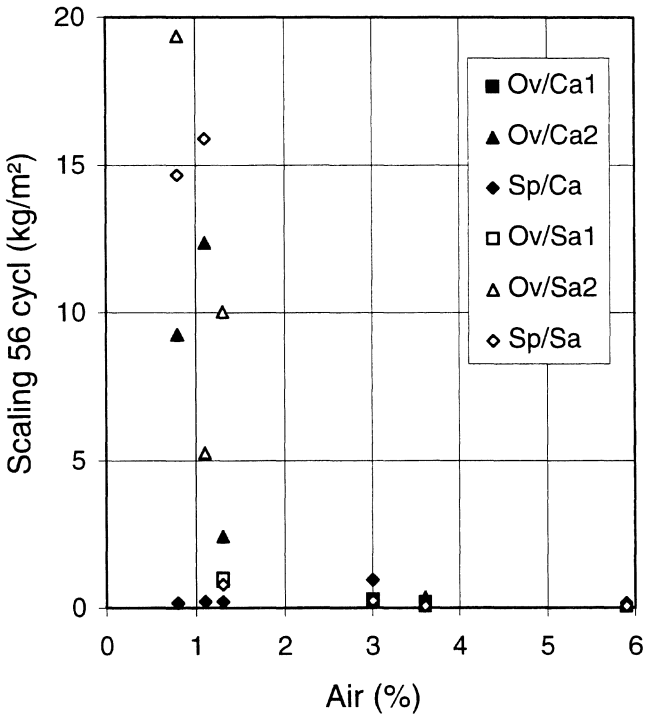

FIGURE 8 *Scaling resistance after 56 cycles as function of air content for the high performance concrete qualities studied. The designations are given in Table 6.*

3 Field exposure tests in an environment with de-icing salts

3.1 Field exposure site at national highway 40 (R40)

In a limited investigation, some qualities of concrete were exposed to an environment along a highway. The goal was primarily to calibrate the freeze/thaw test method SS 13 72 44 against results obtained under realistic exposure conditions.

The exposure site is located immediately outside the road area along national highway 40 (R40), west of Borås. Specimens with the dimensions of 50x150x150 mm were placed in rows in special rigs with ten specimens in each rig. The rigs were oriented in a direction alongside the road and were set into the roadbank so that the test surface was on a level with the surface of the road. As the entire width

of the road is used for traffic along the test area, vehicles passed very close to the specimens, sometimes at a distance of only a few decimetres. The traffic intensity is high and there is intensive use in winter of de-icing agents. This environment can be therefore be considered to be very aggressive for concrete.

The Swedish Road Administration has a weather station located about 300 meters from the test area, which can be reached by telephone. Information is updated every 30 minutes. It was not possible to make continuous registrations, but the weather station was called three or four times each day and their observations were registered.

For the test period, autumn 1990 to spring 1993, observations were made according to Table 8. No temperature registrations were made during the 1993-1994 winter season. As the observations are relatively few, it is likely that the values in the table are somewhat underestimated. The number of "zero point passages" is relevant for the ground close to the road surface, and the lowest air temperatures were probably somewhat lower. The winters in question are considered relatively mild.

TABLE 8 *Climate observations at the exposure site close to R40 during the period from autumn -90 to spring -91.*

Period	Number of passages through 0°C	Lowest temperature (°C)
Nov 90-March 91	46	-10.1
Nov 91-March 92	68	-11.8
Nov 92-March 93	58	-13.3

3.2 Concrete qualities

A total of 15 concrete qualities were included in the investigation, as described in Table 9. The mixtures range from concrete with expected very poor scaling resistance (water/binder ratio=0.90, no entrained air) to very good scaling resistance (water/binder ratio=0.37, 6% entrained air).

Swedish ordinary Portland cement Degerhamn anl was used for all mixtures. As mentioned in section 2.2, this is a low alkaline, sulphate-resistant concrete with low heat development.

The air-entraining agent used is a neutralised Vinsol resin (C88L). In addition to the air-entraining agent, a water-reducing agent, a melamine (V33), was also used for mixtures with the water/binder ratio 0.37. The aggregate used was a natural material, primarily gneiss. The largest particle size was 16 mm.

TABLE 9 Concrete qualities used for the field exposure tests at the R40.

Quality No.	Cement content	W/C	Admixtures	Air	Slump	Compr. strength
	kg/m³			*%*	*mm*	*MPa*
A-37	464	0.37	PL	2.1	80	77.2
A-45	426	0.45	-	1.9	80	65.2
A-60	302	0.63	-	1.7	80	39.8
A-75	278	0.74	-	1.2	85	29.3
A-90	219	0.93	-	1.1	80	16.2
B-37	458	0.37	PL+AE	3.8	80	74.9
B-45	398	0.45	AE	4.2	80	56.4
B-60	310	0.59	AE	4.0	80	36.0
B-75	255	0.72	AE	4.0	85	24.5
B-90	209	0.87	AE	4.0	80	16.4
C-37	449	0.37	PL+AE	5.9	80	70.7
C-45	404	0.44	AE	6.3	80	46.2
C-60	300	0.59	AE	6.3	80	32.3
C-75	240	0.74	AE	6.0	80	20.8
C-90	198	0.90	AE	6.1	80	13.0

1) AE=air entraining agent (C88L), PL=plasticizer (V33)

3.3 Manufacturing and curing of specimens

All mixtures were made in a 350-litre paddle mixer. When an air-entraining agent was used, it was added with the mixing water. When a water reducing agent was used, it was added after the air-entraining agent, with the last mixing water. All batches were mixed for 180 seconds.

Specimens with the dimensions of 50x150x150 mm were manufactured according to the procedure described in section 2.3.2, specimens for normal time tests. Four specimens per concrete quality were used for the normal time test, while two specimens per quality were placed in the test area for field exposure about 28 days after casting.

3.4 Freeze/thaw testing

Normal time testing was carried out according to the methodology described in section 2.4, freeze/thaw testing.

3.5 Results of normal time testing

The results of the normal time tests are reported in Table 10. The results generally agree with expected values and with the results presented in Table 2 in section 2.5 for normal time testing of concrete for Träslövsläge. The results for C-75 may be uncertain, owing to leakage during testing. This quality of concrete was, therefore, not considered in the continued analysis.

TABLE 10 Scaling resistance results (mean values) for normal time tests of concrete used at the field exposure site at R40.

Quality No.	W/C	Air	Scaling (g/m²)					Rating[1]
		%	*7c*	*14c*	*28c*	*42c*	*56c*	
A-37	0.37	2.1	1020	2450	5520	9310	11880	NA
A-45	0.45	1.9	1190	3320	7630	10630	12280	NA
A-60	0.63	1.7	1300	4050	10870	16740	19760	NA
A-75	0.74	1.2	2060	6490	15580	20160	SF[2]	NA
A-90	0.93	1.1	1610	4300	6890	10130	SF	NA
B-37	0.37	3.8	190	430	790	1080	1270	NA
B-45	0.45	4.2	50	70	90	100	110	G
B-60	0.59	4.0	200	440	790	1040	1130	NA
B-75	0.72	4.0	360	700	1210	1460	1600	NA
B-90	0.87	4.0	540	870	1200	1470	1580	NA
C-37	0.36	5.9	30	50	60	70	80	VG
C-45	0.44	6.3	20	30	40	50	60	VG
C-60	0.59	6.3	40	60	70	80	80	VG
C-75	0.74	6.0	250	360	*420*	*440*	*450*	(G)
C-90	0.90	6.1	470	720	940	1040	1130	NA

1) Rating of scaling resistance according to SS 13 72 44;
VG=very good, G=good, A=acceptabel, NA= not acceptable
2) SF means that the specimen is totally disintegrated
3) Accelerated scaling (normally not acceptable according to SS 13 72 44

It is remarkable that scaling is so high for concrete with a water/binder ratio of 0.37 and 4% added air. Its scaling resistance is judged as even worse than that of concrete with the same air content and with a water/binder ratio of 0.45. One probable explanation is that the combination of air-entrainment agent and water-reducing agent, used only for the water/binder ratio 0.37, is unsuitable and gives an unsatisfactory air pore structure. A corresponding effect was reported in /5/.

3.6 Field exposure results

Two specimens of each quality were placed at the field exposure site in October 1990. The aim was to study the development of damage visually. The specimens were taken to the laboratory for examination after one year. A measurement was then made of the volume of each specimen by weighing it in air and in water. The specimens were then again placed at the test area. The same procedure was repeated after two and three years of exposure. Unfortunately, the experiment then had to be stopped, as the road was to be re-built and it was impossible to continue our work.

The volume change after different exposure times proved to be an excellent measure of concrete scaling. Unfortunately, no determination of volume was made before the specimens were first placed at the test site and thus there are no values for the first winter's exposure. The results are shown in Table 11.

TABLE 11 Volume change of the specimens after exposure during three winters at R40. Each value is the mean result from two specimens.

Quality No.	W/C	Air	Volume change (%)			
		%	9110-9209	9209-9311	9311-9407	**1991-1994**
A-37	0.37	2.1	0	0	0.1	**0.1**
A-45	00.45	1.9	0.1	0.9	0.4	**1.4**
A-60	0.63	1.7	0.1	7.8	33.5	**41.4**
A-75	0.74	1.2	0.4.1	95.9	-	**100**
A-90	0.93	1.1	14.2	85.8	-	**100**
B-37	0.37	3.8	0	0	0.1	**0.1**
B-45	0.45	4.2	0	0	0.1	**0.1**
B-60	0.59	4.0	0.1	0.1	0.2	**0.4**
B-75	0.72	4.0	0.2	2.0	0.6	**2.8**
B-90	0.87	4.0	0.4	4.4	1.5	**6.3**
C-37	0.36	5.9	0	0	0.1	**0**
C-45	0.44	6.3	0.1	0	0.1	**0.2**
C-60	0.59	6.3	0	0.3	0.2	**0.5**
C-75	0.74	6.0	0.2	1.6	0.6	**2.4**
C-90	0.90	6.1	0.5	6.1	1.9	**8.5**

It can be seen in the table that the reductions in volume vary from very small, 0.1% after three years of exposure, to total disintegration of the specimens of the poorest qualities. As expected, frost damage was most severe for concrete without entrained air. When air was entrained, 4% and 6% air appears to give the same results.

In Träslövsläge on the Swedish west coast, no damage at all was observed after three years of exposure, with the exception of the poorest qualities. This shows that the road environment is much more aggressive than the marine environment on the Swedish west coast, at least with respect to freeze/thaw and scaling.

Figure 9 shows the volume reduction after exposure over three winters as a function of water/binder ratio and air content. The darker the colour, the stronger the scaling. Concrete with the water/binder ratio over 0.6 and without entrained air was completely disintegrated. Concrete with entrained air with a water/binder ratio of 0.9 also showed severe damage. Very good scaling resistance was achieved for concrete with entrained air when the water/binder ratio was 0.45 or lower, which is in good agreement with present norms. It is also possible to achieve scaling-resistant concrete without air, according to the results in Figure 9, provided there is a low water/binder ratio, in this case 0.37. This is in good agreement with the results from the field tests in Träslövsläge.

Figure 10 shows the relationship between the results from the field exposure tests at R40 and the normal time tests according to SS 13 72 44. Two lines are marked in the figure. The vertical line at 1 kg/m^2 after 56 cycles corresponds to the limit

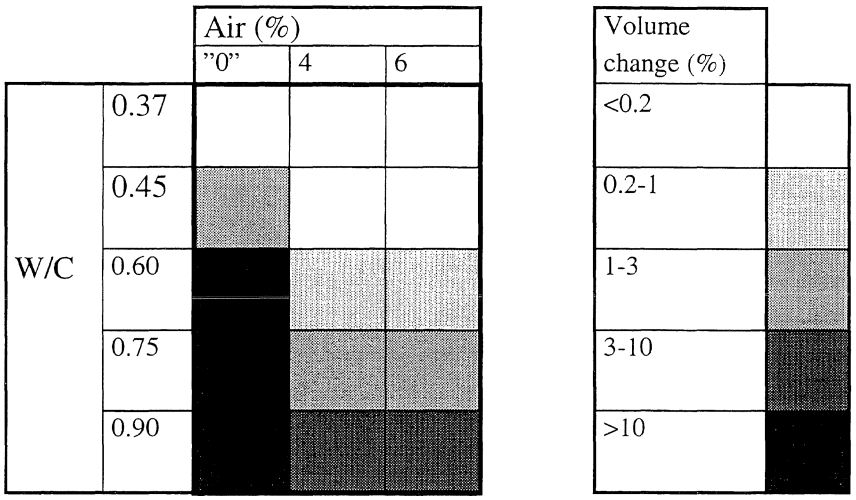

FIGURE 9 *Relation between air content, water/binder ratio and volume change for specimens exposed at the field exposure site at R40 for three winters.*

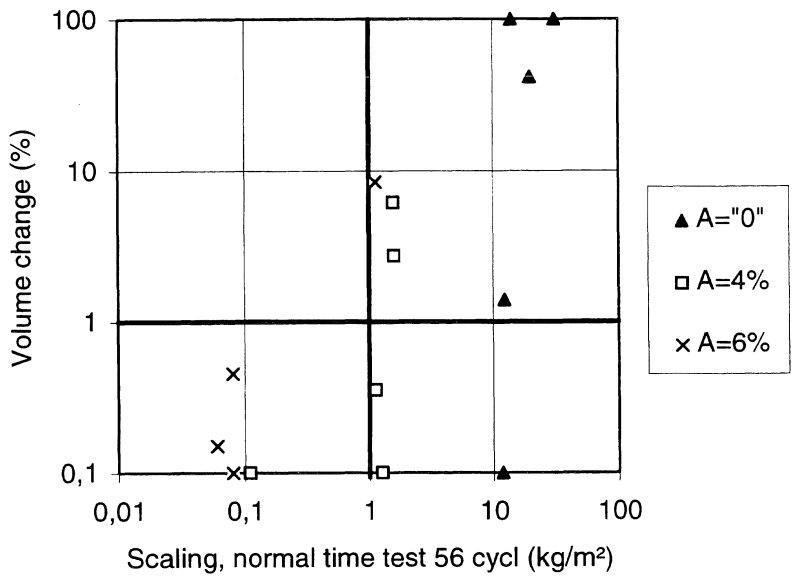

FIGURE 10 *Volume change after three winters at the exposure site at R40 as function of results from normal time tests according to SS 13 72 44.*

for acceptable scaling resistance according to SS 13 72 44. The vertical line at a volume reduction of 1% corresponds to an example of a possible acceptance limit after three years of field exposure.

The figure shows that the four concrete qualities that fulfilled the requirement of 1 kg/m^2 in the normal time test also all fulfilled the requirement of 1% volume change in the field exposure test. Moreover, there were two qualities, air content=4% with water/binder ratios of 0.37 and 0.6, that fulfilled the field exposure requirement and which were at the limit of the acceptable area for the normal time test. Of the other eight qualities that failed to fulfill the requirement for acceptable scaling resistance in the normal time test, seven also failed in the field exposure. The exception is the concrete without added air with a water/binder ratio of 0.37.

Test method SS 13 72 44 thus generally classified the qualities of concrete correctly in 13 of 14 cases. For concrete qualities that are normally used in environments aggressive towards concrete in Sweden, for which the method was primarily developed, i.e. concrete with entrained air and low water/binder ratio, the method classified all eight concrete qualities correctly. The results thus indicate that the method and the acceptance limits are suitable for testing concrete in an aggressive road environment, at least for high quality concrete with entrained air.

The results deviated for concrete without entrained air and with low water/binder ratio (0.37). The normal time test gave a great deal of scaling after 56 cycles, over 11 kg/m^2, while no damage at all occurred during the field exposure period! This observation agrees well with the results of the field exposure in the marine environment in Träslövsläge. Ageing had a positive effect, especially on concrete without entrained air, and when the water/binder ratio is less than 0.40 there were indications that concrete without entrained air also had considerable ability to tolerate freezing in environments aggressive towards concrete.

Concrete with low water/binder ratios (0.30-0.40) and no entrained air is not scaling-resistant in normal time tests, i.e. at an age of about one month. At that time, there is a high amount of freezable water in the capillary pores and without a functioning air pore system, the concrete disintegrates because of freezing. As the concrete ages, hydratation continues, and the volume of the capillary pores, and thus also the amount of freezable water, decreases. If the water/binder ratio is sufficiently low, the capillary pore volume becomes so small and the amount of water that can freeze so little that the concrete is protected from scaling even by a poor air-entrainment system, e.g. by the natural air that always exists in concrete. This is probably the explanation for the differences between the normal time tests and the field exposure tests for the quality of concrete without entrained air and with a water/binder ratio of 0.37. The effect may also be strengthened by other positive ageing effects.

There is also a significant difference between the normal time test and the results of the field exposure tests for the concrete with a water/binder ratio of 0.37 and an air content of 4%. The result in the normal time test is also considerably poorer than the corresponding result for the concrete with the same air content but with a water/binder ratio of 0.45. This is probably explained by the fact that the concrete

mixtures with a water/binder ratio of 0.37 always had an added water-reducing agent, which no other mixtures had. Investigations have shown that the combination of water reducing agents and air-entraining agents often leads to poor air-pore systems /5/. For the concrete with a water/binder ratio of 0.37 and 4% entrained air, there is obviously no protective air-pore system at the normal time test, although such a system is found in the concrete with a water/binder ratio of 0.45. This explains the differences in the normal time tests. With continued hydratation and ageing, the significance of a good air-pore system decreases at low water/binder ratios. For this reason, there are no demonstrable differences between water/binder ratio of 0.37 and water/binder ratio of 0.45 in the field exposure tests.

SS 13 72 44 thus normally underestimates the scaling resistance of concrete without entrained air and low water/binder ratios. In order to be able to fully exploit the potential of such qualities of concrete, the test methodology should be modified. It would probably be advantageous to carry out tests when the specimens are 56 days old or older, or perhaps more preferably, on test specimens that have been allowed to age outdoors for a number of months. The disadvantage is that the required testing time is extended, but it is difficult to see how this can be avoided. Concrete with low water/binder ratios is simply not "mature", from the viewpoint of scaling resistance, at an age of 28 days.

Large differences were seen in the normal time tests between concrete with 4% and 6% entrained air, except when the water/binder ratio was 0.37, and also when the water/binder ratio was 0.6 or higher. No corresponding difference was found in the field exposure tests. This supports the observations at Träslövsläge that indicate that the positive effects of ageing become clearer the poorer the quality of the air pore structure.

4 Conclusions

This paper gives the results of field experiments in which 34 qualities of concrete were exposed to a marine environment on the west coast of Sweden and in which 15 qualities of concrete were exposed to a de-iced road environment along Swedish national highway 40 between Borås and Gothenburg. The conclusions from the investigation can be summarised in the following points:

- Normal time testing according to SS 13 72 44, procedure IA, classified the scaling resistance of the concrete correctly, i.e. in an expected way according to present experience.
- Concrete is often either good or very poor from the viewpoint of scaling resistance and is seldom classified in the classes between good or very poor. A functioning test method must thus primarily be able to distinguish between very good and very poor qualities. The experiments performed here show that SS 13 72 44 does so.
- No visible frost damage could be observed on any of the specimens after three years of exposure in a marine environment, except for specimens with a water/binder ratio of 0.75. These specimens showed surfaces that were weakly etched and edges with frost damage.

- For concrete qualities with entrained air, scaling is often up to ten times less in specimens aged in a marine environment than in specimens that were not aged at all. This difference decreases with increased scaling and, at values of about 1 kg/m^2 after 56 cycles, which is the limit for acceptable scaling resistance according to SS 13 72 44, there no longer seems to be any difference. The present acceptance limit thus seems adequate for concrete with entrained air in the marine environment in Sweden. For concrete with lower scaling, the method gives results that can be said to be on the safe side, i.e. the scaling in the normal time test is higher than the corresponding values for aged specimens.
- The results indicate that SS 13 72 44 underestimates the scaling resistance of concrete without entrained air that has been exposed to a marine environment. However, there is justification for a high safety margin for concrete without entrained air until the destruction mechanisms and ageing effects in the case of salt and frost damage are completely understood.
- For aged specimens without entrained air and with Portland cement as binder, scaling is very limited after 56 freeze/thaw cycles, when the water/binder ratio is 0.4 or lower. This indicates that it may be possible to produce concrete with good scaling resistance in the marine environment without the use of air-entrainment agents, providing that the water/binder ratio is sufficiently low.
- The results from the exposure of concrete to a highway environment indicate that SS 13 72 44 and its acceptance limits are adequate for classifying concrete for use in road environments aggressive towards concrete, at least for high quality concrete with entrained air.
- Ageing has a positive effect, especially on concrete without entrained air. When the water/binder ratio is less than 0.40, concrete without entrained air also seems to have a considerable ability to withstand freezing in an aggressive road environment.
- Many of the specimens exposed to the highway environment showed a great deal of damage after four seasons. This demonstrates that the environment of a highway is significantly more aggressive than the marine environment of the west coast of Sweden, at least with respect to frost damage.
- Concrete manufactured according to present practices, i.e. with a water/binder ratio less than 0.45 and entrainement of 4-6% air, normally has good scaling resistance both in a marine environment and a road environment with de-icing agents.

5 References

1. *Petersson, P-E.* Scaling Resistance of Concrete - Field Exposure Tests. SP-Rapport 1995:73, Swedish National Testing and Research Institute, 1995.
2. *SS 13 72 44.* Concrete testing - Hardened concrete - Frost resistance. Swedish standard, second ed., 1988.
3. *Petersson, P-E.* The influence of silica fume on the salt frost resistance of concrete. SP-RAPP 1986:32, Swedish National Testing and Research Institute, 1986.
4. *Lagerblad, B and Utkin, P.* Silica granulates in concrete - dispersion and durability aspects. CBI-report 3:93, Swedish Cement and Concrete Research Institute, Stockholm, 1993.

5. *Petersson, P-E.* The use of air-entraining and plasticizing admixtures for producing concrete with good salt-frost resistance. SP-Report 1989:37. Swedish National Testing Institute, Borås, 1989.

THE INFLUENCE OF AIR-ENTRAINING AND OTHER MICRO-STRUCTURE PROPERTIES ON THE RESISTANCE OF CONCRETE - A case study

Hannu Pyy, Msc, Senior Researc Scientist
VTT Building Technology
P.O.Box 1805, FIN-02044 VTT, Finland

1. Introduction

Since the early 1980s VTT Building Technology has used microscopic techniques to study the microstructure and composition of concrete and other mineral building materials, mainly mortars and claybricks. The study of petrographic thin sections gives a possibility to look inside the structure of a hardened concrete. This possibility to in situ research has become more and more important when investigating damaged or deteriorated concrete. The most valuable tool it is in the diagnostics of concrete structures and in predicting their service life.

For some 8 - 12 years ago microscopy was not extensively used in the building diagnostics. As a matter of fact systematic diagnostics were not done. We studied separate "cases of damage", as they were called. During those years a lot of experience was gathered. During the last 5 - 8 years the amount of building diagnostics has increased in great numbers. Visible damages are no more needed to start the study. The need to know the state of the facades and the estimated repaire works needed are the shot for these diagnoses. The microscopical studies of thin sections as a central part of these diagnostics have given a view to undrestand the relations between the microstructure and the resistance of concrete.

2. The Pori Project

In 1995 one of the most extencive diagnostics poroject was run in the town of Pori on the western coast of Finland. The work was done in co-operation between VTT Building Technology and Pori University. The site investigations and sample drillings were done by the University and the thin section studies by VTT. The resarch reports were compiled together.

The great advantage of the project was that totaly 34 sites were studied. They situated in 3 suburbs of the town (Fig. 1). During the project more than 200 thin sections were prepared and studied.

All houses were builed between 1966 and 1983. The facades were made of prefabricated sandwich elements. In 32 sites the external skin of the elements was made of exposed aggregate concrete and in one site of painted concrete and in one site of figured white concrete.

Fig. 1. A general view of a typical suburb Sampola. The topography in the area of Pori is very flat and the suburbs are mainly very open. Woods are rare. This makes it easy for the wind and rain to hit the buildings.

In this presentation I am going to concentrate to the microsturcture of the facades made of sandwich elements with the outer skin of exposed aggregate concrete.

3. The sandwich elements

The thickness of the outer skin of the sandwich elements varied between 50 and 70 mm and it was made of two concrete layers. The inner layer was made of a normal "grey concrete" and the outer one of an exposed aggregate concrete. The thickness of the outer layer varied mainly between 30 and 40 mm. The facades were called "dark" or "light" depending on the colour of the exposed aggregate concrete. In the "dark" elements the coarse aggregate was a medium grained red granite and in the "light" elements a coarse grained, white limestone.

In the exposed aggregate concretes the amount of fine aggregate was very low and in some concretes only the coarse aggregate was used. For this reason the paste content in these concretes is high. In exposed aggregate concretes the w/c-ratio was normaly relatively low.

The composition and structure of the "grey"concretes were quite "normal". Granitic aggregate was used and the binder was a portland cement with or without a mineral admixture depending on the year when the house was builed.

4. Air-entrained or not?

The air-entraining of the concretes depended on the year when the houses were builed, as is shown in Table 1.

Table 1. The air-entraining of the extended aggregate concrtes used in the outer skin of the sandwich elements.

The site number	Builed	Air-entrained	Not air-entrained
1	197371974	+	+
2	1979	+	
3	1978	+	
4	1977	+	
5	1978	+	
6	1975	+	+
7	1976	+	+
8	1974		+
9	1974		+
10	1973/1974		+
11	1977	+	
12	1976	+	
13	1970/1971		+
14	1966		+ A)
15	1971		+
16	1969		+
17	1973		+
18	1981	+	
19	1978	+	
20	1977	+	
21	1979	+	
22	1979	+	
23	1972		+
24	1973		+
51	1982	+	
52	1983	+	
53	1980	+	
54	1980		+ B)
55	1979	+	
56	1974		+
57	1973		+
58	1972		+
59	1971		+
60	1973		+

A) Figured white concrete.
B) Painted concrete.

A demand for the use of air-entrained concrete in the facades was presented in 1976 in the publication Durability of Concrete - Guidelines by The Finnish Concrete Assosiation /1/.

5. The microstructure of concretes

The microstructure of the concretes was studied by means of petrographic thin sections. The preparation techniques and the study methods are presented f.ex. in /2/, /3/and /4/.

The air content of the air-entrained concretes was in general high, varying from 5% up to 10%. In concretes where the air content was high a certain amount of agglomeration of air pores was found. This phenomenon is very common in concretes with high air content.

In some air-entrained concretes a part of the air pores were wholly or partly filled with ettringite or calsiumhydroxide. This filling of air pores can radically change the air pore structure of a concrete: the air content, specific curface and spacing factor are changed. The air content has been found to decrease even to half of the original in concretes where the crystallization of ettringite and/or calsiumhydroxide is high. This type of filling of air pores is very common in concretes which are allways or repeatedly wet.

The influence of air-entraining in the microstructure of concretes is illustrated by the microphotographs in Figures 2 - 6.

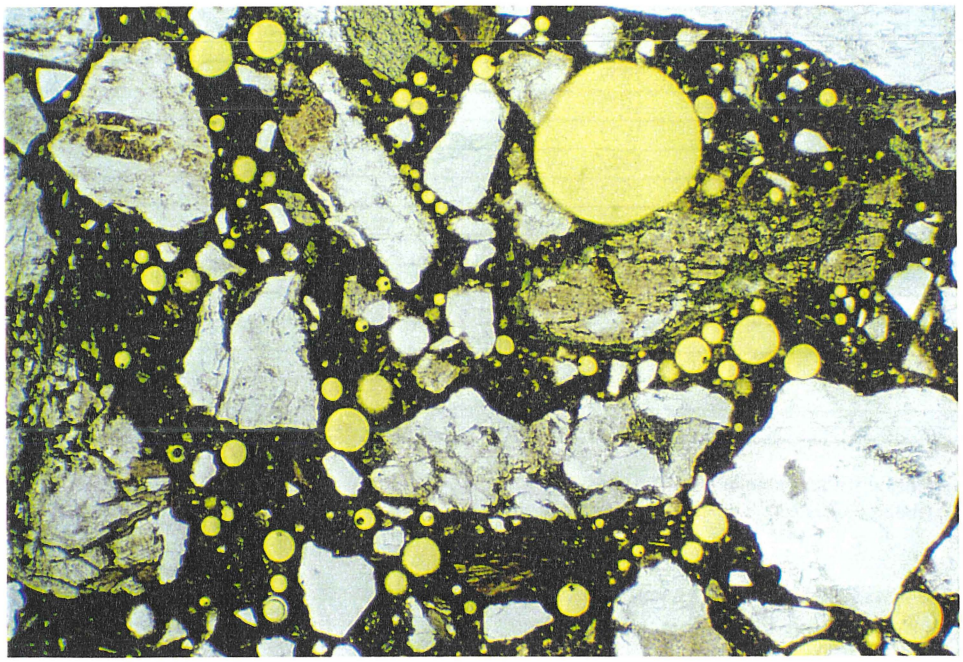

Fig.2. Site 11. A high air content with different size of air pores. The distribution of pores is a bit uneven. The hight of the micrograph is 2,8 mm.

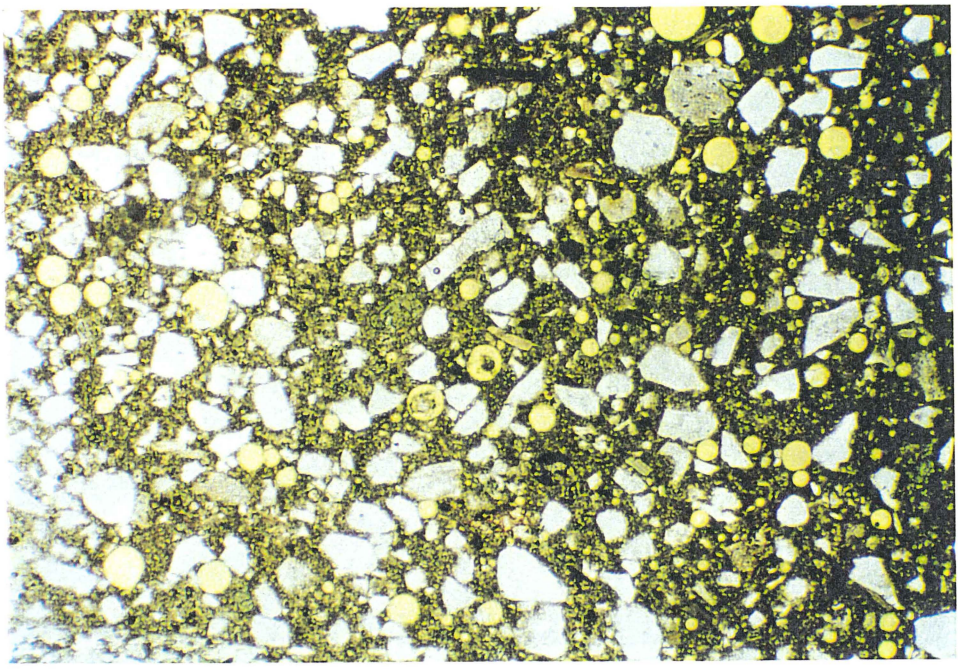

Fig.3. Site 12. A high air content with an even pore size and pore distribution. The hight of the micrograph is 2,8 mm.

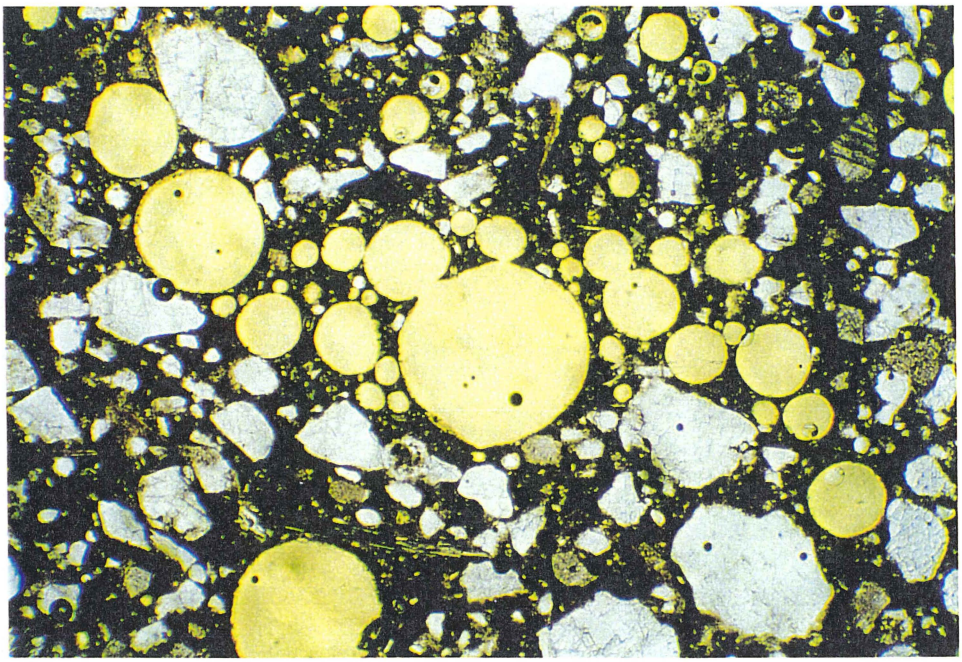

Fig. 4. Site 51. A very high air content often leads to agglomeration of air pores. This has a negative effect to the air pore structure and the strength of concrete. The hight of the micrograph is 2,8 mm.

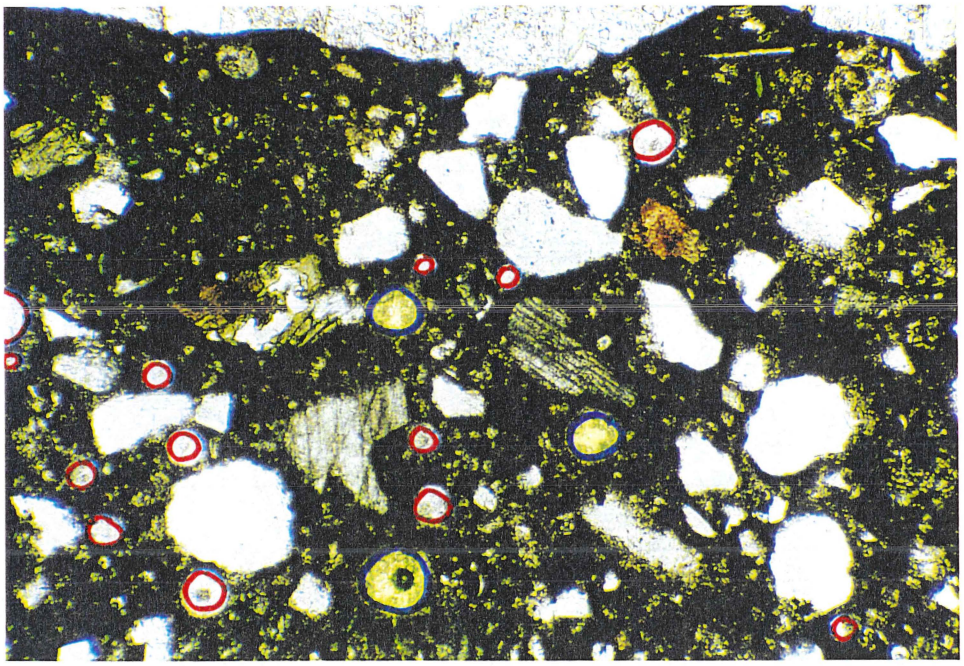

Fig. 5. Site 55. An air-entrained concrete where the original air content has been high but where most of the air pores in the field of micrograph are filled with ettringite. There has been 16 air pores in the area of the micrograp, of which only 3 are still open (marked with a blue circle). 13 pores have been filled with ettringite (marked with red circle). The hight of the micrograph is about 1 mm.

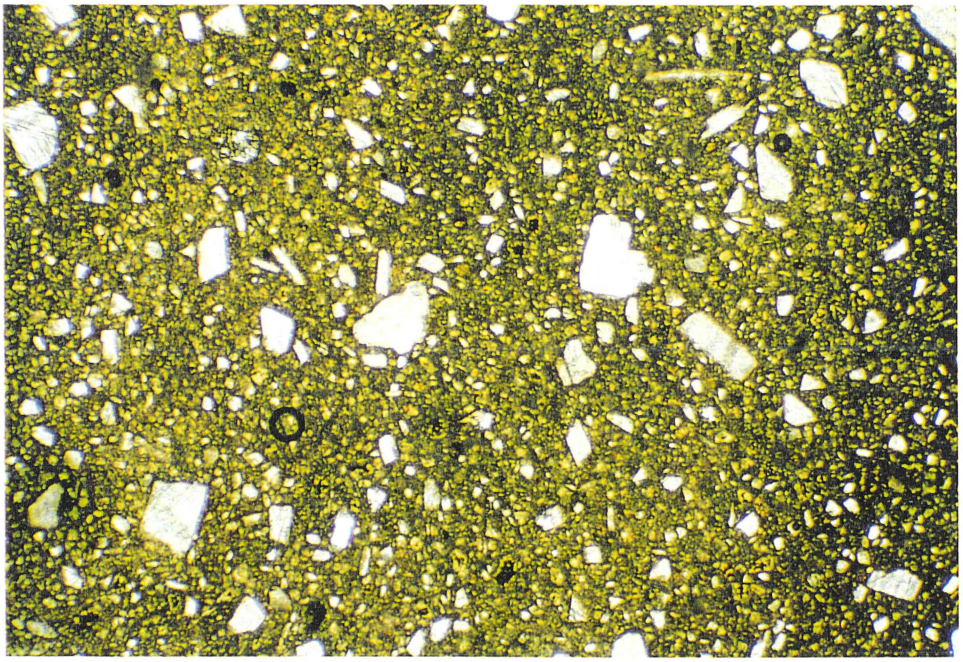

Fig. 6. Site 23. A concrete without air-entraining. No air pores can be seen. The hight of the micrograph is 2,8 mm.

6. Frost damages

Based on the data recived from the site investigations it was expected to find some damages in the concretes.

Because of the high paste content in the exposed aggregate concretes shrinkage cracks were found in a high number of these concretes.

In some buildings (f.ex. in site 6) the exposed aggregate concrete had shown visuable frost damages which had led to impregnation of certain facades. In the studies it was found that impregnation of highly cracked concrete very often does not lead to the wished result: filling of all cracks (Fig. 7).

Frost damages were found in a lot of buildings. The high number of sites in the Pori project gave a possibility to make a statistical study of the damages. The study was done separately to the air-entrained and the unair-entrained concretes. Also the direction of the facades was taken into consideration. The results are given in Tables 2 and 3.

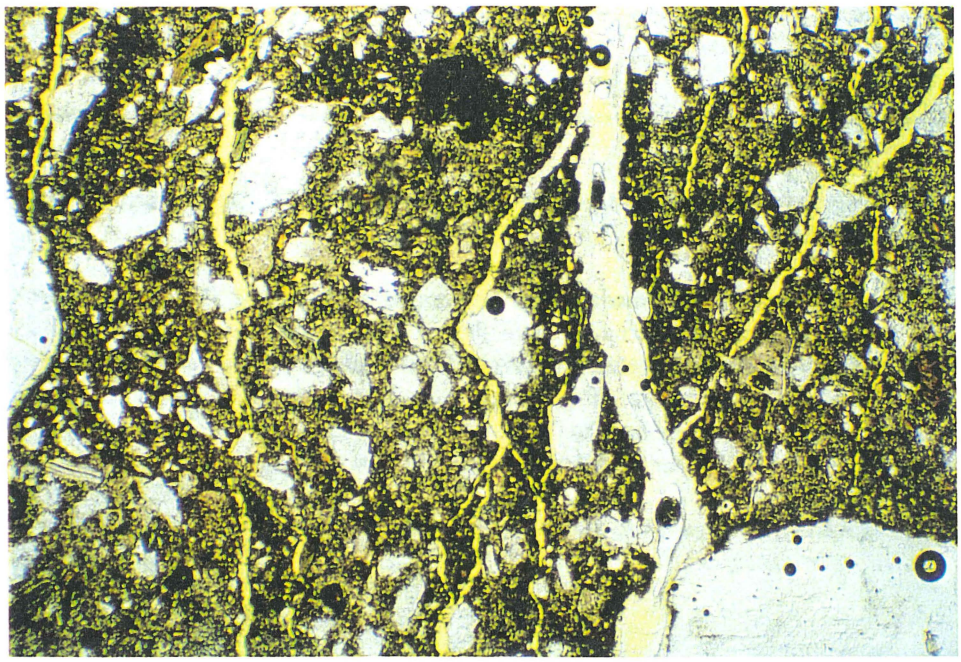

Fig. 7. Site 6. Frost damages in the concrte. The facade has been impregnated. The resin has filled the broadest crack and partly some minor cracks branch out of it. The hight of the micrograph is 2,8 mm.

*Table 2. The frost damages in the **air-entrained** exposed aggregate concrte facades.*

The direction of the facade	Number of facades studied	Number of facades with frost damages	**The amount of frost damages, %**
North	3	0	**0**
Northeast	4	0	**0**
East	4	0	**0**
Southeast	9	0	**0**
South	4	0	**0**
Southwest	9	0	**0**
West	1	0	**0**
Northwest	6	0	**0**
In total	*40*	*0*	***0***

Table 3. The frost damages in the **unair-entrained** *exposed aggregate concrete facades.*

The direction of the facade	Number of facades studied	Number of facades with frost damages	**The amount of frost damages, %**
North	4	2	**50**
Northeast	9	2	**22**
East	4	3	**75**
Southeast	10	7	**70**
South	6	5	**83**
Southwest	9	6	**67**
West	5	4	**80**
Northwest	6	1	**17**
In total	*53*	*30*	***57***

As the results show **no frost damages were found in the facades made of air-entarined concrete.**

The total number of facades made of unair-entrained concrete was 53. In 30 of these more or less serious frost damages were found. This means that **in 57 % of the facades made of unair-entrained concrete frost damages were found.** In many cases it was a question about damages that were just coming. The most "critical" directions were those from East to West via South. South showed to be the most critical direction with 83 % of facedes having some frost damages.

These results are analoguous to the results that have been recieved in a high number of individual studies.

7. Ettringite

In some of the air-entarined concretes ettringite was found in the air pores. The amount of these crystallizations was in general not so high. In some concretes, such as shown in Figure 5, the amount of ettringite crystals was so high that the crystallization

had significantly changed the air pore structure. Only in one of these cases the crystallization had yet caused damages.

8. The general condition of the sites

The general condition of the sites was evaluated. This was based on the results recived in the thin section studies presented in the previous chapters.

The following 4 graded scale was used:

good
satisfactory
fair
poor

The results of the evaluation are shown in Table 4.

Table 4. The general condition of the sites. Evaluated in a scale with 4 grades.

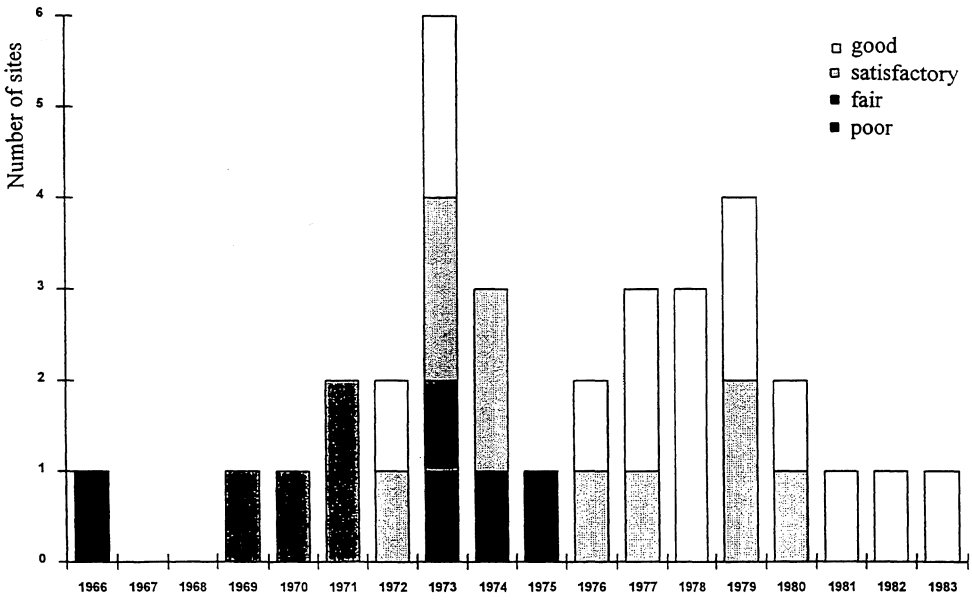

The table shows clearly that the houses builed before 1975 are mainly in a satisfactory or fair condition. Houses builed after 1975 are mainly in a good or condition. This is not only because they are younger. It is mainly because unair-entrained concrete has been used in the facades of the older ones and frost damages were found in them.

9. Other results and what now?

Carbonation was measured both in the thin section samples and the field samples. Based on the field measurements the corrosion rate of the reinforcement was calculated. The results of these studies were included in the project reports and will be published later this year.

Microscopical study of thin sections as a part of building diagnostics has been done for 15 years in VTT Building Technology. This means that a lot of material has been gathered, but no summary has been prepared and presented. The results of the Pori project showed that the time is now. There is a plan to put all the information from previous projects together to get more accurate data about the influence of different microstructural factors on the resistance of concrete. This work is planned to be done this year.

LITERATURE

1. Durability of concrete - Guidelines, BY9 (in Finnish), The Finnish Concrete Assosiation, Helsinki 1976.
2. Concrete, hardened: water-cement ratio. Nordtest method, NT Build 361.
3. ASTM C 856, Petrographic examination of hardened concrete.
4. Pyy Hannu and Raivi Paula, Optical microstructure analysis and the quality of concrete pp. 95-101, in Microstructure and properties of concrete, Edited by Heikki Kukko. VTT Symposium 115, Technical Researc centre of Finland, Espoo 1990.

FROST TESTING OF HIGH STRENGTH CONCRETE: INTERNAL CRACKING VS. SCALING OF OPC AND SILICA FUME CONCRETEs

S. Jacobsen[1)], T.A. Hammer[2)] and E.J. Sellevold[3)]

1) Norwegian Building Research Institute, Oslo, Norway 2) SINTEF - Structures and concrete, Trondheim, Norway 3) Norwegian Institute of Technology, Trondheim, Norway

ABSTRACT

Internal cracking, scaling and increased degree of saturation in concrete freeze/thaw tested in water or salt solution have been studied. Eleven different concretes with normal and light weight aggregates with compressive strengths = 41 - 141 MPa were tested. The investigated test methods were ASTM C666 procedure A (rapid freeze/thaw in water) and SS 13 72 44 (slow cycles with 3 % NaCl solution). Depending on concrete and test, all four combinations of cracking and scaling were observed: no scaling and no cracking, no scaling and cracking, scaling and no cracking, and both cracking and scaling. Both scaling and cracking were associated with increased absorption during freeze/thaw due to a "pumping" effect.

Key words: degree of saturation, deicing salts, frost durability, high strength concrete, internal cracking, laboratory testing, surface scaling

1. INTRODUCTION

When a concrete specimen is exposed to freezing and thawing with water or salt solution, two types of damage can be observed: surface scaling and internal cracking, Powers /1/. Surface scaling is largely amplified by deicer salts, Verbeck and Klieger /2/, and this is considered to be the main type of frost damage in Scandinavia (frost/salt attack). Internal cracking, on the other hand, can affect the whole specimen volume, causing loss of strength and modulus of elasticity without any significant surface damage. According to /1/ also combinations of these two forms of deterioration can occur. There are some main features that are quite similar between internal cracking and surface scaling when freeze/thaw testing OPC concrete. These are: the positive effect of concrete quality, i.e. low w/c-ratio, the positive effect of air entrainment, and the negative effect of freezing and thawing continuously in contact with water/salt solution, /2, 3/.

Both before and after the basic work /1, 2, 3/ a very large amount of research on frost durability of concrete has been performed by numerous researchers. In the last decade a large part of the research into frost action has been devoted to the question of whether high strength/high performance concrete (HSC) needs air entrainment to be protected against frost action, see for example the experimental studies by Perenchio and Klieger /4/, Foy, Pigeon and Banthia /5/, Hammer and Sellevold /6/, Gagné /7/, and the review by Marchand et al /8/. One main observation questioning the need for air entrainment in high performance concrete, is that non-air entrained HSCs with sufficiently low water/binder ratio have proven to perform excellently in salt/frost and internal cracking tests. In some tests it has also been observed that severe cracking can take place on concretes with very good frost/salt durability. Factors affecting the critical w/b-limit for need of air entrainment has been addressed in /4-8/.

The possibilities of bad resistance against internal cracking in rapid freeze/thaw tests, but good resistance against frost/salt scaling in scaling tests point to that different mechanisms are involved in the two types of deterioration. This implies that resistance to one type of

deterioration does not guarantee resistance to the other. Different mechanisms were investigated and postulated by Powers and co-workers in the early research /1, 2, 9, 10, 11/.

In scaling tests (often slab tests with the test surface covered by salt solution during slow freeze/thaw cycles, e.g. ASTM C672, SS 13 72 44) the question of moisture history and ageing is very important. Verbeck and Klieger /2/ noted that specimens dried at 50 % RH for 14 days scaled less than specimens continuously water cured before resaturation with pure water and freeze/thaw tested with salt solution. Sellevold /12/, based on his experiences with low temperature calorimetry and frost/salt testing, found that more severe drying (50 °C) and subsequent resaturation increased both ice formation and the frost/salt scaling dramatically. The effect was found to depend on concrete quality and composition. High strength concretes and silica fume concretes were less susceptible to drying/resaturation activated damage than OPC concretes of lower grade. The drying/resaturation effects make the comparison of cracking and scaling behaviour very complicated. In this paper we have limited the discussion and laboratory investigation to the standard drying procedure in the SS 13 72 44 method (50 % RH). (Ageing might be important also for internal cracking, but the research performed on ageing and frost resistance mainly concerns scaling).

In internal cracking tests (rapid freeze/thaw of beams continuously or periodically submerged (ASTM C666), critical degree of saturation testing (Fagerlund /13/)) the access to water and the degree of saturation are decisive depending on how the test is carried out. In addition, of course, concrete quality, concrete curing, air voids etc. are important, as mentioned above. Degree of saturation has been investigated by several researchers. Among others Whiteside and Sweet /14/, Warris /15/, MacInnis and Beaudoin /16/, Fagerlund /17/ and Vuorinen /18/ studied the critical degree of saturation for different types of concretes, air void contents, test conditions etc. In /13/ Fagerlund developed a test procedure for laboratory measurement of the critical degree of saturation. The "global" degree of saturation for a concrete specimen can be measured in any frost test by rather simple means. However, it is important to remember that in the test method /13/ the degree of saturation is the same in the whole specimen. In the ASTM C666 test, with possibility for absorption (procedure A) and partly drying (procedure B), on the other hand, the degree of saturation may vary greatly during test, and within the specimens due to non-equilibrium conditions caused by continuous absorption from the surface (and also partly drying in procedure B). Fagerlund /19/ called this unsealed testing. In /20/ he suggested that the degree of saturation-approach is valid for scaling with deicing salts.

In this paper internal cracking, scaling and absorption during freeze/thaw have been monitored in both ASTM C666 procedure A (freeze/thaw in water, internal cracking) and SS 13 72 44 (surface scaling with 3 % NaCl) for a variety of concretes, to study the process of deterioration in these two tests.

2. CONCRETE MIXES, MATERIALS AND SPECIMENS

A total of 11 different concrete mixes were investigated. In table 1 concrete mixes are given, and in table 2 properties of fresh and hardened concrete are given. Mixing procedure consisted of 1 minute dry mixing, 2 minutes mixing with water in a horizontal rotating counter current mixer. Naphtalene superplastisizers were mixed with the water whereas melamines were added at the end of wet mixing. Air entraining agents were added after water reducing admixtures, and the mixes were given an additional 1 minute mix with the air entraining agent. Non-air

entrained mixes waited 5 minutes after mixing and were then remixed 1 minute. Then properties of fresh concrete were determined (slump, density and air void content) and specimens were moulded in steel moulds. The specimens were demoulded after 24 hours and cured in water at 20 ° C. Mixes 3 - 6 were cured in water for 4 weeks before start of testing, Mixes 7 - 11 were cured in water for 8 weeks before start of testing. For Mix 5 an additional set of ASTM C666 specimens were made and water cured for 9 months before start of test. The concretes of Mix 1 and 2 were part of the investigations presented in /21, 22/. The curing regimes of the ASTM C666 specimens were not in compliance with the standard curing specified by ASTM C666 (14 days moist curing).

Weight and volume of cubes were taken at demoulding and after water curing to measure absorption and estimate self desiccation during curing for 7 of the concretes (Mix 3-6 and 9-11). In table 3, characteristics of cement and silica fume are given, and in table 4 characteristics for Normal Density (ND) aggregates are given. The cements used were Norwegian High Strength Cements (HS1, HS2) and Norwegian Ordinary Portland Cement (OP1). In addition a Swedish Degerhamn Standard Portland Cement and Finnish Portland Cement P 40/28 were used in Mixes 7 and 8. The details of these concretes are given by Kukko and Paroll, /23/. The silica fume used came from two sources in Norway: one slurry (S) with 50/50 water/solid content from Fiskaa and one dry (D) from Ila and Lilleby. The Quartz Diorite aggregate (QD) consisted of crushed rock in the whole fraction, and had a water absorption of 1.3 % by weight. The natural rocks consisted of gneiss granite rocks and the aggregate of Mixes 5, 6, 9, 10 and 11 contained 20 - 30 % of crushed material of the same type of rock. The water absorption was 0.6 %. The light weight aggregates used were two different types. LW1 (Macrolite) in Mix 2 with particle density of 800 kg/m^3 had a glassy structure and surface and a very low absorption in the fresh concrete. LW2 (Leca 800) had a higher particle density of about 1430 kg/m^3 and also higher absorption (estimated at 6.9 % in the fresh concrete) and is designed to give much higher concrete strength compared to Macrolite. LW1 was used in dry condition whereas LW2 was used either as oven dry (Mix 3 - 3508 LW2 D) or pre-saturated by vacuum (Mix 4 - 3508 LW2 W) resulting in a rather high water content of 31 % by weight or 44 % by volume. The superplastisizers used were either naphtalene (mix 1, 2, 8) or melamine (Mix 3-6 and 9-11) with solid contents of ca 40 % by weight. The air entraining agents were tensides in Mixes 6 and 11 and neutralised vinsol resin in Mix 8. From the measured air void contents and air void characteristics of table 2 it is seen that the air entrained Mixes 6, 8 and 11 had $\overline{L}$ = 0.13 - 0.33 mm whereas the non air entrained mixes had larger $\overline{L}$ in the range 0.75 - 1.30 mm. From table 2 we see that Mix 8 had a very good air void system whereas Mix 6 had higher air void content and lower specific surface than Mix 8.

3. TEST PROCEDURES

ASTM C666 Procedure A, rapid freezing and thawing in water

Freeze/thaw testing was performed in an air cooled freeze/thaw cabinet able to produce 5 cycles pr. day within the limits set by ASTM C666. The cooling rate was 12 °C/h. Three parallel beams 10 by 10 by 34.5 cm were placed in thin metal plate boxes with open tops and 1 - 3 mm water on all sides. A plastic foil was placed in the water on top to prevent evaporation during test. Thermocouples were put in the water of one specimen on each shelf to ensure proper cycle control. The temperature in the centre of a specimen was checked by moulding a thermocouple in a dummy specimen with water/cement ratio 0.40. In figure 1 test set-up and freeze/thaw cycle is shown. At start and during testing (at least each 35 cycles) measurements

were made of transverse resonance frequency by an Ono Sokki CF 910 frequency analyser. The accelerometer was fixed at the end of the beams which were placed on a piece of foam rubber during measurements. The beams were vibrated by hitting lightly with a plastic hammer in the middle of the span. Ultrasonic pulse velocity (UPV) was measured through the length of the beams using a PUNDIT MK V 54 MHz and a water based gel. Scaled material collected in the metal boxes was dried at 105 °C and weighed, and the beams were weighed. For Mix 9 - 11 the volume of each beam was measured at start and during freeze/thaw testing.

SS 13 72 44 - The Borås method, frost/salt scaling

Frost/salt scaling was measured on sawn surfaces of slabs 50 by 150 by 150 mm cut from 150 mm cubes. For each concrete mix four parallel slabs were tested. The slabs were wet sawn with diamond saw from the cubes after water storage. Then the slabs were stored at 50 % relative humidity and 20 °C for 7 days. During this storage the specimens were prepared according to the standard. A non-absorptive rubber cloth was used. Bottom and lateral sides of the slabs were in addition sealed with epoxy paint before the rubber cloth was glued to the specimens to ensure that absorption and scaling would occur only on the test surface. A polyamid amine epoxy paint was used for this purpose. After 7 days the specimens were weighed, and water was put on top of the test surfaces for 3 days. Then the water was removed, the specimens were weighed and a 3 % NaCl solution was poured on the surface up to 3 mm depth. During testing measurements were made of scaled off material, ultrasonic pulse velocity and weight of the specimen after scaled off material had been removed and the test surface had been dried with a paper cloth. Ultrasonic pulse velocity was measured on the rubber (with transmission gel) by the PUNDIT. Figure 2 shows preparation of test specimens and temperature in the salt solution during one freeze/thaw cycle. Cooling rate is approximately 2.5 °C/h. Thermocouples were placed in the salt solution of specimens at the top, middle and bottom of the freeze/thaw cabinets to check that the freeze/thaw cycle was within the specified limits of the standard. The specimens were rotated randomly in the cabinets between each measurement. The scaled off material was brushed off, dried at 105 °C for 24 hours and weighed. In the results, scaling is calculated to the nearest 0.01 kg/m^2.

Compressive strength, air content, porosity, degree of saturation

Compressive strengths (f_{c28} and f_{start}) were measured on three parallel 10 cm cubes for each of the 11 concrete mixes. Air void characteristics (air void content, specific surface and air void spacing factor $\bar{L}$) were measured on two polished sections for each mix (2 x 1500 points) according to ASTM C457 - modified point count method. The sections were sawn perpendicular to the length axis of beams for ASTM C666 procedure A test before freeze/thaw testing. Porosities and moisture contents/degree of saturation were measured by the so called PF-method /24/ with some modifications on slices 10 by 10 by 3 - 4 cm cut from the centre part of the ASTM beams immediately after taking the beams out of water storage (before start of freeze/thaw testing) and after frost deterioration. (Additional tests were performed on 5 by 15 by 15 cm slabs cut from cubes of Mix 3 - 8 and these showed little deviation from the beams). The beams for ASTM C666 procedure A testing were moulded as 50 cm long beams and sawn to 345 mm length (figure 1). The testing procedure consisted of measuring the weight of the slices in different moisture conditions, measuring the volume and then calculate porosities and densities.

Measurements:

m_{act}: specimen mass in actual moisture condition

m_{dry}: specimen mass dried to constant weight (105 °C)

$m_{suction}$: specimen mass after immersion in water (capillary or suction porosity)
$m_{pressure}$: specimen mass after pressure saturation at 10 MPa water pressure
V : volume measured by weighing in water

Calculations:

$\varepsilon_{suction}$	(suction porosity)	$= (m_{suction} - m_{drv})/ V$	(vol-%)
ε_{macro}	(macro porosity, air content)	$= (m_{pressure} - m_{suction})/ V$	(vol-%)
w_{act}	(actual water content)	$= (m_{act} - m_{drv})/ V$	(vol-%)
w_e	(evaporable water content)	$= (m_{act} - m_{drv})/ m_{drv}$	(g/g dry)
w_{stop}	(evaporable water at stop)	$= (m_{stop} - m_{drv})/ V$	(vol-%)
S_{act}	(degree of saturation at start)	$= w_{act}/(\varepsilon_{suction} + \varepsilon_{macro})$	
ΔS	(increase in S	$= (w_{stop} - w_{act})/(\varepsilon_{suction} + \varepsilon_{macro})$	

The suction porosity ($\varepsilon_{suction}$) determined this way is a function of the volume fraction of cement paste, the w/c - ratio and the degree of hydration, assuming that no water is absorbed by the aggregate. The air content is represented by pores that are not filled by capillary suction after immersion in water, but are filled at subsequent application of 10 MPa water pressure. Different densities can be calculated from the data (dry density, solid density). The use of PF-factor for estimating frost durability of concrete was discussed by Vuorinen /18, 25/.

Self-desiccation and water absorption during water curing

Measurements of water absorption were performed to estimate whether air voids were filled during curing. Theoretical total porosities and self desiccation porosities of the cement paste fraction of the concrete according to Powers and Brownyard /26/ can be calculated using the following formulae, /27/:

$$\varepsilon_{tot} = \frac{(w/c - 0.172\alpha)}{(0.321 + w/c)}$$ (to check recipe of mix by comparing $\varepsilon_{suction}$ and ε_{tot})

$$\varepsilon_{sd} = \frac{0.0584\alpha}{(0.321 + w/c)}$$ (to estimate if water absorption fills ε_{sd})

Where:
ε_{tot} : total hardened cement paste porosity
ε_{sd} : self desiccation porosity
α: degree of hydration (must be estimated)

These use of these formula is a simplification since it has been shown by Sellevold and Justnes /28/ that the reaction products with silica fume differ from those with pure cement with respect to amount of bound water and composition of the hydration products. Furthermore, the calculations are based on measurements on concrete specimens assuming that the paste/aggregate ratio is the same in each specimen as in the bulk mix, that there are no effects of the interface zone between paste and aggregate on the properties of the cement paste and that the aggregate does not absorb water during water storage.

4. RESULTS AND DISCUSSION

Absorption during water curing and self-desiccation

In tables 5 and 6 total porosity (ε_{tot}) and self desiccation porosity (ε_{sd}) have been calculated. ε_{tot} and ε_{sd} are given together with absorption during water curing (before frost testing), evaporable water content in virgin state (w_{act}), suction- (ε_{suc}) and macro porosity (ε_{macro}) as measured with the PF-method. The degree of hydration was estimated to be in the range 0.75 - 0.85. For the w/b = 0.35 concrete it is lower, probably around 0.65. Consequently ε_{tot} will be larger and ε_{sd} lower for 035-08 in table 6.

From tables 5 and 6 it is seen that for non-air entrained concretes the absorption is approximately equal to the self desiccation porosity after long time water curing. For the air entrained concrete of table 5 with highest air void content (Mix 6) the absorption is slightly larger than the theoretical self desiccation porosity, indicating that part of the air voids are filled. For Mix 10 and 11 (no air and air entrained) the values of table 5 (10 cm cubes) give no indication of filling of air voids, whereas in table 6 (15 cm cubes) the air entrained Mix 11 absorbs more than the non-air entrained Mix 10, indicating that airvoids take up water during curing, in accordance with Fagerlund /29/. Also the higher absorption during presuction for the frost/salt test for Mix 6 and 11 compared to Mix 5 and 10 given in table 7 indicates that air voids can be filled during isothermal water suction. From table 5 it is also seen that the actual water content in virgin condition (w_{act}) is in the same range as the suction porosity (ε_{suc}) for Mix 5, 6, 9, 10 and 11, indicating that at least the capillary pores were saturated before start of freeze/thaw. By comparing the absorption values of Mix 10 and 11 after two months in water for 10 and 15 cm cubes (comparing tables 5 and 6) we see that there is a clear effect of specimen size since the absorption (vol-% of paste) is smaller in the 15 cm cubes. The effect of prolonged water curing on porosity and estimated degree of hydration is also given in tables 5 and 6: the absorption approaches theoretical self desiccation, total porosity is reduced and self desiccation increases as degree of hydration increases.

Freeze/thaw results

In table 7 and figure 3 results from ASTM C666 procedure A testing are given. It is seen that three concretes have "good" Durability Factor (DF) > 90 : Mix 3, 6 and 8. Mix 1 has a fair DF of 79, whereas Mix 2, 4, 5, 7, 9, 10 and 11 have low DF in the range 2 - 23. For all concretes with Normal Density (ND) aggregate a proper air entrainment is required to obtain good DF. This is seen by comparing the three air entrained mixes Mix 6, 8 and 11 with DF of 94, 91 and 23. Mix 11 has the highest $\bar{L}$ of these three with 0.33 mm, whereas Mix 6 and 8 have lower $\bar{L}$ of 0.16 and 0.13 mm. Mix 1 with the highest strength is the most durable of the non-air entrained ND concretes. For the beams of Mix 5 with prolonged water curing (9 months in water instead of 4 weeks) the DF increased from 11 to 20. The additional water curing therefore had a significant, but limited effect on the resistance to internal cracking.

By comparing the three light weight aggregate concretes we see that Mix 2 with the glassy Macrolite and Mix 4 with the water saturated Leca do not survive the test, whereas Mix 3 with the dry Leca has an excellent freeze/thaw durability with DF = 99. All three light weight aggregate concretes are non-air entrained. The very fast deterioration of Mix 4 with the water saturated Leca is not surprising, but the low durability of Mix 2 compared to Mix 3 (both dry aggregates) indicates that both the type of lightweight aggregate particle (porosity, surface

morphology, water absorption etc.), and concrete properties (strength, air content etc.) influence the freeze/thaw durability.

Scaling

In table 8 and figure 4 results from SS 13 72 44 frost/salt scaling testing are given. Also scaling values taken during ASTM C666 procedure A testing are given. It is seen that for Mixes 1, 2, 3, 6, 8 and 11 the frost/salt scaling durability is very good (scaling < 0.10 kg/m^2 after 56 cycles) according to SS 13 72 44. Mixes 5, 7, 9 and 10 have non-acceptable resistance to frost/salt (> 1 kg/m^2 after 56 cycles) according to SS 13 72 44, and Mix 4 has 0.24 kg/m^2 after 42 cycles. Mix 1, 2 and 11 are examples of concretes with very good durability against frost/salt scaling up to higher number of cycles (205) even though these concretes do not survive internal cracking testing in ASTM C666 procedure A. Mix 5 with w/c+s = 0.35, 8 % silica fume and 28-day compressive strength of 105 MPa has quite high scaling, 2.59 kg/m^2 after 56 cycles. Mix 1 with w/c+s = 0.30, 8 % silica fume and 28 day compressive strength of 110 MPa has 0.02 kg/m^2 after 56 cycles. Mix 4 (lightweight aggregate concrete) with the same binder as Mix 5 but slightly lower w/c+s (approximately 0.33) due to a little higher absorption in the light weight aggregate than anticipated, has very good scaling durability (0.01 kg/m^2 after 56 cycles). Mix 6, which has the same composition as Mix 5 but with air entrainment, has very good frost/salt scaling durability according to SS 13 72 44 with 0.09 kg/m^2 after 56 cycles.

The results show that high compressive strength is not always enough to ensure very good frost/salt scaling durability according to SS 13 72 44. The critical limit of water/binder ratio and compressive strength of ND concrete for the particular binder composition of Mix 3 - 6 is probably around 0.33 and above approximately 110 MPa. The composition of the concrete (type of cement, type of additives etc.) may of course also influence this border value. For Mix 9 and 10 with water/binder ratio of 0.40 and 28-day strengths 69 - 79 MPa the scaling is higher than Mix 5 without air entrainment. Silica fume reduces the scaling a little and air entrainment (Mix 11) results in very good durability according to SS 13 72 44 (0.02 kg/m^2 after 56 cycles). For Mix 11 the air entrainment is sufficient for very good frost/salt scaling durability, but gives a DF of only 23, showing that ASTM C666 procedure A requires better air void system than SS 13 72 44 for the binder composition of this mix. For mixes with very good durability according to SS 13 72 44 that are frost/salt tested beyond the normal 56 cycles (up to 98 or 205 cycles: Mix 1, 2 , 3, 6 and 10) no dramatic acceleration in damage is observed.

The scaling values measured during the ASTM C666 test are all on a low level compared to the frost/salt scaling values, as expected due to no salt (fresh water on undried mould surfaces). It is also interesting to note that the scaling values in ASTM C666 are not very different between the 11 concretes, even though the same concretes show a very large variation in frost/salt scaling. This is clearly seen when comparing scaling in ASTM after 35 or 70 cycles with scaling in SS after 28 or 56 cycles for Mix 3 and 5 - 11. (Mix 1, 2 and 4 have practically no scaling in SS, or test was interrupted before 56 cycles.) Apparently scaling in ASTM C666 procedure A in pure water does not distinguish between good and bad scaling durability as does the frost/salt test.

Absorption during freeze/thaw and salt/frost testing

In table 9 absorption during freezing and thawing is given in kg/m^2. This is the most practical way of comparing absorption in SS and ASTM due to the absorption and possible non-homogeneous moisture content in the specimens, as discussed in the introduction.

For SS 13 72 44 it is seen that the absorption during freezing and thawing increases rapidly and is generally high compared to the absorption during the preceding 3 days presuction with pure water. Absorption during three days of presuction of the SS test is lowest for Mix 2 (the most dense binder in terms of water/binder ratio). If we compare the two sets of mixes with equal binder composition but with and without air entrainment (Mix 5, 6, 10 and 11) the results indicate that the air voids absorb water during the 3 days of absorption with pure water in the SS 13 72 44 test before freeze/thaw. The high absorption of Mix 2 in SS 13 72 44 after 205 cycles is probably because of absorption in the light weight aggregate particles (sawn surfaces).

Also in ASTM C666 the absorption during freeze/thaw testing is significant, but lower than in SS 13 72 44 (comparing 35 cycles ASTM with 28 cycles SS). Reasons for this can be more time for absorption in the SS cycle due to longer time in thawed condition and the increased absorption due to salt /20/. The three mixes that perform well in ASTM C666, Mix 3, 6 and 8, have significant absorption during the test even though no or little reduction in resonance frequency is observed. Mix 1, the densest and highest strength concrete tested in ASTM C666, has very low absorption and no cracking as measured by resonance frequency during the first 200 cycles. After about 200 cycles internal cracking can be measured, see table 7. The absorption is clearly accelerated by the cracking in this case, see table 9. For Mix 2, 5, 7, 9 and 10 (no air entrainment), deterioration starts very fast, and absorption gets very high quickly. It is difficult to judge what comes first: cracking or absorption. The results in table 7 demonstrate that both high scaling in SS 13 72 44 and deterioration due to internal cracking in ASTM C666 procedure A are associated with increases in absorption during the course of freeze/thaw. This indicates a progressive type of deterioration in both methods caused by absorption, in contrast to Fagerlunds method /13/, where degree of saturation is fixed during the freeze/thaw cycles.

Correlation internal cracking - absorption during freeze/thaw

Figures 5 and 6 show absorption vs. internal cracking in SS (measured as pulse velocity) and ASTM (measured as resonance frequency) after 56 and 70 cycles respectively. (In SS 13 72 44 pulse velocity was not measured for three of the concretes). Both plots show good relationships between cracking and absorption - though a little better in ASTM C666 procedure A, figure 7. There is no such correlation between scaling and absorption for the same concretes, even though scaling and absorption both increase for each concrete during the course of freezing and thawing, as mentioned above. Mix 4 (saturated light weight aggregate) has large absorption even though the scaling is not very high. Mix 9 on the other hand has very high scaling and small signs of internal damage as measured by UPV, and with moderate absorption compared to the SS slabs with larger reduction in UPV. It therefore seems that absorption during freezing and thawing correlates better to cracking than to scaling.

If we compare UPV in the same mixes with and without air entrainment (Mix 5 - 6 and Mix 10 - 11, table 10) we see that cracking in the non-air entrained mixes propagate very fast with a significant reduction in UPV, and also high absorption and scaling. Mix 5 and 10 both show an initial loss in pulse velocity and then a significant increase again. Some of this increase is due to the fact that some specimens were removed after 28 cycles due to large internal cracking and leakage of salt solution, but still some increase in pulse velocity was observed after continued testing of the remaining specimens. This can be due to healing of cracks. For mixes with very good scaling durability according to SS 13 72 44, frost/salt tested beyond the normal 56 cycles (up to 98 or 205 cycles: Mix 2, 3, 6, 11) no reduction in pulse velocity is observed. Mix 11

which had very low scaling showed a significant increase in UPV up to 205 cycles, possibly due to continued hydration or increased water content.

Correlation resonance frequency - pulse velocity

In figure 7 a plot of resonance frequency vs. UPV is shown for all ASTM C666 beams tested. The plot shows a good relationship between UPV and resonance frequency. It is seen that the resonance frequency is a more sensitive indicator of internal cracking than UPV. For zero frequency in the most deteriorated beam (Mix 4 - saturated lightweight aggregate particles), there is still a pulse velocity of 50 % of the initial value. Also other researchers, Warris /15/ and Fagerlund /17/, claimed that resonance frequency is more sensitive to internal cracking than UPV.

Comparing internal cracking in ASTM and SS:

In table 10 UPV of eight mixes can be compared in both ASTM and SS (UPV was not measured in SS testing of Mix 1, 7 and 8). The results show that six of the eight concretes have considerable internal cracking in ASTM (Mix 2, 4, 5, 9, 10, 11), whereas only three mixes have cracking in SS 13 72 44 (Mix 4, 5 and 10). Therefore ASTM is tougher than SS with respect to internal cracking for these concretes, as expected. Higher cooling rate and higher surface/volume ratio in the ASTM test are probable causes.

Simultaneous occurrence of cracking and scaling

The results of cracking and scaling measurements on the same concrete mixes demonstrate that depending on test method and concrete composition, one may observe all combinations of cracking and scaling in a laboratory test: cracking and scaling (Mix 5, 7, 10 in ASTM and SS), cracking and no scaling (Mix 1, 2, 11 in ASTM and SS), no cracking and scaling (Mix 8 in ASTM and Mix 9 in SS), no cracking and no scaling (Mix 3 and Mix 6 in ASTM and in SS). With simultaneous cracking and scaling, the scaling was accelerated.

By comparing scaling values and pulse velocities in both test methods (tables 8 and 10) for Mix 9 and 10 (same mix with and without silica fume) it is seen that silica fume reduces the scaling but increases the cracking, as observed by Pigeon et al /30/. However, Hooton et al /31, 32/ observed improved cracking resistance with silica fume in ASTM C666 procedure A. The results indicate that the effect of silica fume on frost durability depends on the test method and concrete parameters (materials, curing etc.).

Volume increase at internal cracking

Table 11 shows the volume increase during deterioration of Mix 9, 10 and 11. It is seen that the volume increases with reduction in dynamic modulus (E_{rel}). By comparing with water absorption in table 13 it is seen that the water absorption is larger than the volume increase, i.e. water filling takes place in created cracks and in already existing pores.

Increased porosity and degree of saturation at internal cracking

In table 12 results are given for porosity and evaporable water content of slices cut from the beams before and after ASTM C666 procedure A. Also the relative dynamic modulus ($E_{relative}$) at stop of freeze/thaw test and the number of cycles to stop are given. Degree of deterioration (relative dynamic moduli) were not equal for the deteriorated concretes at stop of test. It is seen that the freeze/thaw deterioration results both in increased suction porosity (ε_{suc}) and evaporable water content (w_e). Mix 3 and 6, which were not deteriorated in ASTM C666, have clear increase in evaporable water contents, (w_e), but no increase in suction porosity

(ε_{suc}). Compared to the water content at start of test (w_{act}), the increase is 1.1 and 1.3 vol-% (3.4 and 4.1 % of cement paste). It seems that water was transported into air voids/light weight aggregate particles without causing damage during the 300 cycles of the test for these two concretes. The "pumping" effect has been observed and discussed earlier /1, 19, 20/.

From table 13 we see that the degree of saturation of Mix 1 is clearly erroneous since it is larger than 1 both before and after freeze/thaw exposure. The reason can be an error during test. An other explanation might be that for this type of concrete with very low capillary porosity, the degree of saturation cannot be determined by simply drying at 105 °C, using water suction and 10 MPa pressure saturation. However, the results demonstrate that the water content increases during test also for this concrete.

Scatter in scaling testing

Figure 8 shows a plot of scaling after 28 cycles in SS versus coefficient of variation for the 11 mixes. The standard type of relationship is seen: low scatter for high scaling and high and low scatter for low scaling.

5. CONCLUSIONS

The results show that during freeze/thaw in water or 3 % NaCl solution the damage is accompanied by rather large absorption. Good correlation between internal cracking and absorption after a given number of cycles was observed. Also concretes durable against rapid freezing and thawing absorbed water during the 300 cycles without significant damage as measured by loss of resonance frequency. In SS 13 72 44 the absorption due to this "pumping effect" is high compared to the water absorption before start of freeze/thaw.

Measurements of absorption during curing in water and comparison with theoretical values of total hardened cement paste porosity and self desiccation porosity show that practically all self desiccation pores can be filled, and that in an air entrained concrete also some of the air voids may be filled.

Cracking and scaling measurements demonstrate that depending on test method and concrete composition, all combinations of cracking and scaling were observed: cracking and scaling, cracking and no scaling, no cracking and scaling, no cracking and no scaling. Simultaneous cracking and scaling gave acceleration of the scaling.

Comparing pulse velocity measurements for the same concretes tested in the two test methods showed that SS 13 72 44 gives less internal cracking than ASTM C666 procedure A. Comparing scaling in the two test methods showed that the scaling is much lower in ASTM C666 procedure A than in SS 13 72 44 (as expected due to lack of salt), and that concretes with large differences in scaling in SS 13 72 44 show small differences in ASTM C666.

High Strength Concretes (HSC) with sufficiently low w/c - ratio had excellent durability against frost/salt scaling without air entrainment. Further, previous research and this study demonstrate that it is possible to produce HSC without air entrainment which can survive ASTM C666 procedure A, but that this depends on factors like curing conditions and binder composition. It appears that concretes that are close to being salt/frost resistant without air entrainment are particularly sensitive to binder composition since concretes of close water/binder ratios and compressive strengths may exhibit considerable differences in scaling durability in the Borås test (viz. mix 1, 2 and 3 vs. mix 5).

Based on the types of deterioration observed in the two methods it is concluded that SS 13 72 44 is the most suitable test method for simulating durability against frost/salt attack.

6. REFERENCES

/1/ Powers T.C.: A working hypothesis for further studies of frost resistance of concrete, PCA-bulletin 5, 1945

/2/ Verbeck G., Klieger P.: "Studies of salt scaling of concrete", Highway Research Board Bulletin No. 150, 1956

/3/ Highway Research Board Special report 47: Report on Cooperative Freezing-and-Thawing Tests of Concrete, Washington, D.C. 1959

/4/ Perenchio W.F., Klieger P.: Some physical properties of high strength concrete, Research and development bulletin RD056.0IT, PCA, Skokie Illinois 1978

/5/ Foy C., Pigeon M., Banthia N.: Freeze/thaw durability and deicer salt scaling resistance of a 0.25 w/c concrete, Cement and concrete research, Vol.18, No.4, pp.604-614 (1988)

/6/ Hammer T.A., Sellevold E.J.: Frost resistance of high strength concrete, 2nd Int. Symp. on High Strength Concrete, Berkeley, 1990, ACI SP - 121 pp. 457 - 489

/7/ Gagné R.: Frost durability of high performance concretes. Ph.D.Thesis Université Laval, 1992 (In French)

/8/ Marchand J.,Gagné R., Pigeon M., Jacobsen S. and Sellevold E.J.: The frost durability of high-performance concrete, Consec'95, International Conference on Concrete under severe conditions Sapporo, Japan, pp. 273 - 288, Chapmann and Hall, 1995

/9/ Powers T.C.: The air requirement of frost resistant concrete, Proceedings Highway Research Board, V.29, pp.184-211, 1949

/10/ Powers T.C. and Helmuth R.A.: Theory of volume changes in hardened portland cement paste during freezing, Highway Research Board, Proceedings 32 1953

/11/ Powers T.C.: Basic considerations pertaining to freezing-and-thawing tests. Proceedings of the ASTM, Vol.55, 1955.

/12/ Sellevold E.J, Farstad T.: Frost/salt testing of concrete: effect of test parameters and concrete moisture history. Nordic Concrete Research Publ. No.10 1991 pp.121-138.

/13/ Fagerlund G: The critical degree of saturation method of assessing the freeze/thaw resistance of concrete, Materials and Structures no. 10 1977, pp. 217 - 229

/14/ Whiteside T.M and Sweet H.S.: Effect of mortar saturation in concrete freezing and thawing tests. Proceedings of the Highway research board 30, pp.204-216, 1950

/15/ Warris B: The influence of air entrainment on the frost resistance of concrete Part A: Proceedings no 35 (1963), Part B: Proceedings no 36 (1964) Swedish cement and concrete research institute.

/16/ MacInnis C., Beaudoin J.J.: Effect of degree of saturation on the frost resistance of mortar mixes, ACI Journal pp.203-208, March 1968

/17/ Fagerlund G.: Critical degrees of saturation at freezing of porous and brittle materials, Division of building materials, The Lund institute of technology, Report 34 1972 (In Swedish)

/18/ Vuorinen J.: On use of dilation factor and degree of saturation in testing concrete for frost resistance, Nordisk Betong nr. 1 1970.

/19/ Fagerlund G.: Effect of the freezing rate on the frost resistance of concrete. Nordic Concrete Research Publication No.11 pp. 20 - 36 1992

/20/ Fagerlund G.:"Studies of the scaling, the water uptake and the dilation of specimens exposed to freezing and thawing in NaCl solution". Research seminar, RILEM committee 117 FDC Freeze/thaw and deicing resistance of concrete, Report TVBM 3048 Lund Institute of Technology, Sweden, 1991 pp. 37 - 66

/21/ Jacobsen S., Sellevold E.J.: "Frost/salt Scaling and Ice Formation of Concrete: Effect of Curing Temperature and Silica Fume on Normal and High Strength Concrete", The

International Workshop on Freeze-Thaw and Deicing Salt Scaling Resistance of Concrete, Université Laval - CRIB, Québec, Canada, pp.231-246, 1993
/22/ Sellevold E.J., Jacobsen S., Bakke J.A.:"High Strength Concrete without air entrainment: effect of rapid temperature cycling above and below 0 °C", as /21/ pp. 155 - 165
/23/ Kukko H., Paroll H.: Round robin tests on concrete frost resistance, as /21/ pp. 263 - 272.
/24/ Sellevold E.J.:"Hardened Concrete - Determination of air/macro and gel/capillary porosity (PF- method)", Report 0 1731 The Norwegian Building Research Institute, 1986 (In Norwegian with draft method in English)
/25/ Vuorinen J.: On the protective pore ratio of concrete. Proceedings Nordic Workshop Concrete and Frost pp. 283 - 295, The Danish Concrete Association publication no. 22 1985 (in Swedish).
/26/ Powers T.C., Brownyard T.L.: Studies of the physical properties of hardened portland cement paste, PCA bulletin 22 1948
/27/ Sellevold E.J.: Concrete structure, compendium for Course 32586, The Norwegian Institute of Technology 1991.
/28/ Sellevold E.J. and Justnes H.: High strength concrete binders - Part B: Non-evaporable water, self-desiccation and porosity of cement pastes with and without condensed silica fume. ACI Special Publication SP-132, pp. 891 - 903. 1992
/29/ Fagerlund G.: The influence of slag cement on the frost resistance of the hardened concrete, CBI-research Fo 1:82 1982
/30/ Pigeon M., Pleau R., Aitcin P.-C.: Freeze-thaw durability of concrete with and without silica fume in ASTM C 666 (Procedure A) test method: internal cracking vs. scaling, Cement, Concrete and Aggregates Vol. 8, No.2, Winter 1986.
/31/ Hooton R.D.: Influence of silica fume replacement of cement on physical properties and resistance to sulphate attack, freezing and thawing and alkali-silica reactivity, ACI Materials Journal, March-April 1993, pp 143 - 151.
/32/ MacGrath P. and Hooton R.D.: Self desiccation of Portland cement and silica fume modified mortar, Advances in cementitious materials, Ceramic transactions Vol.16, Am. Cer. Soc., Sidney Mindess editor, pp.489 - 501, 1990

7. ACKNOWLEDGEMENT

The work was carried out with financial support from The Norwegian Research Council/ Norcon programme, Public Roads Laboratory, Norcem and Norwegian Contractors. Air void analysis was performed by the first author at Laval University/CRIB, Québec, Canada. Thanks to Jacques Marchand, who provided help for preparation of the polished sections.

Table 1: Concrete mixes

Concrete	w/c+s	s/c+s	Cem. type	SF type	Vol. paste	Cem.	Aggregate type	Aggregate	Super plast.	Air entr.
					vol-%	kg/m^3		kg/m^3	kg/m^3	kg/m^3
1 030-08 QD	0.30	0.08	HS1	S	32	469	ND QD	1650	12	-
2 030-08 LW1	0.30	0.08	HS1	S	32	469	LW 1	300+400 1)	12	-
3 035-08 LW2D	0.33	0.08	HS2	D	32	428	LW 2	585+679 2)	7.80	-
4 035-08 LW2W	0.35	0.08	HS2	D	31	426	LW 2	583+826 3)	6.32	-
5 035-08 ND	0.35	0.08	HS2	D	32	440	ND G	1765	11.92	-
6 035-08 NDA	0.35	0.08	HS2	D	29	401	ND G	1610	8.12	0.53
7 035-00 ND2	0.35	0	OP1	-	26	387	ND G	1921	7.75	-
8 049-00 ND3A	0.49	0	OP2	-	29	357	ND G	1769	-	0.09
9 040-00 ND	0.40	0	OP3	-	31	432	ND G	1799	4.92	-
10 040-05 ND	0.40	0.05	OP3	D	31	409	ND G	1782	6.46	-
11 040-05 NDA	0.40	0.05	OP3	D	31	411	ND G	1703	4.93	0.13

1) Natural sand + light weight aggregate 2) w/c+s corrected for absorption in LW 2
3) LW 2 including water from presaturation

Table 2: Properties of fresh and hardened concrete

Concrete	Fresh concrete			Hardened concrete					
				PF	ASTM C457				
	Slump (cm)	Dens. (kg/m^3)	Air (vol-%)	Air (Vol-%)	Air (Vol-%)	α (1/mm)	$\bar{L}$ (mm)	$f_{c\,28}$ (MPa)	f_c start (MPa)
1 030-08 QD	16	2520	2.0	1.3	1.0	9.1	1.16	110	141
2 030-08 LW1	16	1375	-	-	3.3	8.6	0.81	-	41
3 035-08 LW2D	9	1910	2.4	-	1.7	8.1	1.03	75	75
4 035-08 LW2W	12	2020	2.8	-	1.9	5.8	1.30	72	72
5 035-08 ND	21	2410	1.4	1.8	2.0	7.8	1.04	105	105 1)
6 035-08 ND A	15	2200	9	7.8	13.2	13.3	0.16	65	65
7 035-00 ND2	8	2450	2.7	2.4	3.5	7.3	0.75	73	
8 049-00 ND3 A	8	2300	5.2	3.7	5.8	36.4	0.13	47	
9 040-00 ND	20	2450	1.6	2.0	2.5	6.8	0.99	69	74
10 040-05 ND	19	2450	2.0	2.3	2.0	7.7	0.97	79	83
11 040-05 ND A	21	2350	5.1	4.2	5.3	14.8	0.33	68	73

1) $f_{c\ 9\ mth}$ = 113 MPa

Table 3: Characteristics of cement and silica fume

Component	Cement			Silica fume	
	HS 1	HS 2	OP 1	Slurry (S)	Dry (D)
- SiO_2	22.1	22.1	20.9	> 95	91.2
- Al_2O_3	4.2	4.1	4.6		0.3
- Fe_2O_3	3.4	3.4	3.5		2.8
- CaO	64.1	64.3	63.4		
- MgO	1.4	1.0	1.8		1.5
- SO_3	2.7	3.1	3.1		0.5
- K_2O	0.6	0.4	0.9		0.7
- Na_2O	0.2	0.2	0.4		0.4
- L.O.I.	0.9	1.3	1.0		1.7
Fineness (m^2/kg)	4200	4180	3580		

Table 4: Particle sizes of normal density aggregates, fineness modulus (FM) and density

Aggregate	Sieve size (mm) - % passing								FM	Density
	0.125	0.25	0.5	1	2	4	8	16	ISO	g/cm^3
1 QD	5	9	14	21	28	40	45	100	4.91	2.78
5,6,9,10,11 ND	3	5	12	23	37	48	63	97	4.64	2.67
7 ND2	3	8	21	30	42	52	64	100	4.32	2.67
8 ND3	6	8	13	21	38	55	72	100	4.40	2.67

Table 5: Absorption during curing, theoretical porosities and porosities measured by the PF-method. All values: vol-% of paste. Absorption: 10 cm cubes, PF-method: slices 10 by 10 by 3-4 cm.

Mix	Vol-% absorbed			Theoretical		PF-method		
				ε_{tot}	ε_{sd}	w_{act} 2)	ε_{suc} 3)	ε_{macro}
	1 mth	2 mth	9 mth	$\alpha = 0.75$				
3 035-08 LW2D	3.1			32.9	6.5	1)	1)	1)
4 035-08 LW2W	5.0			32.9	6.5	1)	1)	1)
5 035-08 ND	4.5		6.6	32.9	6.5	35.6	36.6	5.3
6 035-08 ND A	8.1			32.9	6.5	46.2	46.9	26.9
9 04-00	4.7	6.1		37.5	6.1	37.1	36.8	6.5
10 04-05	5.8	5.8		37.5	6.1	37.4	37.4	7.4
11 04-05A	5.2	5.8		37.5	6.1	37.7	39.0	13.5

1) Not relevant due to moisture in light weight aggregate particles
2) Actual (evaporable) water content in virgin condition (after water curing)
3) Suction and macroporosities measured after drying at 105 °C

Table 6: Absorption during water curing and theoretical porosities 040-05 and 040-05A
Effect of curing time (15 cm cubes)

Curing time	Vol-% abs		Theoretical porosity		α
(Months)	040-05	040-05A	ε_{tot}	ε_{sd}	1)
2	3.9	4.5	37.5	6.1	0.75
3	4.5	4.8	36.9	6.3	0.78
6	5.8	6.5	36.4	6.5	0.80
7	5.8	5.5	35.8	6.7	0.83
9	5.6	6.3	35.2	6.9	0.85

1) Linear interpolation of degree of hydration between 2 and 9 months

Table 7: ASTM C666: resonance frequencies and Durability Factors (DF)

Mix	Resonance Frequency (Hz)									
	0	35	70	100	140	205	240	275	300	**DF**
1 030-08 QD	3300	3300	3300	3300	3300	3300	3275	3160	2930	**79**
2 030-08 LW1	2340	2210	2200	1900	1630					**23**
3 035-08 LW2D	2625	2600	2590	2600	2610	2620	2620	2610	2610	**99**
4 035-08 LW2W	2500	0 1)								**2**
5 035-08 ND	2930	2830	1630							**11**
5 9 mth curing	2960	2940	2860	1950	510					**20**
6 035-08 ND A	2640	2590	2580	2610	2590	2600	2590	2580	2560	**94**
7 035-00 ND2	3200	3010	1500							**9**
8 049-00 ND3 A	2960	2880	2860	2850	2850	2850	2840	2830	2820	**91**
9 040-00 ND	2850	2780	2040							**11**
10 040-05 ND	2830	2770	1360							**10**
11 040-05 ND A	2780	2720	2660	2270	1850					**23**

1) At 14 and 29 cycles: 1775 and 1163 Hz 2) 60 cycles

Table 8: Scaling in SS 13 72 44 (3 % NaCl) and ASTM C666 procedure A (kg/m^2)

Mix	ASTM C666 procedure A			SS 13 72 44				
	35	70	300	28	56	98	134	205
1 030-08 QD	0	0	0	0.02	0.02	0.02	0.02	0.02
2 030-08 LW1	0	0 1)		0.02	0.04	0.09	0.14	0.24
3 035-08 LW2D	0.01	0.02	0.14	0.01	0.01	0.03		
4 035-08 LW2W	0.12			0.20	0.24 2)			
5 035-08 ND	0.01	0.02		0.98	2.59	5.69		
6 035-08 ND A	0.03	0.05	0.20	0.06	0.09	0.16		
7 035-00 ND2	0.03	0.09 3)		0.77	1.24			
8 049-00 ND3 A	0.03	0.05 3)	0.55	0.01	0.01			
9 040-00 ND	0.02	0.07		2.12	4.25	5.83 4)		
10 040-05 ND	0.02	0.03		0.80	3.82	10.2	20.8 5)	
11 040-05 ND A	0.02	0.04		0.01	0.02	0.09	0.04	0.18

1) Some pop-outs over light weight aggregate particles 2) Stopped at 42 cycles due to internal cracking 3) 60 cycles 4) Stopped at 77 cycles 5) One specimen without leakage 77 to 134 cycles

Table 9: Absorption during testing in ASTM C666 and SS 13 72 44 (kg/m^2)

Mix	ASTM C 666 proc A				SS 13 72 44						
	35	70	140	300	- 3 d	0	28	56	98	134	205
1 030-08 QD	0.01	0.01	0	0.11	4)						
2 030-08 LW1	0.03	0.11	0.36		0.07	0	0.14	0.17	0.27	0.46	1.07
3 035-08 LW2D	0.04	0.06	0.12	0.23	0.32	0	0.21	0.27	0.34		
4 035-08 LW2W	0.80				0.32	0	1.14	2.03 3)			
5 035-08 ND	0.09	0.29			0.13	0	1.40	1.75	1.97		
6 035-08 ND A	0.11	0.15	0.21	0.29	0.45	0	0.22	0.32	0.40		
7 035-00 ND2	0.09	0.39			4)						
8 049-00 ND3 A	0.01	0 1)	0.01	2)	4)						
9 040-00 ND	0.07	0.27			0.21	0	0.54	0.62			
10 040-05 ND	0.10	0.41			0.16	0	1.15	1.23	1.65	1.92	
11 040-05 ND A	0.04	0.11	0.35		0.18	0	0.20	0.31	0.43	0.49	0.60

1) 0.03 kg/m^2 at 100 cy 2) Apparent weight loss: inaccurate scaling measurements 3) 42 cy 4) Not measured

Table 10: Ultrasonic pulse velocity in ASTM C666 and SS 13 72 44 (m/s)

Mix	ASTM C666 proc. A					SS 13 72 44					
	0	35	70	140	300	0	28	56	98	134	205
1 030-08 QD	5230	5250	5230	5220	4660						
2 030-08 LW1	3900	3790	3730	3500		3610	3660	3630	3690	3600	3600
3 035-08 LW2D	4270	4220	4180	4180	4180	4050	4030	4030	4040		
4 035-08 LW2W	4060	2020				3910	3810	3520[1]			
5 035-08 ND	4600	4060	3130			4380	3410[2]	3780	4010		
6 035-08 ND A	4360	4340	4340	4330	4340	4070	4040	4060	4070		
7 035-00 ND2	4960	4630	3260								
8 049-00 ND3 A	4700	4660	4670	4620	4510						
9 040-00 ND	4540	4400	3620			4280	4240	4290	4310[3]		
10 040-05 ND	4470	4020	2070			4230	3400[2]	3870	3770	3700	
11 040-05 ND A	4350	4330	4180	3320		4030	4070	4120	4180	4200	4230

1) 42 cy, stopped due to cracking 2) 2 spec. with cracks stopped 3) 77 cy, large scaling

Table 11: Volume increase (vol-%) during ASTM C666 procedure A

Mix	0	20	35	70	105	140	$E_{relative}$ at stop
9 04-00	0	0.1	0.2	0.8			0.51
10 04-05	0	0.2	0.3	1.4			0.23
11 04-05A	0	0.1	0.2	0.3	0.6	1.0	0.44

Table 12: Porosities and evaporable water contents before and after frost deterioration

Concrete	$E_{relative}$ at stop freeze/ thaw	No.of freeze/ thaw cycles	Start freeze/thaw				Stop freeze/thaw			
			w_{act} Vol-%	ε_{suc} Vol-%	ε_{macro} Vol-%	w_e g/gdry	w_{act} Vol-%	ε_{suc} Vol-%	ε_{macro} Vol-%	w_e g/gdry
1 030-08 QD	0.79	300	8.5	6.9	1.3	.0345	11.5	11.6	1.4	.0475
2 030-08 LW1	0.49	140	11.0	10.3	1)	.0833	13.1	12.6		.0981
3 035-08 LW2D	0.99	300	14.6	16.1	1)	.0820	16.6	16.0		.0890
4 035-08 LW2W	0	35	28.8	17.8	1)	.165	31.6	23.5		.185
5 035-08 ND	0.31	69	11.4	11.7	1.8	.0487	13.3	13.7	1.5	.0580
6 035-08 NDA	0.94	300	13.4	13.6	7.8	.0640	13.7	12.7	7.8	.0650
7 035-00 ND2	0.22	60	9.4	9.6	2.5	.0410				
8 049-00 ND3A	0.91	300	13.1	12.3	3.7	.0560				
9 040-00 ND	0.51	70	11.5	11.4	2.0	.0497	12.5	12.5	1.9	.0541
10 040-05 ND	0.23	70	11.6	11.6	2.3	.0500	13.2	15.0	2.3	.0584
11 040-05 NDA	0.44	140	11.7	12.1	4.2	.0521	13.4	14.9	4.0	.0602

1) Macropore content inadequate for light weight aggregate concrete due to porous aggregate particles

Table 13: Increased water content during ASTM C666 (Δm) by weighing the beams before and after frost testing and by the PF-method on slices cut from beams before and after frost testing, and degree of saturation at start (S) and increase at freeze/thaw deterioration ($+\Delta S$)

Concrete	$E_{relative}$ at stop freeze/ thaw	No.of freeze/ thaw cycles	Weight during test	PF-method (Sawing and drying of slices)			
			$+\Delta$ m (vol %)	$+\Delta$ m (vol %)	S_{start}	$+\Delta S_{fr/th}$	Δ w_e (g/g_{dry})
1 030-08 QD	0.79	300	0.5	3.0	1.037	0.366	.0130
2 030-08 LW1	0.49	140	4.6	2.1	1)	1)	.0148
3 035-08 LW2D	0.99	300	1.1	2.0	1)	1)	.0070
4 035-08 LW2W	0	35	3.7	2.8	1)	1)	.0200
5 035-08 ND	0.31	69	1.3	1.9	0.851	0.142	.0093
6 035-08 NDA	0.94	300	1.3	0.3	0.626	0.014	.0010
7 035-00 ND2	0.22	60	1.8	3)	0.777		
8 049-00 ND3A	0.91	300	0.1 2)	3)	0.819		
9 040-00 ND	0.51	70	1.2	1.0	0.858	0.075	.0044
10 040-05 ND	0.23	70	1.9	1.6	0.835	0.115	.0084
11 040-05 NDA	0.44	140	1.6	1.7	0.718	0.104	.0081

1) Macropore content not calculated for light weight aggregate concrete 2) 95 cycles, after that no increase was observed due to inaccurate scaling measurements 3) Not measured by PF-method after freeze/thaw

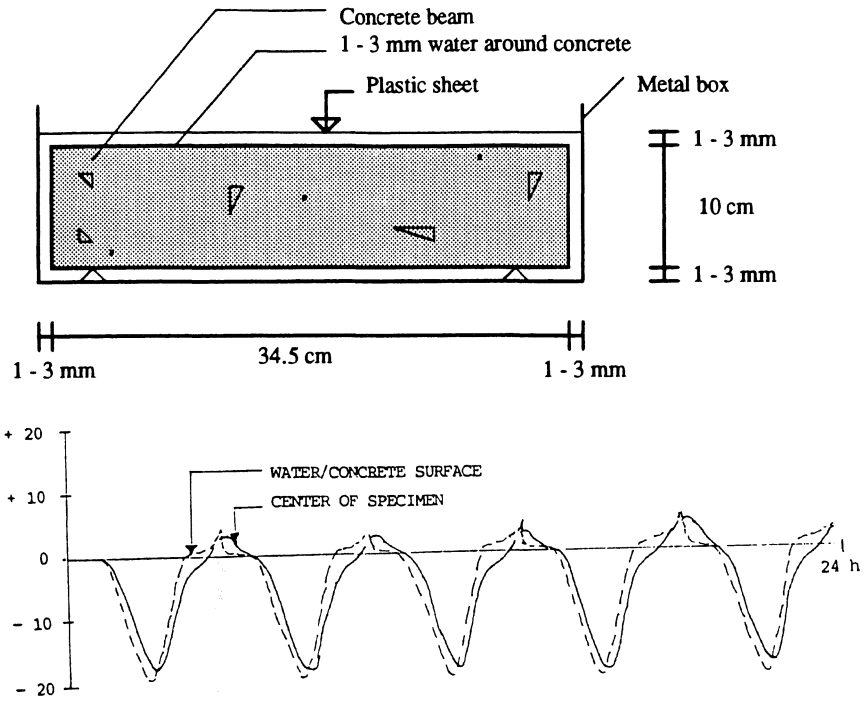

Figure 1: Test set-up and freeze/thaw cycle in ASTM C666 procedure A

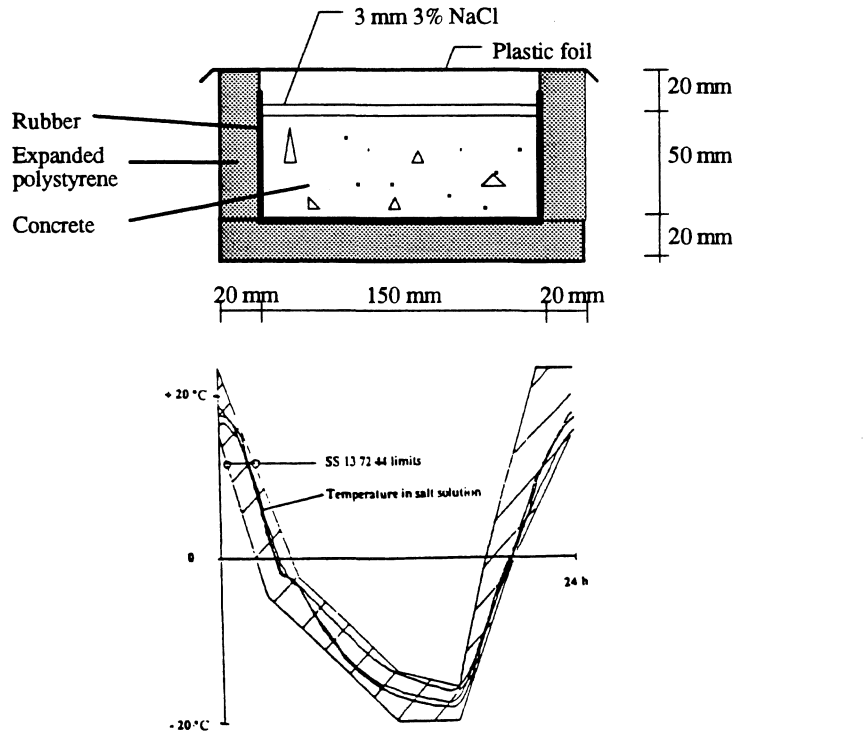

Figure 2: Preparation of test specimens and temperature cycle for SS 13 72 44.

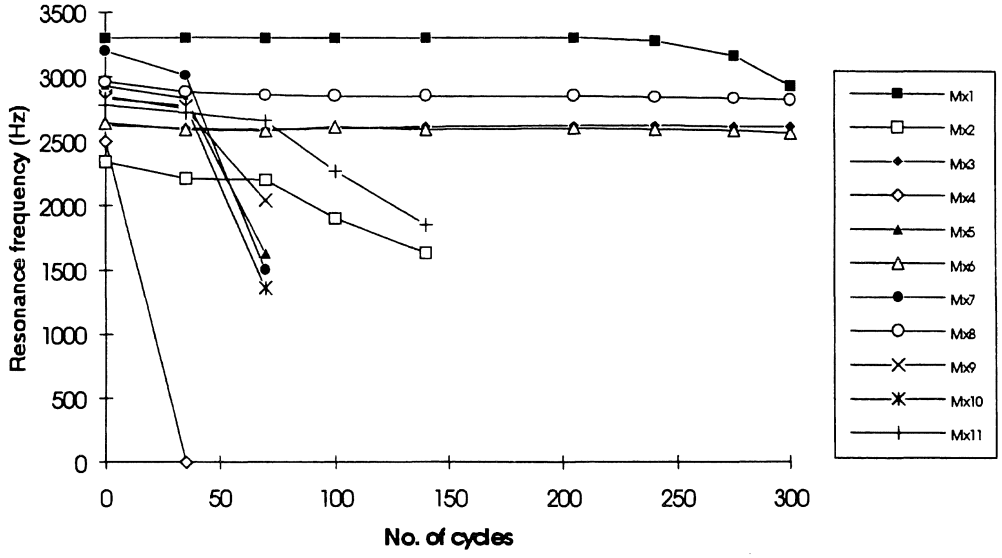

Figure 3: Internal cracking vs. number of cycles in ASTM C666 procedure A, three parallel beams

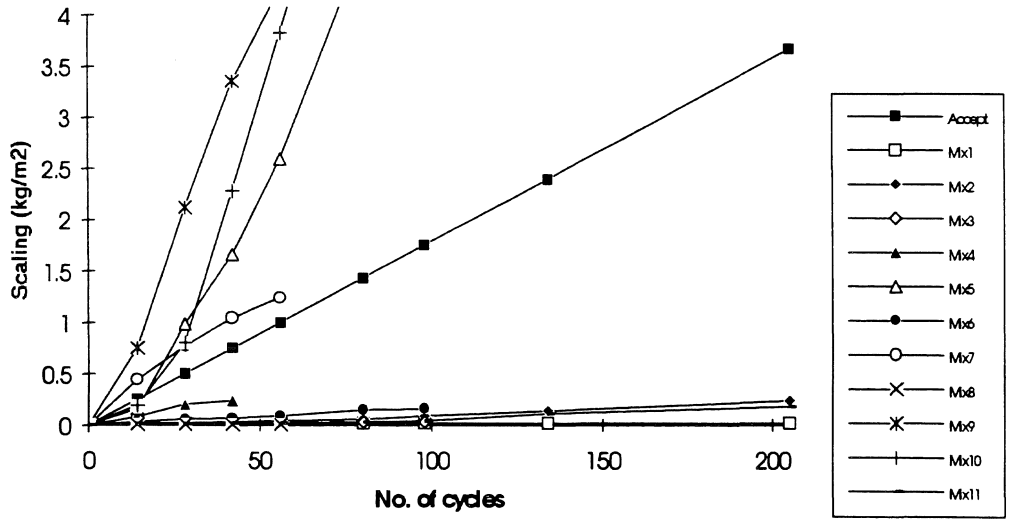

Figure 4: Scaling vs. number of cycles in SS 13 72 44, four parallel slabs for each Mix

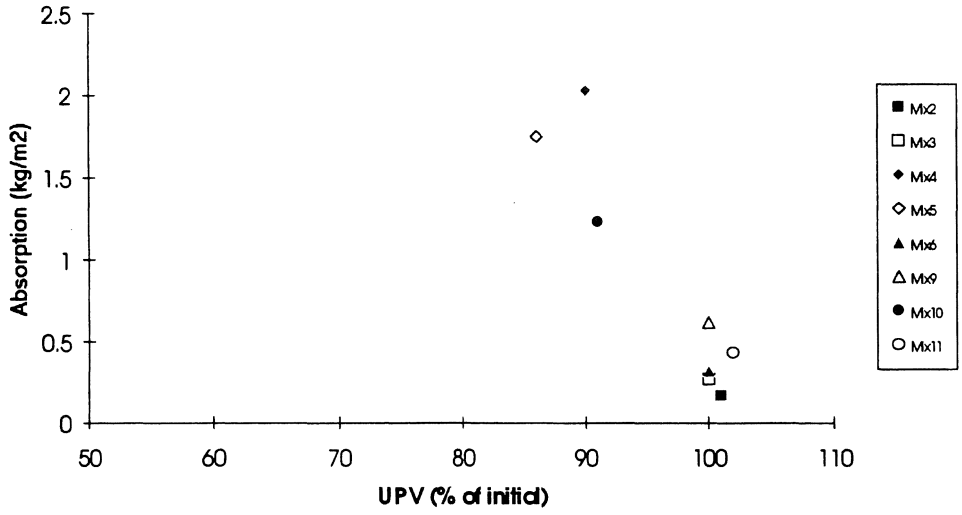

Figure 5: Pulse velocity vs. absorption after 56 cycles in SS 13 72 44.
Abs = -0.11 · UPV + 11.30, r = - 0.93.

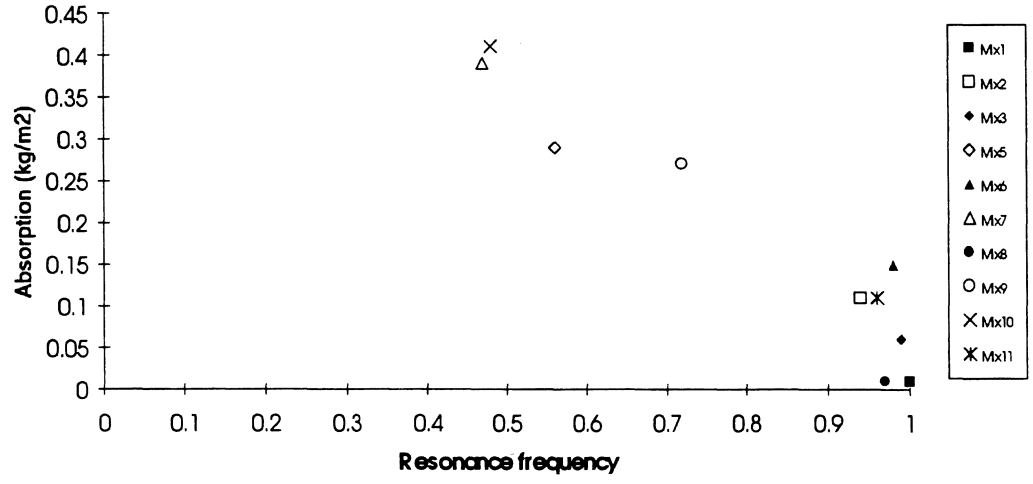

Figure 6: Resonance frequency (normalized to initial value) vs. absorption 70 cycles ASTM C666 proc. A **Abs = - 0.63 · resfreq + 0.69, r = - 0.95**

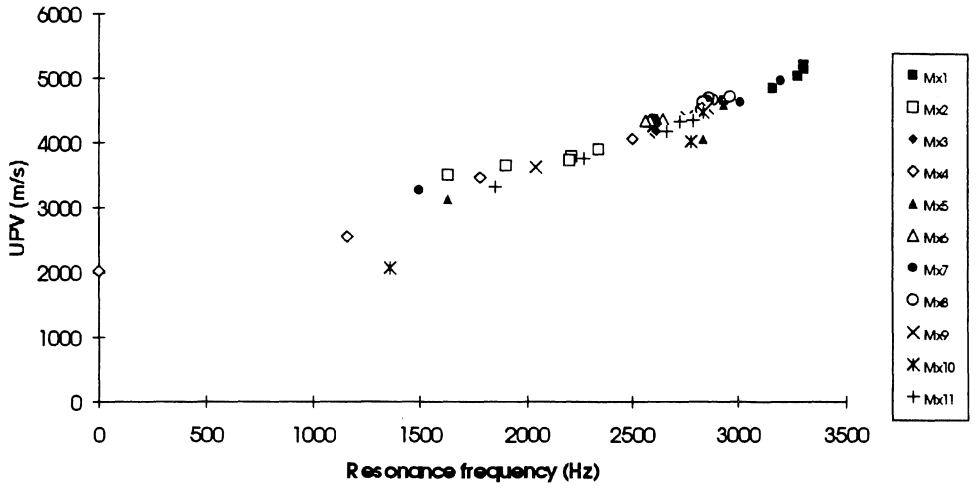

Figure 7: Resonance freqency vs. pulse velocity in ASTM C666 procedure A.
11 concretes up to maximum 300 cycles, max 10 measurements per series,
mean of three beams pr serie, 62 sets of data. **UPV = 1.10 · frequ + 1418, r = 0.96**

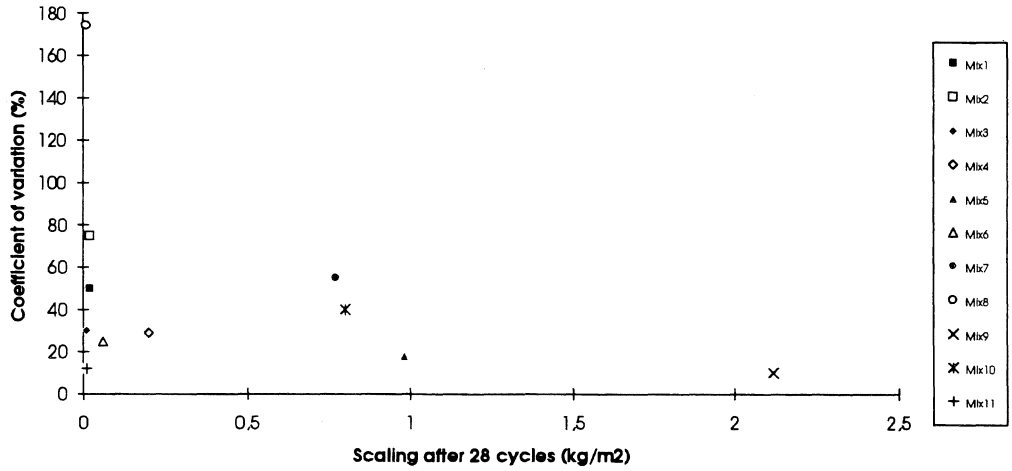

Figure 8: Scaling after 28 cycles versus coefficient of variation, SS 13 72 44

FROST DURABILITY OF HIGH STRENGTH CONCRETE: FROST/SALT SCALING AT DIFFERENT COOLING RATES

Stefan Jacobsen and Dag H. Sæther Norwegian Building Research Institute
Erik J.Sellevold Norwegian Institute of Technology

SUMMARY

The effects of variation of cooling rate and time at minimum temperature on frost deterioration of concrete have been investigated on three non-air entrained and one air entrained concrete. It was found that at equal number of freeze/thaw cycles the frost/salt scaling increased when reducing the rate of cooling for the non-air entrained concretes. Slow cooling rate produced more scaling at comparable periods in frozen condition compared to rapid cooling rate and variable time at minimum temperature. Air entrained concrete with very good frost/salt durability showed no clear effect of freeze/thaw cycle variations. Measurements of resonance frequency at prolonged cycling for two of the concretes (same binder, with/without air) showed that for the air entrained concrete the internal cracking was increased by increasing the rate of cooling. For the non-air entrained concretes the internal cracking was severe for all types of cycles. Measurements of absorption during the tests showed increased absorption with increased damage, and a good correlation between absorption and internal cracking. The scaling was found to accelerate when internal cracking increased. The two types of deterioration (scaling and cracking) therefore appear to be connected in tests where both cracking and scaling occurs. The results of this investigation illustrate an important difference between frost/salt scaling and internal cracking: scaling increased with reduced rate of cooling whereas internal cracking increased with increased rate of cooling.

Key words: concrete, durability, frost, frost/salt scaling, internal cracking, laboratory testing, mechanism of deterioration

1. INTRODUCTION AND PREVIOUS RESEARCH

Deterioration of concrete in freeze/thaw tests with water or salt solution can be due to internal cracking or surface scaling. Internal cracking is normally observed as loss of dynamic modulus of elasticity (measured by resonance frequency) or dilation, whereas surface scaling is seen as scaling of particles from the surface. Depending of concrete and design of test one may observe only scaling or only loss of resonance frequency or combinations of these two, Powers [1]. On a very frost durable concrete no damage is normally seen, even after high numbers of cycles. Deicer salts are known to amplify the scaling damage dramatically compared to pure water (frost/salt attack), Verbeck and Klieger [2]. Following the work [1, 2] and numerous other

studies on frost resistance, test methods have been developed to characterize durability against internal cracking in rapid freeze/thaw cycles (e.g. ASTM C666) and durability against surface scaling with deicer salts in slow freeze/thaw cycles (e.g. ASTM C672). In Scandinavia deicer salts are considered to be the main cause of frost damage. Recently some recommendations for deicer salt tests have been given [3, 4, 5].

Studying the effect of rate of cooling can give information about factors that affect the two modes of deterioration. Previous research on effect of freeze/thaw cycle variations include studies of cooling rate, time at minimum temperature and different minimum temperatures. A limited review points to three reports where internal cracking was found to increase with increased cooling rate, Powers [6], Fagerlund [7] and Pigeon et al [8], and one report where the opposite was found (using wet porous aggregate), Lin et al [9]. Stark [10] found that increased time at minimum temperature increased the cracking. Deicer salt scaling was found to increase by reduced minimum temperature and increased time at minimum temperature down to about - 22 °C, Studer [11], Lindmark [12], Hartmann [13], Petersson [14] and Marchand [18]. Increased cooling rate was found to lead to both reduced scaling, Sellevold et al [15], and increased scaling, Nischer [16], Hammer et al [17], Marchand [18] and Studer [11]. Fagerlund [19] was of the opinion that the design of the freeze/thaw test determines the effect of cooling rate: mainly the ability of the specimen to absorb water during freeze/thaw.

The referred studies of effect of cooling rate on scaling were mostly performed with air cooled freeze/thaw cabinets where it is difficult to perform only variations of cooling rate without affecting time at minimum temperature. The purpose of this study was therefore to investigate the effect on scaling of cooling rate without changing the time at minimum temperature, and also to compare with scaling at variable time at minimum temperature (always - 18 °C) at fixed coolingrate. An effort has also been made to "bridge the gap" between rapid freeze/thaw and slow deicer salt freeze/thaw cycles, by measuring both scaling and cracking during test. Since the degree of saturation is considered very important for the performance of concrete in a frost test, Fagerlund [7, 19], also absorption during test has been measured.

2. FREEZE/THAW CYCLES AND MEASUREMENTS PERFORMED

To be able to control the freeze/thaw cycle in a precise manner during frost/salt testing, the test set-up described by Setzer and Hartmann [3,13] was used (CDF test set-up). This is an upside down test set-up, i.e. the

concrete surface to be tested is facing downward in the salt solution in a steel container. The heat is transferred to and from the salt solution by a glycol bath in which the temperature cycle can be designed very accurately by controlling heating, cooling and flow rate of the glycol. Figure 1 shows test set-up for one specimen. The equipment used was built at The Norwegian Building Research Institute with a powerful cooling and circulation system to be able to run different types of cycles. The apparatus has a capacity of testing six specimens with surface areas of 150 x 150 mm^2 each. In the present experiments two concretes with three parallel specimens each (slabs 45 - 50 by 150 by 150 mm) were tested simultaneously in the test equipment. Temperature homogeneity in the glycol bath was assured by continuous stirring. The temperatures in glycol bath and salt solution were measured at three boxes each. Thermocouple configuration is shown in figure 1. Temperature variations in the salt solution were within 0.5 °C.

Figure 2 shows the freeze/thaw cycles and in table 1 the characteristics of the freeze/thaw cycles are given. The freeze/thaw cycles investigated were designed to study the effect of cooling rate by varying only the rate of cooling (constant time at minimum temperature), and comparing with different periods at minimum temperature (constant rate of cooling).

From figure 2 it is seen that very sharply defined temperature cycles are produced in contrast to normal air cooled systems.

The thawing part was identical for all cycles, and all tests were performed down to - 18 °C, which is the same minimum temperature as in other parts of this study [20]. The rapid freeze/thaw cycle no. 5 (5 cycles per day, 12 °C/h) is approximately the same as in the ASTM C666 procedure A test in [20], whereas the slow cycle no. 2 (2 cycles per day, 2.8 °C/h) has approximately the same cooling rate as the cycle prescribed in The Borås method [4], also used in [20]. Cycles 5, 3b and 2 therefore "bridge the gap" between the rapid freeze/thaw cycles and slow frost/salt cycles. However, it is not expected that this should reveal all differences between the different types of tests, since other experimental details than just temperature at concrete surface vary considerably between the tests. The purpose of this "bridge-the-gap-approach", was mainly to study changes in scaling with different cycles, and also to observe changes in cracking and absorption/degree of saturation.

During thawing the following measurements were performed on the slabs:
- Scaled off material, removed from the test surface and container using pure water from a spray bottle and the type of brush prescribed in [4], dried at 105 °C for 24 hours and weighed (0.01 g accuracy).
- Weight of the slab after removing scaled off material (surface dry).

- Pulse velocity through the slab parallel to the test surface using a 54 MHz PUNDIT and a water based contact gel.
- Resonance frequency using a Ono Sokki CF-910 frequency analyser. The slabs were placed horizontally on a piece of foam rubber. The accelerometer was fixed vertically to a corner of the top surface with putty, and the first node was recorded. The slab was vibrated by light hitting with a plastic hammer. The measurements were found to be very repeatable.

The absorption of salt solution in the specimens during freezing and thawing was calculated by taking into account scaled off mass as described in [21]. This was done since it is recognized that degree of saturation of a concrete is of fundamental importance to its performance, Fagerlund [7, 19, 24].

3. CONCRETES, CURING AND PREPARATION OF SPECIMENS

Materials and concrete mixes:
Four different concretes were tested at five different freeze/thaw cycles. In table 2 concrete mixes and compressive strengths are given. In table 3 characteristics of cement and silica fume are given. The cements used were from Norcem, Dalen in Norway: Ordinary Portland Cement (P 30) and high strength cement (HS 65). The silica fume (dry) was Scancem Micropoz from a plant in Norway (Ila & Lilleby). The aggregate consisted of granite/gneiss rock from Årdal Norway, and data are given in table 4.

The concrete notations give water/binder ratio (e.g. 0.40), silica fume/binder ratio (e.g. 05 = 5 %) and air entrainment (A) or not. Three of the concretes (035-08, 037-00, 040-05) were non-air entrained with air void spacing factors in the hardened concrete 0.97 - 1.04 mm, and one concrete (040-05A) was air entrained with an air void spacing factor of 0.33 mm, [20]. Compressive strengths were measured on three parallel 10 cm cubes and ranged from 73 to 113 MPa at start of test. The concrete mix 040-00 was only tested in cycle 5.

The concretes were mixed in a horizontal rotating counter current mixer type Eirich 50 l. The mix procedure consisted of 1 minute dry mixing and 2 minutes of mixing with water and super plasticizer (melamine). The air entrained concrete was mixed an additional 1 minute with the air entraining agent (tenside). 10 cm cubes for compressive strength and 15 cm cubes for frost/salt testing were moulded in steel moulds in two layers with 15 seconds vibration in each layer.

Concrete curing:
Specimens were stripped after 24 hours and stored in water at 20°C. Due to the limited test capacity of the equipment, one type of freeze/thaw cycle was performed at a time. Therefore each concrete mix had to be tested at different ages for the different freeze/thaw cycles.

The 040-05 and 040-05A concretes were water cured to the start of testing (2 - 9 months). These two concretes were freeze/thaw tested up to rather high number of cycles. The effect of prolonged water curing (from 2 to 9 months) was checked by performing the same cycle (cycle 5) two times on the concretes: at 2 months (first series) and at 9 months curing (last series). As will be seen later, the effect of the prolonged water curing was very small on scaling, but it reduced significantly the internal cracking.

The 037-00 and 035-08 concretes were cured longer, and efforts were taken to make sure that the moisture condition was the same for all specimens even though tested at different times. After initial water curing for 10 and 7 months respectively, the 15 cm concrete cubes were kept at 50 % RH and 23 °C for 2 1/2 months and then sealed in plastic bags. Before preparation of specimens (see below), the weights were checked. No weightloss was observed on any of the specimens during storage in plastic bags (0 - 2 months). The testing of these two concretes lasted only two months, since only 28 cycles were run for each of the 5 different cycles.

In table 5 the curing regimes are given. Table 6 gives absorption on water curing and weightloss on subsequent curing at 50 % relative humidity before preparation of specimens. A net gain of weight was obtained on curing.

Preparation of specimens:
After curing according to table 5 and 6, three slabs of 45 - 50 mm thickness were sawn from each 150 mm cube perpendicularly to the moulded surface. Only sawn surfaces were tested. The slabs were then stored for 7 days at 50 % RH during which time the lateral sides of the slabs were painted with a polyamid amine epoxy paint. A solid tape was used on top of the hardened epoxy paint as reinforcement, since this was found to result in negligible scaling from the lateral surfaces. 20 mm thick polystyrene rubber insulation was placed on top of each specimen to prevent condensation on the top surface during the thawing part of the cycle. This hindered absorption elsewhere than on the test surface. After 7 days at 50 % RH and 23 °C the slabs absorbed pure water for 3 days, and then freeze/thaw testing in 3 % NaCl solution started. The 035-08 concrete was dried at 50 °C for 24 hours in a ventilated oven before the 7 days storage at 50 % RH. This treatment is

known to increase the scaling in a frost/salt test [15], and was used to make this concrete more susceptible to scaling.

The conditioning (except for the 50 °C predrying), is comparable to the procedure used in the Borås method [4]. This was done since some of the concretes were tested in the Borås method in an other part of this study [20].

4. RESULTS

In table 7 scaling values after 28 freeze/thaw cycles are given for all test series and in table 8 the coefficients of variation are given for the same tests. In figure 3 a plot of scaling after 28 cycles vs. time below - 3 °C is shown. Figure 4 shows the absorption during 3 days presuction with pure water, and the subsequent increase in absorption during the first 6 cycles for 040-05 and 040-05A. In figure 5, a plot of absorption vs. scaling at 28 cycles is shown. Figure 6 shows a plot of absorption vs. resonance frequency after 28 cycles. In figure 7 and 8 plots of resonance frequency vs. number of freeze/thaw cycle are shown for 040-05 and 040-05A for the different freeze/thaw cycles. Figure 9 shows resonance frequency vs. pulse velocity. Table 9 gives accumulated scaling (kg/m^2) for all test ages, table 10 gives absorption (kg/m^2) during presuction and during frost/salt testing and table 11 gives resonance frequency (Hz).

5. DISCUSSION

Scaling:
From table 7 we see for the non-air entrained concretes that the scaling after 28 cycles increases with reduced cooling rate. Furthermore we see that for constant cooling rate and variable time at minimum temperature the scaling increases with increased time at minimum temperature. Note that for cycle 1.5 (rapid cooling and long time (11.27 h) at minimum temperature), the period below - 3 °C (13.59 h) is much longer than for cycle 2 (6.69 h) with the slowest cooling rate and almost no time at minimum temperature. Still the scaling increases more by reducing the cooling rate than by increasing the time in frozen condition for 040-05 and 037-00. The dried/resaturated 035-08 has slightly higher scaling for cycle 1.5 than for cycle 2.

From figure 3 it is also seen that the scaling at low rate of cooling is larger than at high cooling rate and increased period at minimum temperature for comparable periods in a frozen condition. From the slopes in figure 3 it appears that increase in scaling per unit time in frozen condition is larger when reducing the cooling rate than when increasing the time at minimum temperature. The results indicate that working in a slow gradient (increased

time at intermediate temperatures with some ice but still considerable amount of unfrozen water according to the phase diagram of water - NaCl) is very important for frost/salt scaling to occur, as proposed by Sellevold [15]. For the air entrained concrete (040-05A) with very good frost/salt scaling resistance there is no significant effect of the cycle variations.

By using lower primary freezing temperatures than - 3 °C for calculation of time in frozen condition per cycle, this time will be shorter for the slow cycles compared to the cycles with rapid rate of cooling and increased time at minimum temperature. Making similar plots to figure 3 with lower freezing temperatures than - 3 °C will therefore amplify the effect on scaling of reduced cooling rate compared to increased time at minimum temperature. However, from figure 2 it is seen that nucleation takes place at about - 3 °C for all tests.

From table 7 we see that the prolonged water curing of 040-05 and 040-05A (+7 months) resulted only in a minor reduction in scaling compared to scaling after 2 months water curing. This slight reduction in scaling of sawn surfaces after prolonged water curing makes sense related to increased hydration and reduced water absorption during 3 days absorption before frost/salt testing (table 10).

Internal cracking:
Figures 7 and 8 show reduction in resonance frequency vs. number of cycles for 040-05 and 040-05A. For the air entrained 040-05A there is a clear effect that rapid cooling rate results in more deterioration than slow cooling rate. 040-05 (no air) is rather quickly deteriorated by all cycles.

From table 11 and figures 7 and 8 we see that the resistance against internal cracking is considerably increased at prolonged water curing (cycle 5 vs. cycle 5 +7 months). It was also noted that at increasing degree of internal cracking (prolonged freeze/thaw cycling beyond 28 - 56 cycles) the slabs taken from the centre of the cubes cracked more than slabs from the sides of the cubes, even though there were no such systematic effects on scaling at 28 cycles. This is possibly a size effect since the outer parts are more wet and hence better hydrated than the centre part of the cubes.

In most of the tests the concretes were deteriorated after high number of freeze/thaw cycles. This was expected since normally an air void spacing factor of about 0.20 mm is required to withstand internal cracking in rapid freezing and thawing. (The present concretes had high spacing factors of 0.33 - 1.07 mm). Table 11 shows that after 28 cycles the dried/resaturated 035-08 had largest loss of resonance frequency (most cracking). 037-00

suffered much less internal cracking. It appears that concrete composition and drying/resaturation treatment, in addition to air entrainment and curing period, affect the susceptibility of concrete to internal cracking.

Appearance of damage and effect of cracking on scaling:
In general scaling was evenly distributed in the cement paste part of the sawn test surfaces. At 28 cycles only a few small aggregate particles scaled, and the main part of the scaling occurred in the cement paste. At higher number of cycles, concretes with severe internal cracking could be freeze/thaw tested to complete disintegration into coarse aggregate and fines.

From tables 9 and 11 we see that when the internal cracking increases, the scaling accelerates dramatically (also for the 040-05A concrete which has very low scaling at low levels of internal cracking). This demonstrates that the frost/salt scaling in a laboratory test may depend on to which degree the test conditions produce internal cracking in addition to scaling. The effect of 5 % silica fume on scaling and cracking is seen by comparing 040-00 and 040-05. At 28 cycles silica fume reduces the scaling. However, at prolonged cycling it appears that silica fume increases the tendency to internal cracking. When cracking occurs, the scaling accelerates dramatically and becomes larger than the scaling of the OPC concrete. In the literature contradictory results exist on the effect of silica fume on frost durability. Important reasons for opposing results of silica fume on frost testing results may be to what extent internal cracking and scaling occurred simultaneously. Also curing conditions are important.

The connection between cracking and scaling has earlier been demonstrated by Petersson [22]. He measured pulse velocity in the slabs during salt/frost testing in the Borås method. Sudden and accelerated scaling was accompanied by abrupt loss in pulse velocity. One important aspect of the increased cracking may be the frost resistance of silica fume concrete (and the choice of appropriate test methods for this type of concrete). A test method that gives less internal cracking may reduce the risk of measuring large acceleration in scaling. This is probably the explanation for the results found by Petersson [23] on his non-air entrained mortar prisms with and without silica fume submerged in salt solution during freezing. At early freeze/thaw cycling the silica fume mortar had lower scaling than OPC mortar. However, at higher number of cycles the scaling accelerated, most likely as a result of extensive internal cracking.

Figure 9 shows the relationship between resonance frequency and pulse velocity for 040-05. The figure shows that the resonance frequency is much

more sensitive than pulse velocity to internal cracking. This is in agreement with measurements performed on beams in the ASTM C666 test, [20].

Effect of absorption during freeze/thaw:
Figure 4 shows absorption during presuction and the increased absorption at start of freezing and thawing for concretes 040-05 and 040-05A tested in the slow cycle 2. The large increase in absorption when freeze/thaw cycling started compared to during isothermal absorption always took place, as observed and discussed earlier, Powers [1], Fagerlund [24], Hartmann [13] and [20, 21].

Figure 5 shows a plot of scaling vs. absorption of salt solution after 28 cycles for all test series. 040-05A always has low scaling and low absorption at 28 cycles. For the two concretes with largest tendency to internal cracking as measured by loss of resonance frequency, (035-08 and 040-05, see table 11) scaling increases with absorption. However, for concrete 037-00 with smaller tendency to internal cracking, there appears to be no such relationship even though the scaling is approximately on the same level and with the same effect of freeze/thaw cycle as 035-08 and 040-05. Therefore it seems that increased absorption at freeze/thaw cycling cannot account for the increased frost/salt scaling for all types of concrete and freeze/thaw cycles.

Figure 6 shows a plot of absorption vs. resonance frequency (normalised to frequency at 0 cycles) after 28 cycles for all test series. For the concretes tested it is seen that the absorption is more strongly related to cracking (loss in resonance frequency) than to scaling, since a good trend of increased absorption at reduced resonance frequency can be seen. The absorption cannot be directly related to a "global" degree of saturation, since the surface part of the slab in the salt solution is expected to have higher degree of saturation than the top surface.

Mechanisms of deterioration:
At low levels of internal cracking ("pure frost/salt scaling"), scaling and internal cracking appear to be governed by different damage mechanisms. This statement is based on the observation that the cooling rate has opposite effect on the two types of deterioration: low cooling rate increases the frost/salt scaling, whereas rapid cooling increases the internal cracking. Powers [25] suggested that osmotic pressure might be an explanation for the increased scaling in the presence of salts. Also in the theory of microscopic ice lens formation postulated by Powers and Helmuth [26], increased time in frozen condition will contribute to build up disruptive pressures, as illustrated by their dilation experiments. In the present experiments the concretes are in constant contact with water or salt solution and they can therefore absorb

water during freezing and thawing. The results are therefore not quite comparable with sealed tests with no exchange of water [7]. However, in the case of scaling damage, the surface must be covered with salt solution during freezing if scaling is to occur, [2]. The present results support that time consuming mechanisms (osmotic or ice lens segregation type [25, 26]) are more important than fast (hydraulic type [6]) mechanisms for the disruptive effect of salt on scaling.

6. CONCLUSIONS

The frost/salt scaling of the non-air entrained concretes at a given number of cycles was increased by reducing rate of cooling and increasing period at minimum temperature.

At comparable periods in frozen condition, higher scaling was observed when reducing the cooling rate than when increasing the period at - 18 °C after a rapid cooling. No significant effect of different freeze/thaw cycles on pure scaling could be seen on the air entrained concrete with very good scaling durability.

Frost damage could be associated with absorption during freeze/thaw. Internal cracking (loss of resonance frequency) was clearly related to increased absorption during freeze/thaw.

The internal cracking was not as clearly and systematically affected by cycle variations as scaling for the different concrete types. For the air entrained concrete, rapid rate of cooling resulted in more internal cracking than slow rate of cooling. Two of the three non-air entrained concretes were deteriorated rather fast by internal cracking in all cycles without any significant differences between different freeze/thaw cycles.

The scaling was found to accelerate when the internal cracking increased. The two mechanisms of deterioration (scaling and cracking) therefore appear to be connected in tests that produce cracking in addition to "pure scaling".

From the present observations it seems that frost salt scaling is governed by a mechanism that requires time to build up disruptive pressure, and that a slowly changing temperature amplifies this disruptive effect. Internal cracking on the other hand, appears to be more governed by pressure generated on rapid freezing of water.

7. REFERENCES

1. Powers T.C., PCA Bulletin 5 (Skokie, Ill. 1945)
2. Verbeck G., Klieger P., Highway Res. Board Bulletin No. 150 (1956)
3. RILEM draft recomm., Mat.&Str. 28 (1995) 175-182
4. RILEM draft recomm., Mat.&Str. 28 (1995) 366-369
5. RILEM draft recomm., Mat.&Str. 28 (1995) 369-371
6. Powers T.C., Proc. of the Highway Research Board 29 (1949) 184-211
7. Fagerlund G. Mat.&Str. 10 (1977) 231 - 254
8. Pigeon M., et al., ACI Journal (Sept.-Oct.1985) 684-692
9. Lin C.-H., et al., Transp. Res. Rec. 539 (1975) 8-19
10. Stark D., PCA Res. and Dev. Bull. RD 096, (Skokie, Ill. 1989)
11. Studer W., The Int. Workshop on Freeze-Thaw and Deicing Salt Scaling Resistance. of Con., Ed. J.Marchand and M.Pigeon (1993) 175 - 187
12. Lindmark S., Report TVBM-7055 Lund Inst. of Tech., (Sweden, 1993)
13. Hartmann V., Dr.Ing. Diss., Univ. Essen, (Germany, 1993)
14. Petersson P.-E., SP-Swed. Nat. Test. and Res. Inst. report 22 (1994)
15. Sellevold E.J, Farstad T., Nord.Conc. Res. Pub No.10 (1991) 121 - 138
16. Nischer P., Zement und Beton Heft 2 (1976) 73 - 77
17. Hammer T.A., Sellevold E.J., ACI SP - 121 (1990) 457 - 489
18. Marchand J. PhD-th. École Nat.des Ponts et Ch.326 p. (France, 1993)
19. Fagerlund G., Nord. Conc. Res. Pub. No.11(1992) 20 - 36
20. Jacobsen S., Sellevold E.J., Hammer T.A., paper to be submitted for publication at the 4th Int. Symp. on High Perf. Concrete (Paris 1996)
21. Jacobsen S., Sellevold E.J., Nord. Conc.Res. Pub No.14, (1994) 26 - 44
22. Petersson P.E., Results presented at a Nordic research seminar on Frost durability of concrete, Lund Inst. of Tech. (Sweden, April 1993)
23. Petersson P.E., SP-Swed. Nat. Test. and Res. Inst. report 32 (1986)
24. Fagerlund G., TVBM 3048 Lund Inst. of Tech.37 - 66 (Sweden 1991)
25. Powers T.C., Proc. of the ASTM, Vol.55 (1955)
26. Powers T.C. and Helmuth R.A., Proc. of the Highway Res. Board 32 (1953) 285-297

8. ACKNOWLEDGEMENT

The research was carried out with financial support from The Norwegian Research Council/ Norcon programme, Public Roads Laboratory, Norcem and Norwegian Contractors.

Résumé

Les effets de la variation du taux de gel et le temps à la température minimale sur la détérioration du béton par écaillage en présence de sel fondant ont été essayés dans le laboratoire. Trois bétons différents sans, et un béton avec entrainêment d'air ont été essayés, et l'écaillage a été comparé au même nombre de cycles de gel-degel. Nous avons trouvé que l'écaillage a augmenté quand le taux de gel a été reduit dans les betons sans entrainêment d'air. En comparaison avec un taux de gel rapide et des périodes aux températures minimales prolongées (toujours - 18 °C), un taux de gel lent a augmenté l'écaillage plus efficace, (avec la même période de gel). Sur le béton avec entrainêment d'air et avec une durabilité forte contre l'écaillage, nous n'avons pu montré aucun effet significant sur les variations de cycles de gel/degel sur l'écaillage. Ce béton avec entrainêment d'air a eu une augmentation de la fissuration quand le taux de gel a été augmenté. Un béton avec la même composition, mais sans entrainêment d'air a été grièvement fissuré par tous les différents types de cycles de gel-degel. L'absorption de l'eau/solution de sel fondant pendant l'essai a été suivi dans toutes les éprouvettes pour connaître les changements de degré de saturation. Le degré de saturation est consideré comme une paramètre très important pour le comportement du béton au gel. Les resultats ont montré un augmentation de l'absorption suivant la destruction par fissuration et par écaillage. Un corrélation entre absorption et fissuration a été montré. On a trouvé que l'écaillage a été accélléré par la fissuration. En conséquence les deux mécanismes de destruction par le gel, fissuration et écaillage, sont liés dans des essais où on trouve tous les deux mécanismes de détérioration. Les resultats de cette recherche ont aussi illustré une différence importante entre détérioration par écaillage en présence de sels fondants et fissuration: l'écaillage en presence de sel fondant augmente quand le taux de gel diminue, tandis que la fissuration augmente quand le taux de gel augmente.

Table 1: Characteristics of freeze/thaw cycles used in the investigation.
All cycles: 1.93 h thawing (- 18 to +7 °C), 0.87 h at 7 °C

No. of cycles pr. day	Cooling rate (°C/h)	Time at - 18 °C (h)	Duration of cycle (h)	Time below - 3 °C (h)
5	12	0.07	4.8	2.39
3 a	12	3.27	8	5.59
1.5	12	11.27	16	13.59
3 b	4.9	0.07	8	4.29
2	2.8	0.07	12	6.69

Table 2: Concrete mixes tested (volume fraction cement paste 0.31)

Mix	w/c+s	s/c+s	Cement kg/m^3	type	Aggr. kg/m^3	SP kg/m^3	AEA kg/m^3	Slump cm	Air vol-%	f_{c28} MPa	$f_{c\ start}$ MPa
040-00 1)	0.40	0	432	P30	1799	4.92	-	20	1.6	69	74
040-05	0.40	0.05	409	P30	1782	6.46	-	19	2.0	79	83
040-05A	0.40	0.05	411	P30	1702	4.93	0.13	21	5.1	68	73
037-00	0.37	0	453	P30	1792	8.62	-	21	1.4	81	-
035-08	0.35	0.08	440	HS65	1761	8.11	-	14	1.5	103	113

1) The 040-00 concrete was only tested in one type of freeze/thaw cycle (cycle 5).

Table 3: Composition of cement and silica fume (%).

Component	Cement		Silica fume
	HS 65	P 30	
SiO_2	22.1	20.9	91.2
Al_2O_3	4.1	4.6	0.3
Fe_2O_3	3.4	3.5	2.8
CaO	64.3	63.4	
MgO	1.0	1.8	1.5
SO_3	3.1	3.1	0.5
K_2O	0.4	0.9	0.7
Na_2O	0.2	0.4	0.4
L.O.I.	1.3	1.0	1.7
Fineness (m^2/kg)	4180	3580	15 -20000

Table 4: Particle sizes of aggregate, fineness modulus (FM) and density

Aggregate	sieve size (mm) - % passing								FM	Density
	0.125	0.25	0.5	1	2	4	8	16	ISO	g/cm^3
Gneiss granite	3	5	12	23	37	48	63	97	4.64	2.67

Table 5: Curing periods of the cubes before sawing and preparation for testing (months)

Mix	Curing in water	50 % RH 20 °C	Sealed (Taped in plastic bags)	Sawing, Preparation Testing
040-05 040-05A	2 - 9	0	0	after water curing
037-00	10	2 1/2	0 - 2	after storage in plastic bags,
035-08	7	2 1/2	0 - 2	before start of freeze/thaw test

Table 6: Moisture changes during curing (vol-% of paste).

Mix	Absorption at water storage	Water loss at 50 % RH
040-05	3.9 - 5.8 1)	(0) 2)
040-05A	4.5 - 6.5	(0) 2)
037-00	6.2	- 5.4
035-08	4.2	- 3.1

1) The two figures refer to after 2 months and after 9 months
2) Only cured in water

Table 7: Scaling after 28 cycles for all test series (kg/m^2), mean of three specimens

No of cy. pr day	Cooling rate	Time at - 18 °C	Time < - 3 °C	Mix 040-05	Mix 040-05A	Mix 035-08	Mix 037-00
	°C/h	h	h	scaling (kg/m^2)			
Reduced cooling rate, constant time at minimum temperature							
5 *	12	0.07	2.39	0.34	0.17	0.22	0.30
5(+7 mths)	12	0.07	2.39	0.27	0.12		
3 b	4.9	0.07	4.29			0.60	0.81
2	2.8	0.07	6.69	1.25	0.13	0.90	1.20
Increased time at minimum temperature, constant rate of cooling							
5 *	12	0.07	2.39	0.34	0.17	0.22	0.30
3 a	12	3.27	5.59	0.53	0.20	0.53	0.69
1.5	12	11.27	13.59	0.83	0.19	1.14	0.99

*: same series, reference cycle for comparing effect of cooling rate and time at - 18 °C.

Table 8: Coefficients of variation (%) of scaling at 28 cycles, three parallel specimens

Cycle	040-05	040-05A	035-08	037-00
5	6	11	6	15
5 (+7mths)	11	8		
3 a	2	5	18	11
3 b			15	4
2	18	25	7	4
1.5	19	18	18	5

Table 9: Accumulated scaling for all test series (kg/m^2)

Cycle	Mix	7	14	28	56	75	100
5	040-00			0.85	2.58	4.51	
	040-05			0.34	10.13		
	040-05A			0.17	0.47	0.81	1.57
13 °C/h	035-08	0.02	0.07	0.22			
0.07 h at -18	037-00	0.04	0.11	0.30			
5	040-05			0.27	1.46	2.98	7.01
(+ 7 months)	040-05A			0.12	0.36	1.00	2.04
3 a	040-05			0.53	3.90	8.86	
	040-05A			0.20	0.63	1.65	
13 °C/h	035-08	0.03	0.12	0.53			
0.07 h at -18	037-00	0.09	0.27	0.69			
1.5	040-05			0.83	4.88		
	040-05A			0.19	0.76		
13 °C/h	035-08	0.05	0.20	1.14			
11.27 h at -18	037-00	0.13	0.39	0.99			
2	040-05			1.25	14.95		
	040-05A			0.13	0.40	0.64	0.93
2.8 °C/h	035-08	0.02	0.14	0.90			
0.07 h at -18	037-00	0.17	0.52	1.20			
3 b							
4.9 °C/h	035-08	0.02	0.11	0.60			
0.07 h at -18	037-00	0.09	0.29	0.81			

Table 10: Absorption during presuction and freeze/thaw testing (kg/m^2)

Cycle	Mix	- 3 days	0	7	14	28	56	75	100
5	040-00	0.31	0			0.48	0.92	1.07	
	040-05	0.24	0			0.77	2.01		
	040-05A	0.25	0			0.35	0.96	1.20	1.52
13 °C/h	035-08	0.44	0	0.11	0.24	0.84			
0.07 h at -18	037-00	0.39	0	0.11	0.26	0.43			
5	040-05	0.17	0			0.47	1.40	1.13	1.60
(+ 7 months)	040-05A	0.19	0			0.22	0.61	0.91	1.12
3 a	040-05	0.19	0			0.85	2.21	1.91	
	040-05A	0.19	0			0.33	0.90	1.24	
13 °C/h	035-08	0.40	0	0.12	0.34	1.33			
0.07 h at -18	037-00	0.31	0	0.10	0.22	0.56			
1.5	040-05	0.12	0			0.97	2.36		
	040-05A	0.16	0			0.35	0.89		
13 °C/h	035-08	0.36	0	0.16	0.52	1.81			
11.27 h at -18	037-00	0.31	0	0.16	0.40	0.92			
2	040-05	0.19	0			1.39	2.53		
	040-05A	0.20	0			0.40	0.86	1.03	1.18
2.8 °C/h	035-08	0.36	0	0.12	0.37	1.33			
0.07 h at -18	037-00	0.29	0	0.10	0.19	0.38			
3 b									
4.9 °C/h	035-08	0.35	0	0.10		1.26			
0.07 h at -18	037-00	0.27	0	0.13		0.62			

Table 11: Resonance frequency (Hz)

Cycle	Mix	0	7	14	28	56	75	100	135	205
5	040-00	4288			3463	2513	1938	750		
	040-05	4300			2425	363				
	040-05A	4150			3913	2763	2225	1730	700	
13 °C/h	035-08	4520	4460	4380	3050					
0.07 h at -18	037-00	4460	4400	4383	4275					
5	040-05	4200			3338	1838	1100	750		
(+ 7 months)	040-05A	4225			4100	2513	3200	3000	2725	2200
3 a	040-05	4225			2513	1100	463			
	040-05A	4163			3888	3188	2775			
13 °C/h	035-08	4400	4350	4070	1540					
0.07 h at -18	037-00	4430	4400	4370	4140					
1.5	040-05	4325			2500	863				
	040-05A	4150			3875	3200				
13 °C/h	035-08	4350	4290	3740	1020					
11.27 h at -18	037-00	4460	4430	4317	3750					
2	040-05	4263			2175	700				
	040-05A	4075			4050	3950	3875	3863	3875	3763
2.8 °C/h	035-08	4430	4350	4040	1420					(175
0.07 h at -18	037-00	4390	4310	4300	4210					cy)
3 b										
4.9 °C/h	035-08	4430	4400	4225	1825					
0.07 h at -18	037-00	4420	4390	4325	4075					

040-05/05A: mean of two specimens (excl. centre specimen)
035-08/037-00: mean of all three specimens

FIGURES

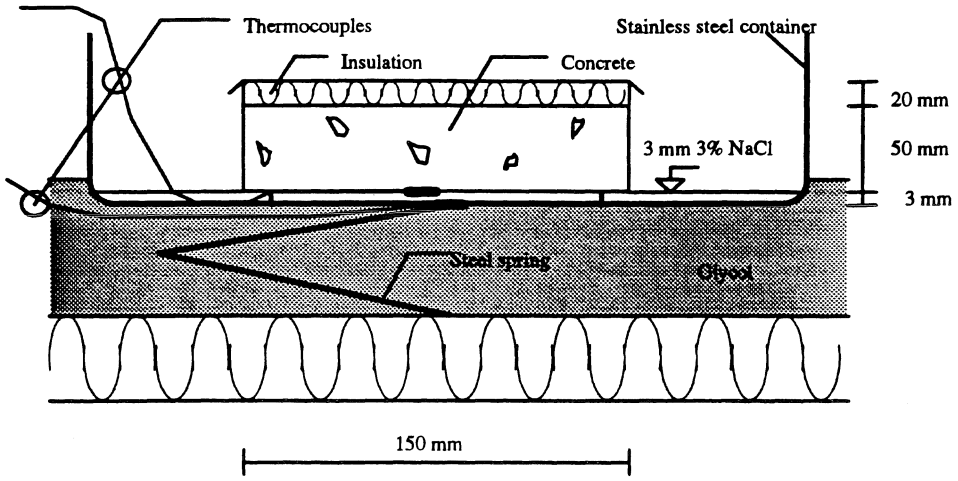

Fig. 1: Test set-up and specimen (slab 45 - 50 by 150 by 150 mm)

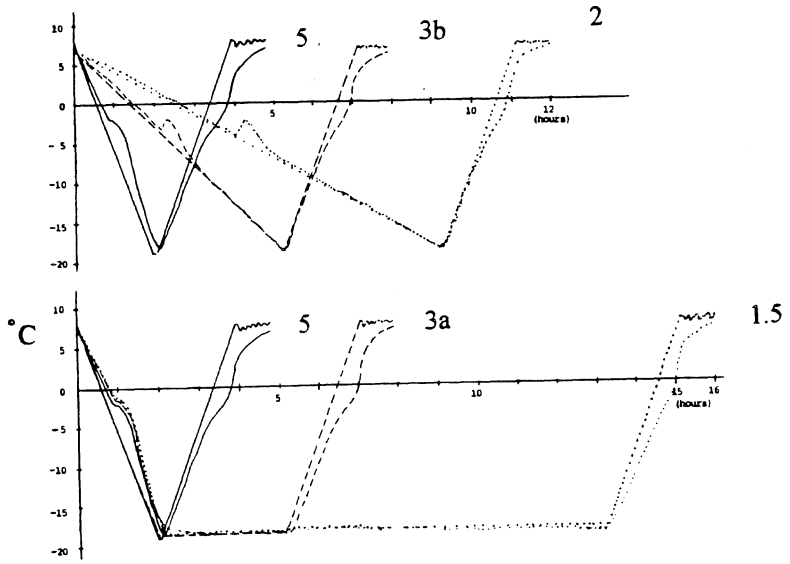

Fig. 2: Freeze/thaw cycles used. Straight lines are glycol temperatures, whereas lines with peaks around - 3 °C are in 3 % NaCl solution on specimen surface.

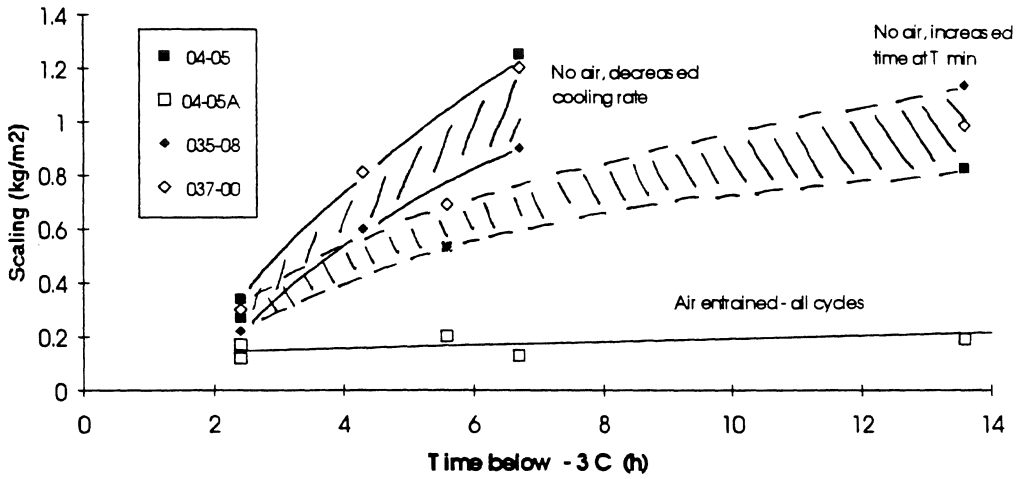

Fig. 3: Time below - 3 °C pr. cycle vs. scaling at 28 cycles for all series

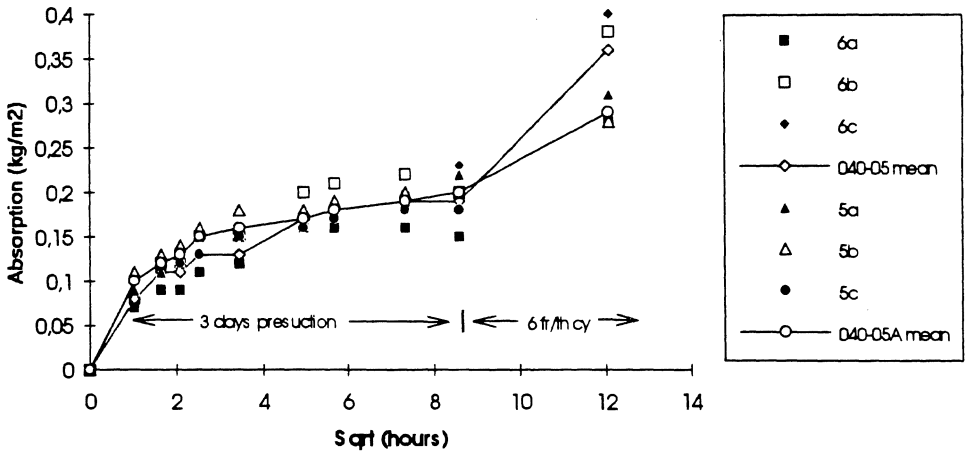

Fig. 4: Absorption during presuction and during the first six freeze/thaw cycles for 040-05 and 040-05A (slow freeze/thaw cycle: 2.8 °C/h)

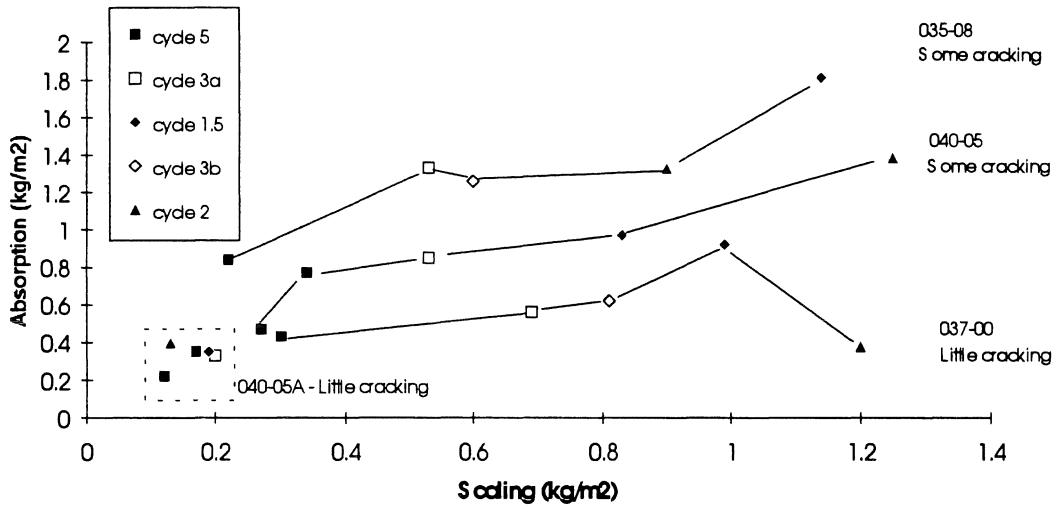

Fig. 5: Scaling vs. absorption at 28 cycles for all test series

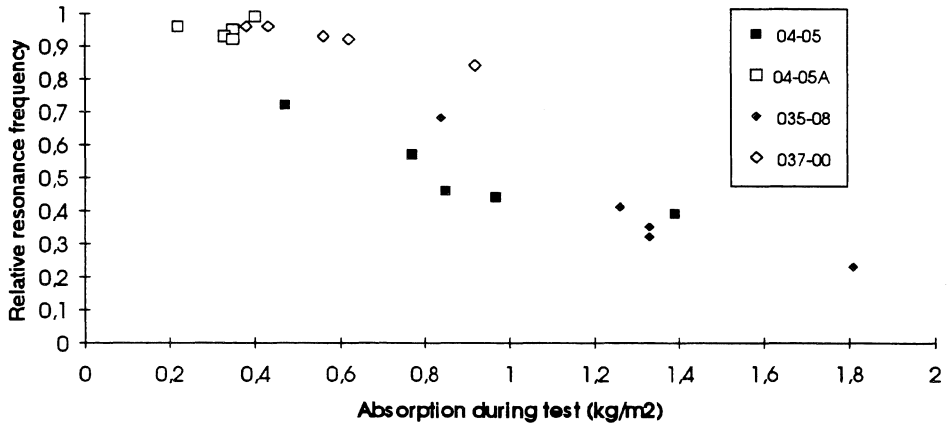

Fig. 6: Absorption vs. normalised resonance frequency at 28 cycles for all test series,
Resonance frequency = - 0.53·Absorption + 1.14, r = - 0.94

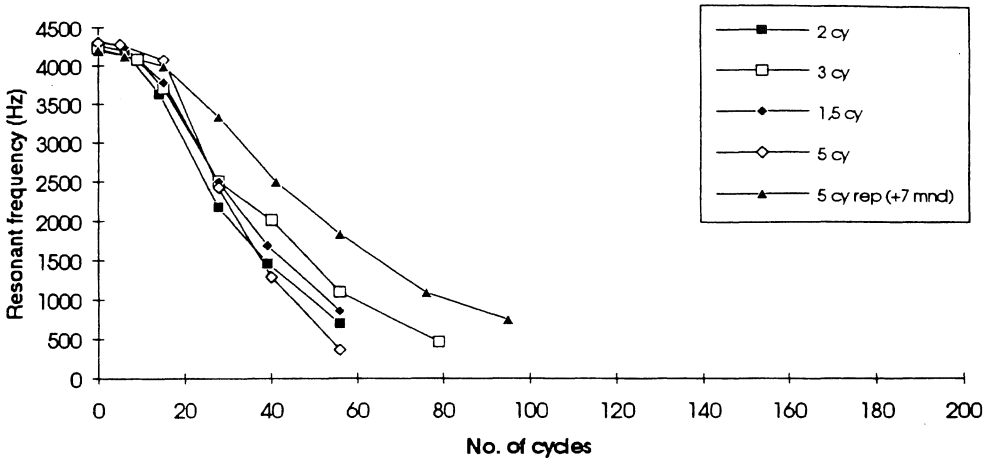

Fig. 7: Resonance frequency vs. number of cycles, 040-05

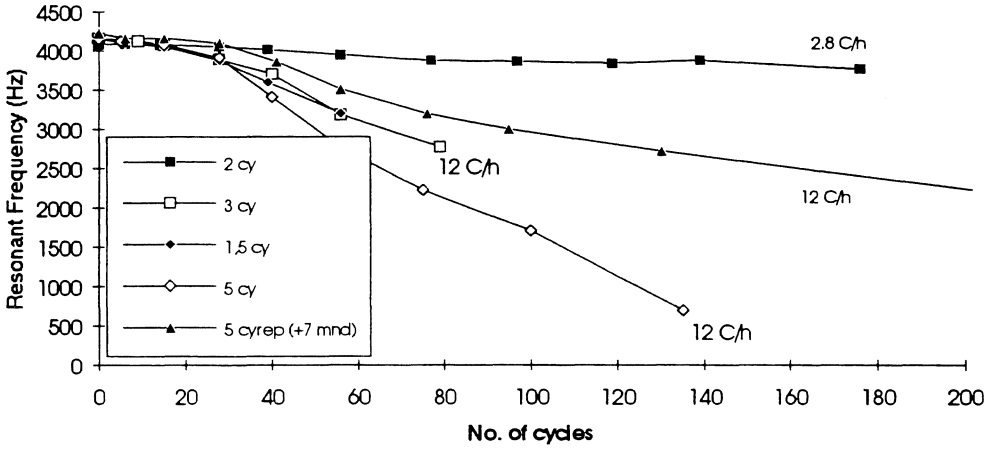

Fig. 8: Resonance frequency vs. number of cycles, 040-05A

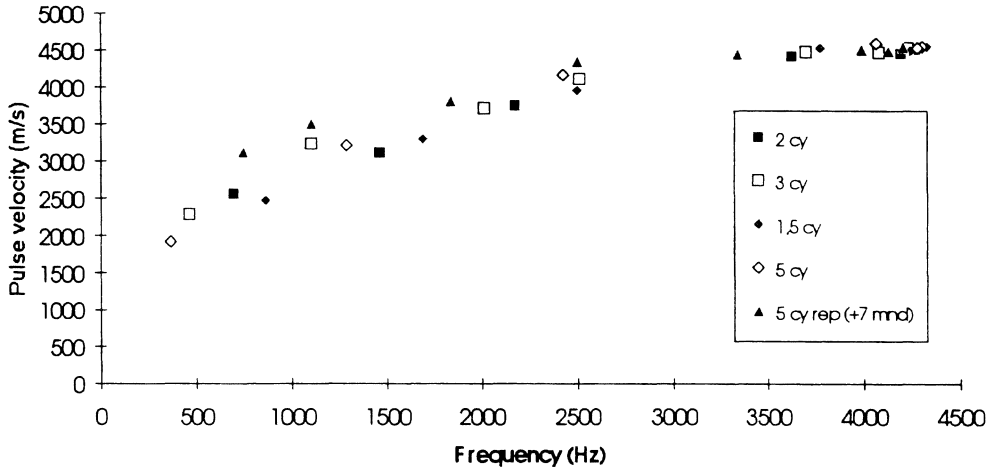

Fig. 9: Resonance frequency vs. pulse velocity for 040-05

FREEZE/THAW TEST OF CONCRETE WITH POTENTIAL FROST SUSCEPTIBLE AGGREGATES

Erik Jørgen Pedersen, B.Sc.
DTI Building Technology
Gregersensvej, P.O.Box 141
DK-2630 Taastrup

Abstract
Analysis of the influence from the amount of potential frost susceptible aggregates on the results of freeze thaw tests on concrete using of methods ASTM C 666 procedurre A and SS 13 72 44 (Borås). And a short comment on the importance of air content in concrete towards frost resistance.

Introduction
Aggregates dredged from the sea or taken from coastal areas can by jigging be upgraded to apply to the Danish requirements for class A materials, materials used for concrete in aggressive exposure class, table 1.

The requirements for the concrete regarding materials and concrete properties including acceptable air content should normally be documented by pretesting.

In the actual case it was for some reason decided to take out cores for testing of the air pore structure. Due to non conformance amount of total air (less than 10 % by volume of the binder) observed on drilled cores from the hardened concrete, the frost resistance now had to be documented by performance testing.

However in an actual case some of the aggregates with density even above 2600 kg/m3 have proven to be frost susceptible, partly by use of the test method for aggregates as drafted in CEN prEN 1367 - 1: "Test for thermal and weathering properties of aggregates - Part 1: Determination of resistance to freezing and thawing", partly by testing concrete by the method: ASTM C 666 procedure A. The use of ASTM C 666 lead to the decision that the aggregates used in the future had to be replaced by granite. So from a problem of showing that the concrete was frost resistant, the problem now was a problem for the producer of the aggregate to show applicability of the materials, which apply to the requirement given in the project.

Test methods
In the case the ASTM C 666 method was chosen. The test procedure was interrupted before the required 300 cycles, due to cracking from aggregates of limestone of paleozoical origin. Apparently the ASTM C 666 A method act as an on/off method in the situation where some of the aggregate particles are frost susceptible.

Therefore the Swedish test method SS 13 72 44 (Borås) were chosen to be able to analyze the impact on frost resistance when the concrete is designed with different amount of the frost susceptible material mentioned.

This method were also used to investigate the difference in frost resistance between concrete using aggregates from the sea and concrete with granite. Both concretes should apply with the requirements for exposure class A; but some of the cores used showed air content less than 10 %.

Results
The freeze thaw test were executed on one half of a core while air pore analysis were executed on the other half. The results are shown in table 2. The conclusion is that both concrete mixes are characterised as "good", referring to the characterisation used in the Swedish standard.

Three levels of potential frost susceptible limestone 5 %, 15 % and 25 % by weight of the aggregates are analyzed using specimens from casted concrete cylinders. From each mix test were made both on sawed surfaces and on surfaces at the form end in order to investi-gate the protective influence from the binder layer. The conclusion is that all concretes are characterised as "good", referring to the characterisation used in the Swedish standard, and that the binder layer has a delaying effect within 56 freeze/thaw cycles on the frost scaling from the aggregates. The results are shown in table 3.

Since the concrete contains potential frost susceptible materials some of these stones could cause internal cracking. Tests using ultrasonic pulse velocity were made on some specimens with the biggest amount of scaling using water cured specimens as references. The pulse direction were along a diameter and near the tested surface. The generally lower velocity in the frost tested specimens is properly due to the difference in the water content between the water cured references and the tested specimens. The results are shown in table 4.
A cross section from the specimen with the lowest velocity was investigated using epoxy effluecense technique and no internal cracking was observed.

The importance of air content in concrete
All specimens tested were characterized by the air pore distribution made on the hardened concrete using the content of total air, air bubbles smaller than 0.35 mm, spacing factor and specific surface of the bubbles as parameters. The content of air is % by volume of the binder, that is the volume which is not fine and coarse aggregates.

While no clear correlation can be shown between the frost scaling and specific surface or by frost scaling and spacing factor, some correlation is found between frost scaling and the air content in the hardened concrete.

It is often stated, that it is the content of small air bubbles which is of the greatest importance and as shown in table 5, a content of 5 to 6 % small bubbles (by volume of the binder) could be a proper threshold limit.

On the other hand a similar correlation can be shown between the frost scaling and the content of the air bubbles bigger than 0.35 mm, table 6. And as shown in table 8 this add up to a correlation between the frost scaling and the total amount of air in the hardened concrete.

No correlation is found between the amount of big air bubbles and small air bubbles as shown in table 7.

The conclusion must be, that in normally used concrete (extremely dense concrete using very low water binder ratio is excluded) the air content provide for frost resistancy. Based on the knowledge and experience of today it is, however, not possible to state other than the hardened concrete shall have a total air con-tent of well distributed bobble sizes at the level of 8 to 9 % by volume of the binder. It should be noticed that these conclusions are based on young, max. 1 year old, concrete.

REQUIREMENTS FOR FROST RESISTANT CONCRETE

EXPOSURE CLASS A

CONCRETE: **CLASS A**

AGGREGATES: **CLASS A**

CONCRETE CLASS A

WATER CEMENT RATIO ≤ 0.45

CHARACTERISTIC STRENGTH ≥ 35 MPa

AIR CONTENT IN FRESH CONCRETE $\geq 15\%$ BY VOLUME OF BINDER
(Binder is the volume of concrete minus the volume of aggregates)

AIR CONTENT IN HARDENED CONCRETE $> 10\%$ BY VOLUME OF BINDER AND
SPECIFIC SURFACE > 25 mm^2 / mm^3

AGGREGATES CLASS A

DENSITY OF THE COARSE AGGREGATES MAX. 1% BY WEIGHT LESS THAN 2400 kg/m^3.

ABSORPTION MAX. 1.1% FOR THE 10% OF THE AGGREGATES WHICH ARE FLINT WITH DENSITY ABOVE 2400 kg/m^3 AND WHICH HAVE THE HIGHEST ABSORPTION.

Table 1

Table 2

Amount of scaling from sawed surface kg/m^2

W/C Air Spec. Spacf. No of cycles	LB59 nr.8 granite 0.42 13.6 36 0.14	LB59 nr.10 granite 0.42 17.7 32 0.14	LB16 A granite 0.40 10.8 37 0.16	LB16 B granite 0.40 8.0 46 0.15	LB27 top granite 0.40 12.8 38 0.14	LB40 top SeaA 0.37 24.4 34 0.09	LB40 midt Sea A 0.37 8.6 40 0.16	LB39 top Sea A 0.37 8.4 51 0.13	LB39 bund SeaA 0.37 19.6 37 0.11
7	0.079	0.094	0.218	0.193	0.250	0.095	0.016	0.023	0.041
14	0.085	0.104	0.304	0.272	0.323	0.116	0.038	0.097	0.105
28	0.087	0.108	0.357	0.325	0.373	0.125	0.072	0.147	0.114
42	0.094	0.110	0.364	0.329	0.384	0.127	0.094	0.173	0.120
56	0.095	0.111	0.364	0.331	0.397	0.127	0.134	0.184	0.147

W/C is the equivalent W/C ratio. Air is % by volume of the binder. Spec. is the specific surface of the air bubbles. Spacf. is the spacing factor of the air bobble system.

Table 4 Pulse velocity [m/sec]

Concrete	A	B	C	D	E	Averidge
-25 In Water Buttom Sawed	4644			4644		4644
	4601	4505	4573	4559	4658	4579
	4545	4518	4464	4601	4573	4540
-15 In Water Buttom Sawed				4573	4732	4653
	4717	4644	4747	4673	4601	4676
	4615	4601	4518	4688	4615	4607
-5 In Water Buttom Sawed		4658	4630			4644
	4412	4545	4823	4630	4451	4572
	4335	4601	4451	4505	4438	4466

DTI Building Technology Gregersensvej 2630 Taastrup	SCALING AS A FUNCTION OF TIME average of 5 specimens pr. term. 7, 14, 28, 42 og 56 cycles
Kunde: Navn:	Ref: Dato:1996-01-04
	Initialer: EJP

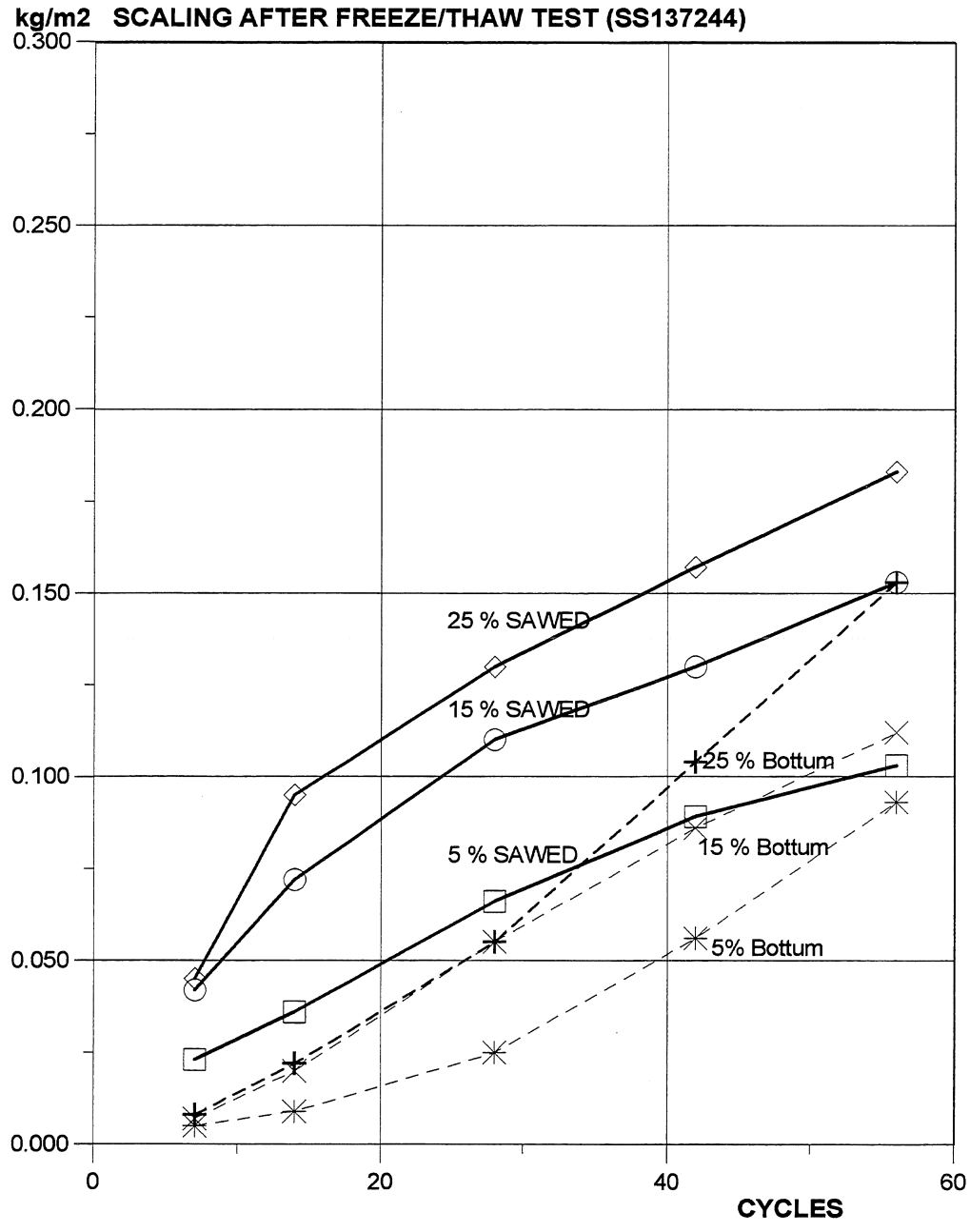

Table 3

25 % SAWED
15 % SAWED
5 % SAWED
25 % Bottum
15 % Bottum
5 % Bottum

DTI Building Technology Gregersensvej 2630 Taastrup	Frost scaling after 56 cycles as a function of the content of small air bubbles < 0.35 mm.
Kunde: Navn:	Ref: Dato: Initialer: EJP

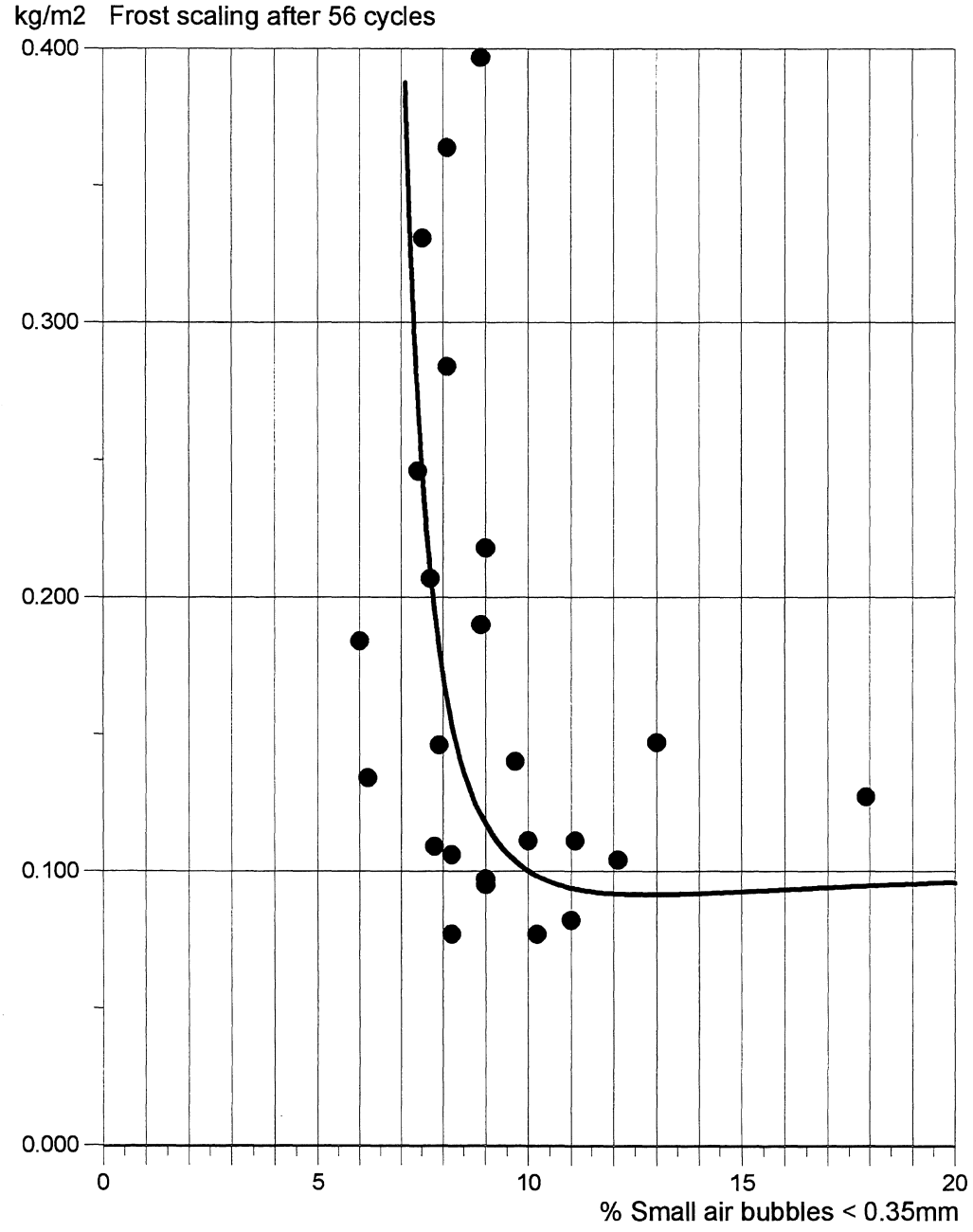

Table 5

The air content is % by volume of the binder

DTI Building Technology Gregersensvej 2630 Taastrup	Frost scaling after 56 cycles as a function of air bubbles bigger than 0.35 mm.
Kunde: Navn:	Ref: Dato: Initialer: EJP

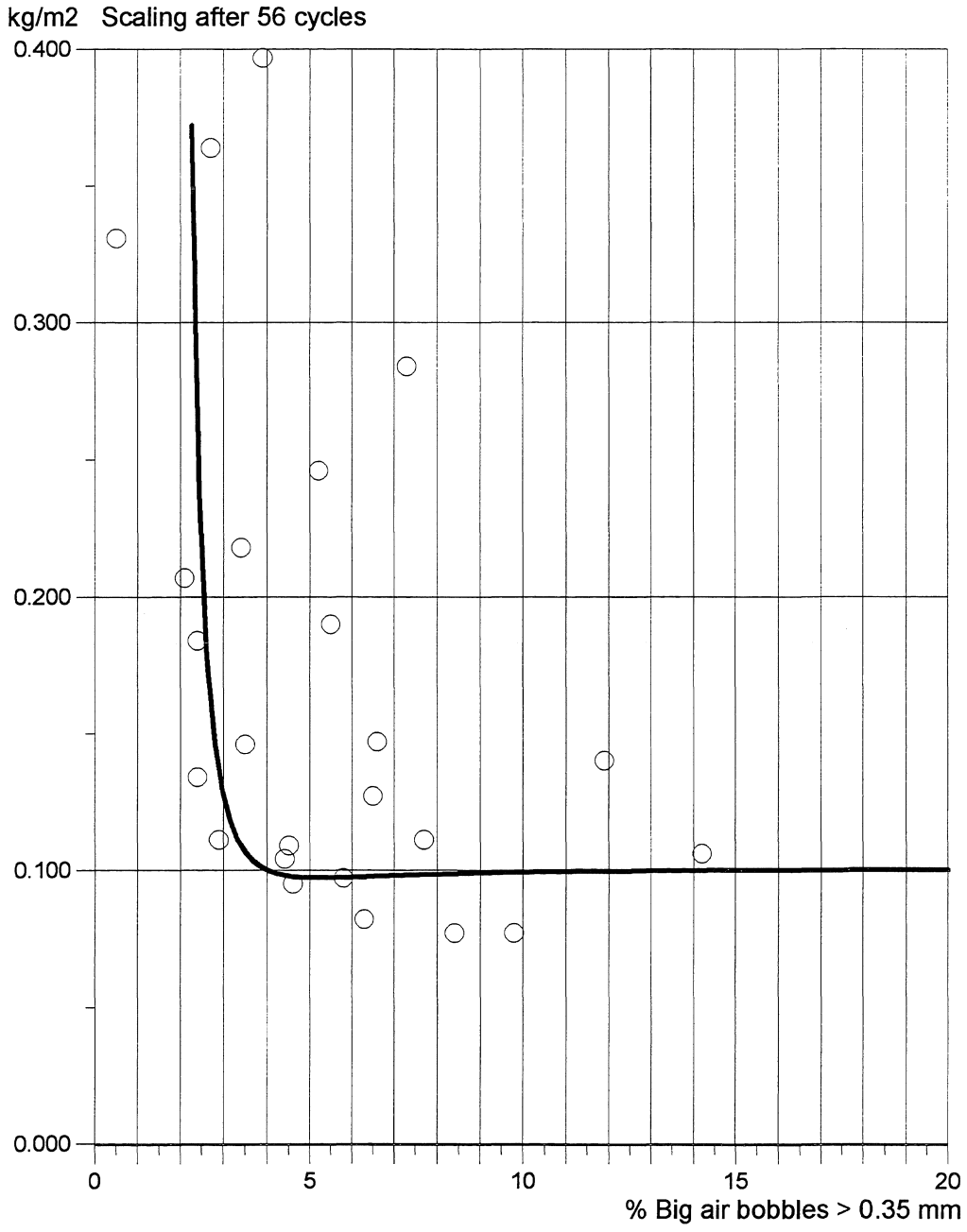

Table 6

The air content is % by volume of the binder

DTI Building Technology Gregersensvej 2630 Taastrup	Content of big air bubbles > 0.35mm as a function of small air bubbles < 0.35 mm.
Kunde: Navn:	Ref: Dato: Initialer: EJP

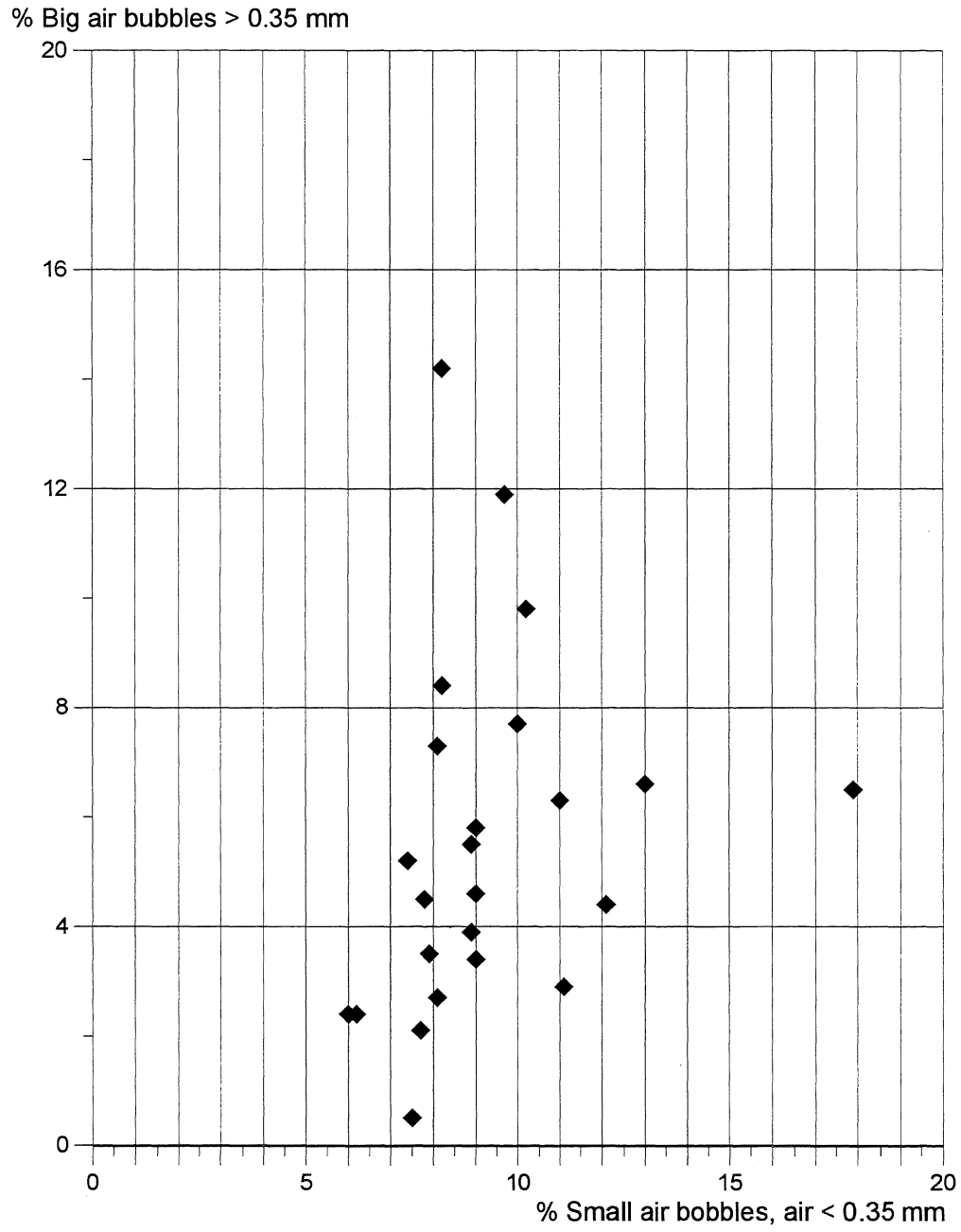

Table 7

The air content is % by volume of the binder

DTI Building Technology Gregersensvej 2630 Taastrup	Frost scaling after 56 cycles as a function of total air bubbles (% of binder)
Kunde: Navn:	Ref: Dato: Initialer: EJP

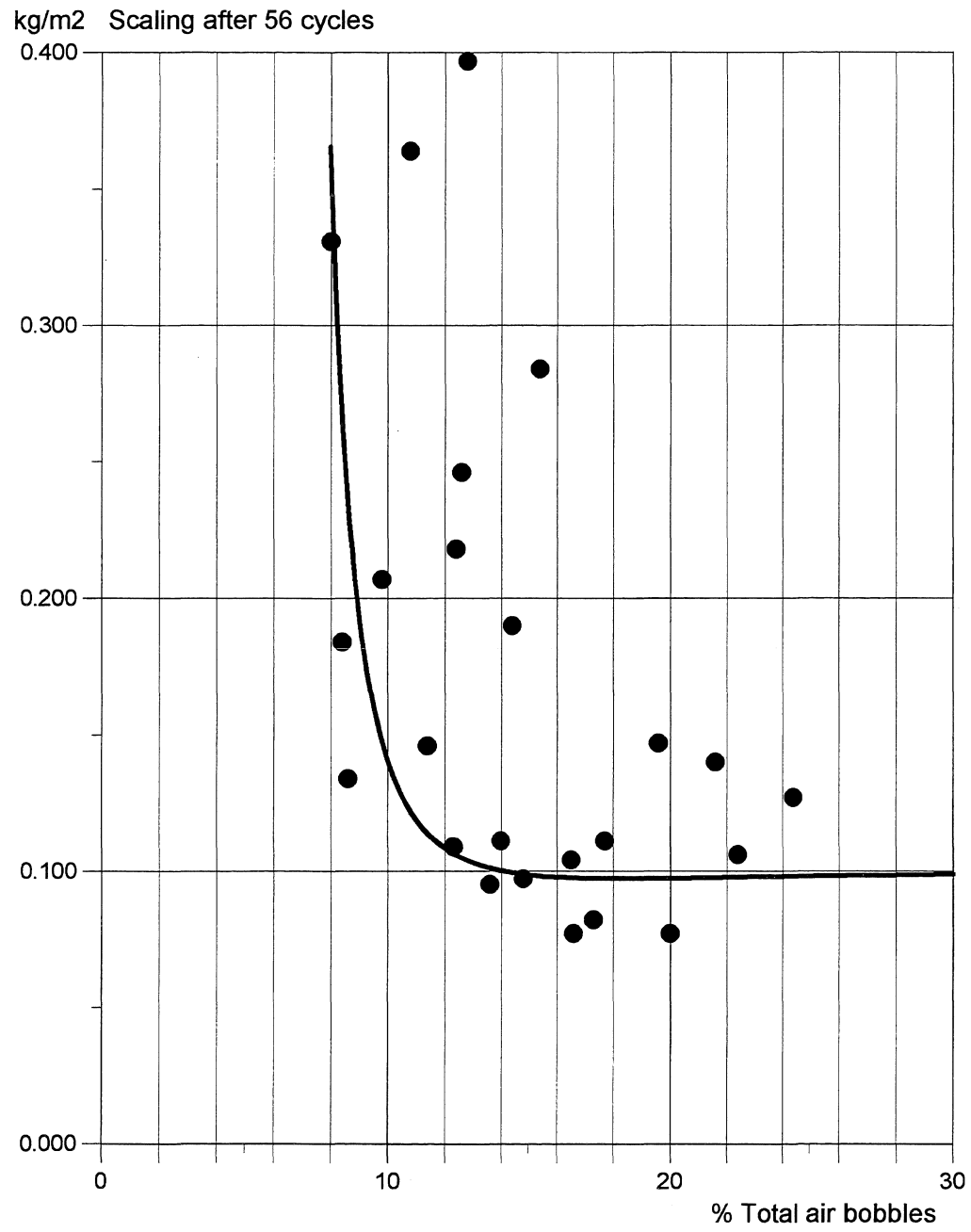

Table 8

The air content is % by volume of the binder

SALT-FROST DETERIORATION OF NATURAL STONE

Lubica Wessman
Division of Building Materials
Lund Institute of Technology
Box 118
S-221 00 Lund
Sweden

Abstract
Some Swedish natural stones have been tested by freezing and thawing in water and in salt solutions. The tested stones were two different calcite bounded sandstones, one limestone and one granite. The used salts were NaCl and Na_2SO_4 * 10 H_2O. Two different test methods have been used; one scaling test and one dilatation test.

In the scaling test the damage is measured as weight loss after a number of freeze-thaw-cycles. The specimens are surrounded by solution during both freezing and thawing. The results show that there exist pessimal salt concentrations. Limestone is extremely sensitive towards freezing and thawing in NaCl-solutions. The granite samples were almost undamaged.

In the dilatation test the damage is measured as the permanent dilatation after one single freeze-thaw-cycle. The specimens, containing different amounts of solution, are wrapped in plastic foil during freezing and thawing. The results show that dilatation is negligible when the samples contain small amounts of solution and that it then increases with increasing amounts of solution. Samples of sandstone containing salt solution dilated more than samples containing pure water. The dilatation of the limestone was very small compared to the dilatation of the sandstone, because of smaller porosity of the limestone and hence smaller water content. The small porosity of granite was also the reason to why it did not dilate.

1 Introduction

Deterioration of ancient buildings and monuments made of natural stone has been a well documented problem for several decades. Since the weathering of stone seems to have become more severe since the start of industrialisation, much of the research concerning this subject has been focused on chemical reactions between minerals of the stone and air pollution. The study presented here, which concerns a physical degradation process – frost – is a complement of such research. Though frost has always existed, it is possible that it causes more severe damage together with air pollution. There are several possible reasons for this:

1) Frost changes the structure of the stone, e.g. by increasing the surface area, so the chemical reactions with air pollution will have more effect.
2) Chemical reaction with air pollution changes the structure of the stone so that frost will have more effect.
3) Solutions (e.g. air pollution solved in water) cause more damage at freezing than does pure water.
4) A combination of 1 and 2 (and 3) above.

Item number 3 above is the one that is treated in the following.

It is a well known fact that ice formation in pores destroy porous building materials like concrete and brick, and that this frost destruction for a fine porous material like concrete is growing worse by the influence of salts and other solutes. Weaker solutions cause more damage than stronger ones [1]. Many studies have been performed in this area, and these studies and the knowledge that has emanated from them has been an important source of inspiration for this study.

2 Materials and salts

The stones tested are presented in Table 1. All tested stones are of Swedish origin.

Table 1. Tested stones.

Stone	Name	Deposit	Porosity (%)
Sandstone (lime-bonded)	Uddvide	Gotland	22
Sandstone (lime-bonded)	Valar	Gotland	17
Limestone	B1 (red)	Horns Udde, Öland	3
Granite	Bohus Röd Bratteby	Hunnebostrand, Bohuslän	0.6

2.1 Sandstones

The colour of the calcite bound sandstones from Gotland is light grey, normally with no tints in it. The type Valar sometimes contains light brown lines, parallel to the bedding. These lines contain more clay minerals and micas than does the light grey parts. Thin section microscopy of the stones shows that it consists almost entirely of quartz grains with empty spaces between them constituting the porosity. The size of the grains is 0.1-0.2 mm in Uddvide and 0.05-0.15 mm in Valar.

The sandstone from Gotland is one of the dominant materials of buildings of historic interest in the Baltic region. It is often used in sculptural decorations, as it is soft and therefore easy to work, but it is also used in facings, mostly from the 17th century. The problems with deterioration of this stone are very extensive.

2.2 Limestone

Limestone, a rock of sedimentary origin, is composed principally of calcium carbonate (calcite). Fossil shells of different form and size are often present. The colour of limestones vary widely; there exist all shades of white, yellow, brown, grey, green and red limestones.

The particular limestone mentioned here is red in colour and fossils, 0.05-0.40 mm in size, are frequently present. In thin section microscopy you can sometimes see thin cracks (5-6 mm in length and only some μm in width) and small holes, less than 0.1 mm, which are probably emanating from loosened fossils, but no pores are visible. Such cracks and holes cannot alone explain the porosity of 3% of the red limestone from Öland. Therefore the porosity of this stone must be made up either by very small pores, invisible in thin section microscopy (i.e. less than 20 μm in size), or by larger, sparsely occurring cracks.

Limestone has been widely used in buildings from the 17th century and is still used in modern buildings. The problems with deterioration are extensive.

2.3 Granite

Granite is a medium- to coarse-grained, igneous rock composed essentially of quartz, feldspar and mica.

The particular granite from Bohuslän mentioned here, has a grey to light pink colour. It is essentially composed of 2-8 mm grains of quartz (about 60%) and feldspar (about 40%). Small flakes of gleaming mica can also be seen. The grains are suited densely together edge by edge. Between the grains tiny cracks in a net-shaped pattern are visible in thin section microscopy. Sometimes cracks exist also within the grains, mainly in the quartz grains. It is difficult to evaluate the porosity caused by these visible cracks, but a rough estimation gives that the porosity of 0.6% can be caused by this kind of cracks only.

Granite is hard, and therefore worked granite was not used frequently in buildings until the middle of the 19th century, when the technique for working of granite was developed. At the turn of the century, granite reached its most popular period as a building material. There are seldom problems with deterioration of granite in buildings, but there are problems with ancient, bronze age rock carvings on exposed granite, as well as with granite rune stones.

2.4 Salts

Two different salts have been tested: NaCl and Na_2SO_4 * 10 H_2O. Both salts are found in considerable amounts as efflorescence (i.e. salt crystals) on facades [2]. The origin of NaCl is mainly ground water and blown sea-spray. The origin of the sulphate is rapid oxidation of sulphur dioxide, which is emanating from air pollution caused by the burning of fossil fuels.

3 Method of freeze-thaw of scaling tests

3.1 Sandstones and limestone

Sawed stone prisms with the dimensions 3 x 3 x 12 cm were dried in an air-circulated oven at a temperature of 105 °C until no more weight loss caused by moisture evaporation occurred (i.e. for at least four days). The prisms were weighed after cooling over silica gel and then placed in standing position in vessels containing salt solutions of different concentration. Eight different concentrations between 0 and 5.3% were used for sandstones exposed to NaCl-solution and six different concentrations between 0 and 4% were used for the limestones and sandstone exposed to Na_2SO_4-solution. The prisms were left in the solutions for four days to be capillary saturated before being freeze-thaw-tested, all the time being surrounded by solution.

Dummies, treated equally to the prisms, but with a thermocouple in a drilled hole in the centre, were also placed in the freezer. They were used to measure the temperature to ensure that the entire prisms reached the desired temperature condition during the freeze-thaw cycling. The freeze-thaw cycle used is showed in figure 1.

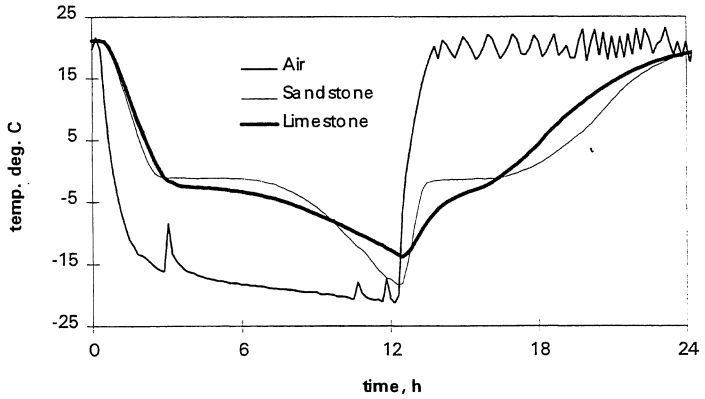

Fig. 1. Freeze-thaw cycle used in the scaling test.

The sandstones and the limestone tested in Na_2SO_4 were freeze-thaw tested 20 cycles, while the limestone tested in NaCl was only freeze-thaw tested four cycles because of the huge weight loss. After the freeze-thaw test, the fragments that had loosened, or could easily be loosened from the specimen with the fingers, were rinsed thoroughly with clean water to remove as much salt as possible. The fragments were then dried at a temperature of 105 °C for at least four days and were then weighed after cooling over silica gel.

3.2 Granite

The granite prisms were treated in the same way as the sandstones and limestone, but instead of being dried at 105 °C they were dried at 50 °C. The prisms were either vacuum saturated by the actual solution or left in the solution for ten days before the vessels containing prisms and solution were placed in the freezer. Only pure water and one concentration of 2% by weight was used for each of the salts NaCl and Na_2SO_4 * 10 H_2O. The freeze-thaw cycle is showed in figure 1. The granite was freeze-thaw tested 35 cycles.

4 Results of scaling tests

The results from the freeze-thaw tests of sandstones and limestone are presented in figures 2 and 3 as weight loss in percent of original weight as a function of the salt concentration by weight. Note the different scales on the y-axes. One dot is one sample.

(The sandstone Valar was not tested in Na_2SO_4-solution.)

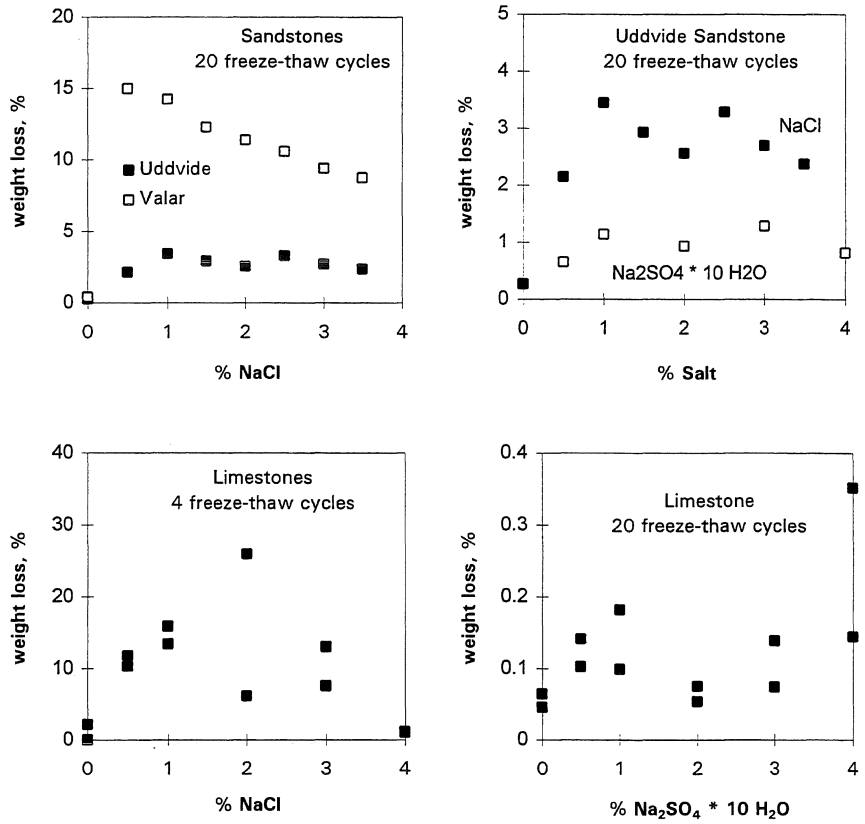

Fig. 2. *Weight loss, expressed in percent of original weight, after freezing and thawing of sandstones and limestone in NaCl- and Na_2SO_4-solutions of different concentrations. Note the different scales on the y-axes.*

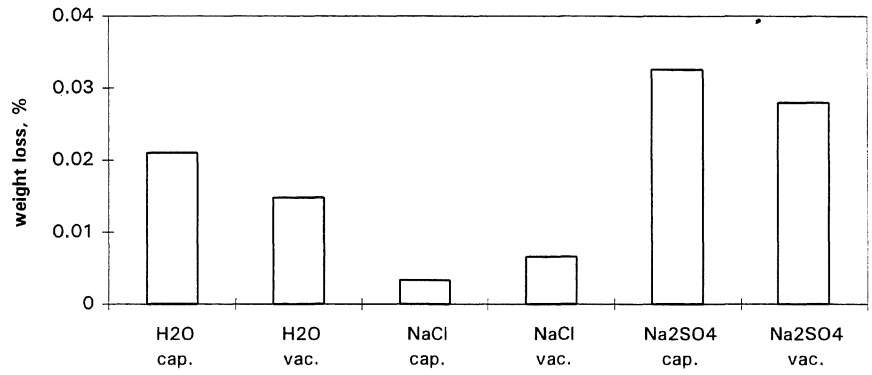

Fig. 3. *Weight loss, expressed in percent of original weight, of granite after 35 cycles of freeze-thaw in pure water and 2% salt solutions of NaCl and Na_2SO_4. * 10 H_2O The specimen were either capillary (cap.) or vacuum (vac.) saturated.*

4.1 Sandstones tested in NaCl

The result shows that the denser sandstone Valar is more sensitive towards freezing and thawing in NaCl-solution than is the more porous Uddvide. The damage of Valar is decreasing with increasing NaCl-concentration, but still, the weakest concentration tested (0.5% by weight) gives rise to considerably more severe damage than does pure water. For Uddvide, there is no clear tendency of decreasing damage with decreasing NaCl-concentration, but pure water left the specimen almost undamaged, as was the case also for Valar. The damage of Uddvide increases with NaCl-concentration up to a value of 1,5%, after which the damage remains constant to 3.5%, which is the highest concentration tested.

4.2 Limestone tested in NaCl

The limestone is very sensitive towards freezing and thawing in NaCl-solution. The most severe damage occurs in NaCl-solutions of a concentration between 1 and 3% by weight. (The large difference between the two limestone specimens that were freeze-thaw tested in the 2%-solution unfortunately cannot be explained.)

4.3 Limestone and sandstone tested in Na_2SO_4

Both the sandstone of the type Uddvide and the limestone obtained smaller scaling when tested in Na_2SO_4 than when tested in NaCl. The difference is considerably larger for the limestone than for the sandstone. The limestone specimens freeze-thaw tested in Na_2SO_4 were almost undamaged compared to the limestone specimens freeze-thaw tested in NaCl. For the limestone the scaling in Na_2SO_4 is so small, that it is not possible to say anything significant about the effect of different salt concentrations.

4.4 Granite tested in NaCl and Na_2SO_4

The granite had a relatively small weight loss after 35 freeze-thaw cycles. The accuracy of the balance and in the experimental method is no more than 0.01 g. The weight loss of granite was between 0.01 and 0.10 g. It is therefore hard to see any difference between the effects of the different salts. But, as can be seen in figure 3, there is a slight tendency of Na_2SO_4 causing more weight loss than does pure water, which in turn causes more weight loss than does NaCl. No significant difference can be seen between capillary and vacuum saturated specimens. The weight loss is mainly caused by loosened flakes of mica.

5 Method of freeze-thaw of dilatation test

Sawed stone prisms with the dimensions 2 x 2 x 15 cm were dried in an air-circulated oven at a temperature of 105 °C, until no more weight loss caused by moisture evaporation occurred (i.e. for at least four days). The prisms were weighed after cooling over silica gel. The sandstone prisms were then conditioned

to contain different amounts of salt solutions. For limestone and granite only completely saturated samples were tested, as the dilatation of these stones was small. Pure water and two different concentrations for each salt: 0,5% and 1,0% by weight, were tested.

The amount of solution inside the specimen was expressed in terms of degree of saturation. Completely saturated samples, where the degree of saturation is 1, were vacuum saturated. To reach the desirable degree of saturation, lower than 1, the samples were either exposed to suction of solution for different long times, or "vacuum"-saturated by sucking the solution after a pre-treatment consisting of evacuation to different residual pressures.

The pre-conditioned samples were provided with measuring knobs at the ends. They were placed in a measuring frame provided with LVDT-gauge for measuring the length change during freezing and thawing. The specimens were wrapped in plastic foil in order to prevent moisture loss or moisture gain during the freeze-thaw cycle. The measuring frame with the specimen was placed in a freezer and exposed to one freeze-thaw cycle of the kind shown in figure 4. The temperature was measured by a thermocouple placed in a drilled hole in the centre of each specimen.

Damage was defined as a permanent dilatation after thawing.

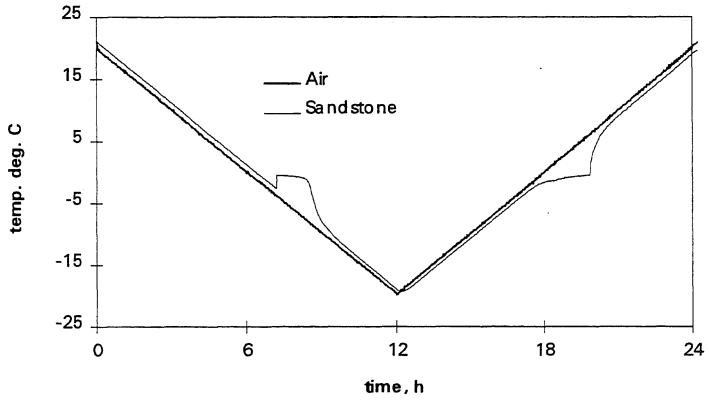

Fig. 4. Freeze-thaw -cycle used in the dilatation test.

6 Results of dilatation test

6.1 Sandstones

The result from the dilatation tests of the sandstones are presented in figure 5 below as permanent dilatation as a function of degree of saturation. One dot is one sample. The conclusions that can be drawn from the figure are the following:

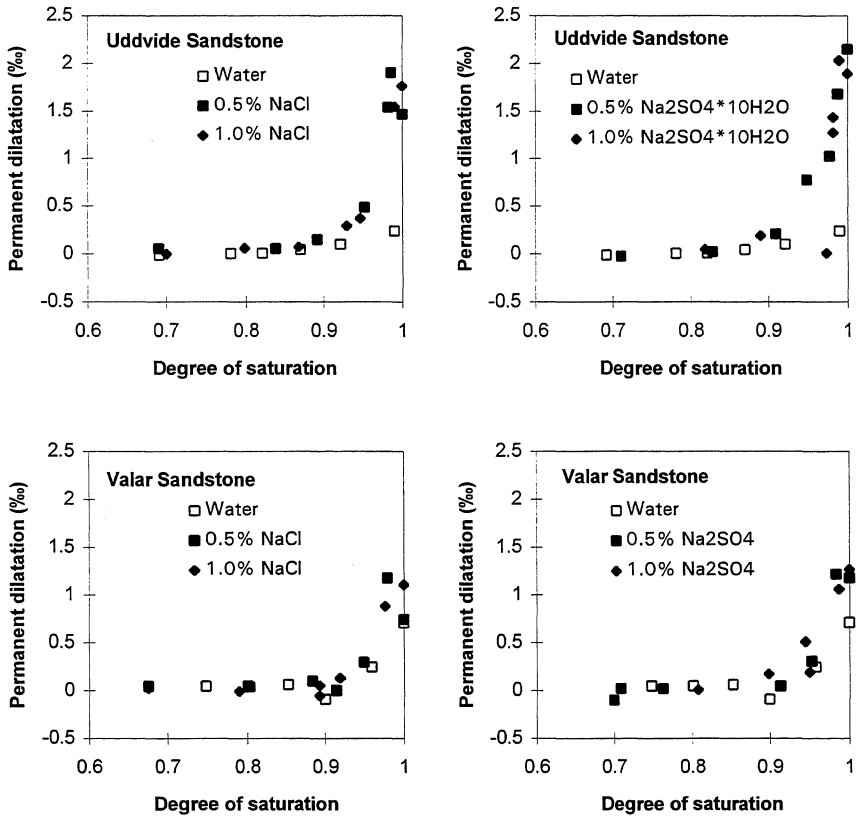

Fig. 5. Permanent dilatation after one freeze-thaw-cycle of sandstones as function of the degree of saturation of NaCl- and Na_2SO_4--solutions of different concentrations.

At low degrees of saturation (below 0.9) almost no permanent dilatation occurs for neither of the samples. Differences between the types of salt, concentrations and the types of stone can therefore only be seen at higher saturation - the higher the degree of saturation, the more obvious the differences.

Salt solutions give larger permanent dilatation than does pure water. There is no visible difference, however, between the different salt concentrations (0.5 and 1.0%).

A slight difference between the different salts can only be seen for the sandstone Uddvide: At high degrees of saturation Na_2SO_4-solution gives larger permanent dilatation than does NaCl-solution.

The more porous sandstone Uddvide obtains larger permanent dilatation than the denser sandstone Valar, except for pure water, where the opposite is valid.

6.2 Limestone and granite

The permanent dilatation for completely saturated limestone samples after one freeze-thaw cycle are presented in table 2.

Table 2. Permanent dilatation (‰) for completely saturated limestone samples

Pure water	0.5% NaCl	1.0% NaCl	0.5% Na_2SO_4	1.0% Na_2SO_4
≈ 0	≈ 0	0.18	0.22	0.29

As can be seen, the permanent dilatation is small compared to the dilatation for completely saturated sandstones. This depends on the relatively small porosity of the limestone. As for the sandstone, there is a tendency of Na_2SO_4 causing larger dilatation than does NaCl. There is also a small tendency of higher salt concentration causing larger dilatation.

The small porosity of granite is probably the reason why no dilatation occurred upon freezing of saturated granite.

7 Comments

The results from the two test methods contradict each other in many ways:

- In the scaling test, limestone is considerably more sensitive against freezing and thawing in NaCl-solution than in Na_2SO_4-solution. In the dilatation test the difference between the salts is almost negligible.
- In the scaling test, the denser sandstone Valar is considerably more sensitive against freezing and thawing in NaCl-solution than is the sandstone Uddvide. In the dilatation test the opposite is valid.

These contradictions depend, among other things, on the fact that the scaling test is an "open test", where moisture can flow out of and in to the specimens during the test, while the dilatation test is performed with sealed specimens. The damage is also measured in different ways in the different tests. This means that the stones can dilate also in the scaling test, but the dilatation does not necessarily cause damage in the form of scaling. In the scaling test the specimens are also affected by the surrounding ice formed at freezing.

8 Acknowledgements

The author acknowledge professor G. Fagerlund for advice and guidance and the technical staff of the department for practical help and assistance. A special thank to Thomas Carlsson, who has prepared the samples and evaluated the results from thin section microscopy. This work is financially supported by the Central Board of National Antiquities in Sweden.

9 References

1. Verbeck, G. J. and Klieger, P. (1957) Studies of "salt" Scaling of Concrete. *Highway Research Board, Bulletin 150.*
2. Nord. A. G. and Tronner. K. (1991) The Central Board of National Antiquities and the National Historical Museums, Conservation Institute, Report RIK 4, *Stone Weathering, Air pollution effects evidenced by chemical analysis.*

INFLUENCE OF ASR EXPANSION ON THE FROST RESISTANCE OF CONCRETE

Jan Trägårdh
Swedish Cement and Concrete Research Institute
100 44 Stockholm, Sweden

Björn Lagerblad
Swedish Cement and concrete Research Institute
100 44 Stockholm, Sweden

Abstract
Results are presented of water absorption and freeze-thaw tests carried out on laboratory concretes casted with and without a deleterious amount of reactive aggregates and a high alkali cement. A petrographic study including thin section study, SEM-EDAX analysis and image analysis was carried out on both laboratory and field concretes. Prior to the freeze-thaw and water absorption tests the laboratory concrete specimens have been stored in a 100% humidity room for three and a half years. During this time the concrete which contained reactive material developed ASR expansion and cracking. The concretes were prepared with two different dosages of an air-entrainment agent and with two different W/C ratios (0.40 and 0.55). For the concretes which developed cracks due to ASR expansion, it is shown that the frost resistance is significantly decreased. This is more pronounced for the specimens with the lower W/C ratio and air-void content. For these specimens it is also shown that the level where the concrete reaches a critical water saturation is decreased when it is affected by ASR. It was also found that the expansion caused by frost action during freze-thaw testing is directly proportional to the initial crack widths caused by ASR.

A microscope analysis showed that frost action induces cement deterioation. This is brought by microcracking followed by leaching of calcium hydroxide and sulphates from cement components. The dissolution and leaching is caused by water movements during recurrent cycles of freezing and thawing which eventually leads to the breakdown of cement gel components. The dissolved constituents precipitate in cracks and air voids as secondary products such as portlandite and ettringite/monosulphate. In the microscope it is observed that microcracks filled with portlandite radiate out from air voids which indicate expansion of water in air voids during freezing.

A petrographic examination of core samples from field structures which showed cracking due to both ASR and frost attack was carried out. Crack pattern, cement deterioation and alteration products were the same for field and laboratory concretes. Cracks caused by ASR can be distinguished from cracks caused by frost attack. Geometry, spacing and crack widths are different.

Introduction

ASR may influence the frost resistance of concretes in several ways. ASR cause internal cracks which emanate at the concrete surface . If the cracks are left open and then water filled freezing may induce such a pressure that the deterioration of concrete increases in comparison with uncracked concrete. Concrete members with exposed horizontal surfaces are especially potentially susceptible to frost attack.

Another effect of ASR is that it produces gel which can fill the air-voids and result in a reduced amount of active air-voids and an increasing spacing factor. ASR-gel can also densify the cement paste structure which results in a decreased capillary pore volume and thus a decrease in the permeability to displaced water caused by freezing. This may change the conditions for water migration which in turn will reduce the frost resistance.

This investigation includes studies on laboratory samples as well as petrography of field concrete in case objects. Water absorption/desorption test and freeze-thaw testing on primarily air-entrained concrete was made. Prior to the testing, some of the specimens had developed cracks due to ASR.

Investigation

Laboratory investigation

Cube samples with the side 150 mm were cast with reactive aggregates and a high alkali cement. The samples were stored at 20 °C and 100 % relative humidity. After three and a half years storage the samples had developed cracks due to ASR and were subjected to water absorption and freeze-thaw tests and microscope analysis.

The reactive component in the aggregate phase was flint and the cement used was Slite Std portland cement with an alkali content of 1.2 weight % Na_2O equivalent. Reference samples were prepared with a non-deleterious aggregate. The concrete mixes had an alkali content of 4.6 kg/m^3 and an aggregate content of about 1700 kg/m^3. The size range of the aggregates was 0-8 mm. The aggregates can be considered as non-porous with a water absorption value below 1 %. Two different dosages of an air-entrainment agent were used in order to reach a moderate (4.6 vol. %) and a high (7.5 vol. %) air content in the hardened concrete. The water - cement ratios were 0.40 and 0.55. *Table 1* show the concretes subjected to water absorption and freeze-thaw tests.

Table 1. Crack width, W/C-ratio, ait-void content and spacing factor for the investigated laboratory concretes.

Batch no.	Sample	W/C ratio	Crack width (mm)	Air void content (vol.%)	Power's spacing factor (mm)
1	Flint 1	0.40	0.1-0.2	4.60	0.235
1	Flint 2	0.40	0.1	4.65	0.230
1	Flint 3	0.40	0.2-0.3	4.72	0.237
1	Flint 4	0.40	0.4-0.8	4.70	0.225
1	Ref. 1	0.40	no cracks	5.0	0.220
1	Ref. 2	0.40	no cracks	5.10	0.230
2	Flint 5	0.55	0.5-0.7	7.72	0.190
2	Flint 6	0.55	0.2	7.69	0.195
2	Flint 7	0.55	0.6-1.0	7.65	0.190
2	Ref. 3	0.55	no cracks	7.95	0.185
2	Ref. 4	0.55	no cracks	7.90	0.180
2	Ref. 5	0.55	no cracks	8.0	0.180

Investigation of bridge structures

Two railway bridges in central Sweden were selected as case studies. The bridges were erected in 1940 and 1962. The climate in the region is normally rather wet summers with long cold winters with many freeze-thaw cycles. The aggregates from the region are dominated by slowly reacting metevolcanic rocks.

The structures showed surface-parallel cracking with spalling and leaching of calcium hydroxide superimposed on a map cracking pattern conspicuous for ASR. This was predominantly observed on sidebeams and sidewings. The surface-parallel cracks develop in sequential stages, progressing from the horizontal surface and the edge of a concrete member to the vertical face. This leads eventually to disintegration of the cement paste and spalling of the concrete cover down to the reinforcement. This type of cracking and spalling of the concrete is confined to the most exposed parts of the structure such as sidebeams and horizontal parts of sidewings where the concrete has reached a critical degree of water saturation.

Reinforcement corrosion does not seem to start until the cover is completey lost. In some cases it was observed that the rebar was unaffected by corrosion even if the conrete was laminated by cracks down to the level of the reinforcement. This could be due to the high water saturation which is indicated by the limited carbonation in the cover. Carbonation is predominantly confined to areas close to cracks.

The cracks which are attributed to a map cracking pattern conspicuous for ASR measured about 0.3 mm in the bridge from 1940 and 0.5-1.0 mm in the bridge from 1962.

Results

Water absorption and freeze-thaw tests of laboratory concretes

The volume of pores filled by capillary action as % of specimen volume and the degree of capillary saturation (S,cap) was measured in accordance with a method developed by Fagerlund (1977) for RILEM Committee 4 CDC. Before the water absorption test started, the samples were dried until constant weight was recorded.

The diagrams in *Fig. 1* (batch 1) show that the total pore volume is reduced in samples damaged by ASR leading to a smaller total water uptake in kg/m^3. In *Fig. 2* (batch 1) it is also shown that the ASR damaged samples reached a higher degree of capillary saturation than the reference samples. The fact that the degree of capillary saturation is higher at the same time as the total water uptake in kg/m^3 is decreased compared to ASR unaffected samples indicates that the structure has been densified by ASR and that the pore volume has been reduced. The degree of capillary saturation (S,cap) was calculated from the values obtained by the water absorption test. In the microscope it was observed that the amount of coarse capillary pores and small air pores have been gel-filled.

The freeze-thaw test was done in accordance with Swedish standard SS 13 72 44, with the exception that the nunber of freeze-thaw cycles was increased. A rubber insulation was put on all sides of the sample, except the upper horizontal side which was covered by 1-2 mm thick film of pure water. The same specimens were used as in the water absorption test, but they were dried before the freeze-thaw test. Metal studs were applied on oppsite sides and perpendicular to the freezing surface. The expansion was measured regularly during the freeze-thaw testing.

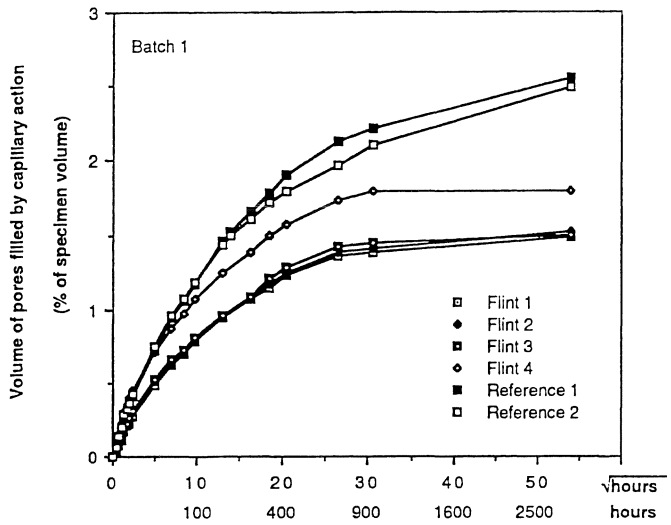

Fig. 1 . Water absorption test of samples in batch 1. ASR damaged samples (Flint 1-4) show a smaller volume of pores filled by water absorption than the reference samnples (% of specimen volume). W/C ratio 0.40.

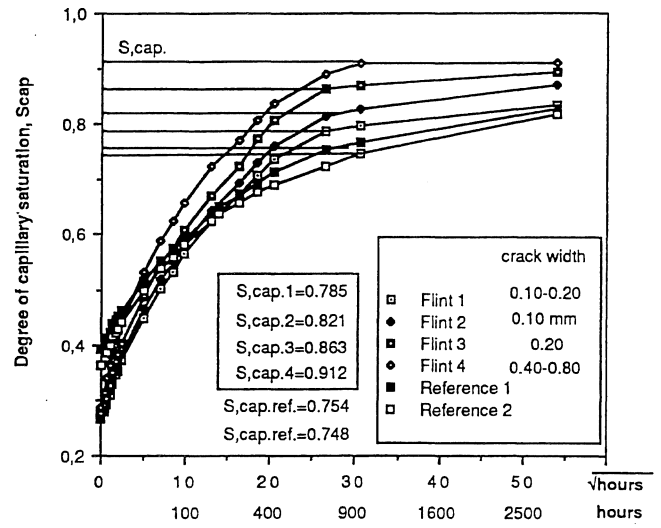

Fig. 2. Diagram showing the capillary degree of saturation (S,cap) for samples in batch 1. The ASR damaged samples show a higher degree of water saturation than the reference samples.

During the freeze-thaw test the samples absorbed water which made it possible to determine the degree of capillary saturation periodically with an interval of approximately 20 freeze-thaw cycles. This was done by measuring the weight of the samples and relating the amount of water absorbed to the corresponding degree of capillary saturation which was obtained earlier from the water absorption test. Pure water was added regularly in order to keep a 1-2 mm thick waterfilm on the top surface. At the same time expansion measurements perpendicular to the freezing surface were carried out. This made it possible to determine the critical degree of capillary saturation (S,cap,crit.). The critical degree of saturation is defined as the degree of saturation when the samples started to expand due to internal damage caused by ice formation.

The diagrams in *Fig. 3* and *Fig. 4* show the critical degree of capillary saturation for the samples in batch 1. The ASR damaged samples showed a decreased critical degree of capillary saturation compared to the reference samples. The amount of damage (expansion) is also increasing with increasing crack width. The critical degree of saturation for ASR damaged samples was reached at 15-30 freeze-thaw cycles and at a capillary degree of saturation of 60-80%, depending on the crack width. At the same time the reference samples did not show any sign of internal damage at a degree of capillary saturation of 95 % and more than 200 freeze-thaw cycles.

Petrography of laboratory concretes

The cement paste structure in the ASR damaged samples show alteration due to freezing and thawing. Wide ASR-induced cracks are open and empty to depths of about 40-50 mm from the surface. The cement paste around these vertical cracks is recrystallized and attains a "grainy" texture due to portlandite crystallization. The crack walls are carbonated. Below 40-50 mm the cracks contain gel fragments surrounded by ettringite needles. The ettringite formation indicate moist migration along the cracks. At even greater depths the crack thins out and is filled with massive deposits of finely crystalline, brownish grey ettringite with a core of gel. When the cracks can be followed into a reactive aggregate particle they are often filled with massive ASR-gel.

From the surface and down to depths about 20-30 mm, a network of microcracks radiating out from air voids exist. This is also observed at much greater depths around the ASR-induced cracks which can be followed from the surface. Both air voids and microcracks are often completely filled with portlandite and ettringite. The interpretation is that these microcracks have been caused by frost action when water filled air voids expanded. It seems that migrating water in concrete subjected to feezing and thawing can dissolve and precipitate calcium hydroxide more efficiently than water migration under normal temperature conditions. The temperature controls whether calcium hydroxide is dissolved or precipitated and frost action leads to increased water movements in the cement paste. The increased amount of secondary portlandite in frost damaged concrete can thus be explained by the fact that the solubility of calcium hydroxide is about 2.5 g/l higher in pure water at temperatures around zero than at 20 °C.

Apart from recrystallization of calcium hydroxide, recurrent freezing and thawing which induces water migration in cracks and capillary pores, also increase the rate of crystallization of secondary ettringite in air voids. The air voids often show an outer shell of dense portlandite and a core of ettringite. Air voids up to about 0.2 mm are often completly filled, while larger air voids only have a coating on the wall leaving most of the air void empty. If the wall coating consists of dense portlandite the air voids can still be considered as inactive. At greater depths the air voids are commonly filled with ASR gel instead of portlandite and ettringite. The radiating microcracks from air voids are interconnected to a fine network pattern which join ASR-induced cracks.

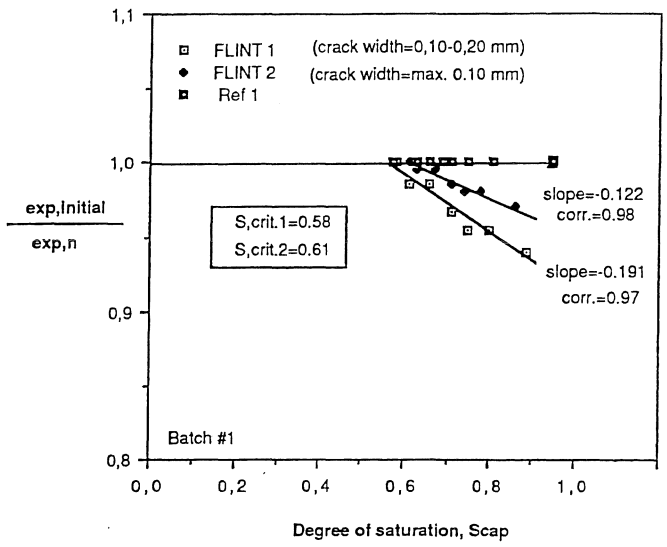

Fig. 3. Diagram showing the critical degree of saturation (S,crit.) from freeze-thaw testing of samples in batch 1. The amount of expansion and the expansion rate (steepness of curves) is increasing with increasing crack width.

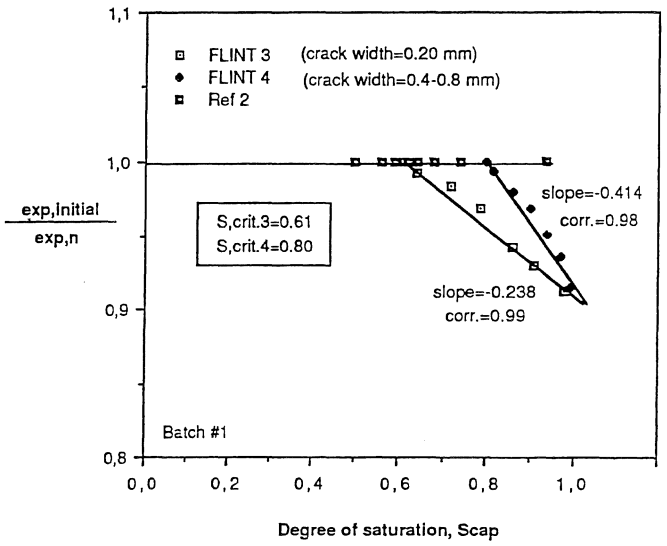

Fig. 4. Same as Fig. 3.

The above observations indicate that ASR cracking opens the concrete structure and can make the concrete more susceptible to frost attack if the cement paste is near saturated state and if the cracks become water filled.

Petrography of field concretes

After examination of thin sections from core samples from the structures, evidence for both frost attack and ASR was observed. The core samples were drilled perpendicular to the horizontal surface on sidewings and sidebeams. *Fig. 5* shows a sketch of the crack pattern from a petrographic examination of a core sample. The microscope examination revealed three types of cracks in the upper 30-40 mm. The wide vertical cracks emanating at the surface contain carbonated gel remnants on the crack walls which make it probable that these cracks are related to ASR cracking. The vertical cracks are intersected by a set of fairly straight and wide horizontal cracks which laminates the upper part of the concrete. The third type of cracks form a network of microcracks radiating out from air voids resembling a map cracking pattern. The radiating microcracks are related to the expansion of air voids which indicate that the air voids have been water filled during freezing.

The horizontal cracks partially contain portlandite and ettringite and the microcracks and smaller air voids (< 0.3 mm) are completely filled with portlandite and ettringite. At deeper levels ASR related cracks dominate and cracks as well as air voids are patially or completely filled with gel and secondary ettringite.

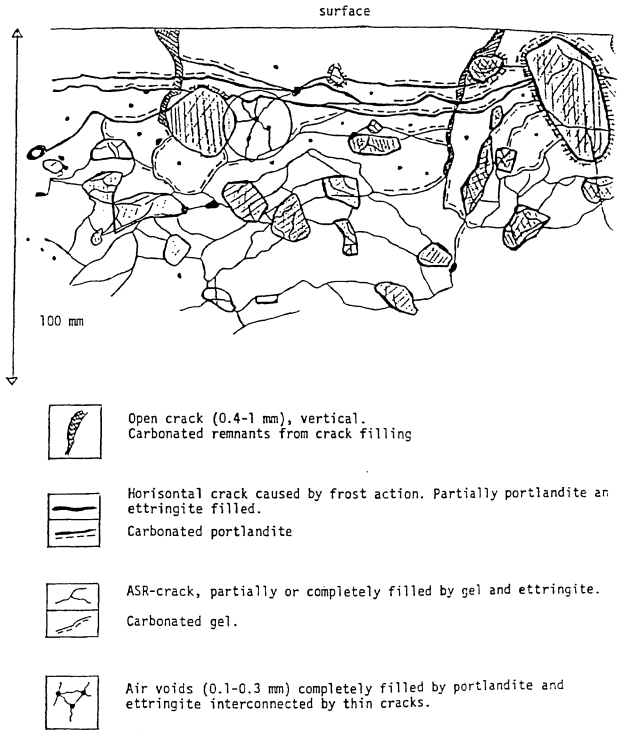

Fig. 5. Sketch showing the crack pattern in a drill core from one of the bridge structures. The core was drilled perpendicular to the horizontal surface on a sidebeam. In the upper part the wide ASR-induced vertical cracks are overprinted by horizontal cracks caused by frost action. The framed area (circule) symbolize radiating cracks from ettringite and portlandite filled air voids. Shaded aggregates = reactive aggregates.

Water absorption of field concrete

A water absorption test was carried out on ASR cracked and uncracked core samples from one of the structures. The test showed that the ASR affected concrete absorbed less water in kg/m^3 than the unaffected concrete. However, the rate and the degree of water saturation was higher for the ASR affected concrete than for the unaffected concrete. This is in agreement with the results from the water absorption test with the laboratory samples.

Conclusions

The results from water absorption tests, freeze-thaw tests and microscope analysis of field and laboratory concretes indicate that cracking due to ASR can significantly decrease the frost resistance. It should be pointed out that the concrete must reach a critical degree of saturation (S=S,crit.). Factors which have an influence on the critical degree of saturation are: cracks which provide easy accsess of water into the concrete, amount of active air voids in the size range of about 0.030-0.80 mm, spacing factor and the geometry and structure of the capillary pore system (W/C ratio). Frost attack is most likely to occur in concrete members which have exposed horizontal surfaces or if the concrete is exposed to a constant moisture load.

From the laboratory tests it can be concluded that compared with uncracked concretes the ASR-cracked concretes show a decreased critical degree of saturation at the same W/C ratio. It can also be concluded that ASR-cracked concretes show a decreased volume of coarse capillary pores and small air voids filled by water. At the same time the level of water saturation is higher in ASR affected concretes. This indicates that the cement paste structure has been densified by ASR. It is also shown that the degree of capillary water saturation is higher for samples with the larger crack widths. Especially crack widths wider than about 0.3 mm result in a high degree of capillary water saturation.

The amount of expansion, which can be regarded as a measure of the internal stress forces built up in the concrete, was found to be proportional to crack widths. This is true for W/C ratios about 0.40, air void contents of about 5 % and a spacing factor of about 0.23 mm. In concretes with higher W/C ratios (0.55) and air void contents (about 7 %) the effect of crack widths on expansion seemed to diminish.

From the petrographic examination of field and laboratory concretes it is shown that not only ASR-gel fills and inactivates the air voids, but also secondary alteration products caused by water movements during freezing and thawing fill the air voids. Such secondary products are portlandite and ettringite. The secondary products indicate leaching of components in the cement paste during freezing and thawing. This will eventually lead to decomposition of the cement paste.

The investigation show that if ASR-induced cracking is present in a structure the rate and the susceptibility to frost attack can increase. This aspect of synergism must be considered when ASR is identified in a structure. Even if ASR itself will not destroy the structure it can induce frost damage which will lower the residual service life of the structure. The frost damage will lead to scaling and reduction of the concrete cover which eventually will cause corrosion of the reinforcement. It is important to consider the detailing of the structure as the freezing will occur in concrete details with poor drainage.

References

Blight, G.E. The moisture conditions in an exposed structure damaged by alkali-silica reaction. Magazine of concrete research, Vol. 43, no. 157, pp 249-255. 1991.

Fagerlund, G. Critical degree of saturation method of assessing the freeze-thaw resistance of concrete. Materials and Structures, Vol. 10. No. 58. pp 217-253. 1977.

Fagerlund, G. The long time water absorption in the air pore structure of concrete. progress report to the BRITE/EURAM project, BREU-CT92-0591, The residual service life of concrete structures. 1993.

Idorn, G.M. Durability of concrete structures in Denmark. A study of field behaviour and microscope features. Ph.D thesis, Technical University of Denmark, 1967. 203 p.

Lagerblad, B. and Trägårdh, J. Slowly reacting aggregates in Sweden - Mechanism and conditions for reactivity in concrete. proceedings 9th International Conference on Alkali-Aggregate Reaction in Concrete, pp 570-578. 1992.

Lagerblad, B. and Trägårdh, J. Alkali-silica reaction in high strength concrete. Proceedings of the International RILEM Workshop, Durability of High Performance Concrete (editor H. Sommer), pp 143-153. 1994.

FROST DURABILITY VERSUS AIR ENTRAINMENT SYSTEM IN HARDENED AND FRESH MORTAR

Thomas Carlsson, Lic Eng
Royal Institute of Technology
Department of Built Environment
Materials Technology
Gävle, Sweden

Introduction

A project was started in the spring of 1992, in order to establish the inter action between the air entrainment system and the properties in plaster and mortar. 53 different mixes of mortar were tested. The same mixing recipe was used for all mixes. In order to obtain different air entrainment systems in the mortar, different types and different amounts of air entraining agents were used. The other mixing and hardening variables were, as far as possible, kept constant. Parameters of the air entrainment system in the hardened mortar were determined by thin section technique and microscopic analysis. Air content and air void distribution of the fresh mortar were measured by the use of a "DBT-luftpormätare". This apparatus is specially designed and manufactured by a danish company, Dansk Beton Teknik.
A complete account of the project, on which this paper is founded, is to be found in [1].

Frost durability test

Frost durability of the hardened specimens (170*25*25 mm) was determined by measuring their dynamic modulus of elasticity. The specimens were capillary saturated and sealed with a plastic film, whereafter they were exposed to cyclic freezing and thawing in a freezer. After a predefined number of test cycles the dynamic modulus of elasticity of the thawed specimens was measured. A decrease of the dynamic modulus of elasticity, compared to the start value, indicates that the specimen is frost damaged. The frost durability test continued until the specimen was considered as damaged or for a maximum of approximately 300 test cycles. Frost durability was defined as the number of test cycles that the specimen passed before a "permanent and pronounced" decrease in dynamic modulus of elasticity were noticed.

Results

Frost durability in hardened mortar

A comparison between frost durability and the three traditional structure variables (total air content, specific surface and spacing factor) of the mortar, does not show any certain relation to the mortars frost durability. This is particularly serious in the case of total air content, since this variable traditionally has been used as a measure of frost durability. However, a fourth structure variable, air void distribution, shows a significant relationship to the frost durability. In figure 1, six different samples with varying frost durability and air content are marked. Air void distribution for the same six samples is to be found in figure 2. It should be noted that the samples have been chosen in pairs. In each air content interval, one durable and one non durable sample are marked. The relationship between frost durability and air void distribution is very pronounced. A frost resistant mortar is characterized by a large volume of small voids, in spite of the mortars total air content. This pattern is the same for all mortars that have been

tested within the project. The accumulative distributions may be conversed into an equivalent air content regarding air voids smaller than a certain size. Figure 3 shows the frost durability versus air content of air voids smaller than 200 microns in diameter, L200. The figure clearly shows that L200 should be 2-3 % in order to make the mortar frost durable. In consequence, a mortar may become frost durable at a very low total air content, on condition that the air void distribution can be completely controlled.

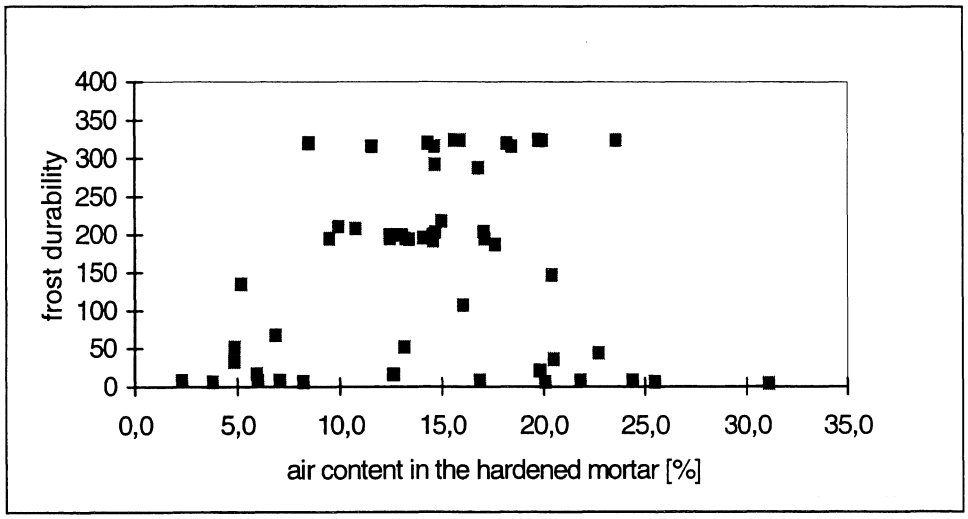

Figure 1. Air content versus frost durability

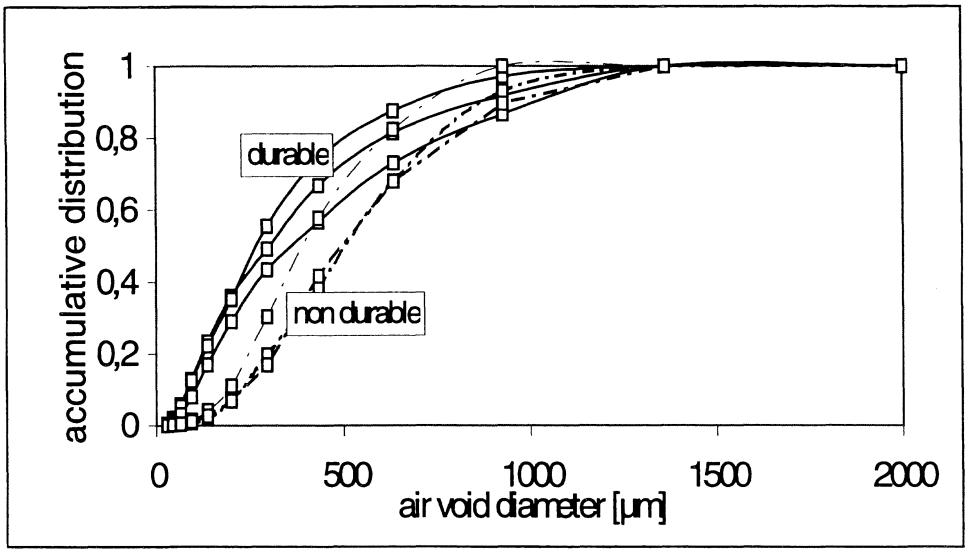

Figure 2. Accumulative distribution versus air void diameter.

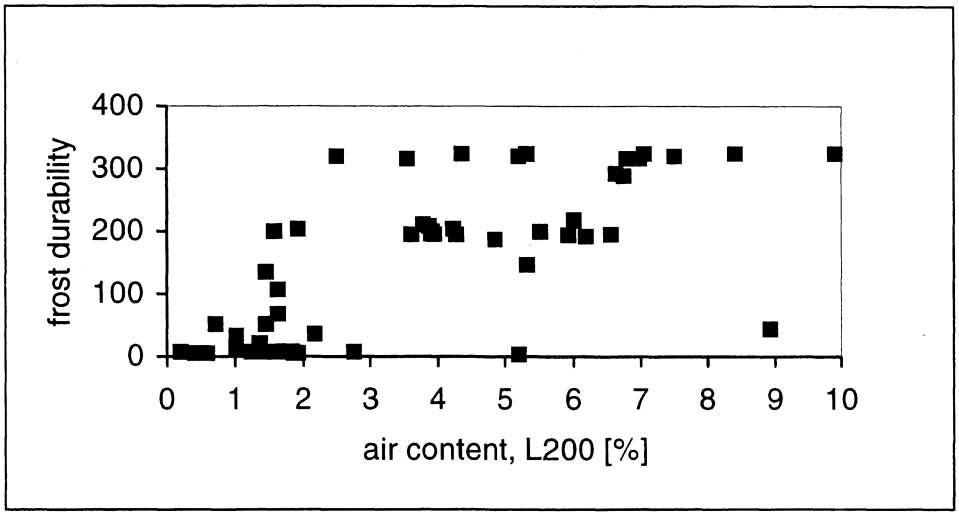

Figure 3. Frost durability versus air content.

Air content and air void distribution of fresh mortar

Measurements of total air content and air void distribution of the fresh mortar, were done in connection to the casting of specimen. The DBT-equipment consists, in general terms, of a cylinder filled with a special fluid. The mortar sample is placed in the bottom of the cylinder and stirred. At the top of the cylinder a scale pan of a electronic balance collects the rising air bubbles and measures their "lifting force". Different void sizes gives different rate of rise through the fluid. A small computer is then able to calculate an air void distribution. The whole equipment is mobile and can easily be used at any working site. A comparison between the total air content in the hardened mortar, obtained from a microscopic analysis, and values obtained from measurements in the fresh mortar, shows a very good agreement, as seen in figure 4.

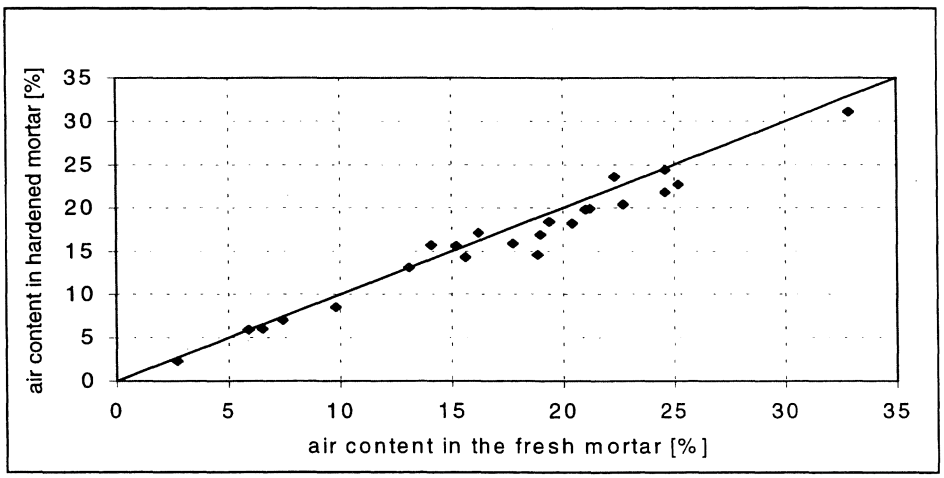

Figure 4. Air content.

The air void distribution for the same six samples as in figure 2 are shown in figure 5. In the critical void size range, less than approximately 300 microns in diameter, figure 2 and 5 are almost identical. For void sizes greater than 300 microns, there are a obvious disagreement between figure 2 and 5. This disagreement is completely a consequence of different size class interval. Furthermore, also the variable L200 in the fresh mortar shows good agreement to L200 in the hardened mortar, as seen in figure 6.

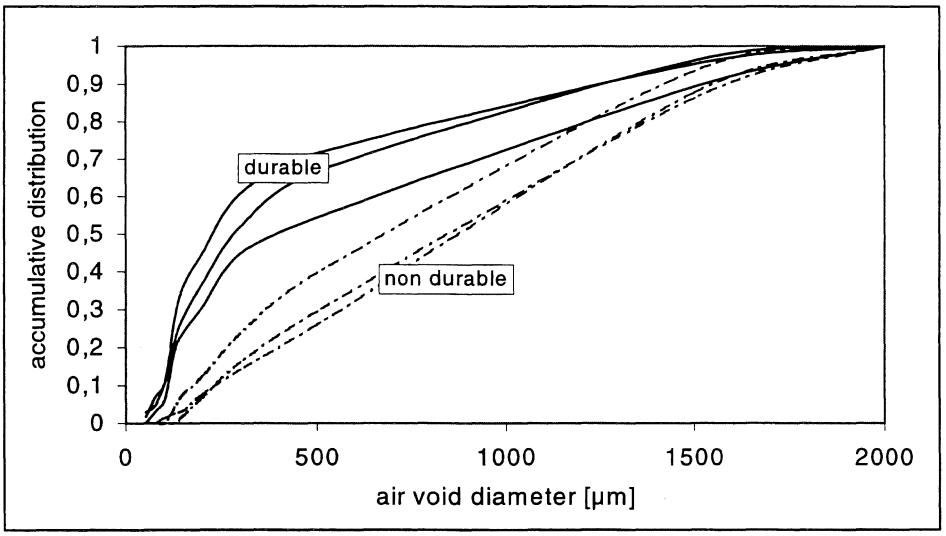

Figure 5. Accumulative distribution versus air void diameter.

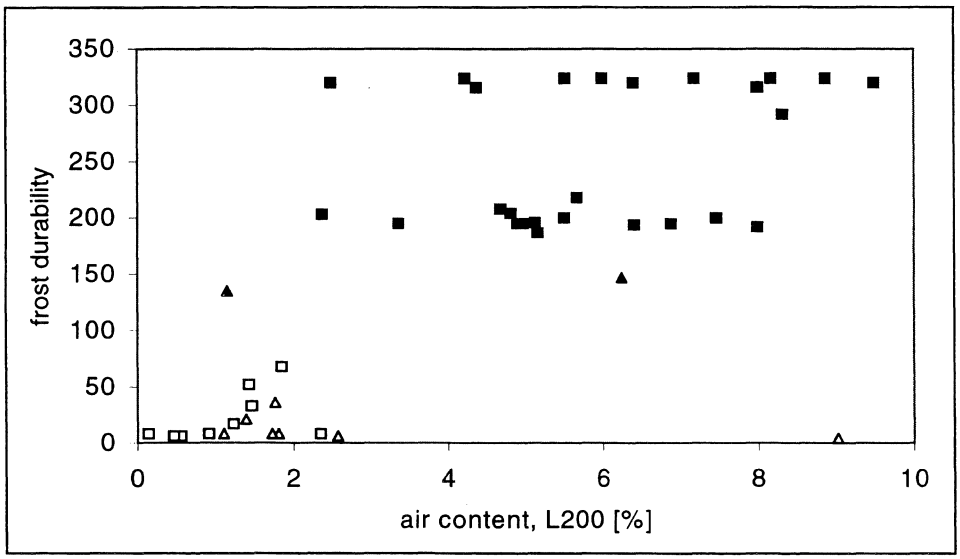

Figure 6. Frost durability versus air content.

Conclusions

The above presented results indicate that there is a possibility to determine the total air content and air void distribution in fresh mortar. This means that the frost durability can be determined at an early stage. The DBT-equipment is quite expensive, which restricts the use at working sites. However, when it comes to R&D, the possibility to determine air void distribution in fresh mortar comes in handy. It should finally be emphasized that the presented results is valid for a normal mortar, and will not of necessity be applicable to other materials, for example concrete, without further experiments.

References

[1] Carlsson, T. (1995) Luftporstrukturens inverkan på egenskaperna hos puts- och murbruk. Lund Institute of Technology, TVBM-3066, Lund. (in Swedish).

MODELLING CRITICAL DEGREES OF SATURATION OF POROUS BUILDING MATERIALS SUBJECTED TO FREEZING

Ernst Jan de Place Hansen, MSc, PhD
Department of Structural Engineering and Materials, Technical University of Denmark, Lyngby, Denmark

Abstract
Frost resistance of porous materials can be characterized by the critical degree of saturation, S_{CR}, and the actual degree of saturation, S_{ACT}. An experimental determination of S_{CR} is very laborious and therefore only seldom used when testing frost resistance. A theoretical model for prediction of S_{CR} based on fracture mechanics and phase geometry of two-phase materials has been developed.

The degradation is modelled as being caused by different eigenstrains of the pore phase and the solid phase when freezing, leading to stress concentrations and crack propagation. Simplifications are made to describe the development of stresses and the pore structure, because a mathematical description of the physical theories explaining the process of freezing of water in porous materials is lacking.

Calculations are based on porosity, modulus of elasticity and tensile strength, and parameters characterizing the pore structure and its effect on strength, modulus of elasticity and volumetric expansion. Also the amount of freezable water and thermal expansion coefficients are involved. For the present, the model assumes non air-entrained homogeneous materials subjected to freeze-thaw without de-icing salts.

The model has been tested on various concretes without air-entrainment and on brick tiles with different porosities. Results agree qualitatively with values of the critical degree of saturation determined by measuring resonance frequencies and length change of sealed specimens during freezing.

The reliability and usefulness of the model are discussed, e.g. in relation to the description of the pore structure. Based on this analysis, some new adjustments of the model are indicated. When further knowledge of the values and the importance of the different parameters is obtained, several of the tests involved will be unnecessary, making the model more useful in practice.

Keywords: Brick tile, concrete, critical degree of saturation, eigenstrain, fracture mechanics, frost resistance, pore size distribution, pore structure, stress development, theoretical model.

1 Introduction

To characterize the frost resistance of porous building materials a large number of standardized test methods exist. The methods are designed to imitate and accelerate natural degradation. Still they are time consuming and not always sufficiently reproducible and they do not explain *why* some porous materials are characterized as frost resistant and others not.

Fagerlund has shown experimentally the existence of critical degrees of saturation, S_{CR}, by freeze-thaw of porous materials. He has also shown that degrees of saturation can be used to express the frost resistance of the material, [1] [2]. The method has the advantage compared to standardized test methods that it distinguishes between the dependence of the properties of the material, expressed by the critical degree of saturation, S_{CR}, and the influence from the environment, expressed by the actual degree of saturation, S_{ACT}. S_{ACT} is normally determined approximately by capillary water uptake.

When separating the properties of the material and the influence of the environment it is easier to understand *why* porous materials are damaged or not by freeze-thaw. The drawback of the method is that it is very laborious to determine S_{CR} with a reasonable precision. Besides, it is for the present not proven experimentally whether the method can be used in connection with deicing salts, [3].

The alternative to an experimental determination of S_{CR} is to make a theoretical model. The problem is that the circumstances when water in porous materials freezes are not fully understood; different theories are developed to explain what is happening physically, e.g. [4] [5]. A more detailed mathematical description of these is lacking. This complicates the description of the relation between the pore structure and the frost resistance, a relation which is fundamental to understand the nature of freeze-thaw.

2 Modelling frost degradation and pore structure

No matter which theory is used to explain the freezing process in porous materials, stresses will be generated. These stresses will eventually result in crack propagation and degradation of the material. The pore structure, including the pore size distribution, is of crucial importance to the development of stresses. Therefore a quantitative description of the pore structure and a model for the development of stresses is necessary, although some simplifications have to be made at this stage.

Frost degradation of (partly) saturated porous materials is modelled as being caused by different eigenstrains of the pore phase and the solid phase when subjected to freeze-thaw, [6]. This leads to stress concentrations and crack propagation as described by fracture mechanics, e.g. [7] [8] [9] [10]. A parameter takes into account that ice formation can progress very slowly, cf. microscopic ice lens growth, [5].

For calculations of stresses, a system of equations based on linear elasticity is used. Such a system is relatively simple but without a direct relation to the theories of frost degradation.

The pore structure is described 1) by a shape factor, μ_0, that indicates to which degree the pore system consists of cracks, as shown in Figure 1, 2) by a parameter B that takes the deviation from pure cylindrical pores as indicated in Figure 1 into account.

In a pore system with almost no bottlenecks and a smooth pore surface, the expansion at freezing can take place almost without stress development and thereby no outward expansion, expressed by $B \approx 0$. With a rough surface and a high amount of bottlenecks the stresses generated as a result of the expansion at freezing will give rise to a great outward expansion (higher B). In other words, by introducing B only that part of the expansion by freezing that leads to generation of stresses (called effective expansion) is involved in the calculation.

Methods to determine μ_0 and B directly on basis of the pore structure are lacking at the moment, although some qualitative considerations can be made. Instead the parameters are determined 1) based on expected relations between modulus of elasticity (*MOE*), pore shape and porosity, cf. Figure 2, 2) by expressing mathematically an experimentally determined relationship between effective volumetric expansion and the degree of saturation, [6], [11], cf. the above and Figure 3.

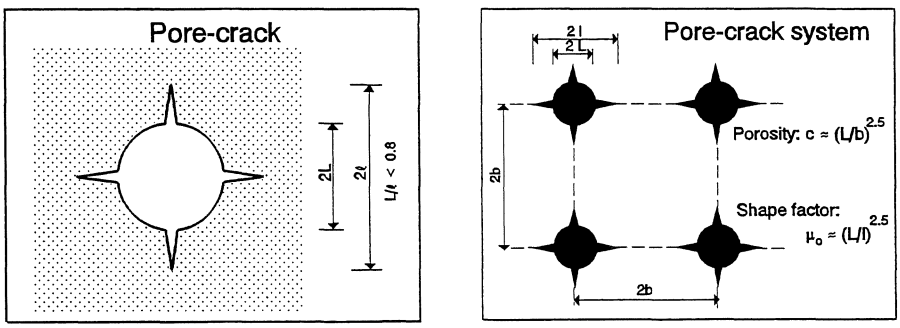

Fig. 1. System of pore-cracks (spherical or cylindrical voids) used in the model. Fracture mechanics can be used when $L/l < 0{,}8$.

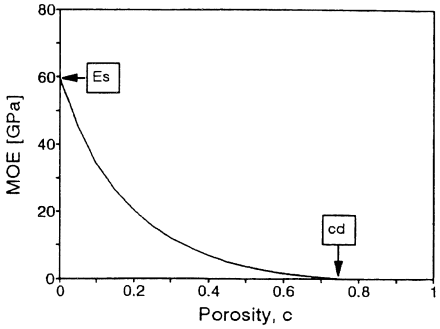

Fig. 2. Modulus of elasticity as a function of porosity. The shape factor μ_0 can be determined from the bending of the curve, cf. (2), (3).

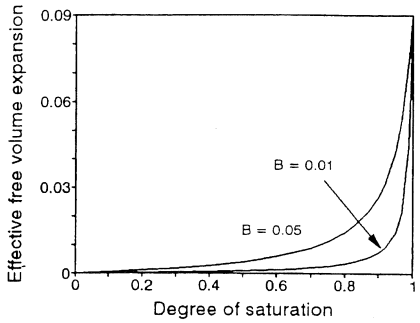

Fig. 3. Effective free volume expansion as function of degree of saturation[1]. B expresses the deviation from pure cylindrical pores (Figure 1).

When the temperature is less than 0°C the pore system is filled with ice, non-frozen water and air. The amount of ice, water and air depends on the liquid water saturation (Figure 4), the pore size distribution and the temperature. The amount of ice as well as the position of the ice in the pore system are of importance to the *MOE* and the stresses in the pore system, as well as the porous material in general.

An equivalent material is introduced to represent the mixture of ice, water and air, described by a shape factor A, and the degree of saturation of freezable water β. *MOE* of this material, E_P^*, is expressed as

$$\frac{E_P^*}{E_I} = \frac{A\beta}{A+(1-\beta)} \tag{1}$$

cf. [6] [11], corresponding to the description of porous material (subscript 0) in general, cf. [12] [13]

$$\frac{E_0^*}{E_S} = \frac{\mu(1-c)}{\mu+c} \quad ; \quad \mu = \mu_0\left(1-\frac{c}{c_d}\right) \tag{2}$$

E_I and E_S is *MOE* of ice and solid phase, respectively, c is the porosity and c_d is the critical porosity, cf. Figure 2. μ and μ_0 describes the pore shape at porosity c, and porosity $c \approx 0$, respectively.

For the present, the model assumes isotropic, homogeneous materials *without* air-entrainment or coarse cracks and subjected to freeze-thaw *without* de-icing salts, which simplifies the calculations. As by an experimental determination of critical degrees of saturation, e.g. [1] [14], a limited temperature gradient is assumed.

1. Free expansion means stress-free expansion. In [6] [11] is shown how the real expansion is determined. In Figures 5, 7 and 17 the real expansion as it is measured in dilation tests is used.

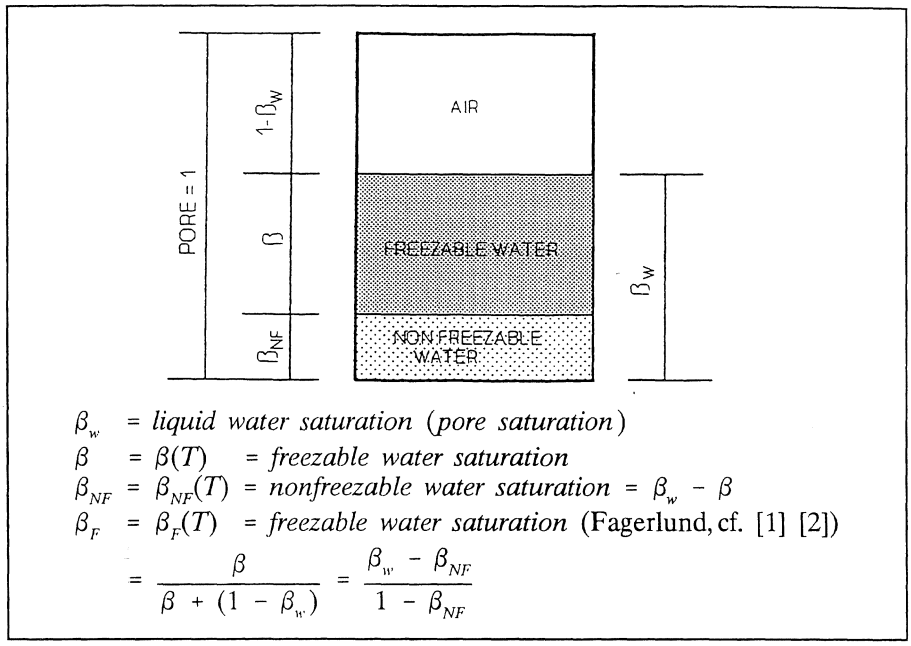

β_w = *liquid water saturation (pore saturation)*
β = $\beta(T)$ = *freezable water saturation*
β_{NF} = $\beta_{NF}(T)$ = *nonfreezable water saturation* = $\beta_w - \beta$
β_F = $\beta_F(T)$ = *freezable water saturation* (Fagerlund, cf. [1] [2])

$$= \frac{\beta}{\beta + (1 - \beta_w)} = \frac{\beta_w - \beta_{NF}}{1 - \beta_{NF}}$$

Fig. 4. Definitions of degree of saturation.

The degree of saturation and thereby the critical degree of saturation can be expressed in several ways as shown i Figure 4. T is temperature. For materials with coarse pores, e.g. tile, $\beta_w \approx \beta \approx \beta_F$. For fine porous materials, the critical degree of saturation will be a function of the minimum temperature, no matter which of the definitions is used.

β_F is used when results from concrete are used to analyse the model (section 5), because the development of stresses is dependent on the amount of ice. Critical degrees of saturation are therefore determined as $\beta_{F,CR}$. On the other hand, β_w is more handy when the results are used in practice, where the pore size distribution seldom is known in detail. Actual values of β_w are measured very simply and $\beta_{w,CR}$ can be calculated from $\beta_{F,CR}$, cf. Figure 4.

3 Test programme

Most of the parameters involved in the model are determined experimentally directly or indirectly as listed in Table 1. Some are determined by table references, e.g. thermal expansion coefficient and E-modulus of ice. Also the critical degree of saturation and the degree of saturation by capillary water uptake are determined. Degrees of saturation are always related to vacuum saturation.

The choice of materials for the different tests has been based on the assumptions mentioned in section 2. Concrete without air-entrainment with water/

cement ratio 0,3, 0,45 and 0,7 and tile bricks with four different additions of saw dust and water are produced, as shown in Tables 2 and 3.

Table 1. Experimentally determined parameters.

Parameter	Method
Parameter B describing the amount of bottlenecks and the roughness of pores, cf. Figure 3	*Dilation* test (measurement of length changes on sealed specimens during freezing). Minimum temperature: -20°C.
Porosity Pore size distribution	Vacuum saturation Sorption, scanning microscopy
Tensile strength and modulus of elasticity	Uniaxial tensile loading
Shape factor of pores, critical porosity	Using corresponding results for E-modulus and porosity, cf. Figure 2
Experimental determination of S_{CR} to compare with calculations based on the theoretical model	*Dilation* test and measurement of *resonance frequency*
Actual degrees of saturation	Capillary water uptake

- By comparing actual degrees of saturation with S_{CR} the frost resistance can be expressed, [1]. This is *not* a part of the theoretical model but is made to support the calculations.
- *Dilation* expresses the deviation from the *linear* thermal deformation during freezing, cf. [15]. Volume expansions (used in the model) are conversed to length changes and vice versa when model and test results are compared.
- The *resonance frequency* is a measure of the dynamic E-modulus, which decreases with increasing frost degradation, cf. [16].

Table 2. Concrete mixtures. Amounts in [kg/m^3].

	Type/Origin/Class	Concrete 0.30	Concrete 0.45	Concrete 0.70
Cement	ASTM Type III	426	349	264
Water	Tap water	109	155	185
Superplasticizer	Peramin F	27,7	3,5	0
Fine aggregate	Ry 0-4 mm, kl SA	643	643	643
Coarse aggr. 1	Glensanda 4-8 mm, kl A	189	189	189
Coarse aggr. 2	Glensanda 8-16 mm, kl A	1058	1058	1058

Table 3. Tile, laboratory mixtures. Amounts in weight units.

		Tile A	Tile B	Tile C
Clay	Prøvelyst tilery[1] (yellow bricks) (= Tile 0)	60	30	20
Saw dust	Build. Mat. Lab.[2]	3	3	3
Water	Tap water	5	4	5

1. Prøvelyst tilery, Karlebo, 2. Building Materials Lab., Tech. Univ. of Denmark.

In both cases the purpose is to make simple comparable materials with different porosities. One of the tile series is a common product from a tilery (series 0), the rest are made by hand at a laboratory (series A, B and C).

4 Test results

The critical degrees of saturation, S_{CR}, determined experimentally 1) in dilation tests, 2) by measuring the resonance frequencies are in general in good agreement. At the same time it is ascertained that S_{CR} has to be determined with some uncertainty, cf. the spread of the results, e.g. Figures 5 to 8.

The dilation tests show, that it is possible to determine the parameter B, expressing the importance of bottlenecks and roughness of the pore surface on S_{CR}, using corresponding values of degree of saturation and expansion, e.g. Figures 5 and 7, although the values have to determined with some uncertainty.

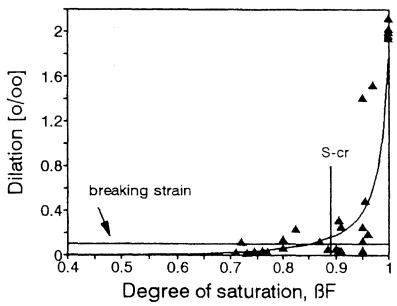

Fig. 5. Results from dilation test, concrete 0.70. Curved line is based on parameter B. Dilation is the deviation from the linear thermal deformation. Temperature -20 °C.

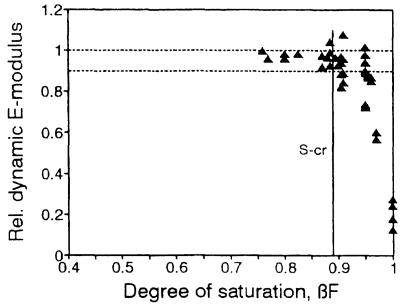

Fig. 6. Results from measurement of the resonance frequency expressed as relative dynamic E-modulus. Concrete 0.70. The horizontal line at 0,9 is defined as the criterion for damage, cf. [16].

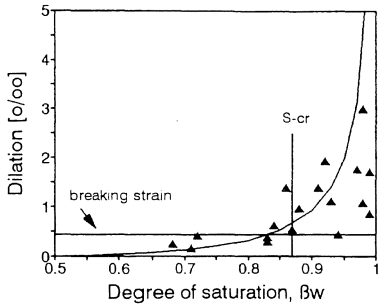

Fig. 7. Results from dilation test, tile B. Curved line is based on parameter B. Temperature -10 °C.

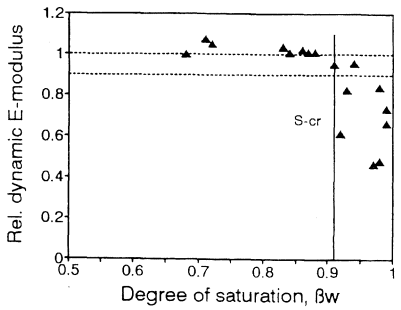

Fig. 8. Results from measurement of the resonance frequency. Tile B.

The tensile strength and the E-modulus are, as expected, strongly dependent on the porosity, cf. Table 4. Also the dilation (non-linear length change) during freezing increases with the porosity.

The amount of coarse pores increases with an increased water/ cement ratio (concrete), and increased porosity (tile), respectively, while the amount of small pores is almost unchanged, cf. Figures 9 and 10. Coarse pores are capillary pores (concrete), and pores with radius greater than 5 - 10 μm (tile), respectively.

Generally, the concretes are very dense and differences in pore structure are difficult to observe when microscopes are used. Still, there seems to be more cracks of a crackwidth of 1 - 2 μm with increasing water/cement ratio. As expected, bricks made at a tilery (series 0), where the production facilities are automated, are more dense than bricks made in the laboratory.

When experimentally determined critical degrees of saturation (S_{CR}) and degrees of saturation at capillary water uptake (S_{CAP}) are compared, the influence of the water/cement ratio on the frost resistance ($F = S_{CR} - S_{CAP}$) is clearly seen, cf. Figure 11. A corresponding dependence is seen when exposing the concretes to standardized freeze-thaw as described in [17].

There is no dependence of the porosity on the frost resistance of tile bricks, cf. Figure 12. The increased porosity is seen as a higher amount of pores greater than 5 - 10 μm, cf. Figure 10. These pores are only filled with water at capillary water uptake with difficulty.

Table 4. Tensile strength (f_t), E-modulus (E_0^*) and porosity (c).

Average values	Concrete 0.30	0.45	0.70	Tile 0	A	B	C
f_t [MPa]	4.5	3.4	2.3	2.6	1.4	0.9	0.5
E_0^* [GPa]	46	40	30	8.7	4.3	2.3	1.4
c	0.08	0.11	0.14	0.42	0.50	0.55	0.62

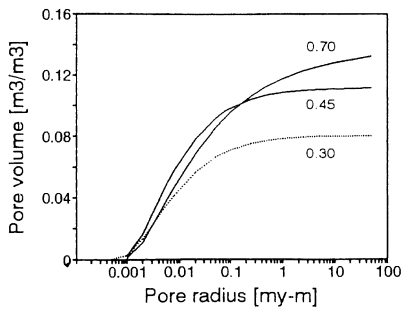

Fig. 9. Pore size distribution, concrete.

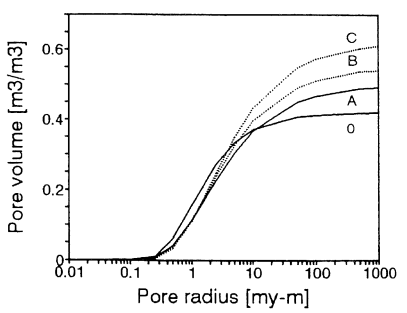

Fig. 10. Pore size distribution, tile.

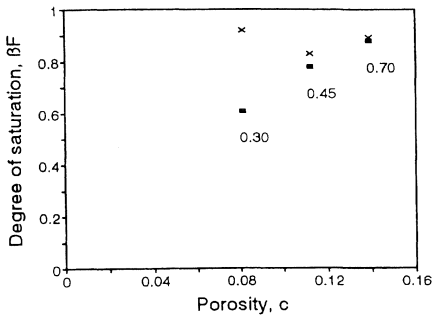

Fig. 11. Experimentally determined critical degree of saturation (x) and degree of saturation at capillary water uptake (■) as function of porosity. Concrete. Average values.

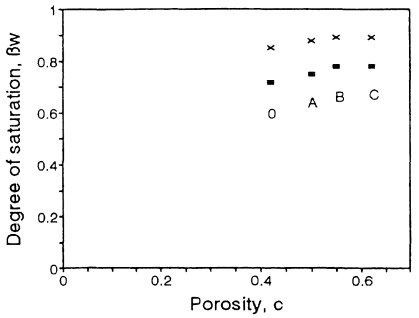

Fig. 12. Experimentally determined critical degree of saturation (x) and degree of saturation at capillary water uptake (■) as function of porosity. Tile. Average values.

5 Discussion of the theoretical model for prediction of S_{CR}

Based on the test results, calculations are made with the theoretical model using an algorithm made for computer. Generally, the calculations give lower values of S_{CR} than the experimentally determined, typically 0,1 - 0,15 lower, e.g. Figures 13 and 14. Such a deviation is acceptable being aware of the simplifications of the calculations, cf. section 2.

5.1 Degree of saturation and pore structure

To establish the relation between degree of saturation and volumetric expansion, calculations show that it is necessary to take into account that some parts of the pore system is filled with non-freezable water, dependent on the temperature, especially in concrete. Thereby, the model supports Fagerlund's definition of the degree of saturation of freezable water, β_F in Figure 4.

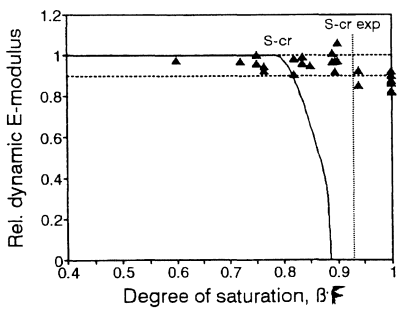

Fig. 13. Relative dynamic E-modulus as function of degree of saturation, calculated (bold line) and experimentally determined (▵). Concrete 0.30.

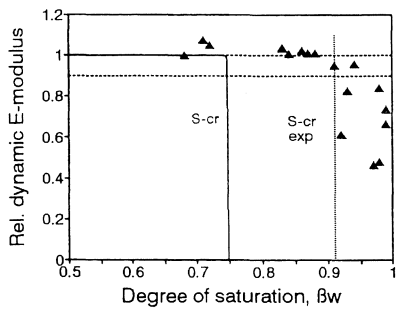

Fig. 14. Relative dynamic E-modulus as function of degree of saturation, calculated (bold line) and experimentally determined (▵). Tile B.

Calculation of the E-modulus of the material when subjected to freeze-thaw is made using an analogy between a porous material and the pore phase perceived as a porous material with ice as solid phase, cf. (1) and (2). However, this analogy assumes that the amount of freezable water is related to the *total* pore volume, β in Figure 4.

It is possible to relate the amount of freezable water to the *total* pore volume when calculating the E-modulus and at the same time taking into consideration that the pore system is partly filled with non-freezable water when calculating degrees of saturation. Thereby, the difference between the calculated and the experimentally determined S_{CR} is decreased by 0,05 - 0,1 for concrete compared to Figure 13.

For brick tile there is no difference between the two definitions of the degree of saturation, β_F and β, since there is almost no non-freezable water.

The use of different definitions of the degree of saturation is somewhat confusing. This is one of the primary reasons why some of the expressions in the model are adjusted at the moment. The shape factor A describes the position of ice in the pore system, or more correctly the shape of that part of the pore system *not* filled with ice. A has been held constant in this study, but in practice the position of the ice, and thereby the value of A, will be dependent on the amount of freezable water β (Figure 4), and thereby the temperature. Expressions involving B and other parameters are adjusted too.

5.2 Usefulness of the model

When the critical degree of saturation is exceeded a great spread of results is expected. Therefore it is not surprising that the curve based on parameter B only to some extent corresponds with the results of the dilation test, especially in Figure 7. The analysis in [11] shows that the critical degrees of saturation calculated using the model are dependent on how precisely the parameter B is determined. This expresses the close relationship between the pore structure (roughness, bottlenecks) and the critical degree of saturation, and increases the need for a quantitative description of B directly on basis of the pore structure.

The other parameters describing mechanical properties, pore size distribution, shape factor etc. (Table 1) can be determined allowing for some uncertainty assuming that a reasonable basis exists.

Whether the importance of B is overestimated because of the simplifications of the model, primarily when calculating stresses in the material, will be studied in the near future. Also the importance of how the degree of saturation is defined will be investigated.

Especially for tile, the model simplifies the circumstances when the critical degree of saturation is exceeded, e.g. bold line compared to "▵" in Figure 14. This is probably caused by the fact that the importance of cracks on the strength is expressed by a simple crack model (Griffith), e.g. [7] [9], modified as described by [8].

Also the fact that calculations of stresses are based on a system of equations without direct linkage to the theories of frost degradation is of importance. At the same time, it is shown that the model *is* capable of taking into account that concrete has some amount of toughness, e.g. Figure 13.

6 Further perspectives

Although there are disagreements between calculated and experimentally determined values of critical degrees of saturation, the analysis shows the perspectives in using a theoretical model. For instance, the model supports Fagerlund's definition of degree of saturation and the existence of critical degrees of saturation.

It is possible to determine all the parameters in the model, although some have to be determined indirectly. The assumptions concerning the relation between the modulus of elasticity, shape factor and porosity seems to be sufficiently precise, cf. Figures 15 and 16.

The need for a direct, quantitative description of the relation between pore structure and degree of saturation is stated. An expression involving the volume expansion and the parameter B which both are dependent on the pore structure is used. This expression has shown to be relevant, but very dependent on the parameter B. Adjustments of the expression are under consideration.

The system of equations for calculations of stresses has to be more directly related to physical theories of freezing. Also, it must be investigated, whether the model used for crack propagation (Griffith) is sufficiently precise.

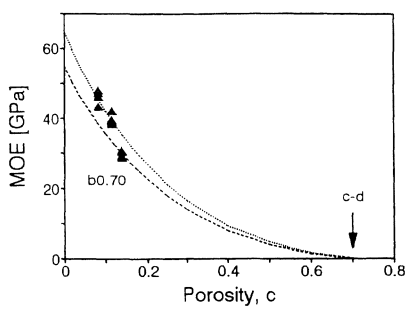

Fig. 15. E-modulus as function of porosity, concrete. Curved lines are based on (2), Section 2.

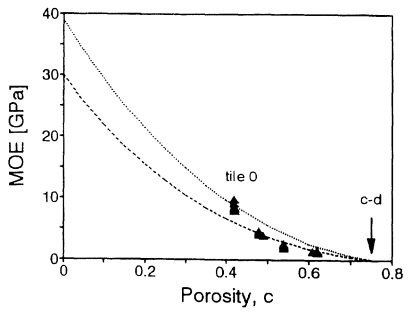

Fig. 16. E-modulus as function of porosity, tile. Curved lines are based on (2), Section 2.

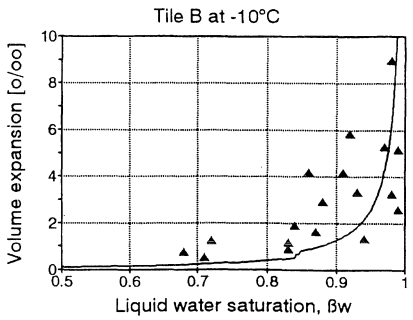

Fig. 17. Results of dilation test shown as volume expansion, tile B. Curved line is based on parameter B. The model is adjusted compared with Figure 7 as indicated in Section 5.1.

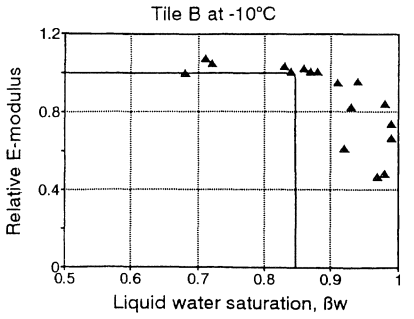

Fig. 18. Relative E-modulus as function of liquid water saturation, calculated (bold line) and experimentally determined (▵). Tile B. The model is adjusted compared with Figure 14.

Preliminary results of the adjustments of the model as indicated in Section 5.1 are shown in Figures 17 and 18. Notice, that the results from dilation test are shown as volume expansion and that the circumstances when the critical degree of saturation is exceeded still are to simplified, Figure 18.

If used on air-entrained materials, inhomogeneous materials and/or by combined freeze-thaw and deicing salt exposure changes in the model are necessary, as suggested in [18]. For instance the modelling of stress-development must be modified when deicing salts are involved.

6.1 Computer modelling of pore structure

A general problem of the calculation of frost resistance based on degrees of saturation is the difficulty of describing, in a simple way, the pore structure and its importance to transport of moisture and to critical degrees of saturation. This is also the reason why the parameters describing the pore structure at present are determined indirectly.

Today methods are developed based on a more detailed description of the pore structure, e.g. on series of two-dimensional photos or on a three-dimensional description of the surface, [19] [20]. A three-dimensional computer model for simulation of the hydration of cement and - especially important in this connection - the formation of a system of capillary pores in the cement paste (percolation theory) is developed in the USA, [21] [22]. With this model it is possible to follow how the connectivity of the pore system is formed.

Such systems must be involved in the future to obtain a more precise description of the relation between pore structure, moisture transfer and critical and actual degrees of saturation.

Acknowledgement
This paper is based on a PhD-study on frost resistance of building materials, [11]. The financial support from the Danish Research Academy, Århus and the Danish Building Research Institute, Hørsholm is gratefully acknowledged.

References

1. Fagerlund, G. (1972) *Critical degrees of saturation at freezing of porous and brittle materials* (in Swedish), Thesis, Report 34, Div. of Building Technology, Lund Institute of Technology, Lund.
2. Fagerlund, G. (1975) Significance of critical degrees of saturation at freezing of porous and brittle materials. *ACI Special Publ.* SP-47. pp.13-65.
3. Fagerlund, G. (1992) *Studies of the scaling, the water uptake and the dilation of mortar specimens exposed to freezing and thawing in NaCl-solution*, pp.35-66 in: Freeze-thaw resistance of concrete. Research seminar held in Lund, June 17, 1991. RILEM Committee TC-117 FDC (edited by G. Fagerlund, M.J.Setzer). Report TVBM-3048, Division of Building Materials, Lund Inst. of Technology. Lund.
4. Powers, T.C. (1949) The air requirement of frost-resistant concrete. *Proc. Highway Research Board*, Vol.29. pp.184-211.
5. Powers, T.C. and Helmuth, R.A. (1953) Theory of volume changes in hydrated Portland cement paste during freezing. *Proc. Highway Research Board*, Vol.32. pp.285-297.
6. Nielsen, L.F. (1993) *Mechanics of composite material subjected to eigen-stress. With special reference to frost resistance of porous brittle material.* SBI Bulletin 96, Danish Building Research Institute, Hørsholm.
7. Griffith, A.A. (1920) The phenomena of rupture and flow in solids. *Trans. Royal Soc.*, Vol.221, London.
8. Dugdale, D.S. (1960) Yielding of steel sheets containing slits. *Journ. Mech. and Phys. Solids*, Vol.8. pp.100-104.
9. Nielsen, L.F. (1986) *Material mechanics.* (textnotes in Danish), Technical Report 169/1986, Building Materials Lab., Technical University of Denmark, Lyngby.
10. Nielsen, L.F. (1988) *Material mechanics II.* (textnotes in Danish), Technical Report 189/1988, Building Materials Lab., Technical University of Denmark, Lyngby.
11. Hansen, E.J. de Place (1995) *Frost resistance of building materials - modelling the critical degree of saturation* (in Danish). Ph.D.-thesis, Danish Building Research Institute, Hørsholm and Building Materials Lab., Technical University of Denmark, Lyngby, 197 + 111 p.

12. Nielsen, L.F. (1982) Elastic properties of two-phase materials. *Materials Science and Engineering*, Vol.52, No.12. pp.39-62.

13. Nielsen, L.F. (1984) Elasticity and damping of porous materials and impregnated materials. *Journ. Am. Ceram. Soc.*, Vol.67, No.2. pp.93-98.

14. Fagerlund, G. (1977) The critical degree of saturation method of assessing the freeze/thaw resistance of concrete. *Materials and Structures*, Vol.10, No.58. pp.217-253.

15. ASTM C-671 (1986) *Standard Test Method for Critical Dilation of Concrete Specimens Subjected to Freezing. ASTM C 671-86*, nov 1986. American Society for Testing and Materials. Annual book of ASTM standards, vol.04.02.

16. Warris, B. (1964) *The influence of air-entrainment on the frost resistance of concrete. Part B: Hypothesis and freezing experiments*, Proc. no.36, Swedish Cement and Concrete Research Institute, Stockholm.

17. Swedish Standard SS 13 72 44 (1988) *Concrete testing - Hardened concrete - Frost resistance*. Byggstandardiseringen.

18. Hansen, E.J. de Place (1996) Testing a model for the critical degree of saturation at freezing of porous building materials. Accepted for presentation at *7th Int. Conf. Dur. Build. Mat. & Comp.*, Stockholm, Sweden, May 19-23, 1996.

19. Nakamura M., Ohnishi T. and Kamitani M. (1991) Quantitative analysis of pore structure on frost durability of inorganic building materials. *Journ. of Ceramic Society Japan, Int. Edition*, Vol.99. pp.1074-1079.

20. Issa, M.A. and Hammad, A.M. (1994) Assessment and evaluation of fractal dimension of concrete fracture surface digitized images. *Cement and Concrete Research*, Vol.24, No.2. pp.325-334.

21. Bentz, D.P. and Garboczi, E.J. (1991) Percolation of phases in a three-dimensional cement paste microstructural model. *Cement and Concrete Research*, Vol.21, Nos.2/3. pp.325-344.

22. Garboczi, E.J. (1993) Computational materials science of cement-based materials. *Materials and Structures*, Vol.26, No.158. pp.191-195.

A HYPOTHESIS ON THE MECHANISM OF SURFACE SCALING DUE TO COMBINED SALT FROST ATTACK

Sture Lindmark, MSc Civ. Eng.
Lund Institute of Technology
Div. of Building Materials
Box 118
221 00 LUND
SWEDEN

Abstract
A hypothesis on the mechanism of "salt-scaling" of porous building materials based on theories for frost heaving in soils and observations made by Powers and Helmuth /1953/ is described. Though the text mainly deals with cement based materials, the mechanism described should be valid for any brittle, porous material. A simplified calculation of possible scalings shows that the hypothesis predicts reasonable values. Results from a first qualitative test support the hypothesis.

Background
In /1943/, Arnfelt investigated damages observed on Swedish concrete roads and also performed some laboratory experiments which clearly showed that weak solutions of different salts would cause severe surface damages when the concrete was exposed to frost. These results also proved valid for solutions of urea and ethyl alcohol, which are both non ionic. For this reason, Arnfelt came to the conclusion that the mechanism was of physical rather than chemical nature. Brick and sandstone were tested too, but in these cases, pure water caused worse damages than did the solutions that were used. The damages observed on bricks (used for roofing) were of another kind than the ones seen on concrete, and it was not as clear that the bricks were subject to a surface attack. Sandstone showed larger scaling the less the salt concentration used. Arnfelt proposed this was due to the different pore size distribution of sandstone as compared to concrete.

Verbeck and Klieger /1957/ presented results from tests on surface scaling resistance of concrete exposed to frost attack and solutions of different de-icers. Their results showed that the combined frost de-icer attack causes much worse surface damages than does pure water. Also, it was concluded that a moderate concentration of de-icer, 2-4 percent by weight, causes worse damage than do lower as well as higher concentrations.

The results from Verbeck and Klieger are very similar to those of Arnfelt, and similar results have also been achieved later by other researchers. Some attempts have been made to explain the observed results, e.g Pühringer / 1994/, Powers /1965/, Browne&Cady /1975/, Petersson /1984/ and others, but none of them has been found fully satisfactory.

Many qualitative observations have been reported which help in understanding the phenomena of "salt scaling". For example, Verbeck and Klieger observed that there would be no scaling if no solution was applied on the specimen surface. I believe another and complementing observation made in our laboratory should be mentioned here: It has been proposed that as de-icers will be differently concentrated in pores of different size, osmotic phenomena will be responsible for "salt scaling". However, in laboratory studies which are to be published at our department, it has been observed that specimens in which there is a salt concentration gradient close to the surface and on which salt scaling has occured in previous frost cycles in which the specimens were covered with a salt solution, scaling will be discontinued if the specimen is frozen without any salt solution on its surface.

The aim of this text is to present a hypothesis based on theories for frost heaving in soils. After a short description of basic thermodynamical principles, a physical model is presented and with that model as a basis some speculations on the consequences of some variations of parameters in a testing procedure will be given.

Thermodynamic basis in short

In figure 1, which was drawn according to Everett /1961/, two perfectly rigid containers are connected by a narrow channel of radius *r*. The pistons make it possible to adjust the volume of each container. Both containers are initially water filled, but ice formation is initiated in A, the upper one. As the level of free energy of ice is lower than that of water, the water will now "condense" on the ice surface and continue to do so until both phases reach the same level of free energy. To reestablish equilibrium at constant temperature and in the abscence of solutes, a pressure difference is needed between ice and water.

Assuming the contact angle to be 0°, the radius of the meniscus separating the phases when equilibrium is established may be calculated using the LaPlace equation:

$$\Delta P = \frac{2\sigma}{r}$$

in which ΔP = Pressure difference required for equilibrium, Pa
σ = Interface tension ice-water, J/m²
r = Kelvin radius of the meniscus, m

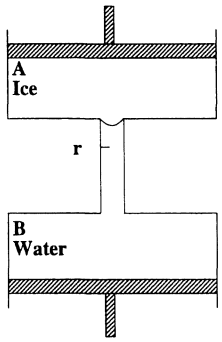

Fig 1: Ice and water at thermodynamical equilibrium (and equal temperatures), with a spherical meniscus of radius r separating the phases. Everett /1961/.

It is thus seen that if the radius of curvature of the meniscus is 10 nm, a pressure difference of about 6.6 MPa is needed to maintain equilibrium.

If the upper container is initially completely filled with water, pressure will raise heavily on ice formation and the process will be stopped. On the other hand, if the degree of saturation is such that the upper one contains just a small fraction of the total water content, no pressure will arise in the ice. Instead, as water is transferred to the ice phase, container B will be partly emptied. This will give rise to a negative pressure in the water and the requested pressure difference may be reached.

Within a certain interval, equilibrium will be established as a combination of positive pressure in the ice and negative pressure in the water. For lower degrees of saturation, no positive pressure will exist in the ice, and for higher degrees of saturation, no negative pressure will exist in the water. Somewhere within this interval, there will be a critical degree of saturation at which the material will be damaged due to micro ice lens growth. As the isothermal compressibilities of both water and ice are quite low, this interval is likely to be rather narrow.

If both pistons are free to move, no pressures, neither negative nor positive, will appear in any of the phases. This means the ice will continue to feed from the water container until all the water has been consumed. It also means that if the liquid phase is very much larger than the solid phase, the negative pressure in the liquid will be negligible in comparison to the pressure difference needed for equilibrium and thus the ice will grow and start to exert a pressure on the container walls.

Hypothesis

In /1953/, Powers and Helmuth proposed a mechanism of inner frost damage in concrete specimens, which has later been referred to as the theory of micro ice lens growth. Observations like the one shown in figure 2 formed the basis for this theory, according to which ice lenses which form in capillary pores are able to feed from the unfrozen water in nearby pores. This process is due to the different

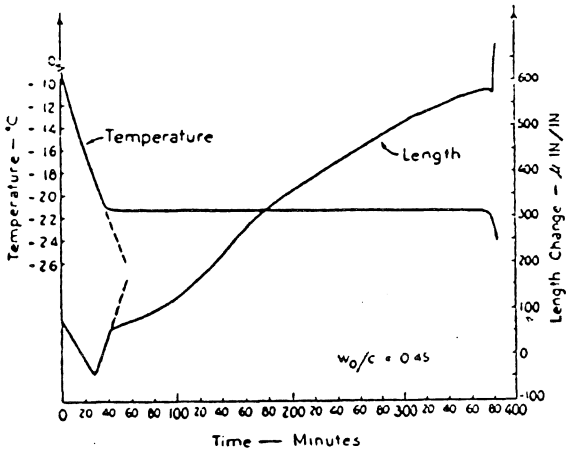

Fig. 2: Expansion of paste specimen during period of constant temperature. Powers and Helmuth/1953/.

levels of free energy in unfrozen water and ice, which are caused by differences in temperature and pressure. The process will be active also between two ice crystals of equal temperature and pressure, if they are of different size, as surface tension adds to the level of free energy.

This harmful process will come to a stop when the levels of free energy are equal. A stable temperature gradient between the pores, the presence of solved salts in the pore water or a pressure difference between the phases are different ways of reestablishing equilibrium. Obviously, any combination of these opportunities may do as well.

The first case, a stable temperature difference, is very unlikely to occur between two adjacent pores. Actually in an ordinary specimen, the temperature would have to be higher in the unfrozen portion of water and lower in the frozen one, which must be considered an impossible situation. It may therefore be considered as impossible to stop the process by the aid of local temperature differences.

As described above, a pressure difference between solid and liquid phase may bring the two phases into thermodynamic equilibrium. This means that freezing, i.e. growth of the solid phase, will continue at a rate predicted by the heat flow as long as the pressure difference is too small. If the ice phase starts to exert a pressure on the pore walls surrounding it or if the pore system is drained to such an extent that the remaining water is exposed to a negative pressure, the required pressure difference may be obtained.

If salts are present in the pore water, the level of free energy of the water is reduced and ice will not start to form until temperature has declined to a certain extent below 0°C, a temperature which we may call T_c. As temperature continues to fall, more ice will form and the ice crystals may start to exert a pressure on the pore walls. However, the pressure difference required for equilibrium to exist between pure water and ice as described above, is reduced if the water contains salts. This means that if the pores contain a large enough quantity of salt, no

pressure difference is needed between the phases to maintain equilibrium and no ice lens growth will occur at temperature above T_c. (Obviously, no amount of salts can protect the paste from damage due to in-site formation of ice during cooling, but this requires that the degree of saturation be high enough and makes use of another type of deterioration mechanism.)

As the results of Powers and Helmuth /1953/ showed that the specimen expands during a period of constant temperature, there has to be an inner expansive pressure. This means that the amount of naturally dissolved salts in the pore system is not large enough to protect the cement paste from damage by micro ice lens growth. Instead, there is an overall competition between ice lenses for the available unfrozen water and the entire specimen volume is damaged.

By combining the container-model described by Everett and the theory proposed by Powers and Helmuth, a hypothesis for the mechanism of surface scaling due to combined salt frost attack may be proposed. In figure 3, a principal sketch shows a small pore located a certain distance dx beneath the surface of a concrete specimen. The surface is covered with pure water. A narrow channel connects outer water and pore solution. Heat flows perpendicularly to and unidirectionally from the water surface into the air. In this way, temperature is first lowered at the upper surface. (All other edges are sealed to any kind of flow.)

Water on top of the specimen will start to freeze when the temperature reaches 0°C. Possibly, some supercooling may occur, but that is not very likely in a real case, and will not be considered here. This means that a meniscus will form at the upper end of the channel connecting the outer water and the solution of the pore. The exact location of this meniscus will probably be dependent on chemical composition of the pore solution and pore size distribution. As no pressure difference exists at this stage, the meniscus will initially be plane. As long as the temperature of the outer ice as well as the pore solution is 0°C, the two phases will exist in equilibrium. If now temperature were lowered in both phases, a difference in level of free energy would occur. As a consequence, the pure ice on the surface would feed from the pore solution, reducing the water content of the pore system. If the cooling is done slowly enough, water may be transported at a rate high enough to prevent ice formation in the pores. This means that pure water on the surface will act protectingly on the uppermost layer of the specimen. As the

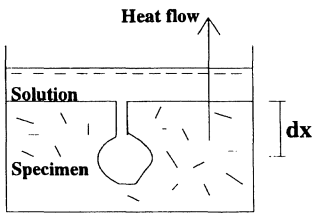

Fig 3: Model pore close to the specimen surface.
Pore size is in the nm-scale.

pressure in the pore solution is lowered, the meniscus will adopt a certain radius of curvature, which may be calculated as described above.

Now let heat flow in the opposite direction. In this way, the specimen is cooled before the remaining unfrozen water, and so the pore solution will start to freeze before the water on the surface does (provided the pore solution does not contain dissolved salts or something else that lowers its freezing temperature too much). Now, a meniscus will form at the lower end of the channel, with its convex side facing the channel. This means the ice formed in the pore will feed from the surface water via the channel. As the outer water volume is at constant pressure, the pressure difference needed for equilibrium must be achieved as a positive pressure in the ice. As a consequence, the ice in the pore is likely to grow and exert pressure on the pore walls. In the case of ordinary building materials, this pressure will easily be large enough to damage the material. This process is the same as that taking place in frost heaving of soils. It has also been observed, that surface scalings are more severe when a concrete specimen is tested in this way than when cooled from the surface side /1995/.

If there had been no water on the surface, a meniscus between water in the channel and outside air would have formed, and on ice lens growth a negative pressure in the water would have appeared. Under ideal circumstances this negative pressure might have been large enough to prevent the ice from destroying the specimen. It is unlikely though that the specimen would remain completely free of damages if completely or almost completely water saturated at the start of cooling. However, the important point is that the damages would have been spread across the entire specimen volume. Actually, the surfaces should be the least damaged part, as ice lenses close to the surface would have had only half as much moisture available as the ones in the interior! Compare this with the results of Powers and Helmuth: Their specimens were isolated to moisture ingress, and so inner processes were everywhere the same (except possibly at the surfaces), causing an overall damage.

Once again, let heat flow from the specimen surface but this time replace the outer water with a salt solution with a freezing point depression ΔT. For the sake of simplicity, we shall presume the pore solution to be pure water. When temperature reaches 0°, no ice will form in the outer solution, but ice will start to form inside the specimen (certainly, 0° will be reached slightly later in the pores than in the surface water, but the delay will be very small under usual testing conditions). This time, the meniscus will form at the lower end of the channel and water transport will be directed towards the ice crystal. As the outer liquid phase and thus also the remaining pore solution will remain at atmospheric pressure, the ice crystal will be able to grow unrestrictedly. Initially, the available moisture will be the pore solution which we have said to consist of pure water and so it will in no way retard the speed of ice lens growth. In fact, the ice lens will not stop growing until the water transported to it contains a large enough amount of solutes. Depending on the depth of the ice lens below the surface, more or less pore solution will be available before the ice crystal is surrounded by water containing solutes. In this way, conditions for ice lens growth close to the surface have been

drastically improved as compared to the case of pure water as well as to that of no water on the surface.

Some qualitative predictions may now be made as on how the system will react to certain changes of conditions. But first a simplified calculation will show that the order of size of predicted scalings is correct:

The pressure difference required for equilibrium may be calculated from the Clausius-Clapeyron equation using the temperature below 0°C at which ice and water are to exist, or one may use the width of the channel separating the containers. The latter approach was used by Everett, but as we cannot correctly predict the width of the open channels, it seems more convenient for our purpose to use the former one. This has been done, for instance, by Knutsson /1985/, who has given the following formulation:

$$\Delta P = \frac{(T_0 - T)}{T} * H * \rho$$

in which ΔP = Pressure difference required for equilibrium, Pa
T_0 = 273.15 K
T = Present temperature, K
H = Heat of fusion (333 kJ/kg at 273.15 K)
ρ = Density of water, 1000 kg/m³

Suppose the temperature is -10°C. For ice and water to exist in equilibrium at that temperature, a pressure difference of 12.2 MPa is required.

As was said above, ice lensing will progress at a speed set by the current heat flow. The only restriction is that unfrozen water has to be available. This means that ice lensing will take place in places where heat flow balances the heat of fusion released on freezing. At the crystal surface, water condenses at a rate predicted by the heat flow, and the ice crystal grows in a direction which offers the least resistance. The transfer of water to the ice crystal may thus be thought of as a short cut diffusion process. However, when a certain volume of water disappears from the pore solution, it has to be replaced or else a negative pressure will occur. This means there has to be a flow of water in the pores. As long as the ice crystal and its surrounding pore solution are not in equilibrium, water will keep flowing. If the resistance to flow becomes too large, either because the permeability is too low or because the available water is too far away, ice lens growth will stop and the frost front will progress into the specimen. The depth of balance, dx in figure 3, may be calculated by applying Darcy's law:

$$G = B * \frac{dP}{dX}$$

in which G = Flow rate, kg/(m²*s)
dP = Pressure difference, Pa

dX = Flow distance, m
B = Coefficent of permeability, s

At some depth dX below the surface, heat flow will balance the heat of fusion which is released on freezing of the water which flows from the surface to the ice crystal. Close to the surface, the heat flow may be estimated from the following expression:

$$q = V * \rho * c * \frac{dT}{dt}$$

in which q = Heat flow, J/(m²*s)
V = Volume of water covering the specimen surface, m³/m²
ρ = Density of water, 1000 kg/m³
c = Specific heat of water, 4.2 kJ/(kg*K)
dT/dt = Cooling rate, K/s

Under normal testing conditions (as in the Swedish standard SS137244), water depth and cooling rate are 3 mm and 3 K/h, respectively. This means the heat flow is 10.5 J/m²*s. The heat of fusion is 333 J/g, and so this heat flow corresponds to an ice formation rate of 10.5/333 = 0.0315... g/m²*s. The water flow reaching the ice crystals thus has to be 0.0315 g/m²*s in order to balance the heat flow.

The mean temperature during a frost cycle like the one used in SS137244, may be set to be -10°C. At this temperature, the required pressure difference is about 12.2 MPa as estimated above. For cement paste with a water to cement ratio of 0.40, B may be estimated from Powers et al /1954/ to be $2*10^{-15}$ s.

Solving for dX, we get

$$dX = B * \frac{dP}{G} = 2 * 10^{-15} * \frac{12.2 * 10^{6}}{0.0315 * 10^{-3}} = 0.77mm$$

In the laboratory, surface scaling flakes have been measured to be up to about 0.9 mm. Certainly, the exact figures shall not be focused upon too much, but this very simple calculation shows that the proposed mechanism predicts values of correct order of size. Most probably, ice lenses will not form in just one single layer, but rather at many different depths and thus flakes will be of many different thicknesses.

Obviously, one may question the use of a non-existing pressure as a driving force for water flow and the use of a permeability as measured for water flow under an outer overpressure. However, the explanation given above and the fact that

geologists use this approach, should make it reasonable to believe these principles will hold also in the case of porous building materials.

Consequences - Predictions

We may now turn to the qualitative predictions mentioned above. As will be evident, any single change will affect the system in many ways and as a consequence the discussion will have to be limited, otherwise it will not serve its purpose of clarifying the basic principles.

The predictions are essentially divided into two groups: Reactions caused by changes in outer circumstances, and reactions caused by changes in material properties.

Permeability

Permeability governs the water flow under conditions of constant pressure difference and flow distance. In this way, permeability plays a major role in that it decides the maximum depth at which ice lensing may take place. As mentioned above, using the permeability to water flow as measured for water flow at conditions of an outer overpressure may not be correct, but irrespective of what parameter is chosen for flow calculations, the principles given below will apply.

Permeability to water flow through discs of cement paste has been studied by many researchers. Though, as far as the author knows, no studies have been reported on water permeability of partly frozen cement paste or mortar. Such measurements are undoubtedly very difficult to accomplish, but should prove very useful for more precise predictions of the phenomenon described. In the lack of proper data, the simple relation between capillary porosity and permeability given by Powers et al in /1954/, will be used to demonstrate possible effects.

As is seen in figure 4, permeability may be described in terms of capillary porosity. When calculating the depth of balance between heat flow and water flow, either one of two simple ways of estimating permeability at temperatures below 0°C may be used. The first and simplest way certainly is to estimate, for the water to cement ratio in question, a mean permeability, likely to be valid throughout the period of freezing. The second way is to reduce capillary volume by the volume of ice formed in the pores. This is doubtful though in that we do not know exactly how much ice has formed, neither do we know where it has formed: If it forms only as micro ice lenses growing in relatively coarse capillary pores (or even entrained air pores), a case which will be possible under conditions of slow cooling, the remaining capillary porosity is unchanged and thus permeability is likely to remain constant too. In this case permeability may be chosen directly from figure 4 for the particular water to cement raio. On the other hand, if the material is cooled rapidly, ice is more likely to form in site in the capillary pores, causing a large decrease in permeability.

According to the equations given above, a lower permeability will reduce the possible maximum depth of ice lensing, and so scaling will be reduced. Here a

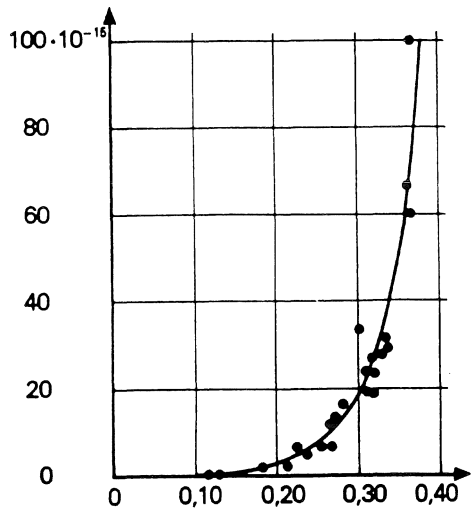

Fig 4: Water permeability (B, unit: second) vs. capillary porosity. From /1982/ after Powers et al /1954/

first complication on predicting effects of different frost cycles may be discerned: Depending on the foregoing cooling rate, conditions for ice lens growth will vary at subsequent temperatures and cooling rates.

Permeability may also be affected by temperature. Probably though, these effects are small and as a first approximation they may be omitted.

Pore size distribution

Three main types of pore size distribution will be treated: Uniformly coarse distributions, uniformly fine distributions and finally well spread distributions comprising a wide range of sizes. Permeability is closely related to pore size distribution, but will be discussed only briefly in the following.

In a material with coarse porse of one single and quite large size, all water will freeze almost simultaneously just slightly below 0°C. After that, no pores will be open and no water transport may take place any more. This means the proposed mechanism will not be active.

A material with a pore size distribution of this kind will be very sensitive to anomalies in its pore size distribution. If there are some larger pores present in which the very first ice formation is likely to take place, permeability will still be high and thus conditions for continued growth of the crystals formed in these pores will be very good.

In the case of uniform and very fine porous materials, very low temperatures will be needed for any ice formation at all to take place. Once ice crystals have started to form, permeability will be reduced just as in the former case, and thus the possibilities for micro ice lens growth are once again strongly restricted, but just as in the former case this pore system too will be sensitive to anomalies. Due to its very minute pores, permeability of the fine porous system will be very much lower than that of the uniformly coarse pore system, and thus this fine porous system will not be as badly damaged as the depth of balance between heat- and water flow can not be very large.

The two cases described are impossible, though, as it is presumed that their pore size distributions are perfectly uniform. This will never be the case in any real kind of building material. Instead in reality the suggested anomalies will always be present more or less pronouncedly and thus a coarse porous material will probably not be able to withstand a combined de-icer and frost attack. The fine porous one might suffer no or only very limited damage as ice will not start to form unless very low temperatures are applied and when that eventually happens the limited permeability of such materials should set limits on the ice lensing depth.

The third pore system contains all pore sizes between the two extreme cases treated above. In such a pore system, ice will start to form when temperature is lowered slightly below 0°C but that some water will still remain unfrozen at temperatures well below those normally occuring either in the laboratory or in nature. In such a pore system, permeability may still be quite high even after extensive ice formation has occured. This will make it possible for ice lensing to occur even at relatively large depths. As a consequence scaling may be severe, depending on the cooling rate.

Pore solution

Generally, the described scaling mechanism is favoured if the pores contain pure water, as any presence of solutes will reduce the pressure difference needed for equilibrium and thus will reduce the maximum possible pressure that ice lenses may exert.

Outer de-icer concentration

This is perhaps the most interesting question as any hypothesis put forward on the mechanism of salt-frost scaling has to be able to explain the maximum in damages at a solute concentration of about 2-4 percent by weight observed by many researchers. Unfortunately, the hypothesis does not provide any simple explanation. From the foregoing it is evident though that scalings are likely to increase the lower the de-icer concentration in the pores, while as a de-icer has to be present in the solution covering the specimen surface for any scaling to be possible at all. Before commencing any detailed analysis, it may therefore be concluded that maximum scalings are likely to occur when a test is performed in such a way that de-icers do not enter the pore system and in such a case scaling will also be independent of saltconcentration, provided there is always a large enough amount of moisture available. (As temperature drops, ice will be segregated from the solution and so the available liquid phase will be reduced. In the extreme case all this liquid may be consumed by the ice crystals and as a

consequence no ice lens growth due to the presence of an outer liquid phase will be possible. This extreme case may be realized if the de-icer concentration is too low in comparison to the initial amount of solution applied) Possibly, the maximum in damages caused by a 3% solution is simply the result of these two conflicting requirements and possibly the 3% level is the one that does not reduce possible ice pressure too much. It must be remembered however that damages do not disappear completely when stronger concentrations are used!

What amount of de-icer will be present at any given depth in the specimen is mainly a question of what time is avilable for diffusion (or any other transfer mode) of the de-icer into the pores to take place before freezing starts. Certainly, some diffusion may take place even after freezing has been initiated, but the main conditions will already be set by then. This means we may distinguish three principally different cases: In the first one no de-icers have entered the pore system, in the second one the de-icer is uniformly distributed in the entire pore system and in the third case their is a concentration gradient close to the surface. In all three cases it is presumed that the de-icer concentration in the outer solution is such that de-icers do not leave the pores.

The first case is the same as the situation described above where the pore solution consists of pure water. This means ice lens growth may take place anywhere in the pore system and also that no limits are layed upon maximum ice pressure.

In the second case where a strong concentration is present everywhere, ice lenses will not start to form until a certain temperature T_c below 0°C is reached. This temperature T_c is dependent on the salt concentration. For temperatures lower than T_c, the maximum pressure that an ice crystal may exert is reduced. For example if the relative vapour pressure of water is reduced from 100% to 96% by adding salt (about 6.3% by weight NaCl), the equilibrium pressure difference will be reduced by about 4.5 MPa (the effect will be dependent on temperature). If the requested pressure difference has to be established as an overpressure in the ice phase (i.e. assuming the liquid phase to remain at atmospheric pressure) the overpressure at -10°C may be calculated to be about 11.6 MPa. When the salt is added this is reduced to about 7.1 MPa. Probably, an ice pressure of 7.1 MPa will be enough to damage the pore walls, but it is clearly seen how salts in the pore water reduce the damaging effect of ice lens growth.

In the third case in which the de-icer is not uniformly spread there is reason to believe ice lens growth will occur: When ice starts to form in one pore there will always be nearby pores containing cleaner water from which the ice crystals may feed. Especially, it is likely that pores of different sizes will contain different amounts of dissolved salts after a given, short period of salt ingress.

The maximum in damage observed at about 3% by weight concentration of NaCl is possibly explained by the fact that the maximum pressure that an ice crystal may exert is not reduced too much while the depth of ice lensing is still quite large.

Cooling rate

Generally, slow cooling, i.e. low heat flows, will promote ice lens growth, but at low cooling rates, the ice lens growth will take place closer to the surface than the permeability would permit and thus scaling will not be the worst possible. Such low heat flows may be named suboptimum heat flows, as there is a certain heat flow, which will make full use of the available permeability. The optimum heat flow on the other hand, is likely to vary with temperature in the case of a material with a wide spread pore size distribution as the amount of freezable water varies with temperature in such a material.

Suboptimum heat flows though has another advantage: After flaking off a first layer, another level of ice lens growth may be established and in this way multiple flakings may occur during one single frost cycle. Whether this outweighs the negative effect of a seemingly suboptimum heat flow is impossible to say.

Minimum temperature

There have been some discussions on the importance of choice of minimum temperature when testing concrete for salt frost resistance. Ordinarily, the minimum temperature is in the range -15 to -22°C. The following discussion refers to a range of this size and is not aimed at explaining phenomena that might be observed if temperature is allowed to vary in a range like -2 to -50°C.

The lower the temperature, the more ice will form in a material with a certain spread in pore size distribution. In this way there will be more sites in which ice lenses may start to grow unless larger ice crystals in the vicinity of these pores have already consumed what water was ever available in them. Furthermore, at a given depth, larger ice crystals in other places are likely to be more able to benefit from the improved moisture accessibility close to the surface. Thus the minute ice lenses that might form at very low temperatures probably will have to be located very close to the specimen surface to be able to grow in site. That is, the minute ice crystals have to be closer to the specimen surface and the moisture available there than to their nearest ice crystal neighbour. This means the extremly fine pores will add to total scaling only when cooling is so rapid that only very shallow ice lens depths are possible. (Once again: This means choice of lowest temperature should play a role only under circumstances of quite rapid cooling.)

Depth of solution covering the specimen surface

Provided cooling is kept constant, depth of the surface solution will play only a second role. In the calculation given above, it was seen that water flows into the specimen will be something like 100 g/m²*h. Very probably, large deviations from this figure may occur. Anyway, it still is interesting as it indicates that under some circumstances, all available liquid on the specimen surface may be consumed and thus ice lens growth will be interrupted. (With an initial amount of 3l/m² of 3% NaCl solution, there will remain 0.6 l/m² of liquid phase at -10°C. If nothing else would change and all of this solution would be available for ice lens growth, it would take 6h at -10°C to consume it all. Of course conditions will not be this ideal but the calculation indicates that the total amount of solution on the surface specimen at the beginning of a test might be important.)

Initial test

As was mentioned above, damages should be independent of salt concentration if an ordinary scaling test were carried out in such a way that no salts were present in the pores. Therefore, such a test was run as a first test of the hypothesis. Only a short review of the test will be given here, for a complete report, the reader is referred to our department.

The main interest thus lay in using different saltconcentrations. This was accomplished by pouring 26 ml of pure water on the specimen surfaces at +20° and then when the temperature of the surface solution had reached 0°, another 13 ml of different cooled NaCl-solutions were added. By using NaCl-solutions 3 times more concentrated than the desired ones, the solution covering the surface would be correct after dilution.

Three cement mortars of different water-cement ratios (0.45, 0.50, 0.65) were used. The air contents were 6.6, 6.2 and 6.7% respectively. The total paste content was about 45% and thus a moderate or low frost resistance was expected. Maximum aggregate size was 3 mm.

Specimens were circular discs with a diameter of 127 mm and a thickness of 25 mm. The specimens were heat isolated as shown if figure 5 and a lid was put on to prevent any evaporation.

All specimens were water cured for at least 6 weeks. Half of the specimens were slightly dried in a climate chamber (60%RH/18°C) for two days and were then water stored another three days before starting the test.

Because the specimens of water cement ratio 0.50 were run as a pre-series, these were treated slightly different than the others. As the differences are generally believed not to influence very much on the principal results, they will not be commented upon here, all such details are given in the complete report. There is one major difference though: The 0.50s were tested with salt solutions with concentrations of 0, 1.1, 2.3 and 5.6% respectively, while as the others were tested with 0, 1, 3 and 7.5%.

The specimens were run through 7-10 frostcycles. The temperature cycle is given in figure 6. The salt solutions were immediately removed and replaced with pure water when temperature once again reached 0°C. In this way, no salt solution was present during the hours when temperature was above 0°C.

The main results are given in figures 7-9.

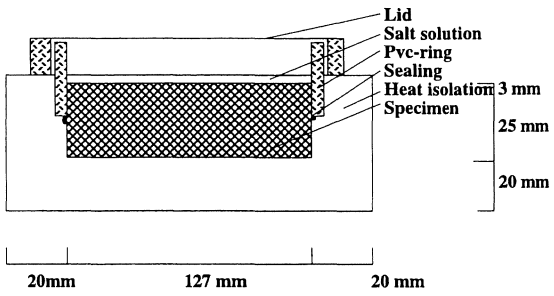

Fig 5: Test setup for salt-scaling tests.

Specimens are identified by their water cement ratio, next with a letter combination (D or ND) indicating whether the specimen has once been dried and remoistened or not, after that the salt concentration that was applied to it and finally a letter to show which one of two identical specimens is in question. 45ND3A thus means water cament ratio 0.45, Never Dried, 3%, specimen A.

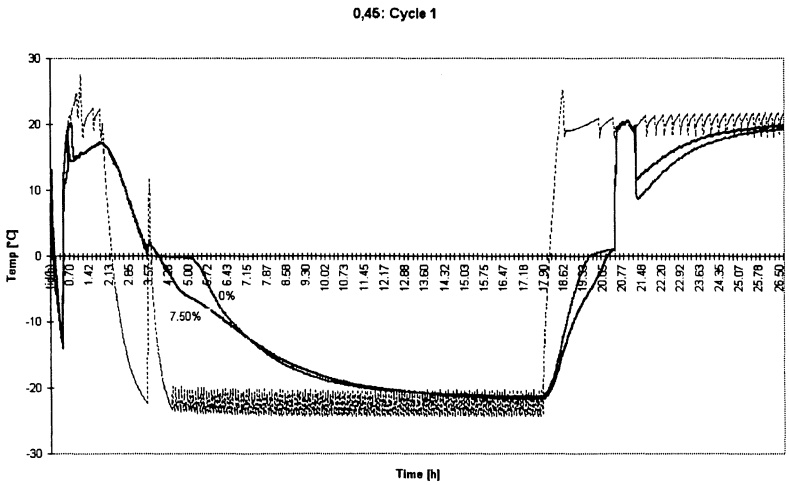

Fig 6: Temperature cycle as measured in the solution covering specimen surfaces. (Dashed line shows air temperature)

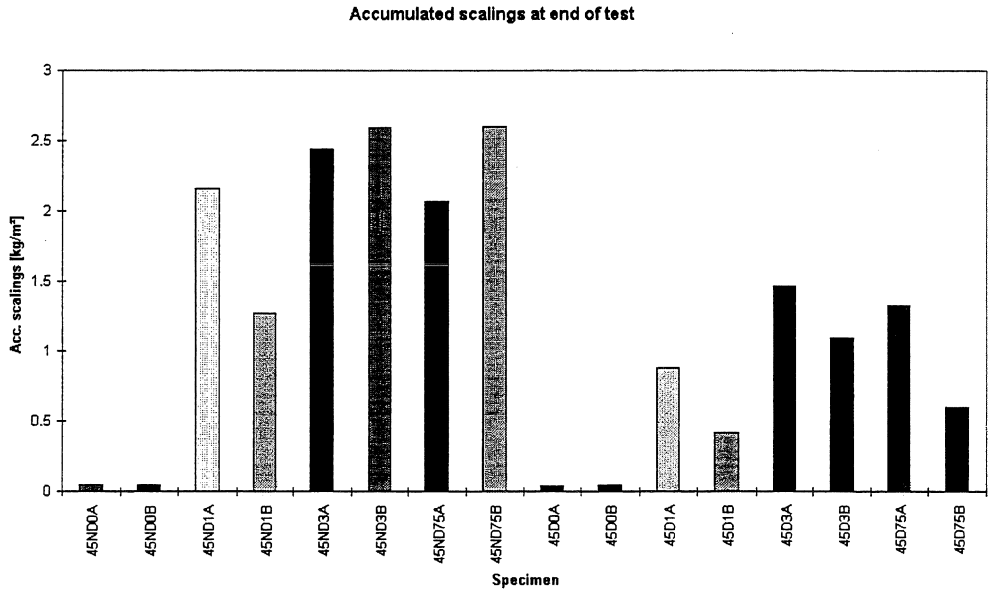

Fig 7: Final accumulated scalings (W/C 0.45, 10 cycles)

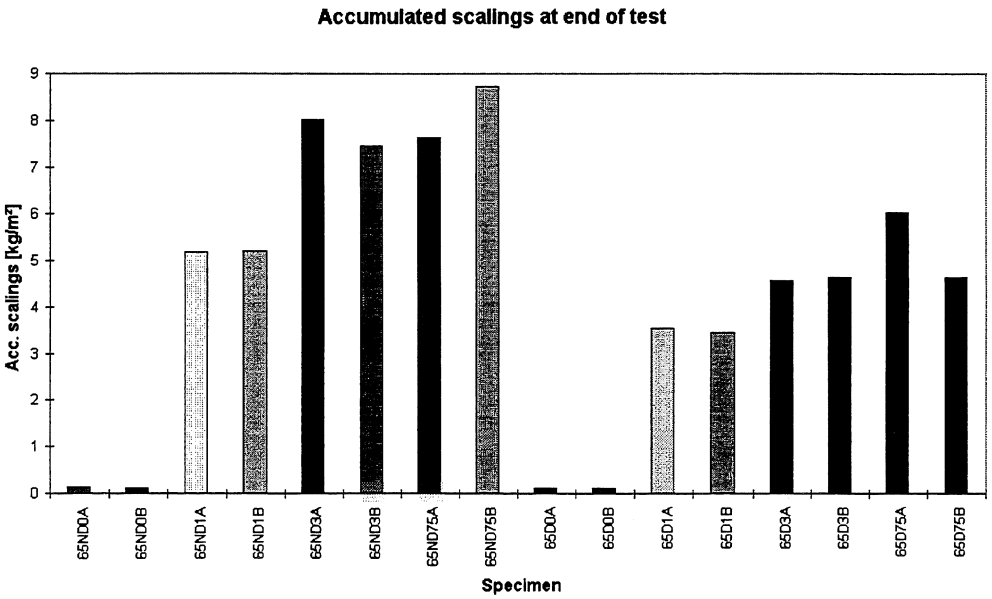

Fig 8: Final accumulated scalings (W/C 0.65, 9 cycles)

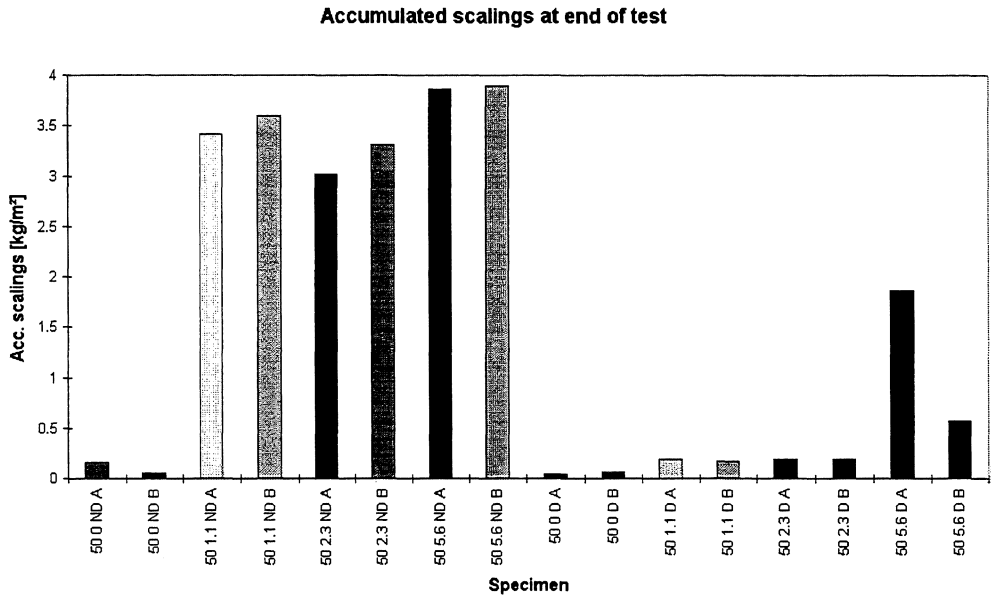

Fig 9: Final accumulated scalings for the pre-series (W/C 0.50, 7 cycles)

For specimens that were never dried, it is clearly seen that there is no damage maximum at a concentration of about 3%. Rather, damages seem to be independent of salt concentration.

Results from a test of this kind should be treated with great care as there are so many other variables which also affect the results. Nevertheless, from previous experience it was expected for a mortar of this kind to show a clear damage maximum at the 3% concentration. Therefore it seems reasonable to state that these results support the hypothesis.

One interesting observation was made during the test: Specimens that had once been dried and remoistened, were able to withstand a few cycles but when scaling finally commenced, the complete surface was scaled off in almost one single, coherent layer, about 0.8 mm thick. This behaviour was repeated in subsequent cycles, although less pronounced. Specimens that were never dried did not show the same "one-single, coherent-layer"-behaviour. Still the flakes measured up to about the same thickness.

References

1943 Arnfelt, H: "Damage on concrete pavements by wintertime salt treatment" Meddelande 66, Statens Väginstitut, Stockholm 1943 (In Swedish)

1953 Powers, T C, Helmuth, R A: "Theory of volume changes in hardened portland-cement paste during freezing", Higway Res. Board, Proceedings, 32/1953.

1954 Powers, T.C, Copeland, L.E, Hayes, J.C, Mann, H.M: "Permeability of portland cement paste", ACI Proceedings V26, No 3, Nov. 1954

1957 Verbeck, G and Klieger, P: "Studies of "salt" scaling of concrete", Higway Res. Board, Bull. 150, Washington DC.

1965 Powers, T.C: "The mechanism of frost action in concrete". Stanton Walker Lecture Series, Lecture No. 3, Presented at University of Maryland, Nov.1965

1975 Browne, F.P, Cady, P: "Deicer scaling mechanisms in concrete", ACI Special Publication 47-6

1985 Knutsson, S: "Några synpunkter på tjälningsprocessen och dess termodynamiska bakgrund", 85:08, Avdelningen för Geoteknik, Tekniska Högskolan i Luleå. (In Swedish)

1982 Betonghandbok Material, Svensk Byggtjänst.

1984 Petersson, P-E: "Inverkan av salthaltiga miljöer på betongs frostbeständighet", Statens Provningsanstalt, SP-Rapp 1984:34 ISSN 0280-2503

1994 Pühringer, J: "Zur materialzerstörung durch tausalzfrostwechsel - über die 3%ige NaCl-lösung"

1995 Fagerlund, G: Personal communication.

INGRESS OF MOISTURE DUE TO FREEZE/THAW EXPOSURE

Mette Geiker, Specialist
COWI
Parallelvej 15
DK-2800-Lyngby

Niels Thaulow, Head of Dept.
G.M. Idorn Consult, RAMBØLL
Bredevej 2
DK-2830-Virum

Abstract
Concrete exposed to salt solution during freeze/thaw testing absorb more water than concrete in contact with pure water. An explanation of the observed effect is suggested.

Introduction

Increased mositure content of concrete causes an increased risk of frost damage. The importance of the degree of saturation with respect to frost damage appears first to have been emphasised in (Hirschwalt, 1910). Based on the theories of Powers, a critical degree of saturation above which the material is damaged during freeze/thaw exposure has been proposed (Fagerlund, 1977).

Exposure to salt/salt solution increases the freeze/thaw damage considerably, e.g. (Jacobsen and Sellevold, 1994). According to (Fagerlund, 1993) the dominating effect of salt on the degree of freeze/thaw deterioration is the increased absorption in the surface layer.

Concrete tends to suck water when subjected to repeated freeze/thaw cycles. Exposure to salt solution has been reported to cause an increased rate of moisture ingress, ref. e.g. (Fagerlund, 1992), (Jacobsen and Sellevold, 1994).

At present there appears to be no commonly recognized explanation of the mechanism of absorption. Ingress of salt has been said to be facilitated by osmosis. Due to the very small difference in ion concentration of salt water and pore liquid this effect is questioned by the authors. According to (Setzer, 1993) the increased absorption during freeze/thaw exposure can be explained by a pumping effect due to the high thermal expansion of water compared to ice and the freeze/thaw hysteresis.

Ingress of Moisture

The following hypoteses explaining the effect of salt is hereby presented for discussion.

Assume concrete is freezing from the surface. As ice takes up 9% more room than water, the surplus pore liquid may be pushed into the concrete in front of the ice.

Also, assume the concrete thaws from the surface. The thawing creates a low pressure in the pores because the pore liquid takes up less room than the ice. Therefore, if liquid is present at the surface it will be sucked into the concrete. (The ice not yet thawed is acting as a barrier against the interior of the concrete).

This means that the concrete will have a higher degree of water saturation after each freeze/thaw cyclus.

Influence of the Environment

Thawing of water is heat consuming (an endothermal process). The temperature of the system where melting ice is in contact with liquid pore solution will be at constant temperature (i.e. the freezing-point) until no more ice with the actual freezing-point is present.

Concrete in Contact with Air

Normally, thawing will take place from the concrete surface. When frozen concrete is thawing in air and a low pressure is formed in the concrete, no water is available for absorption by the concrete. Thawing in air is therefore generally mild, because the degree of water saturation will not be increased for each freeze/thaw cyclus.

Concrete in Contact with Pure Water

If the surface of the concrete is covered by pure ice (without salt) when the temperature is rising, the ice inside the concrete may melt before the pure ice on the surface due to different melting-points for the two types of ice. The melting point of the ice of the pore liquid is from 1 to 3°C lower than that of pure ice because of dissolved alkali salts, see Table 1. If the temperature rises slowly the pore liquid may be sucked back from the inside of the concrete, as no water can be absorbed from the surface, which is covered by unmelted pure ice. Furthermore, the pure ice acts as a barrier against suction of air.

Table 1. Freezing-point depression for different concentrations of potassium hydroxide and sodium chloride. (The pore liquid in concrete mostly consists of potassium hydroxide). Data from (Handbook, 63rd edt.).

Substance	Concentration		Decrease of freezing-point, °C
	mole/l	%	
KOH	0.270		0.924
	0.548		1.886
	1.066		3.747
NaCl		0.5	0.299
		3	1.790

The possibility of back-sucking of pore liquid is less in case of thick frozen concrete layers and quick thawing, as the pure ice on the outside of the concrete can melt in time.

Concrete in Contact with Salt Water

On the other hand, if the concrete is covered by saline ice, this ice will melt at a lower temperature than pure ice. The concrete will therefore experience wet surroundings at a lower temperature than would be the case with pure ice on the surface; maybe even at a time when the inside ice of the concrete has not yet melted. Thus there is a greater risk that the concrete can absorb water (salt water) from the surroundings during thawing, taking place from the exterior and inwards.

Thawing in saline ice is therefore worse than thawing in pure ice, as the water saturation is increased for each freeze/thaw cycle. Penetrating sea water or 3% NaCl solution will not change the freezing point of the pore liquid of the concrete substantially.

Conclusions

The following mechanism of mositure ingress due to freeze/thaw exposure is suggested: Soluble salts will reduce the freezing-point of a liquid. The freezing point of the pore liquid is -1 to -2°C (-3°C), whereas a 3% sodium chloride solution freezes at -2°C. During melting the temperature will only increase after all the ice with the actual freezing-point has melted. Thawing of water is accompanied by a volume contraction. If pure ice is present on the surface when the ice in the pores melt, the concrete may maintain its original degree of saturation. However, if the surface is exposed to a liquid salt solution, some of this solution will be absorbed. The determining factor is thus the difference in freezing-point between the pore liquid and the liquid of exposure.

References

Fagerlund, G. (1993): Studies of the scaling, the water uptake and the dilation of mortar specimen exposed to freezing and thawing in NaCl solutions. Proceedings of RILEM TC-117 Research Siminar, Lund, Sweden. Edt. by G. Fagerlund and M.J. Setzer (Refered in Marchand et al (1994): The decicer salt scaling deterioration of concrete - an overview. 3rd Int. Conf. on Concrete Durability, Nice)

Fagerlund, G. (1977): The critical degree of saturation method assessing frost action. Materials and Structures, Vol. 10, No. 58.

Fagerlund, G. (1993): Frostangrepp, beskrivning av verkande mekanismer. Seminar: Marina betongkonstruktioners livslängd. Cementa AB, Danderyd

Jacobsen, S. and Sellevold, E.J. (1994): Frost/salt scaling testing of concrete - importance of absorption during test. Nordic Concrete Research, Publ. No. 14, 1/1994

Handbook of Chemistry and Physics, 63rd Edt., p. D-253

Hirschwalt (1910): Mineralogical-Berlin, Vol. 1, p. 20 (referred in CordonW.A. (1966): Freezing and thawing of concrete mechanisms and control. ACI Monograph No. 3

Setzer, M.J. (1993): On the abnormal freezing of pore water and testing on freeze-thaw and deicing salt resistance. Int. Workshop on Freeze-Thaw and Deicing Salt Scaling Resistance of Concrete, Quèbec, Canada, August 30-31, pp 3-20 (Referred in (Jacobsen and Sellevold,1994)

THE REQUIRED AIR CONTENT IN CONCRETE

Göran Fagerlund
Div. of Building Materials
Lund Institute of Technology
Box 118
S-221 00 Lund, Sweden

Summary

A model for the water absorption in the air-pore system of the concrete is outlined. This absorption causes a gradual increase in the spacing between pores that are air-filled. After a certain critical absorption the remaining air content is too low to protect the concrete. This critical absorption depends on the pore size distribution and on the critical true spacing factor.

By numerical examples it is shown that the inactivation of the air-pore system by water, dependes very much on the fineness of the pore system and on the general shape of the pore system. The finer the pores, the more rapid the absorption. This leads to the seemingly paradoxical results that a concrete with a very fine air-pore system might need more air than a concrete which is more coarse-porous. It also leds to the logical result that a higher air content is required when the concrete is more moist.

In the report a quantitative approximative relation between the time of continuous water storage and the air requirement is presented.

The traditional way of calculating the air requirement, by the use of the Powers spacing factor, is an approximation that can only be used for normal situations as regards moisture load, frost load and air-pore system. It cannot be applied universally.

Previously presented at the Japanese-French Workshop on "Mass-Energy Transfer and Deterioration of Building Components - Models and Characterization of Transfer Properties". Paris February 9-11, 1995.

Published in Building Research Institute. Ministry of Construction, Japan. BRI Proceedings No 2, 1996.

1. The traditional method. The Powers spacing factor

Traditionally, the air requirement in concrete is calculated by the so-called Powers spacing factor assuming all air-pores actually staying air-filled also during moist out-door conditions. The air requirement is either calculated by eq (1a) which is valid for air-contents that are lower than a limiting value, or by eq (1b) which is valid for bigger air contents; /1/[1,2] .

$$a_{req}=V_p/\{0{,}364[(\alpha_o \cdot L_{CR}/3)+1]^3-1\} \quad \text{for } a_{req} \le 0{,}23 \cdot V_p \qquad (1a)$$

$$a_{req}=V_p/\{\alpha_o \cdot L_{CR}\} \quad \text{for } a_{req} \ge 0{,}23 \cdot V_p \qquad (1b)$$

Where

a_{req}	the required air content (% of the concrete)
V_p	the cement paste exclusive of air (% of the concrete)
α_o	the specific area of the entire air-pore system (m^{-1})
L_{CR}	the critical Powers spacing factor (m)

In eq (1a) it is assumed that all air-pores are of equal size. This is determined by the specific area α_o; i.e. the diameter of the average pore is $6/\alpha_o$. It is also assumed that all air pores are placed in a loose-packed array where L_{CR} is the distance from the corner of the cement paste cube to the periphery of the air pore in the centre of the cube; see Fig 1a.

In eq (1b) it is assumed that the air-entrained cement paste is composed of a layered structure of air-free cement paste and air; see Fig 1b.

Eq (1) is plotted in Fig 2 which can be used for an estimation of the air requirement, once the values of the three coefficients V_p, α_o and L_{CR} are known. V_p is obtained by the concrete recipe. α_o is found by an air-pore analysis using the linear traverse method /4/. L_{CR} must be found by other means. Normally, the critical spacing factor is determined by comparing the calculated spacing factor for a large number of concretes with the behaviour of the same concretes exposed to freeze-thaw. Concretes which are not damaged by frost have spacing factors below the critical value, and vice versa.

---

[1] In fact, as shown in the derivation of the Powers spacing factor, /1/, and as pointed out in /2/, theoretically it would be better to use the parameter Φ as a measure of frost resistance. Φ is defined:

$\Phi=L^3/r+3 \cdot L^2/2$

Where r is the radius of an air pore corresponding to α_o; i.e. $r=\alpha_o/3$

[2] The formulas are based on very idealistic models of the air-pore structure ; see Fig 1. A more realistic air content can be calculated on the assumption that the air-pore system has a certain size distribution. The following formula can be used; /3/:

$$a_{req} \cdot \{1+L' \cdot \alpha_o+L'^2 \cdot \alpha_o \cdot ([u]_1/[u]_2)+1{,}33 \cdot L'^3 \cdot \alpha_o \cdot ([u]_o/[u]_2\}=C$$

Where L´ is a statistical spacing factor defined by the requirement that all points in the cement paste shall, with a certain probability, lie within the distance L´ from the periphery of the nearest air-filled pore. $[u]_i$ is the i:th statistical moment of the air-pore system. The constant C depends on the level of probability chosen. For 63% probability, C=1. For 90% probability, C=2,3.

Some examples of such determinations are seen in Fig 3 and 4. Other examples can be found in /5/ where an analysis of the concept critical spacing factor is also performed.

The critical spacing factor depends on environmental factors; mainly the presence of de-icing salts. From the data in Fig 3 and 4 the following values can be deduced:

* Freezing in pure water: $L_{CR} \approx 0{,}23$ à $0{,}25$ mm
* Freezing with de-icing salts: $L_{CR} \approx 0{,}20$ mm

By these values it is very easy to calculate, by eq (1), the air-requirement for concretes with different types of air-pore systems; i.e. pore systems with different values of the specific area α_o.

This "traditional" theory for calculating the required air content was first developed by Powers /1, 6/.

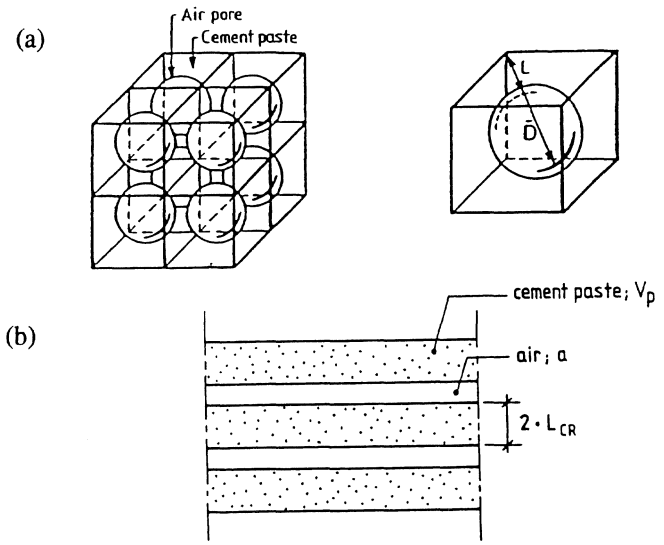

Figure 1: Definition of the Powers spacing factor. (a) low and moderately high air contents. (b) high air contents.

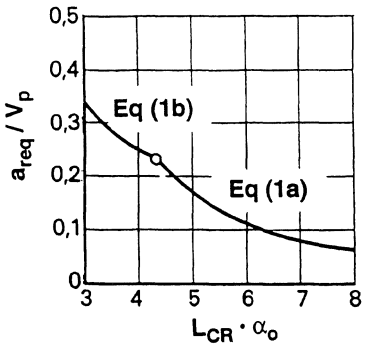

Figure 2: Diagram for determination of the air requirement; plot of eq (1).

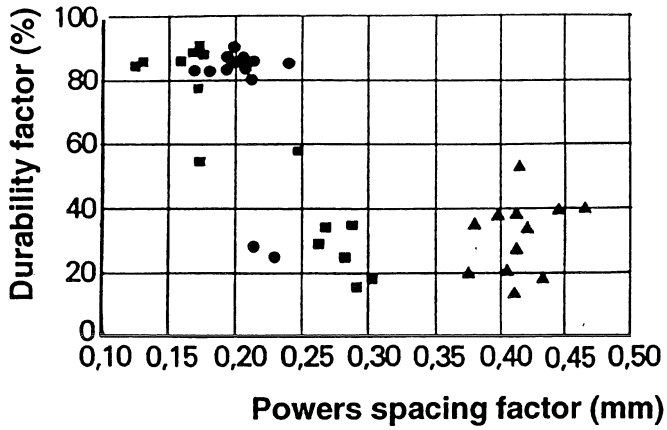

Figure 3: Experimental determination of the durability factor for freeze/thaw in pure water versus the Powers spacing factor; /11/.

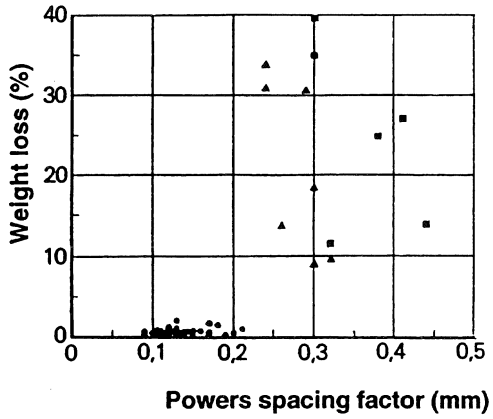

Figure 4: Experimental determination of the salt scaling resistance versus the Powers spacing factor; /12/.

2. Failure of the traditional method

The values of the critical spacing factor shown above are by no means indisputable. As will be shown below in Fig 5-7, quite other values have been found in other experiments,. It seems as if at least the following two factors are important for the value of the critical spacing factor:

1: *The characteristics of the freeze/thaw test.* Two examples are seen in Fig 5 and 6. According to Fig 5, the critical spacing factor for freeze/thaw in 3% NaCl-solution is closer to 0,18 mm than to 0,20 mm as it is according to Fig 4. The two tests are not identical; for instance, the test used in Fig 5 reaches a lower temperature than the test used in Fig 4.

According to Fig 6 the spacing factor for freezing in pure water is very high while it is only 0, 25 mm according to Fig 3. The reason is most probably that the test in Fig 3 is very moist. The specimens have no chance to dry and the water content is probably increasing during every freeze/thaw cycle. The test in Fig 6 is rather dry.

Almost no water uptake is possible during the test. Besides, it is a unidirectional test in which only the bottom of the specimen is exposed to the salt solution. In the test in Fig 4 the specimen is immersed in salt solution.

2: *The characteristics of the air-pore structure.* As will be shown theoretically below, the air pores will absorb water in nature and during a freeze/thaw test. A smaller air-pore takes up water more rapidly than a bigger pore. Therefore, theoretically one cannot find one single critical spacing factor by the traditional method used; i.e. by comparing the Powers spacing factor of the empty pore system with the result of freeze/thaw tests. Examples ot the big spread in results when a large number of concretes with many different air-pore systems are tested by the same salt scaling method are seen in Fig 7. All parameters except the air-pore structure, such as the water/cement ratio, the curing procedure and the freeze/thaw test were kept constant.

By Fig 7 it is not possible to find any well-defined value of L_{CR}. Some concretes need a spacing factor as low as 0,12 mm in order to be salt scaling resistant while 0,27 mm is sufficient for other concretes. The most plausible explanation is the different ability of different air-pore systems to take up water during the salt scaling test.

These discrepancies between the results of different tests can be understood by the theory derived below, in which consideration is taken to the natural water absorption in the air pores during a freeze/thaw experiment or in the practical situation.

The air requirement calculated by the traditional method is very sensitive to the choice of the critical spacing factor. This is best shown by an example. Let V_p be 30% and α_o be 25 mm^{-1} (average pore diameter 240 μm):

L_{CR}=0,25 mm: a_{req}=3,1 %
L_{CR}=0,23 mm: a_{req}=3,7 %
L_{CR}=0,20 mm: a_{req}=5,1 %
L_{CR}=0,18 mm: a_{req}=6,4 %
L_{CR}=0,16 mm: a_{req}=8,3 %

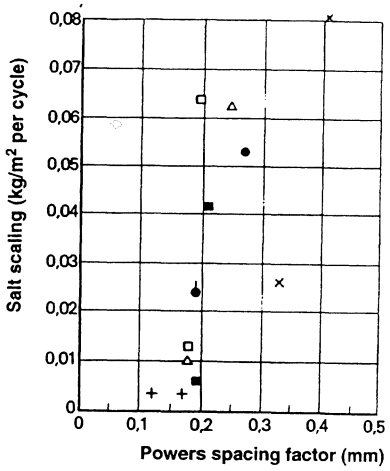

Figure 5: Experimental determination of the salt scaling resistance versus the Powers spacing factor; /13/.

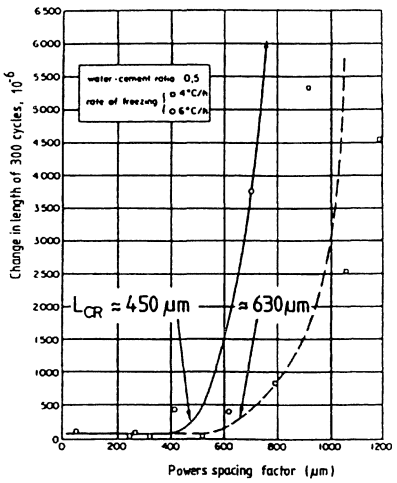

Figure 6: Experimental determination of the durability factor for freeze/thaw in pure water and the Powers spacing factor. Two different rates of freezing; /14/.

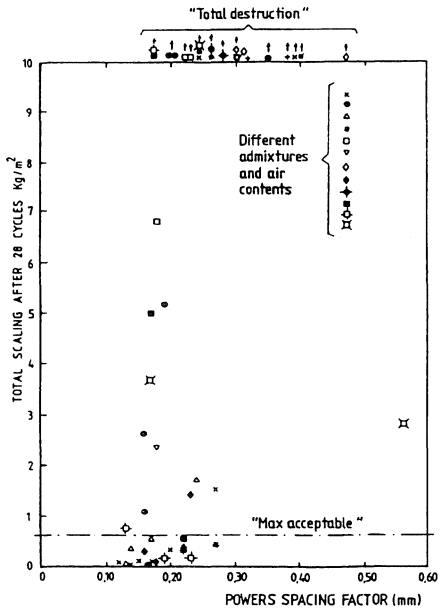

Figure 7: Experimental determination of the salt scaling resistance versus the Powers spacing factor. Different air-entraing admixtures, different plasticizing agents, different consistency levels; /13/.

3. Water absorption in the air-pore system

When the concrete is stored in water, either before the freeze/thaw test starts or during the test, water enters the air-pore system. The process has been described in detail in /7/. The driving force is the over-pressure inside air-bubbles that are enclosed in air-pores. The over-pressure is caused by the curved miniscus between the enclosed bubble and the pore water. Due to this over-pressure, air is dissolved in the water. The smaller the bubble, the bigger the over-pressure, and the bigger the solubility of air in the pore water.

One can calculate the water volume V_w needed in order to completely dissolve a bubble of radius r. It is; /7/:

$$V_w=[4\cdot\pi/3]\cdot[\rho_o/s]\cdot[1+P_o/\Delta P]\cdot r^3 \quad (2)$$

Where

ρ_o	the density of air at 1 atm and +10°C (1,25 kg/m^3)
s	the solubility of air at 1 Pa and +10°C [$3\cdot10^{-2}$ kg/(m^3·Pa)]
P_o	the atmospheric pressure (10^5 MPa)
ΔP	The over-pressure in the air bubble (Pa)

The over-pressure is given by the Laplace law:

$$\Delta P=2\cdot\sigma/r \quad (3)$$

Where

σ	The surface tension between air and water (N/m)

According to eq (2) a water volume of $1{,}36\cdot10^{-12}$ m^3 is needed to completely dissolve an air-bubble of the radius 10 μm. This corresponds to a sphere with a radius as small as 69 μm. It is therefore quite clear that small air-bubbles will become water-filled already after a short time of water storage.

One can also calculate the required thickness of a saturated cement paste shell surrounding the bubble of radius r. It is:

$$t > \{[1+(\rho_o/s\cdot\varepsilon_{tot})\cdot(1+10^5\cdot r/(2\cdot\sigma)]^{1/3}-1\}\cdot r \quad (4)$$

Where

t	the thickness of the required cement paste shell (m)
ε_{tot}	the total porosity of the cement paste (m^3/m^3)

For a mature cement paste with the water/cement ratio 0,50 the porosity is about 43 %; /8/. The average spacing between the air pores is supposed to be 0,15 mm; i.e. the average thickness t of the cement paste shell is 0,075 mm. According to eq (4), this means that all pores with radii smaller than about 30 μm will become water-filled already due to a local dissolution of its air.

Pores that are bigger than those calculated by eq (4), will stay air-filled for a certain time. There will, however, be a diffusion of air from a smaller pore to a bigger adjacent pore. This process is hard to describe exactly. One can, however, consider a simple two-pore system consisting of one big and one small pore separated by a saturated cement paste. When the bigger pore is very much bigger than the smaller, the air flow can be described by a simple equation:

$$q\approx\delta\cdot(L+r_1)\cdot4\pi\cdot s\cdot2\sigma/L \quad (5)$$

Where

q	the air flow (kg/s)
δ	the diffusivity of dissolved air (m^2/s)
L	the distance between the pores (m)
r_1	the radius of the smallest air-bubble (m)

It is reasonable to assume that the pore spacing is proportional to the size of the small pore; $L \approx \eta \cdot r_1$. Then the diffusion can be described by:

$$q \approx \delta \cdot [1+1/\eta] \cdot 4\pi \cdot s \cdot 2\sigma \qquad (6)$$

This means that the rate of air flow from a pore is independent of the size of the pore.

Let η be 5. This, for example, means that the spacing for a pore with diameter 100 μm is 500 μm. Then, by introducing numerical data for s and σ at +15°C ($2{,}5 \cdot 10^{-7}$ kg/(m^3·Pa) and 0,074 N/m) the equation can be written:

$$q \approx 5{,}6 \cdot 10^{-7} \cdot \delta \text{ kg/s} \qquad (7)$$

This equation is of course very approximative. It can however be used for an estimate of the time it takes to fill an air-pore with water. The time is proportional to the volume of the bubble:

$$t_{req} = V \cdot \rho_o / (5{,}6 \cdot 10^{-7} \cdot \delta) = (4 \cdot \pi/3) \cdot r^3 \cdot \rho_o / (5{,}6 \cdot 10^{-7} \cdot \delta) \qquad (8)$$

Where

t_{req}	the time needed for filling the pore (s)
V	the volume of the pore to be filled (m^3)

The diffusivity of dissolved air is unknown. Diffusivity of air in bulk water is $2 \cdot 10^{-9}$ m^2/s. There is reason to believe that it is at least 10^2 to 10^3 times lower in a dense cement paste.; i.e. values of the order of size 10^{-11} to 10^{-12} m^2/s are imaginable.

In Fig 8 the time versus the pore radius is shown. Pores smaller than 30 μm (diameter 60 μm) are filled within 1 to 10 days. For coarser pores the time needed is 1 year or more. This is the reason why a concrete can be frost resistant also when it is stored in water for a long time.

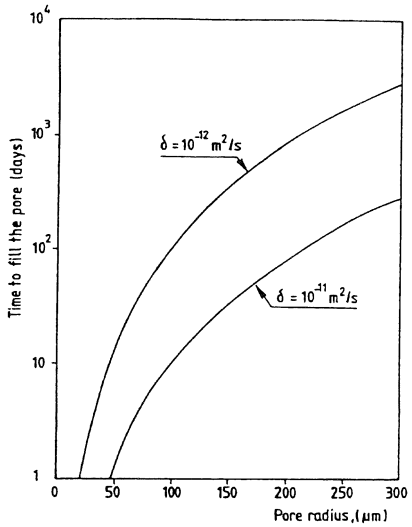

Figure 8: Time needed to completely water-fill an air-pore; eq (8).

4. Effect of water absorption on the spacing factor

The gradual water absorption changes the spacing between pores that are air-filled. The bigger the absorption, the bigger the spacing. The new spacing factor L_r after a certain water absorption can be calculated if the air-pore size distribution is known. The following equation, based on eq (1), is used:

$$L_r=(3/\alpha_r)\cdot\{1,4[(V_p/a_r)+1]^{1/3}-1\} \quad \text{for } a_r/V_p\leq 0,23 \tag{9a}$$

$$L_r=V_p/(a_r\cdot\alpha_r) \quad \text{for } a_r/V_p\geq 0,23 \tag{9b}$$

Where

a_r	the residual air content (% of the concrete)
V_p	the cement paste exclusive of air (% of concrete)
α_r	the residual specific area of the air-filled pore system (m^{-1})
L	the residual Powers spacing factor (m)

It is assumed that a smaller air pore is water-filled before a coarser. Then, the parameters a_r and α_r are unique functions of the size distribution:

$$a_r=\int_{r_w}^{r_{max}} f(r)\cdot(4\cdot\pi/3)\cdot r^3\cdot dr \tag{10}$$

Where

f(r)	the frequency function of air-pores
r_{max}	radius of the biggest pore (m)
r_w	radius of the biggest water-filled pore (m)

$$\alpha_r=\int_{r_w}^{r_{max}} [f(r)\cdot 4\cdot\pi\cdot r^2/a_r]\cdot dr \tag{11}$$

r_w at acertain water absorption time is given by eq (8).

The size distribution can be determined by automatic image analysis or by the linear traverse method /4/.

One example of a calculation of the change in the parameters a_r, α_r and L_r is shown in Fig 9. The total air content of the empty pore system is 4%. The size distribution is described by:

$$f(r)=\kappa\cdot \ln b/b^r \tag{12}$$

Where

κ	a constant
b	a coefficient determined by the fineness of the air-pore system. b=1,03 in the actual example; i.e α_o=30 mm^{-1}
r	the pore radius (μm, NOTE the unit)

The spacing factor increases from 0,19 mm for the empty pore system to about 1 mm when all pores with radius smaller than 200 μm are water-filled. This corresponds to a water-filling of about 90% of the entire pore system.

In a more coarse-porous system, the same time of water-filling (the same value of r_w) gives a smaller water absorption and also a smaller residual spacing factor. Thus, a coarser pore system can be favourable and lead to a smaller required air content. This will be further discussed below.

5. The critical true spacing factor

As said in paragraph 1, the Powers spacing factor is based on the idea that no air-pores take up water. In reality they do. Therefore, the real spacing factor will be a function of the wetness of the test used for its determination. The Powers spacing factor therefore is a sort of *fictitious* critical spacing factor which cannot be universally applied.

There is reason to believe that a true spacing factor exists, which is independent of the wetness of the test. The critical true spacing factor can be calculated from a determination of the critical degree of saturation $S_{a,CR}$ of the air-pore system in combination with information of the size distribution of the pores. From $S_{a,CR}$ the critical residual air content $a_{r,CR}$ can be calculated:

$$S_a=1-a_r/a_o \quad \text{and} \quad S_{a,CR}=1-a_{r,CR}/a_o \qquad (12)$$

Where

S_a the degree of saturation of the air-pore system (m^3/m^3)

a_o the total air content (m^3/m^3)

$a_{r,CR}$ the minimum allowed air-filled part of the air-pore system (m^3/m^3)

Then, by using eq (10) the size of the biggest air-pore r_w that can be allowed to be water-filled can be found. By inserting this value in eq (11), the critical residual specific area $\alpha_{r,CR}$ can be calculated. Finally, the critical spacing factor can be calculated by eq (9) by insering the valueas of $a_{r,CR}$ and $\alpha_{r,CR}$.

Such determinations have been made for some concretes. A review is given in /5/. It seems as if a value of the order of size 0,35 to 0,40 mm is valid for a portland cement concrete with a water/cement ratio of about 0,45, under the assumption that freeze/thaw takes place in pure water.

In Fig 9 the value 0,40 mm was used for the critical spacing factor. Then, as shown by Fig 9, for the actual air content 4% and the actual pore size distribution, only pores smaller than 105 μm can be allowed to be water-filled. This corresponds to a water absorption time that can be estimated by eq (8) provided the diffusivity of air in pore water is known.

Probably the critical spacing factor is a function of the water/cement ratio. Some theoretical estimates based on the hydraulic pressure theory, /1/, have been made in /9/. If the critical spacing factor is 0,40 mm for w/c=0,40 it should be about 0,43 mm for w/c=0,35, 0,29 mm for w/c=0,50 and 0,25 mm for w/c=0,60.

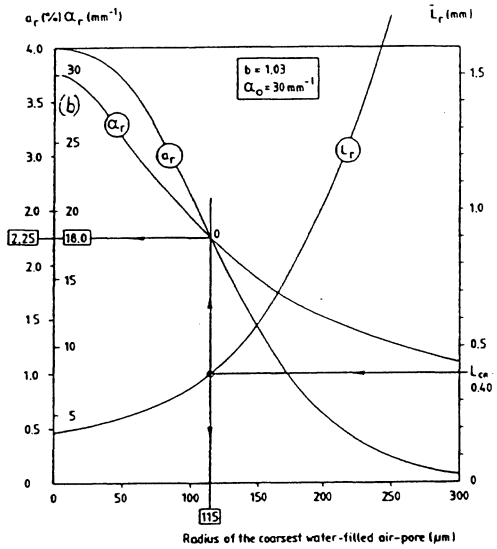

Figure 9: Influence of a gradual water-filling of the air-pore system on the air content, the specific area and the spacing factor. Assumptions: L_{CR}=0,40 mm, pore size distribution according to eq (12) with b=1,03 (α_0=30 mm^{-1}), air content 4%. Cement paste content 30%.

6. A new definition of the required air content

The minimum air requirement can be calculated by the following expression:

$$a_{req}=a_w+a_{CR} \qquad (14)$$

Where

a_{req}	the required total air volume of a concrete in which all pores smaller than r_w are water-filled
a_w	the water-filled air volume
a_{CR}	the critical air volume for the given residual specific area α_r

Each radius r_w of the biggest water-filled pore corresponds to a certain value a_w/a_0= 1-a_r/a_0 of the water-filled part of the pore system and to a certain value α_r of the specific area of the air-filled part of the pore system. These relations are given by the pore size distribution. By using the values of α_r and the true critical spacing factor L_{CR}, the critical air content a_{CR} can be calculated by eq (1). Then, for a given value of r_w, the required air content is calculated by:

$$a_{req}=a_{CR}/(a_r/a_{req}) \qquad (15)$$

Such calculations have been made for two different types of air-pore system:

a) The exponential function:

$$f(r)=\kappa\cdot\ln b/b^r \qquad (12)$$

b) The power function:

$$f(r)=\lambda\{1/r^c-1/r_{max}{}^c\} \qquad (16)$$

Where

κ and λ constants

b, c coefficients determined by the fineness of the pore system. They are functions of the specific area of the empty pore system; /7/.

In the calculations made below, using eq (16), the smallest radius is supposed to be 10 μm and the biggest 1000 μm. When using eq (12), r_{min} is supposed to be 0. The error made by also considering pores in the range 0-10 μm is negligible for this type of distribution. The two types of distributions are shown in Fig 10 for different values of the coefficients b and c; i.e. for different values of the specific area α_o.

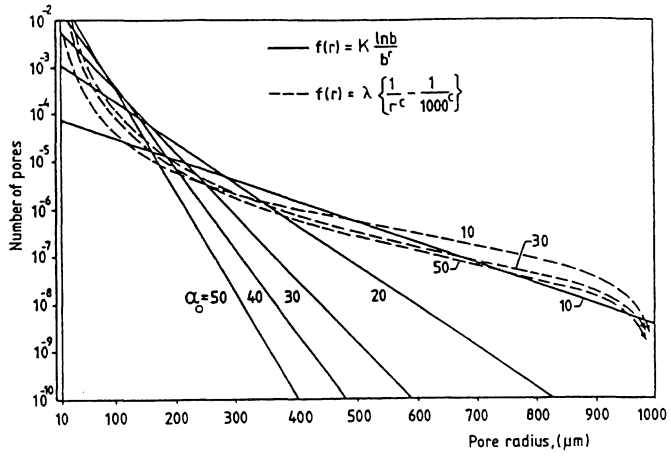

Figure 10: The frequency functions of different air-pore size distributions.

The corresponding values of r_w, α_r, a_w/a_o, a_r/a_o, a_{CR} and a_{req} for a case where $V_p=1$ (pure cement paste) and the critical spacing factor is 0,35 mm are listed in Tables 1 and 2 in the APPENDIX. (Note, air is not included in V_p)

In Fig 11 the fraction of pore volume of completely water-filled pores is plotted versus the size of the biggest filled pore. The big difference between different types of pore size distribution is clearly shown; the exponential air-pore size distribution giving the biggest relative absorption. The figure clearly shows that a more fine-porous system obtains a considerably higher water absorption than does a coarse-porous system.

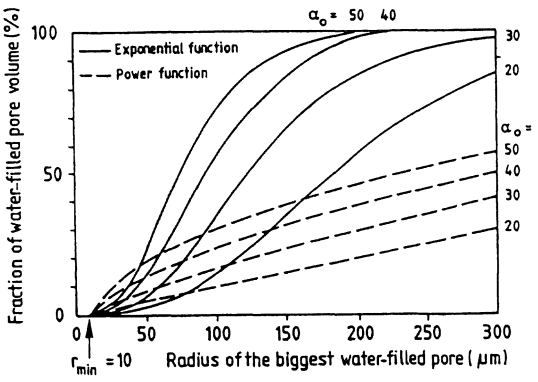

Figure 11: Influence of a gradual water-filling on the residual air content; eq (10).

In Fig 12 the residual specific area is plotted versus the size of the biggest completely water-filled pore. It is interesting to see that the power function gives the biggest reduction in specific area which is a consequense of the big number of very small pores in this type of distribution; see Fig 10. On the other hand, the required air content at a certain water-filling is lower for the power function. The reason is the smaller water-filled pore volume.

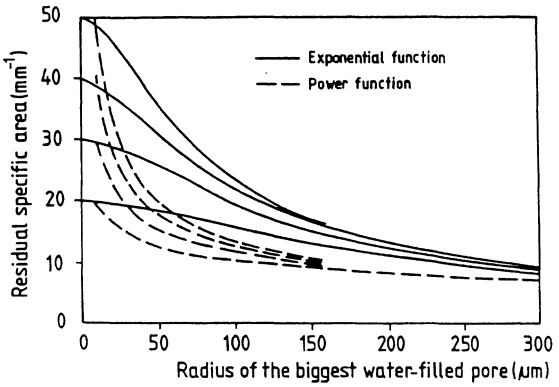

Figure 12: Influence of a gradual water-filling on the residual specific area; eq (11).

In Fig 13 and 14 the required air content is plotted versus the fineness of the pore system which is expressed in terms of the specific area α_0 of the empty pore system. The parameter in the figures is the size of the biggest water-filled pore. The critical true spacing factor is supposed to be 0,35 mm. The following observations can be made:

1: When there is no water absorption, $r_w=r_{min}$, the air requirement is lower the higher the specific area α_0 of the pore system. In this case, the air requirement can be calculated by eq (1) using the values of the true L_{CR} and the specific area α_0.
2: The air requirement increses with increasing water absorption.
3: The bigger the water absorption, the smaller is the effect of the initial fineness of the air-pore system on the required air concent
4: The required air content is almost the same in all pore systems when all pores smaller than 100 µm are water-filled.

5: When pores bigger than 100 μm are water-filled,the air requirement is higher the finer the air-pore system

Therefore, the analysis show that the initial fineness probably is of much smaller importance for the air requirement than has previously been assumed, e.g. when the Powers spacing factor, as it is normally defined, is used in eq (1). In the figures have also been plotted the required air contents based on the usually accepted figures of the Powers spacing factor, 0,25 and 0,20 mm.

NOTE: in the calculations it is assumed that all air-pores are isolated from each other by water saturated cement paste. In some cases, with unstable air pore systems, the air-pores coalesce and form continuous channels. Such air-pore systems suck water rapidly when the concrete is exposed to liquid water. They do therefore not fill by the slow dissolution process desribed above, being the basis for the theoretical analysis above.

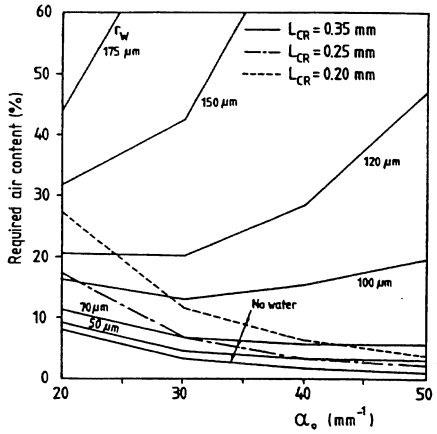

Figure 13: The required air content as function of the size of the biggest water-filled pore. Exponential pore size distribution; eq (12). Pure cement paste.

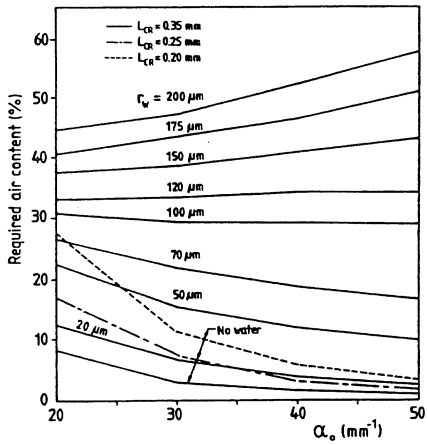

Figure 14: The required air content as function of the size of the biggest water-filled pore. Power type of pore size distribution; eq (16). Pure cement paste.

7. The required air content as function of the required service life

The calculations made in the previous paragraph make it quite clear that the required air content is determined by the "wetness" of the environment in which the concrete is placed; the wetter the environment, the bigger the water absorption, and the bigger the required air content. Theoretically, one can calculate a relation between the time a concrete is stored in water and the air requirement. In this calculation the time axis is obtained by eq (8) giving the relation between the air-pore radius and the time to fill the pore. According to this expression there is a certain relation between the biggest water-filled pore, r_w, and the water absorption time. As shown in the previous paragraph there is also a certain relation between the biggest air-filled pore and the air requirement. Examples of the latter relation for some air pore distributions are listed in the APPENDIX and are shown in Fig 13 and 14.

Thus, there is a unique relationship between the water absorption time t and the air requirement. This relationship depends on the diffusivity of dissolved air, δ, and it depends on the pore size distribution, f(r).

$$a_{req}(t)=f(\delta,t)\cdot F[f(r),f(L_{CR})] \qquad (17)$$

Where

$f(\delta,t)$ and $F[f(r),f(L_{CR})]$ are functions of the diffusivity, the time, the pore size distribution and the critical true spacing factor.

Examples of a calculation of the air requirement as function of the water absorption time are shown in Fig 15.The exponential distributions used above -Fig 10- is used in the calculation. It is assumed that the true critical spacing factor is 0,35 mm.

Fig 15 shows that the air requirement is a function of the water absorption time. It is also a function of the type of the pore size distribution. It is also clear that a very fine-porous system is highly sensitive to the water absorption time. This can explain why fine air-pore systems sometimes have behaved quite bad in freeze/thaw tests. One example is concrete with so-called hollow microspheres. Such concretes were found to have a good performance in a salt scaling test during the first part of the test period. When the test was prolonged, severe scaling appeared more or less suddenly; /10/. The best explanation is that the pore system gradually became inactivated by absorption. After a certain test period the volume of air still remaining air-filled was too small to prevent the concrete from being damaged.

8. Some comments on salt scaling

The theory presented above for calculating the air requirement is derived for pure frost attack. When salts are present, more severe damage often occurs. Besides, the salt frost attack usually is a surface attack, or so-called salt scaling. Probably, the air requirement for this type of attack can be calculated by the same theory as that presented above. The following factors might contribute to the observed effect of salt:

1: Dissolved salt in the pore water might change the critical true spacing factor; either increasing it, or decreasing it. Some preliminary tests indicate that the critical spacing factor actually might increase, /5/.

2: Salt concentrations inside the concrete cause moisture movements that lead to an increase of the water absorption in the air-pores at the surface part of the concrete.

3: The dissolved salt makes the concrete take up more moisture.

4. The diffusivity of dissolved air in the pore water is higher when this contains dissolved salt. This would increase the rate of water absorption.

None of these hypotheses has been experimentally confirmed or rejected.

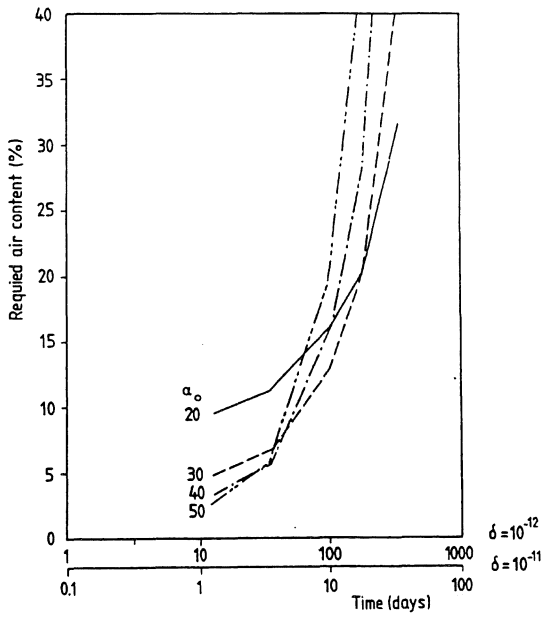

Figure 15: The reqired air content as function of the water absorption time. Exponential pore size distribution; eq (12). Diffusivity of dissolved air, $\delta=10^{-11}$ or 10^{-12} m^2/s.

References

/1/ Powers T.C.: The air requirement of frost resistant concrete. Proc. Highway Res. Board, 1949, 12, 184-211.

/2/ Danielsson. U. , Wastesson. A.: The frost resistance of cement paste as influenced by surface-active agents. Swedish Cement and Concrete Research Institute, Proceedings Nr 30, Stockholm 1958, 38 pp.

/3/ Fagerlund G.: Equations for calculating the mean free distance between aggregate particles or air-pores in concrete. Swedish Cement and Concrete Research Institute, Research Nr 8:77, Stockholm 1977, 38 pp.

/4/ ASTM: Designation C-457: Microscopical determination of air-void content and parameters of the air-void system in hardened concrete.

/5/ Fagerlund G.: The critical spacing factor. Div. of Building Materials, Lund Institute of Technology, Report TVBM-7058, Lund 1993. 50 pp.

/6/ Powers T.C.: Void spacing as a basis for producing air-entrained concrete. ACI Journal May 1954, Proc. Vol 50, p 741-760.

/7/ Fagerlund G.: The long time water absorption in the air-pore structure of concrete. Div. of Building Materials, Lund Institute of Technology, Report TVBM-3051, Lund 1993, 73 pp.

/8/ Powers T.C.: Physical properties of cement paste. Proc. Fourth Int. Symp. on The Chemistry of Cement, Washington 1960, National Bureau of Standards, Monograph 43, Vol II, Washington D.C., p 577-609.

/9/ Fagerlund G.: Frost resistance of high performance concrete- some theoretical considerations. Div. of Building Materials, Lund Institute of Technology, Report TVBM-3056, Lund 1993, 37 pp.

/10/ Sommer H.: Ein neues Verfahren zur Erzielung der Frost-Tausalz-beständigkeit des Betons. Zement und Beton, 1977, p 124-129. (in German)

/11/ Ivey D.L., Torrans P.H.: Air void systems in ready-mixed concrete. J. of Materials Vol 5, Nr 2, 1970, p 492-522.

/12/ Bonzel J., Siebel E.: Neuere Untersuchungen über die Frost-Tausalzwiderstand von Beton. Betontechnische Berichte, 1977, Betonverlag GmbH, Düsseldorf, 1977, Heft 4, p 153-157+Heft 5, p 205-211+Heft 6, p 237-244. (In German).

/13/ Sjöblom C.: Investigation of some air-entraining admixtures. Div. of Building Materials, The Royal Institute of Technology, Diploma work, 1976:2, Stockholm 1976, 45 pp. (in Swedish).

/14/ Pigeon M., Prévost J., Simard J-M.: Freeze-thaw durability versus freezing rate. ACI Journal Sept.-Oct., 1985, p 684-692.

/15/ Fagerlund G.: Effects of air entraining agents and other admixtures on the salt scaling resistance of concrete. In "Durability of Concrete". Int. Seminar Gothenburg, April 1986. The Swedish Council for Building Research, Document D1:1988, p 233-266.

APPENDIX: Effect of water absorption on properties of the residual air-pore system and on the required air content

Table 1: Effect of water absorption in the pore system on the required air content. Exponential pore size distribution.The critical true spacing factor is 0,35 mm.

α_0 (mm^{-1})	r_w (mm)	α_r (mm^{-1})	a_w/a_0	a_r/a_0	a_{CR} (%)	a_{req} (%)
	50	18,6	0,018	0,982	9,4	9,6
	70	17,5	0,052	0,948	10,8	11,4
20	100	15,7	0,140	0,860	13,8	16,0
	120	14,6	0,216	0,784	16,2	20,6
	150	13,0	0,346	0,654	20,8	31,8
	175	11,9	0,456	0,544	24,0	44,1
	200	10,9	0,559	0,441	26,2	59,4
	50	25,7	0,063	0,937	4,5	4,8
	70	23,1	0,156	0,844	5,8	6,8
	100	19,5	0,343	0,657	8,5	12,9
30	120	17,8	0,482	0,518	10,4	20,1
	150	15,1	0,646	0,354	15,0	42,4
	175	13,6	0,758	0,242	18,9	78,0
	50	31,2	0,136	0,864	2,8	3,3
	70	26,9	0,296	0,704	4,0	5,7
	100	21,8	0,575	0,425	6,6	15,5
40	120	19,3	0,691	0,309	8,7	28,1
	150	16,3	0,838	0,162	12,7	78,2
	50	35,5	0,230	0,770	2,1	2,7
	70	29,6	0,445	0,555	3,2	5,8
50	100	23,6	0,718	0,282	5,5	19,4
	120	20,4	0,835	0,165	7,7	46,4

Table 2: Effect of water absorption in the pore system on the required air content. Power type of pore size distribution.The critical true spacing factor is 0,35 mm.

α_o (mm^{-1})	r_w (mm)	α_r (mm^{-1})	a_w/a_o	a_r/a_o	a_{CR} (%)	a_{req} (%)
	20	16,5	0,011	0,989	12,3	12,5
	50	12,9	0,044	0,956	21,2	22,2
	70	11,6	0,065	0,935	24,6	26,3
	100	10,4	0,097	0,903	27,5	30,4
20	120	9,7	0,118	0,882	29,3	33,3
	150	9,0	0,149	0,851	31,7	37,3
	175	8,5	0,175	0,825	33,6	40,7
	200	8,1	0,201	0,799	35,3	44,2
	300	6,9	0,303	0,697	41,4	59,4
	350	6,5	0,354	0,646	44,2	68,4
	20	22,3	0,026	0,974	6,3	6,4
	50	15,5	0,086	0,914	14,2	15,5
	70	13,5	0,120	0,880	19,2	21,8
	100	11,6	0,166	0,834	24,6	29,5
30	120	10,7	0,195	0,805	26,7	33,2
	150	9,7	0,235	0,765	29,5	38,5
	175	9,1	0,266	0,734	31,4	42,8
	200	8,6	0,296	0,704	33,3	47,4
	300	7,1	0,407	0,593	40,1	67,6
	350	6,6	0,501	0,499	43,3	86,8
	20	28,2	0,047	0,953	3,6	3,8
	50	17,9	0,137	0,863	10,3	11,9
	70	15,1	0,183	0,817	15,0	18,4
	100	12,6	0,240	0,760	22,3	29,3
40	120	11,5	0,274	0,726	24,8	34,2
	150	10,3	0,319	0,681	27,7	40,7
	175	9,6	0,354	0,646	29,8	46,1
	200	8,9	0,386	0,614	32,1	52,3
	300	7,3	0,497	0,503	39,1	77,8
	350	6,8	0,546	0,454	42,2	93,1
	20	33,8	0,068	0,932	2,3	2,5
	50	19,9	0,189	0,811	8,1	10,0
	70	16,4	0,243	0,757	12,5	16,5
	100	13,1	0,309	0,691	20,5	29,6
50	120	12,8	0,346	0,654	22,3	34,1
	150	10,8	0,394	0,606	26,5	43,7
	175	9,9	0,429	0,571	28,9	50,5
	200	9,2	0,462	0,538	31,1	57,7
	300	7,4	0,570	0,430	38,5	89,4

MODELLING OF FROST ATTACK FOR SERVICE LIFE DESIGN OF CONCRETE STRUCTURES

Erkki Vesikari, MScTech
VTT Building Technology
Kemistintie 3, FIN-02044 VTT, Finland

1. What is service life design?

Using the well known concepts of load, S, and resistance, R, the difference between traditional structural design and service life design can be characterized as:

Traditional design:	Service life design:
$R - S > 0$	$R(t) - S(t) > 0$

What sets the service life design apart from traditional design is the dimension of time. The requirement of R being greater than S must apply not only at the start of service life but also at the end of it. The structure is designed to meet the requirements throughout its service life.

In principle, S and R may not necessarily be mechanical quantities. If service life design is understood in a wider sense, S may be a physical, chemical, biological or other load and R whatever response to the load. However, in this context the main emphasis is on the mechanical service life design, where S is assumed to be a mechanical load and R the load-bearing capacity.

The reason why the dimension of time must be taken into account is that degradation in materials of a structure gradually lower its resistance. Even the load may be time dependent. The degradation of materials is taken into account using degradation models, which express the rate of degradation as a function of various material, structural and environmental parameters.

Below is a short review on the basic concepts of service life design of concrete structures. A fuller description of the theory and procedure of service life design is given in the report of the RILEM committee 130 CSL /1/.

2. Formulation of mechanical service life design

As traditional mechanical design also the mechanical service life design is based on the theory of reliability. The theory is only extended to apply with time dependent loads and resistances. New concepts are defined to characterize time related quantities. The target service life, t_g, is the required minimum service life; the design service life, t_d, is the service life applied in the calculations, and the lifetime safety factor, γ_t, is the ratio between the design service life and target service life. By the lifetime safety factor the fulfilment of the target service is ensured (Figure 1).

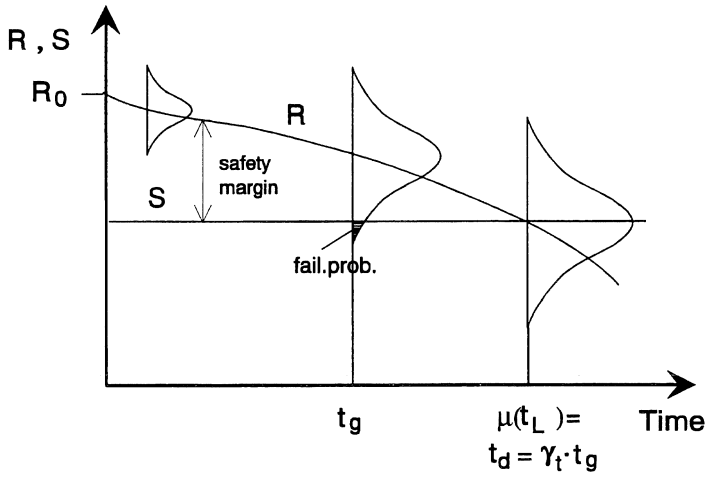

Fig 1. Meaning of the lifetime safety factor for the safety of a structure.

The design formula for mechanical service life design is written as shown in Formula 1. The determinative time in the design formula is the design service life. In structural durability design the design formula can be written as:

$$R_d(t_d) - S_d(t_d) \geq 0 \qquad (1)$$

where

S_d is the design value of the load (the loads are multiplied by the corresponding load safety factors),

R_d the design value of the resistance (the material strengths are multiplied by the corresponding material safety factors),

t_d the design service life (the target service life is multiplied by the lifetime safety factor).

Because of the degradation of materials the cross-sectional area and possibly also the strength of concrete and steel are reduced with time. The effect of degradation

on the load-bearing capacity is evaluated by degradation models which are incorporated in the design formulae. This procedure is exemplified by the design formulae for simple column (Fig 2 and formulae 2 - 6). The measure c' denotes the depth of deteriorated concrete (loss of effective load-bearing concrete) which is subtracted from the width of the column b_o. d' denotes the depth of corrosion (at cracks) and is subtracted from the diameter of the steel bar respectively.

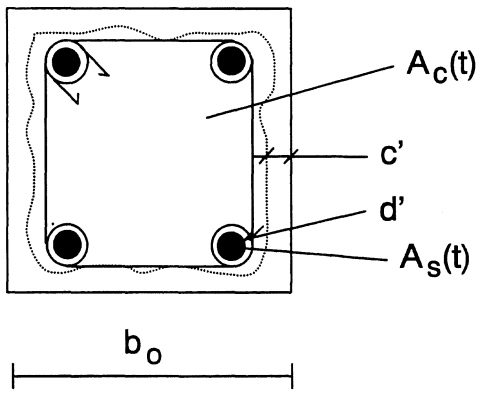

Fig 2. Cross-section of a column.

$$R_d(t_d) - S_d \geq 0 \quad (2)$$

$$S_d = \gamma_g \cdot F_g + \gamma_p \cdot F_p \quad (3)$$

$$R_d(t_d) = A_c(t_d) \cdot f_c/\gamma_c + A_s(t_d) \cdot f_y/\gamma_s \quad (4)$$

$$A_c(t_d) = (b_o - 2 \cdot \mathbf{c'(t_d)})^2 \quad (5)$$

$$A_s(t_d) = 4 \cdot \pi (D_o - 2 \cdot \mathbf{d'(t_d)})^2/4 \quad (6)$$

Result : b_o, D_o

Durability models may depend on many variables, such as the properties of concrete, dimensions of the structure and aggressiveness of the environment. These variables become new parameters of the structural design. Of course c' and d' also depend on the design service life.

In general, the effects of degradation in the mechanical performance of concrete structures exposed to outdoor conditions can be classified into the following structural deterioration mechanisms:

1. Frost attack or other surface deterioration, causing a reduction in the cross-sectional area of concrete.
2. Corrosion of reinforcement

a) at cracks in the concrete, causing a reduction in the cross-sectional area of steel bars and
b) at all surfaces of the concrete (general corrosion) causing, as a result of the cracking of concrete, a reduction in the bond of structural reinforcement and in the cross sectional area of the concrete.

3. Modelling of frost attack

Frost attack may have two kinds of structural effects on concrete structures. They are:

1. Reduction of the strength of concrete
2. Reduction of the dimensions of the structure.

In practical design, the effect of frost attack could be taken into account in both ways. The frost attack model could be a strength model which would show the reduction of concrete compressive strength with time. However, as the reduction of compressive strength is always more or less an edge phenomenon, a strength model as applied to the whole cross-sectional area of concrete would not yield a correct measure of the reduction of load-bearing capacity.

Thus a model that expresses the loss of effective load-bearing concrete at the edges of the structure has been assumed to work better in structural applications. The model is applicable for both types of deterioration. Even in cases where real disintegration of concrete does not occur, the model would evaluate the apparent loss of concrete from the dimensions of the structure corresponding to the reduction in strength at the edges of the structure.

Figure 3 shows the model for disintegration of concrete. Actually the process occurs as a series of steps, which can be small or large depending on e.g. the presence of chlorides or other degradation factors that may promote disintegration. The model straightens the steps to a linear process. This simplification is justified by the fact that also during the dormant phases of the steps (when no real disintegration occur) the reduction in compressive strength nevertheless continues.

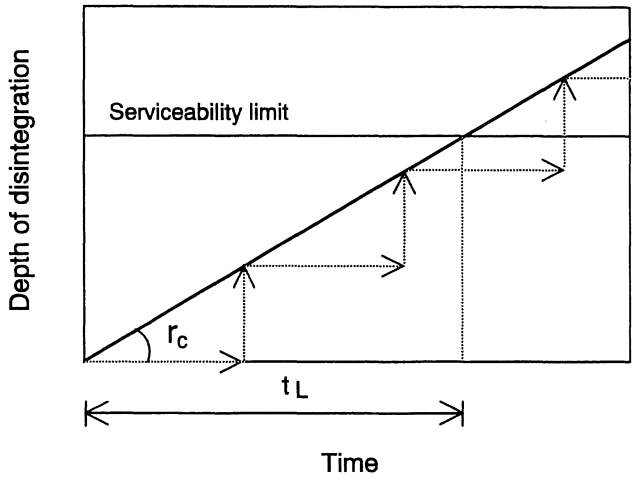

Fig 3. Model of disintegration of concrete due to frost.

The rate of disintegration, r_c, is evaluated by the frost-resistance index, P, and the environmental factor, K_e. The frost resistance index is a material property and takes into account all the material-related impact on the rate of disintegration. The environmental factor accounts for the entire contribution from the environment. The frost resistance index is inversely proportional to the rate of scaling in the frost-salt test (SFS 5449).

$$r_c = \frac{K_e}{P} \tag{7}$$

$$c' = r_c \cdot t \tag{8}$$

where

r_c	is the rate of disintegration of concrete (mm/year),
K_e	the environmental factor,
P	the frost resistance index of concrete ($20 < P < 80$),
c'	the depth of disintegration (mm),

The environmental factors applicable to the design of concrete bridges are presented in Table 1 /2/.

Table 1. Environmental factors for bridge design.

STRUCTURE	ENVIRONMENTAL FACTOR, K_e		
	Environmental class E1b		Environ-mental class E2b
	1. Moderate load	2. Severe load	
Super structure			
Beams, deck	2	3	2
Edge beam	6	10	4
Substructure			
Basement slab	-	-	-
Abutment and intermediate post	4	6	3
Intermediate column	6	10	4
Edge beam	6	10	4
Structure in sea water	6	10	4

If the concept of P is generally known, as in Finland, the structural designer sets the requirement of the frost resistance index only. The responsibility of the contractor is to prove the fulfilment of the requirement of P. However, as the frost resistance index depends on the compressive strength of concrete, which is also set by the designer, it is essential for the designer to check that the requirement of frost resistance index is consistent with the requirement of strength.

If the concept of P cannot be used as such, indirect formulae for P, as presented in the following, may be used in the structural design. In that case P in Formula 7 is replaced by these formulae. Consequently the air content, curing time, and the constituents of the binder become new parameters of the mechanical service life design.

4. Frost resistance index

Matala developed a model for the frost resistance index, P, from a statistical study of the results of some 280 frost-salt tests on different concretes /3/. The model is based on the parameters of fresh concrete, the air content and the reduced (water+air)/cement ratio. The aging of concrete is taken into account by the aging coefficient which depends on the binder used in the concrete, and the efficiency of curing is taken into account by the curing coefficient.

$$P = \frac{46 \cdot c_{cur} \cdot c_{age}}{\frac{10 \cdot W_{red}^{1.25}}{a^{0.50}} - 1} \quad (9)$$

$$W_{red} = \frac{w + (a-2) \cdot 10}{q_{pc} + 2.5 \cdot q_{si} + 0.3 \cdot q_{fa} + 0.8 \cdot q_{bs}} \quad (10)$$

$$c_{cur} = 0.85 + 0.17 \cdot \log_{10}(t) \quad (11)$$

$$c_{age} = 1 - 0.045 \cdot p_{si} - 0.008 \cdot p_{bs} - 0.001 \cdot p_{fa} \quad (12)$$

The notations in the formulae are:

P	frost resistance index,
W_{red}	reduced (water+air)/cement ratio,
c_{cur}	curing coefficient
c_{age}	aging coefficient
a	air content of fresh concrete (%).
w	water content (kg/m^3),
q_{pc}	content of Portland cement in the concrete (kg/m^3)
q_{si}	content of silica fume in the concrete (kg/m^3)
q_{fa}	content of fly ash in the concrete (kg/m^3)
q_{bs}	content of blast furnace slag in the concrete (kg/m^3)
t	curing time
p_{si}	portion of silica fume of the total amount of binder (w-%)
p_{fa}	portion of fly ash of the total amount of binder (w-%)
p_{bs}	portion of blast furnace slag of the total amount of binder (w-%)

From Formula 9 another formula was derived for the frost resistance index by replacing the reduced (water+air)/cement ratio by the compressive strength of concrete /10/:

$$P = \frac{46 \cdot c_{cur} \cdot c_{age}}{\frac{10 \cdot \left(\frac{28.8}{13.5 + f_{cm}}\right)^{1.25}}{a^{0.5}} - 1} \quad (13)$$

where

f_{cm} is the mean cubic compressive strength of concrete (MPa) at the age of 28 d.

Table 2 shows the values of P as a function of compressive strength and air content. The mean compressive strength of concrete has been replaced by the characteristic strength K, which is assumed to be 8 MPa less than the mean. The coefficients c_{cur} and c_{age} are assumed to be 1.

Table 2. Values of frost resistance index P as a function of tcompressive strength K and air content a (c_{cur}=1 ja c_{age}=1).

K-strength	Air content, %						
MPa	1	2	3	4	5	6	7
20	8.3	13.2	17.3	21.2	25.1	29.0	33.0
30	12.0	10.0	25.7	32.4	39.6	47.2	
40	16.0	26.4	37.2	49.1	62.8		-
50	20.8	36.2	53.9	76.1	-	-	-
60	26.7	49.6	80.3	-	-	-	-
70	33.9	69.0	-	-	-	-	-
80	43.0	99.1	-	-	-	-	-
90	54.7	-	-	-	-	-	-
100	70.3	-	-	-	-	-	-

Formula 14 was derived to simplify the formula for P. With low or moderate values of P ($P \leq 45$) the Formulae 13 and 14 yield closely similar values. If the compressive strength of concrete and the air content are both high Formula 14 is rather conservative and gives the design extra safety.

$$P = 0.0752 \cdot c_{cur} \cdot c_{age} \cdot a^{0.7} f_{cm}^{1.4} \qquad (14)$$

5. Concluding remarks

The frost attack model presented in this article has been developed for the mechanical service life design of concrete structures. The model is applicable for structures exposed to frost-salt action, such as bridges.

The accuracy of the model could be further improved through appropriate experimental and theoretical research. To widen the applicability of the model, the environmental coefficients should be studied with a profound analysis of the environmental stresses.

LITERATURE

1. Sarja, A. & Vesikari, E. (ed.) Durability design of concrete structures. Chapman & Hall 1995. Final report of Rilem Technical Committee 130-CSL. RILEM Report 14. 163 s.
2. Proposal for the service life design of concrete bridges. VTT Building Technology (draft).
3. Matala, S. Service life model for frost resistance of concrete based on properties of fresh concrete, Nordisk Vägtekniska Förbundet, Broseminarium, Korsär, Denmark 1991, 18 p.

Lund University
Lund Institute of Technology
Division of Building Materials
Box 118
S-221 00 Lund, Sweden

KFS AB, Lund 1996